AN INVESTIGATION OF THE ANTI-CANCER EFFECTS OF APPLE FLAVONOIDS FRACTION 4 ON BREAST CANCER CELLS

by

Chao-Yu Loung

Submitted in partial fulfillment of the requirements
for the degree of Master of Science

at

Dalhousie University
Halifax, Nova Scotia
July 2018

Table of Contents

LIST OF TABLES

LIST OF FIGURES

ABSTRACT

Cancer remains to be the one of the leading causes of death in Canada and the United States. In Canadian and American women, breast cancer is the second leading cause of cancer-related deaths behind lung cancer, despite large advancements in our understanding of the disease. One major reason for this is the lack of novel therapeutics that can selectively target triple-negative breast cancers. This project attempts to solve this problem using a collection of phytochemicals found in the peels of Northern Spy apples, called AF4. Using a variety of flow cytometry techniques and western blotting, apple flavonoids fraction (AF4) was found to kill triple-negative breast cancer cells while being non-toxic to healthy epithelial cells. This cell death occurred without the cleavage of caspases or poly (ADP-ribose) polymerase 1 (PARP1) and was determined to be at least in part dependent on reactive oxygen species (ROS). In addition, AF4 inhibited the proliferation of triple-negative breast cancer cells via G1 cell cycle arrest. AF4 seems to inhibit the phosphorylation of Akt via a ROS-dependent mechanism; however, inhibition of the PI3K/Akt pathway does not seem to be responsible for decreased proliferation. In addition, AF4 altered the expression of enzymes involved in epigenetic modulation in both triple-negative breast cancer and epithelial cell lines. The findings of this project highlight the potential of AF4 as a possible selective triple-negative breast cancer treatment.

LIST OF ABBREVIATIONS USED

7-AAD	7-Amino Actinomycin D
Ab	Antibody
AF4	Apple flavonoids fraction 4
Akt	Protein kinase B
ANOVA	Analysis of variance
ATP	Adenosine Triphosphate
BRCA	Breast cancer type 1 susceptibility protein
°C	Degrees Celsius
CaCl2	Calcium chloride
Caspase	Cysteine aspartate-specific protein
CDK	Cyclin-dependent kinase
cDMEM	Complete Dulbecco's Modified Eagle's Medium
CM-H2DCFDA	5-(and-6)-chloromethyl-2',7'-dichlorodihydrofluorescein diacetate, acetyl ester
cm^2	Centimeters squared
ddH_20	Double distilled water
DFE	Deferiprone
DiOC6	3,3'-dihexyloxacarbocyanine iodide
DMEM	Dulbecco's Modified Eagle's Medium
DMSO	Dimethylsulphoxide
DNA	Deoxyribonucleic acid
DNase	Deoxyribonuclease

DNMT	DNA methyltransferase
EDTA	Ethylene diamine tetraacetic acid
ERα	Estrogen receptor alpha
ERK	Extracellular signal–regulated kinase
EtOH	Ethanol
FACS	Fluorescence-activated cell sorting
FBS	Fetal bovine serum
Fe	Iron
g	Gravity
G0	Quiescent Phase
G1	Gap Phase 1
G2	Gap Phase 2
h	Hours
HAT	Histone acetyltransferase
HDAC	Histone deacetylase
HEPES	5 mM N-2-hydroxyethylpiperazine-N-2ethanesulfonic acid
HER	2 Human epidermal growth factor receptor 2
HI-FBS	Heat-inactivated FBS
HRP	Horseradish Peroxidase
JNK	c-Jun N-terminal kinase
kDa	Kilodalton
M	Molar
M phase	Mitotic Phase

MAPK	Mitogen-activated protein kinase
mg	milligram
min	minute
ml	milliliter
mM	millimolar
mTOR	Mammalian target of rapamycin
MTT	3-(4,5-Dimethylthiazol-2-yl)-2,5-diphenyltetrazolium bromide
NaCl	Sodium chloride
NaOH	Sodium hydroxide
NFκB	Nuclear factor kappa light chain enhancer of activated B cells
nm	nanometer
p21	21 kDa Cyclin-dependent kinase inhibitor
p38	38 kDa mitogen-activated protein kinase
p53	53 kDa tumour suppressor protein
PARP1	Poly (ADP-ribose) polymerase-1
PBS	Phosphate buffered saline
PDK1	Phosphoinositide-dependent kinase-1
PFA	Paraformaldehyde
pH	Power of hydrogen (measure of acidity)
PI	Propidium iodide
PI3K	Phosphatidylinositol-3-kinase
PIP_2	Phosphatidylinositol 4,5-bisphosphate

PIP_3	Phosphatidylinositol (3,4,5)-trisphosphate
PMSF	Phenylmethyl sulfonyl fluoride
PP2A	Protein phosphatase 2
PR	Progesterone receptor
PTEN	Phosphatase and tensin homolog
RNA	Ribonucleic acid
RNase	Ribonuclease
ROS	Reactive Oxygen Species
RTK	Receptor tyrosine kinase
S phase	Synthesis Phase
SEM	Stand Error of the Mean
SD	Standard Deviation
SDS	Sodium dodecylsulphate
TET	Tet methylcytosine dioxygenase
Tris-HCl	Tris-Hydrochloric acid
Triton-X 100	Octylphenolpoly(ethyleneglycolether)x
TrypLE	Phenol red negative trypsin replacement
T-TBS	Tween Tris-buffered saline
µg	Microgram
µL	Microlitre
µM	Micromolar
w/v	Weight by volume

ACKNOWLEDGEMENTS

This project would not have been possible without the support of countless individuals who have aided with project troubleshooting and helped me adapt to life in graduate studies. First of all, I would like to thank my supervisor Dr. David Hoskin for the opportunity to work in his lab. Your guidance and support over the course of my project will leave me with lessons that I will carry for the rest of my life. Thank you for always having my best interests in mind and providing an environment that not only provided me the tools to further my training as a scientist, but one that allowed for personal growth as well.

Thank you to my committee members Dr. Vasantha Rupasinghe and Dr. Paola Marcato. To Dr. Rupasinghe, thank you for entrusting me with your AF4 project and always being supportive when my experiments failed and for your encouraging words after every committee meeting. To Dr. Marcato, thank you for your input and for teaching me so much about cancer epigenetics. Although I was not able to apply all the knowledge I have learned from you into my project, I am grateful to you for showing me how cancer epigenetics is so much more complex than I thought.

To my lab members, thank you all for providing such a supportive and fun environment to work in. You all have taught me so much, and I am eternally grateful to you all for being patient with me and treating me as an equal even though I had little prior experience in this field. To Wasu, thank you for all the troubleshooting and knowledge you provided throughout my project. This project would not have been completed in this timeframe nor would it have as much data without the vast amounts of information that you somehow store in your brain. To Andrea, Javad, Emma, Madu, Taylor, Alicia, Anna, Jordan, Bronwen, and Jasmine, thank you for making the lab such a lively place and full of friendly conversation and discussion. You all made my graduate experience incredibly memorable.

To the Pathology Department members, thank you for the support throughout my project and constructive criticism provided in seminars and presentations. To the graduate students, thank you all for being so friendly, willing to help troubleshoot with my project, and sharing reagents.

Lastly, thank you to all my friends and family for the constant support. The encouragement and understanding allowed me to push forward in times of heavy workloads and failed experiments.

CHAPTER 1: INTRODUCTION

1.1 Cancer

Cancer is one of the leading causes of death in developed countries and is characterized by the unregulated growth of cells. The growth of these cells affects the functions of the organs in which they reside, ultimately posing a risk to life. Although recent advances in the understanding of cancer and how to prevent, treat, and screen for this disease has lead to a decrease in the amount of cancer deaths per year, in Canada alone it is estimated that 206,200 Canadians were diagnosed and 80,800 Canadians have succumbed to cancer in 2017 (Canadian Cancer Society, 2017; Siegel et al., 2018). In addition, it is estimated that 1 in 2 Canadians will develop cancer in their lifetimes, with roughly half of these cases being lung, colorectal, breast, or prostate cancers. As for prognosis, its estimated that a startling 1 in 4 Canadians are estimated to die of cancer (Canadian Cancer Society, 2017). Given the severity and prevalence of this disease, many resources have been utilized to better understand cancer with the ultimate goal of achieving a cure. However, cancer is a complicated disease. Given that cancer cells arise from normal human cells, the search for a cure is limited by the side effects produced.

1.2 Breast Cancer

Of all cancers, breast cancer is the most commonly diagnosed cancer in women, with an estimated 1.38 million new diagnoses per year worldwide (Ferlay et al., 2010; Jemal et al., 2011). Although numerous advances in therapeutics and screening programs have reduced the mortality rates significantly, breast cancer remains the second leading cause of cancer deaths in North American women (Siegel et al., 2018).

1.2.1 Breast Cancer Subtypes

Breast cancers can be clinically subtyped by the expression of the hormone receptors estrogen receptor α (ERα), progesterone receptor, and epidermal growth factor receptor 2 (HER2). The presence of estrogen and progesterone receptors and overexpression of HER2 receptors on breast cancer cells contribute to dysregulated cell growth via the activation of a variety of signalling pathways which lead to transcriptional and non-transcriptional cellular responses that favour cell proliferation and survival (Lim et al., 2012; Martin et al., 2014). Triple-negative breast cancers express no hormone receptors nor do they overexpress HER2, and are most aggressive and hardest to treat (Boyle, 2012).

In addition to clinical subtypes, molecular subtypes of breast cancer have been described. This system of breast cancer classification utilizes the gene expression of breast cancers rather than the expression of estrogen, progesterone, and HER2 receptors (Dai et al., 2015). Breast cancers within the same clinical subtype group can be dramatically different from one another while being similar to cancers in another clinical subtype, with differences in sensitivity to certain drugs and cancer aggressiveness. However, clinical subtypes are still the main determinant of treatment due to current limitations in molecular subtyping research (Reis-Filho and Pusztai, 2011). Although there exist many different classifications of breast cancers based on gene expression, the best-known classification includes six different molecular subtypes of breast cancer: luminal A, luminal B, HER2 over-expressing, basal-like,, and the most recent addition, claudin-low. Each of these subtypes takes into account the expression of estrogen,

progesterone, and HER2 receptors, in addition to the expression of other markers for growth such as Ki-67 (Dai et al., 2015; Prat et al., 2010). In general, both luminal A and luminal B breast cancers express estrogen and progesterone receptors, while luminal A cancers do not overexpress HER2 and luminal B includes cases of both HER2 overexpressing and non-overexpressing. HER2 overexpressing breast cancers include those that are estrogen and progesterone positive and HER2 overexpressing. Basal-like and claudin-low breast cancers are triple-negative. The expression of these receptors are not a strict requirement for classification into these molecular subtypes, as the expression of many other genes is also taken into account. In theory, the classification of breast cancers into these groups allows for better clinical outcomes by guiding the utilization of drugs that are known to work in similar breast cancers. This would allow the development of treatments that target more specific pathways present in each group. Although the implications of clinical subtyping are promising, much more work needs to be done before it can fully replace clinical subtyping and allow the use of more personalized cancer treatments.

1.2.2 Current Treatments for Breast Cancer

As the presence of hormone and HER2 receptors directly contributes to the growth of certain breast cancers, these same receptors can be targeted for therapy. Hormone positive cancers can be treated with estrogen receptor antagonists such as tamoxifen or fulvestrant (Lim et al., 2012). Aromatase inhibitors that inhibit estrogen production can also be used as an alternative to hormone therapies (Lim et al., 2012). Although expression of the progesterone receptor is used to classify breast cancers, there are

currently no treatments that target this receptor. Trials with the first generation of progesterone antagonists produced severe side effects and have not been the focus of further research (Brisken, 2013). Lastly, HER2 receptors are targeted with the monoclonal antibody trasztuzamab, which binds to the receptor and prevents its activation. This in turn inhibits cell division via induction of cell cycle arrest at the G1 stage (Hudis, 2007). In addition to these targeted treatments, breast cancers that express hormone receptors or overexpress HER2 are also treated with less selective but more aggressive chemotherapies (Martin et al., 2014). These include taxanes such as paclitaxel and anthracyclines such as doxorubicin (Hudis and Gianni, 2011). Taxanes function by acting as mitotic poisons, stabilizing microtubules and preventing cell division while inducing apoptosis, while anthracyclines act as DNA intercalators and topoisomerase II inhibitors to interrupt DNA replication in cell division (Abal et al., 2003; Thorn et al., 2011). Both taxanes and anthracyclines target rapidly dividing cells rather than cancer cells specifically, which brings about the well-known side effects of chemotherapies such as hair loss, loss of immune function, and damage to the nervous system (Shapiro and Recht, 2001). In the case of triple-negative breast cancers, these chemotherapies are the only choice for treatment (Oakman et al., 2010). To allow for synergistic effects, taxanes and anthracyclines may be used in conjunction with platinum DNA-intercalating agents, like cisplatin or carboplatin (Petrelli et al., 2014). As triple-negative breast cancer can only be treated with therapeutics that have a greater effect on rapidly dividing cells rather than cancer cells, many consider triple-negative breast cancer to lack selective therapies.

1.2.3 Triple-Negative Breast Cancer

As previously mentioned, triple-negative breast cancers are aggressive and hard to treat. It is estimated that about 15% of breast cancers are triple-negative and have the worst prognosis out of all the breast cancers (Dent et al., 2007). This is because there a currently no therapeutics that can selectively target triple-negative breast cancers. Triple-negative breast cancers also have high rates of metastasis and relapse, as well as high tumor grades and size at the time of diagnosis (Dent et al., 2007). Although numerous attempts have been made to target mutations present within most triple-negative breast cancers, these clinical trials have been at best minimally successful. One example of this is the use of PARP1 inhibitors in triple-negative breast cancers to exploit the fact that most triple-negative breast cancers have BRCA1 deficiencies (Foulkes et al., 2003; Lakhani et al., 2005). As both these proteins are involved in DNA repair, this combination was predicted to be more detrimental to the cancer cells compared to normal cells, which would have normal BRCA1 levels (Zhang and Powell, 2005). In conjunction with conventional chemotherapies, it was thought that PARP1 inhibition would allow for the treatment of triple-negative breast cancers with fewer side effects (Alli et al., 2009; Bryant et al., 2005). However, clinical studies of PARP1 inhibitor iniparib in combination with gemcitabine and carboplatin in triple-negative breast cancer patients showed no benefit when compared to treatment with gemcitabine and carboplatin alone (O'Shaughnessy et al., 2011, 2014). The prevalence of triple-negative breast cancer, lack of selective treatments, and poor prognosis for patients highlights the need for novel therapeutics that can be used alone or in combination with other treatments to improve patient outcomes.

1.3 Cell Survival and Proliferation Pathways

To find a way to treat triple-negative breast cancers, we must first find differences between these cancer cells and normal cells. Numerous cellular pathways involved in cell survival and proliferation are dysregulated in many cancers through a variety of different mechanisms such as receptor overexpression or gene mutation. These pathways play a crucial role in allowing cancers to grow uncontrollably and act as attractive targets for the treatment of cancers.

1.3.1 PI3K/Akt

The phosphoinositide 3-kinase (PI3K)/ protein kinase B (Akt) pathway is one of the best understood cell survival and proliferation pathways and has been the target of many prospective anti-cancer agents (Figure 3). Signalling through this pathway is initiated with external growth factors that bind to extracellular receptor tyrosine kinases, which phosphorylates PI3K, activating it (Nicholson and Anderson, 2002). PI3K can then phosphorylate phosphatidylinositol 4,5-bisphosphate (PIP_2) to PI-3K generating phosphatidylinositol-3,4,5-trisphosphate (PIP_3), which then phosphorylates and activates phosphoinositide-dependent kinase-1 (PDK1). PDK1 phosphorylates Akt, allowing it to phosphorylate and activate mTOR, which is directly involved in maintaining cell survival signals. The tumor suppressor gene PTEN works in opposition to PI3K, whereby phosphorylation of this gene product leads to dephosphorylation of PIP_3 to PIP_2 to reduce signalling through the Akt pathway.

Although the best known activator of Akt is PI3K, recent studies suggest that there are PI3K-independent pathways for the activation of Akt through kinases such as protein phosphatase 2 (PP2A) and IKB kinase ε (Carracedo and Pandolfi, 2008; Hemmings and Restuccia, 2012; Verhelst et al., 2013; Xie et al., 2011). In addition, there are multiple downstream targets for Akt, such as FOXO, GSK3, and NF-κB (Kane et al., 1999; Manning and Toker, 2017; Nidai Ozes et al., 1999; Song Gang et al., 2007). Together, these downstream targets of Akt signalling induce a wide variety of cell functions that are essential for cell survival, such as regulation of apoptosis, cell growth and proliferation, protein synthesis and angiogenesis (Gilmore, 2006). These proteins, which serve a critical role in the regulation of cell proliferation, are often dysregulated in cancer through mechanisms that vary from cancer to cancer based on receptor expression and mutations (Gilmore, 2006). The capability of Akt to affect multiple signalling pathways gives it many roles in cancer progression. For example, Akt is involved in cell proliferation and survival, as well as being involved in metastasis, angiogenesis, and drug resistance (Davies, 2011; Martin et al., 2014)

1.3.2 ERK/MAPK

Another well-studied signalling pathway with implications in cancer progression is the extracellular signal–regulated kinases (ERK)/ mitogen-activated protein kinase (MAPK) pathway. This pathway is initiated by the binding of extracellular growth factors, which activate Ras binding of GTP (Figure 3). Ras can then phosphorylate and activate Raf, followed by MAPK kinase (MEK), and finally ERK1 and ERK2 (Downward, 2003). The activation of ERK1 and ERK2 then signal for cell growth and survival. Given the

role of the ERK/MAPK in pathway in cell growth, it's no surprise that this pathway is commonly dysregulated in cancer (McCubrey et al., 2007). Studies also suggest that the ERK/MAPK pathway and PI3K/Akt pathways interact with each other to regulate cell growth. Not only can Ras proteins activate Akt , but Akt can also phosphorylate different Rafs (Downward, 2003; McCubrey et al., 2007). The ERK/MAPK pathway has been the focus of many studies attempting to downregulate cancer cell growth, reduce malignancy, and overcome drug resistance (McCubrey et al., 2007).

1.4 The Cell Cycle

Downstream of the cell proliferation signalling pathways is the cell cycle, which comprises the processes responsible for cell division. There are four growth stages in the cell cycle that follows the G_0, or non-growth phase: the first growth phase, G_1; the DNA synthesis phase, S; the second growth phase, G_2; and the mitotic phase, M (Figure 2; Satyanarayana and Kaldis, 2009). Passage through the stages of the cell cycle is tightly regulated through many different pathways, that ultimately converge on the regulation of two groups of proteins involved in cell cycle regulation: cyclins, and cyclin dependent kinases (CDK). Upon activation, cyclins bind to CDKs, activating them and allowing them to exert their effects on the cell cycle (Malumbres, 2014). Cyclins-CDK complexes each have distinct roles in the cell cycle. The D cyclins couple with CDK4 and CDK6 to phosphorylate the tumor-suppressor protein retinoblastoma protein (Rb), inactivating it and allowing the cell to progress through the G_1 stage of the cell cycle into the S phase, which also requires the activation of CDK2 coupling with the E cyclins. Progression through the S phase to the G_2 phase requires that CDK2 associates with the A cyclins.

Finally, progression from the G_2 phase into the M phase requires CDK1 to be activated by both A and C cyclins. At this point the cell undergoes mitosis and the cycle can start again (Satyanarayana and Kaldis, 2009). The ability of cancers to grow at such a high rate can be attributed to the dysregulation or mutation of proteins involved in the cell cycle. In multiple types of cancers, CDKs are overexpressed or mutated, allowing for uncontrolled cell proliferation (Peyressatre et al., 2015). Mutations of other important cell cycle proteins, such as Rb, are also common (Nevins, 2001).

1.5 Oxidative Stress

Oxidative stress occurs in cells when cellular antioxidants fail to scavenge the reactive oxygen species (ROS) within the cell. This allows these free radicals to react with important intracellular components, most notably cellular DNA (Kryston et al., 2011). Damage to cellular DNA carries the risk of causing mutations in tumor suppressor genes and oncogenes, altering the activity of the translated proteins which may contribute to the cancer phenotype. Although many DNA repair mechanisms exist within cells to counteract DNA mutations, these repair mechanisms are also prone to mistakes, and prolonged oxidative stress may overwhelm these error-correcting mechanisms. Certainly, ROS plays an important part in cancer progression, and has been the focus of many chemoprevention studies that attempt to utilize anti-oxidants to prevent the ROS-induced mutations that can lead to cancer development. However, more recent studies have highlighted the need of ROS within cells. ROS also play a role in various signal transduction pathways, and a small amount of ROS may be able to induce the expression of genes responsible for the defense against oxidation, thus protecting the cell and

organism from future oxidative stress through a mechanism called hormesis (Ristow and Zarse, 2010). With these findings, it is clear that ROS balance within the cell plays an important part in the well-being of organisms.

1.5.1 ROS as second messengers

Although it is clear that oxidative stress has many negative effects on the cellular level, as well as on the whole organism level, ROS is also necessary for certain functions within the human body, such as cell signalling, gene expression, and regulation of the immune system (Bouayed and Bohn, 2010). Furthermore, studies on the impact of antioxidant supplementation after muscle injury find that ROS is needed for proper muscle recovery, likely due to the involvement of ROS in signalling to the immune system to clear the site of injury for wound healing (Michailidis et al., 2013). It is clear that ROS has important functions within the human body, and that its role can be best described as a double-edged sword.

1.5.2 ROS-mediated cell death

Given the many negative consequences of oxidative stress within cells, it comes as no surprise that multiple mechanisms exist to either prevent oxidative stress or manage the negative consequences of this condition. However, excessive production and accumulation of ROS can overwhelm these defenses. At this point, if the cell were to survive and continue proliferating, the risk of mutations and cancer increases. Fortunately, as a fail-safe mechanism, cells that have extensive damage to their DNA are programmed to commit suicide via a variety of programmed cell death pathways, with ROS being one

of the main inducers of cell death. A variety of proteins involved in cell death are thought to be affected by ROS, such as the MAPK c-Jun N-terminal kinase (JNK) and PP2A (Dhanasekaran and Reddy, 2008; Jiang et al., 2017; Shen and Liu, 2006). After sensing excessive oxidative stress, these proteins can either signal the increase of pro-apoptotic proteins such as Bax, signal for the decrease of pro-survival proteins such as Bcl-2, or both, leading to cell death (Dhanasekaran and Reddy, 2008; Korsmeyer et al., 1993).

1.6 Cell Death Pathways

1.6.1. Apoptosis

Apoptosis, the best understood pathway of programmed cell death, is tightly regulated by the balance between pro-survival and pro-apoptotic proteins such as Bcl-2 and Bax (Raisova et al., 2001). Apoptosis serves multiple functions, allowing for the separation of toes and fingers during embryogenesis as well as the removal of damaged cells (Brill et al., 1999). There are a variety of morphological and biochemical changes that occur in a cell undergoing apoptosis, such as cell shrinkage, membrane blebbing, chromatin condensation, DNA fragmentation, and translocation of the phospholipid phosphatidylserine from the inner leaflet of the cell membrane to the outer leaflet (Collins et al., 1997; Elmore, 2007; Lee et al., 2013).

There are two pathways that trigger apoptosis: the intrinsic pathway, and the extrinsic pathway, which are initiated by different signals and caspases, although both converge on the cleavage of the executioner caspases 3, 6, and 7 (Slee et al., 2001). Activated caspases cleave proteins that are necessary for cell survival and cell division. Examples of substrates for executioner caspases include the structural protein vimentin,

which comprises the cytoskeleton; DNA topoisomerase I, which is required for unwinding DNA during DNA synthesis; and poly [ADP-ribose] polymerase 1 (PARP1), which plays a major role in DNA repair (Decker and Muller, 2002; Slee et al., 2001; Tetsuo et al., 1990; Wang, 2002). The disruption of these crucial cellular functions ultimately causes the cell to die (Nicholson, 1999; Slee et al., 2001; Thornberry and Lazebnik, 1998). During apoptosis, the cell is compartmentalized into apoptotic bodies through budding of the plasma membrane, which keeps the cytoplasmic contents confined. These apoptotic bodies are then be engulfed by macrophages to recycle the cellular components (Elmore, 2007).

The intrinsic pathway of apoptosis, also known as the mitochondrial pathway, is initiated by cell damage caused toxins, hypoxia, or ROS (Elmore, 2007). These stimuli cause the loss of mitochondrial transmembrane potential via the opening of the mitochondrial permeability transition pore in the inner mitochondrial membrane, which in turn allows for the release of a variety of proteins from the intermembrane space of the mitochondria, most notably cytochrome c. Cytochrome c binds to apoptotic protease activating factor-1 (Apaf-1) forming an apoptosome which binds to and activates caspase 9, allowing it to cleave caspase 3 (Chinnaiyan, 1999; Elmore, 2007; Pop et al., 2006).

The extrinsic pathway of apoptosis, as its name suggests, relies on the binding of external factors to transmembrane receptors located on the plasma membrane of the target cell (Elmore, 2007). These receptors, which include Fas and TRAIL are present specifically for the initiation of apoptosis and are aptly named death receptors. Upon binding of the ligand onto these death receptors, the protein FADD is recruited to bind

with procaspase 8, forming the death-inducing signaling complex (DISC) and activating caspase 8, allowing it to cleave caspase 3 (Elmore, 2007).

Recent advances have expanded our current understanding of cell death pathways, and more and more regulated cell death pathways that are biochemically distinct from apoptosis are being discovered.

1.6.2 Ferroptosis

Ferroptosis is another form of programmed cell death that is dependent on iron, with the Fenton reaction ($Fe2+ + H_2O_2 \rightarrow Fe3+ + \cdot OH + -OH$) playing a large but not essential role (Xie et al., 2016). Ferroptosis is characterized by lipid peroxidation, mitochondrial shrinkage and increased mitochondrial membrane density; however, ferroptosis involves signalling mechanisms that are distinct from those involved in apoptosis (Xie et al., 2016; Yu et al., 2017). In addition, ferroptosis is suggested to play a role in cell proliferation, highlighting its role in preventing the proliferation of cells with dysregulated growth pathways (Yu et al., 2017). Some currently approved anti-cancer agents, such as sorafenib, are able to induce ferroptosis (Yu et al., 2017). In addition, certain phytochemicals are capable producing ROS through the Fenton reaction, such as artesunate, carotenoids, and myricetin, with artesunate being shown to induce ferroptosis (Eling et al., 2015; Knickle et al., 2018; Polyakov et al., 2001). Although currently not well understood, ferroptosis seems to be another pathway that could potentially be used to combat cancers.

1.6.3 Necrosis

The classic counterpart to apoptosis is necrosis, which is an unregulated form of cell death. Unlike apoptosis, necrosis involves leakage of cell cytoplasmic contents, which induces inflammation (Kroemer et al., 2009). Necrosis can occur when cells are damaged in a way that leads to the immediate permeabilization cell membranes, rupture of the cell and lysosomal degradation of cellular components (Long and Ryan, 2012; Vandenabeele et al., 2010).

1.6.4 Necroptosis

Necroptosis is similar to necrosis in that cellular contents leak out of the cell rather than being compartmentalized for removal by macrophages. However, necroptosis is a form of programmed cell death initiated via cellular signals. It has been suggested that necroptosis provides an alternative cell death pathway that is independent of caspase activation, in order to circumvent certain viruses that express caspase inhibitors (Vandenabeele et al., 2010). Similar to the extrinsic pathway of apoptosis, the binding of external death signals such as tumor necrosis factor (TNF) to a cell surface receptor can trigger cell death by necroptosis. In addition, ROS has been proposed to play a large role in the regulation of necroptosis (Goossens et al., 1999; Kim et al., 2007). Although the mechanisms behind necroptosis are not very well understood, it is known to involve activation of receptor-interacting protein kinase 1 and 3 (RIPK1 and RIPK3, respectively) as well as inhibition of apoptosis (Vandenabeele et al., 2010).

1.7 Immunogenic Cell Death

In contrast to the cell death pathways that involve strictly intracellular signalling, immunogenic cell death results in recognition of target cells by the immune system. The immune system is programmed to ignore healthy cells under normal conditions, however, damaged cells within the body must signal for their elimination. This is accomplished through the secretion of damage-associated molecular patterns (DAMPs), some of which are secreted as a part of programmed cell death pathways such as apoptosis (Garg et al., 2012). In cancer, DAMPs release is inhibited to allow cancers to evade elimination by the immune system (Hanahan and Weinberg, 2011). However, some currently approved cancer therapeutics can induce immunogenic cell death, as well as being directly cytotoxic to cancer cells. Examples include anthracyclines such as doxorubicin and platinum agents such as oxaliplatin; immunogenic cell death highlights the role of the immune system in eliminating cancer cells (Galluzzi et al., 2016; Garg et al., 2010).

1.8 Epigenetic Targets for Cancer Treatment

Targeting epigenetic mechanisms for cancer treatment is a relatively new area of consideration. Epigenetic changes make a major contribution to the changes in cell physiology that are required for cells to enter a cancerous state (Hanahan and Weinberg, 2011). For example, functional tumour suppressor genes such as PTEN may be hypermethylated at the DNA level and hypoacetylated at the histone level, both of which contribute to decreased gene expression via hydrophobic and ionic forces (Brait and Sidransky, 2011; Sharma et al., 2010). Given that epigenetic changes are reversible, finding a way to reverse the epigenetic changes commonly seen in cancers may be

enough to cause cancer cells to undergo apoptosis. Although other epigenetic modifications such as histone methylation or phosphorylation, and non-coding RNAs such as microRNAs (miRNAs) and long non-coding RNAs (lncRNAs) have been suggested to play a role in cancer, DNA methylation and histone acetylation are the best understood (Chrun et al., 2017; Füllgrabe et al., 2011). Nevertheless, targeting epigenetics as a way of modifying gene expression for anti-cancer purposes shoes promise in preclinical studies.

1.8.1 DNA Methylation

DNA methylation, which occurs when a methyl group is added onto the 5' position of cytosine is accomplished with DNA methyltransferases (DNMTs) utilizing S-adenosylmethionine (SAM) as a co-factor. There are three isoforms of DNMT: DNMT1, which is responsible for maintaining the methylation profile of daughter strands as DNA is being replicated, and DNMT3A and DNMT3B, which are responsible for *de-novo* methylation, or the addition of methyl groups onto new sites in the DNA. All three isoforms of DNMT seem to be important for the cancer phenotype, however, DNMT3A and 3B are thought to play the most important role in carcinogenesis due to their *de-novo* methylation capabilities (Issa and Kantarjian, 2009). DNMT-mediated addition of methyl groups exclusively on cytosines that are followed by a guanine ensures that DNA methylation occurs on both sense and antisense strands. Moreover, methylation usually occurs in CpG islands, which are regions of the genome that possess a large number of CpG motifs. These CpG islands are usually located in or near the transcription start site of genes, although in these cases these cytosines remain unmethylated to allow for gene

transcription. In cancer, however, hypermethylation of tumor suppressor gene promoters is commonly seen (Esteller, 2007; Kopelovich et al., 2003). In addition, global hypomethylation is also commonly seen in cancers, which contributes to the genomic instability of malignant cells (Gama-Sosa et al., 1983; Sharma et al., 2010).

Due to methyl group additions being very stable, the removal of methyl groups from DNA requires the excision of the base by DNA repair enzymes. Before the methylated cytosine can be removed, it first must be converted to a nucleotide intermediate via deamination by the AID/APOBEC family of deaminases or by hydroxylation by teneleven translocation (TET) enzymes. These intermediates are then modified even further with a variety of different pathways. The products of each pathway are then recognized by base-excision repair pathways and cleaved off, which allows a naked cytosine to be placed into the resulting excision (Moore et al., 2012). DNA demethylation pathways and their importance in cancers are currently not well understood, but it seems that TET genes, and especially TET2, are found to be frequently mutated in various cancers (Kohli and Zhang, 2013).

Currently, the DNMT inhibitors 5'-azacytidine, and 5'-aza-2'-deoxycitidine are approved for treatment of hematological malignancies (Müller and Florek, 2010). However, the mechanism of action in this case may not be epigenetic. 5'-azacytidine, and 5'-aza-2'-deoxycitidine act as cytosine analogues, thus enzymes that would normally use cytosine take up 5'-azacytidine, or 5'-aza-2'-deoxycitidine instead, which covalently binds to the active site and prevents the enzyme from functioning (Kelly et al., 2010; Müller and Florek, 2010; Plimack et al., 2007). These enzymes include DNMTs, as well as enzymes involved in transcription and translation. With higher doses of 5'-azacytidine,

or 5'-aza-2'-deoxycitidine, the cellular levels of enzymes involved in cell replication and protein synthesis are depleted and the cell undergoes apoptosis before any epigenetic changes can affect the cell (Kelly et al., 2010). Although recent studies on solid tumors have shown that long term treatment with low dose DNMT inhibitors produces anti-cancer effects, the mechanism is currently a controversial. Reduced DNA methylation in the genome is suggested to activate viral DNA elements that were inserted in the genome many generations ago; expression of these elements allows the immune system to recognize these cancer cells and target them for elimination (Roulois et al., 2015).

1.8.2 Histone Acetylation

Histone acetylation is catalyzed by histone acetyltransferases (HATs), which transfer acetyl groups onto lysine residues. The removal of these acetyl groups is catalyzed by histone deacetylases (HDACs). The presence of multiple acetyl groups on histones causes the histones to repel each other due to the negative charge of acetyl groups. This results in an open chromatin structure that enables transcription factors to bind to DNA. In contrast, histone deacetylation condenses chromatin and represses transcription, as transcription factors are now physically unable to access the genes of interest. In humans, 25 HATs and 18 HDACs have been identified. HATs are divided into multiple classes based on structure, homology, and histone specificity: GNATs (hGCN5 and PCAF), MYSTs (MYST and Tip60), p300/CBP (p300/CBP), SRC (SRC-1), and TAFII250 (TAFII250) (Bannister and Kouzarides, 2011). HDACs are divided into class I, II, III and IV HDACs based on homology, size, expression within the cell, and number of enzymatic domains (Mottet and Castronovo, 2008). HDACs 1, 2, 3, and 8 comprise class I, HDACs 4, 5, 6, 7,

9, and 10 comprise class II, and class IV HDACs have HDAC11 as their sole member. Class III HDACs consist of seven members named sirtuins, and are structurally unrelated to the other classes of HDACs (Sauve et al., 2006). Studies on the roles of specific histone modifications in cancer, such as acetylation at lysine 9 and 27 of histone subunit 3 (H3K9 and H3K27, respectively), have shown linkage to carcinogenesis and cancer progression, but surprisingly also certain anti-cancer effects (Ding et al., 2016; Kalle et al., 2010; Roche et al., 2013; Zhang et al., 2017). However, the exact mechanisms are still currently unknown.

1.9 Anticancer Effects of Phytochemicals

The idea of using plants to heal disease dates back thousands of years and is still prevalent today in the form of commercial natural health products as well as certain anti-cancer drugs such as paclitaxel, which are derived from taxanes found in *Taxus brevifolia* trees (Greenwell and Rahman, 2015). These drugs utilize the bioactive ingredients in plants, called phytochemicals, in an effort to prevent and fight diseases such as cancer. However, the cellular pathways affected by phytochemical exposure are generally still not well understood. Recent studies into phytochemicals as potential anti-cancer agents have found that these chemicals affect many different signalling pathways that are involved in cancer (Kale et al., 2008; Yao et al., 2011). With further research, plant-based therapeutics for the prevention or treatment of cancer may be possible.

1.9.1 Apple Flavonoids Fraction 4

Apple flavonoids fraction 4 (AF4) is a collection of phytochemicals isolated from the peels of Nova Scotian Northern Spy apples. AF4 contains a wide variety of phytochemicals but is composed mostly of quercetin glycosides (Table 1; Sudan and Rupasinghe, 2014). These quercetin glycosides differ from their parent compound by the addition of a simple sugar on the 3' position. Structures of the major components of AF4 can be found in Figure 3. Some of these phytochemicals have shown a variety of anti-cancer effects and will be explained in detail in the following section (Table 2). Studies on the effects of AF4 as a whole are currently limited but promising. One study on the effects of AF4 on HepG2 hepatocarcinoma cells shows that AF4 has selective cytotoxicity via the activation of caspase 3, leading to apoptosis of the liver cancer cells (Sudan and Rupasinghe, 2014). At the same dose of AF4, normal healthy liver and lung cells undergo minimal cell death. This effect was compared to those of Sorafenib, a monoclonal antibody used in the treatment of liver cancer that inhibits signalling through receptor tyrosine kinases such as VEGFR and Raf (Keating and Santoro, 2009; Wilhelm et al., 2008). Compared to Sorafenib, AF4 was more selective for cancer cells. In addition, AF4 induces G_2/M cell cycle arrest, and acts as a DNA topoisomerase II inhibitor (Sudan and Rupasinghe, 2014). Given the known anticancer effects of AF4 and its potential to outperform current therapeutics, AF4 is predicted to act as a selective therapeutic for triple-negative breast cancers.

1.9.2 Quercetin

Quercetin is a well-studied phytochemical that is found in a variety of foods such as red wine, onions, green tea, and apples. Quercetin possesses numerous anti-breast cancer activities, such as the ability to induce oG_2/M phase cell cycle arrest, and trigger cell death by apoptosis or necroptosis (Khorsandi et al., 2017; Rivera Rivera et al., 2016). In the ERα and progesterone-positive MCF-7 breast cancer cell line quercetin decreases the expression of the pro-survival protein Bcl-2 while increasing pro-apoptotic Bax expression. In addition, quercetin, in the presence of the necroptosis inhibitor necrostatin-1, failed to affect Bax expression, leading to an increase in cell viability, when compared to cells treated with quercetin alone (Khorsandi et al., 2017). In MDA-MB-231triple-negative breast cancer cells and hormone receptor-negative HER2 overexpressing MDA-MB-435 breast cancer cells quercetin inhibits signalling through Akt and AMPK pathways to inhibit mTOR activation., which results in a decrease in breast cancer cell proliferation and induction of apoptosis (Rivera Rivera et al., 2016). Although the epigenetic effects of quercetin in breast cancers are not yet known, quercetin is able to inhibit DNMT1 activity (Lee et al., 2005). In another study that utilized gold nanoparticles to aid in the absorption of quercetin in hepatocarcinoma cells, quercetin-loaded gold nanoparticles decrease DNMT1, as well as HDAC 1 and 2 expression, which correlates with the modulation of p21, CDK1, and phosphorylated Akt (Bishayee et al., 2015). However, no studies to date have investigated the effects on quercetin on DNA methylation or chromatin structure.

1.9.3 Epicatechin

Catechins, which are flavonoids that are commonly found in tea, exist in many isomers, the most common being (+)-catechin and (-)-epicatechin. Given its abundance, most studies on catechins focus on epigallocatechin gallate (EGCG), also known as epigallocatechin-3-gallate. *In vitro* studies of the effects of EGCG on breast cancer cell lines has shown that this phytochemical has a variety of effects. For example, EGCG induces apoptosis of breast cancer cells via caspase 3 and 7 cleavage, and has been reported to be capable of inducing cell cycle arrest at the G_2/M phase (Gianfredi et al., 2017). In addition, EGCG downregulates NF-κB activation to inhibit cell survival and proliferation and also exhibits epigenetic modulatory abilities (Gu et al., 2013). In the case of DNA methylation, catechins are capable of inhibiting DNMT1 with IC50 values ranging from 210 to 470 nM. In addition, molecular modeling of EGCG and DNMT interactions suggests that EGCG can form hydrogen bonds within the active site of DNMTs, (Lee et al., 2005). EGCG also inhibits histone acetyltransferase, with global specificity for the majority of histone acetyltransferase enzymes. However, EGCG does not affect histone deacetylases, SIRT1, and histone methyltransferases (Choi et al., 2009; Lee et al., 2012).

1.9.4 Cyanidin-3-O-galactoside

Although cyanidin-3-0-galactoside is present in moderate amounts in AF4, this anthocyanin conjugate is currently poorly understood. Moreover, the effects of anthocyanins on breast cancer cells are not-well studied, although anthocyanins seem to have a wide range of effects on esophageal, colon, and skin cancers cells that include

anti-proliferative effects via inhibition of D and A cyclins and the selective induction of apoptosis (Wang and Stoner, 2008). These anticancer effects are accomplished via inhibition of signalling through the Pi3K/Akt pathway, inhibition of ERKs, and inhibition of NFκB (Wang and Stoner, 2008). To date, no studies on the epigenetic effects of anthocyanins have been conducted.

1.9.5 Phloridzin

Phloridizin is a phytochemical best known for its ability to inhibit the uptake of glucose via the transport of the sodium and glucose cotransporter SGLT1, making it an anti-diabetic drug of interest (Nelson and Falk, 1993a). However, compared to other phytochemicals, phloridizin is not as well studied. Phloridizin inhibits the growth of rat mammary adenocarcinoma and bladder carcicnoma cell lines *in vivo*, however, the mechanism of inhibition is unclear (Nelson and Falk, 1993b). Recent studies on phloridizin have used fatty acid esters of phloridzin that work to increase bioactivity via increased cell uptake (Fernando et al., 2016; Nair et al., 2014). Studies on a variety of fatty-acid esters of phloridzin in hepoatocarcinoma cell lines have shown that these esters inhibit DNA topoisomerases IIα activity, induce apoptosis via caspase 3 activation, and reduce the expression of a variety of proteins including mTOR, KRAS, CDK2, and HDACs. In contrast, phloridzin alone does not have any significant effects on hepatocarcinoma cells (Nair et al., 2014). Further studies on the docosahexaenoic acid ester of phloridzin, also known as PZ-DHA, in breast cancer show promising results. PZ-DHA exerts selective cytotoxicity towards breast cancer cells but not healthy cells. Cytotoxicity is due to induction of apoptosis by a ROS-independent mechanism, as well

as inhibition of proliferation of triple-negative breast cancer cells via G_2/M arrest and downregulation of cyclin B1 and CDK1. Again, phloridzin on its own does not have any effects on breast cancer cells (Fernando et al., 2016).

1.10 Research Objectives and Approach

Given the diverse effects of the individual AF4 components on cancer cells as well as the effects of AF4 on liver cancer, this project investigated the effects of AF4 on triple-negative breast cancer cells in comparison to the effects of AF4 on healthy epithelial cells. With the multiple phytochemicals present within AF4, it was hypothesized that this would lead to a greater effect due to the disruption of multiple cancer-related pathways rather than disruption of a single pathway. This enhanced effect would also allow for greater selectivity towards cancer cells, as healthy epithelial cells would be more capable of adapting to smaller amounts of several compounds rather than a large dose of a single compound. Lastly, as glycosylated phytochemicals are capable of affecting different signalling pathways in cancer cells when compared to their parent compounds and are not commercially abundant, AF4 may produce combinations of anti-cancer effects that may not yet be feasible to achieve with current chemical synthesis techniques. Thus, AF4 was hypothesized to be capable of inhibiting the proliferation of triple-negative breast cancer cells via the induction of cell cycle arrest, selectively induce cell death in triple-negative breast cancers, as well as inducing changes in the expression of epigenetic enzymes.

CHAPTER 2: MATERIALS AND METHODS

2.1 Cell Lines

The triple-negative MDA-MB-231 breast cancer cell line was provided .by Dr. S. Dover (Memorial University of Newfoundland, NL), while the triple-negative MDA-MB-468 breast cancer cell line was provided by Dr. P. Lee (Dalhousie University, NS). Murine triple-negative 4T1 cells were provided by Dr. D. Waisman (Dalhousie University, NS). Estrogen and progesterone positive MCF-7 breast cancer cells were provided by Dr. J. Blay (Dalhousie University, NS). HER-2 overexpressing SK-BR-3 breast cancer cells were provided by Dr.G. Dellaire (Dalhousie University, NS). The transformed human epithelial cell line MCF10Awas provided by Dr. P. Marcato (Dalhousie University, NS). The transformed murine epithelial cell line HC11 was provided by Dr. P. Lee (Dalhousie University, NS).

2.2 Culture Medium and Incubation Conditions

All breast cancer cells were cultured in Dulbecco's Modified Eagle's Medium (DMEM) supplemented with 10% heat-inactivated (HI) (56°C for 30 min) fetal bovine serum (FBS), 2 mM L-glutamine, 5 mM N-2-hydroxyethylpiperazine-N'-2-ethanesulfonic acid (HEPES) buffer (pH 7.4), 100 U/mL penicillin, and 100 µg/mL streptomycin, subsequently referred to as complete DMEM (cDMEM). The transformed human epithelial cell line MCF10A was cultured in Dulbecco's Modified Eagle Medium/Nutrient Mixture F-12 (DMEM/F12) supplemented with 10% HI horse serum, 10 µg/mL recombinant human insulin, 20 ng/mL recombinant human epidermal growth factor, 0.5 µg/mL hydrocortisone, and 100 units/ml penicillin and 100 µg/ml streptomycin. This

medium will be referred to as complete DMEM/F12 (cDMEM/F12). The transformed mouse epithelial cell line HC11 was cultured in DMEM supplemented with 5% HI FBS and 100 U/mL penicillin, and 100 μg/mL streptomycin. All cell lines propagated as required in T-75 mm^2 tissue culture flasks and maintained in humidified incubators at 37°C with 10% or 5% CO_2 for cancer cells and epithelial cells, respectively.

2.3 Cell Line Seeding

With the exception of the 4T1 and HC11 cell lines, 96-well plates were seeded at a density of 5,000 cells per well, 24-well plates at 20,000 cells per well, and 6-well plates at 50,000 cells per well. T75 flasks for western blot analysis were seeded with 700,000 cells per flask for 24-h time points, 400,000 cells per flask for 48-h time points, and 300,000 cells per flask for 72-h time points. 4T1 and HC 11 cells were plated at 1000 cells per well in 96-well plates.

2.4 Cell Harvesting

Cells were harvested following AF4 or control treatment. Cell supernatant was first transferred into a tube. Adherent cells were then detached with TrypLE express (Gibco Life Technologies Inc., Burlington, ON) for 3 minutes at 37°C. The detached cells were then recombined with their respective supernatants containing non-adherent cells prior to centrifugation at 500 x g for 5 min and washed with 1X PBS. The isolated cells were then lysed or stained for further experimentation.

2.5 Reagents

AF4 was obtained from Dr. H.P. V. Rupasinghe (Dalhousie University, NS). In short, AF4 was extracted from the peels of Nova Scotian Northern Spy apples with ethanol and stored at -80 °C (Keddy et al., 2012). To prepare AF4 samples for cell treatment, ethanol was evaporated under nitrogen gas, dissolved in ddH_2O and stored at -20 °C. MTT (3-(4,5-demethylthiazol-2-yl)-2,5-diphenyltetrazolium bromide), Dimethyl sulfoxide (DMSO), Triton X-100, phosphate buffered saline (PBS), bovine serum albumin (BSA), sodium acetate, acid phosphatase substrate, insulin, hydrocortisone, N-acetylcysteine (NAC), and phenylmethylsulfonyl fluoride (PMSF) were purchased from Sigma-Aldrich (Oakville, ON). Cell TraceTM Oregon Green® 488 carboxylic acid diacetate was purchased from Molecular Probes (Eugene, OR). Trypan blue dye, L-glutamine, penicillin (10,000 units/mL) and streptomycin (10,000 units/mL) solution, 1M N-2-hydroxyethylpiperazine-N-2-ethane sulfonic acid (HEPES), fetal bovine serum (FBS), horse serum, 0.25% trypsin-EDTA, TrypLE™ Express, propidium iodide (PI), DMEM, phenol red free DMEM, and DMEM/F-12 were purchased from (Gibco Life Technologies Inc., Burlington, ON). 7-Amino Actinomycin D, annexin-V 488, 5-(and-6)-chloromethyl-2',7'-dichlorodihydrofluorescein diacetate, acetyl ester (CM-H2DCFDA, or DCFDA), and Amplex Red® was purchased from Thermo Fisher Scientific Inc. (Burlington, ON). Acrylamide/bis-acrylamide (29:1, 30% solution), sodium dodecyl sulfate (SDS) ammonium persulfate (APS), Tween-20, tetramethylethelyenediamide (TEMED), and Tris-HCL were purchased from BioShop Canada Inc. (Burlington, ON). Luminata™ Forte Western horseradish peroxidase (HRP) substrate and calcium chloride ($CaCl_2$) were all purchased from EMD Millipore (Etobicoke, ON).

2.6 Antibodies

Unless otherwise specified, all primary antibodies were obtained from Cell Signaling Technology Inc. (Beverly, MA). These included antibodies against human caspase 3, caspase 7, PARP1 CDK1, CDK4, CDK6, phospho-PTEN (Ser380), total PTEN, phospho-PDK1 (Ser241), total PDK1, phospho-Akt (Ser473), phospho-Akt (Thr308), total Akt, phospho-mTOR (Ser2448), phospho-RAF (Ser259), phospho-ERK 1/2 (Thr202/Thr204), total ERK 1/2, PP2A subunit C, phosphor-p38 (Thr 180/Tyr182), total p38, total JNK, phospho-GSK3β (Ser9), total GSK3β, β-catenin, DNMT1, DNMT3A, DNMT3B, HDAC1, HDAC4, HDAC6, PCAF, Ac-CBP/p300 (Lys1535/Lys1499), total CBP/p300, GCN5L2, acetylated H3K9, acetylated H3K27, tubulin, GAPDH, β-actin (HRP-conjugated) and caspase 8, CDK2, cyclin A, cyclin B1, cyclin D3, cyclin E1, phospho-JNK (Thr183/Tyr195), phospho-GSK3β, HDAC2, and HDAC3. Antibodies against total mTOR, total RAF, TET2, and secondary antibodies HRP-conjugated donkey anti-rabbit and HRP-conjugated goat anti-mouse were obtained from Santa Cruz Biotechnology (Santa Cruz, CA). Antibodies were diluted in 5% w/v skim milk or 5% w/v BSA in pH 7.6 TTBS (20 mM Tris-HCl, 200 mM NaCl, 0.05% Tween-20), as per the manufacturer's instructions.

2.7 Flow cytometry

Flow cytometry experiments were performed on a FACSCalibur flow cytometer with Becton Dickinson (BD) CellQuest™ software (version 3.3; BD Biosciences, Mississauga, ON). Data analysis was performed using FCS Express software (version 3.0; De Novo Software, Thornhill, ON). For each sample, a total count of 10,000 cells were acquired.

In the case of the cell death and mitochondrial membrane stability assays, the cell count included both live and death cells, while in Oregon Green and cell cycle analysis only counted live cells. Cell cycle analysis was run with a maximum acquisition rate of 50 cells per second to ensure single cell acquisition.

2.8 Morphological Changes

AF4-induced morphological changes in MDA-MB-231, MDA-MB-468, and MCF10A cells were investigated after 24 h of treatment. Cells were plated in 6-well plates and allowed to adhere for 24 h prior to AF4 treatment. Following treatment, pictures of cells were taken with a Nikon Eclipse TS 100 phase contrast microscope at 200 x magnification.

2.9 MTT Assay

An MTT colorimetric assay was used to determine the effects of AF4 and quercetin treatment on cell growth at various concentrations and at 24-, 48-, and 72-h timepoints. MTT, a yellow tetrazolium salt, is converted in cells by mitochondrial succinate dehydrogenase to insoluble purple formazan crystals. Differences in viable cell number results in a respective change the amount of formazan crystals produced. Following formazan crystal solubilisation in DMSO, formazan levels can be quantitated by colorimetric analysis (Mosmann, 1983). Cells were plated in quadruplicate on 96-well flat-bottomed plates and allowed to adhere for 24 h prior to treatment. Cells were then treated with AF4 or control and cultured for the desired time. Following culture, MTT was added to each well to a final concentration of 0.5 μg/ml then plates were incubated

for 2 h at 37°C to allow the formazan crystals to form. After incubation, the cells were centrifuged at 1400 × g for 5 min and the supernatant was discarded. 100 µl of DMSO was then added to each well and shaken on a plate shaker to solubilize the formazan crystals. Sample absorbance at 570 nm was determined on an Expert 96 microplate reader (Biochrom ASYS, Cambridge, UK). Treatment results were compared to the medium control using the following equation: ((experimental reading - experimental blank)/ (medium control reading – medium control blank)) × 100%.

2.10 Acid Phosphatase Assay

An acid phosphatase assay was used to confirm MTT assay results. The acid phosphatase assay utilizes the activity of the cytosolic enzyme acid phosphatase to determine viable cell number. Viable cells utilize acid phosphatase to hydrolyze the substrate p-nitrophenyl phosphatase, which turns yellow in the presence of a strong base (Yang et al., 1996). Cells were plated in quadruplicate on 96-well flat-bottomed plates and allowed to adhere for 24 h. Cells were then treated with AF4, quercetin, or control for 24, 48, and 72 h to a final volume of 100 µl per well. Following culture, cell supernatants were removed, and cells were washed with 100 µl of PBS. To each well, 50 µl of fresh PBS and 50 µl of acid phosphatase buffer (0.2 M sodium acetate, pH 5.5; 0.1% Triton X-100; 4 mg/mL phosphatase substrate) was then added. Plates were then incubated in low light conditions for an additional 90 min at 37°C. Following incubation, 10 µl of 1 M NaOH was added to each well to stop the reaction and induce colour change. The plates were then shaken, and the absorbance of each well was read at 405 nm on an Expert 96 microplate reader (Biochrom ASYS, Cambridge, UK). The absorbance values of treatment conditions were

compared to the medium control using the following equation: ((experimental reading - experimental blank)/ (medium control reading – medium control blank)) × 100%.

2.11 Trypan Blue Viability Assay

AF4-induced changes in cell viability were also determined by trypan blue staining. Trypan blue, a membrane impermeable dye, is excluded from viable cells but can enter and stain cells with compromised membrane integrity (Strober Warren, 2001). Cells were seeded in 24-well plates and left to adhere for 24 h. Cells were then treated with AF4 or its vehicle and cultured for 24, 48, or 72 h. Following culture, supernatants were collected, cells were detached with TrypLE, and then recombined with their respective supernatants. In the case of MDA-MB-231 and MDA-MB-468 cells, cells were centrifuged at 500x g for 5 min. Cell supernatant was discarded and cells were resuspended in 2 mL of cDMEM. Alternatively, MCF10A cells were centrifuged at 300 x g for 5 min and resuspended in 2 mL of supplemented DMEM/F12. Cells suspensions were then combined in a 1:1 ratio with 0.4% trypan blue dye and cell counts were performed by microscopy using a hemocytometer (Hausser Scientific, Horsham, PA). AF4-induced changes in viable cell numberare shown relative to the untreated control.

2.12 7-AAD Assay

AF4-induced breast cancer cell death was determined using 7-AAD, a cell membrane impermeable fluorescent dye that can be detected by flow cytometry. Dye is excluded from viable cells but can enter and bind to the GC regions of DNA in cells with compromised membrane integrity (Zembruski et al., 2012).. Cells were plated in 6-well

plates and allowed to adhere for 24 h prior to treatment with AF4 or its control for 24, 48, and 72 h. Cells were then harvested and stained with 5 µl of 7-AAD solution for 5 minutes and changes in 7-AAD fluorescence were determined by flow cytometry.

2.13 Annexin-V-488/PI Assay

An annexin-V-488/propidium iodide (PI) assay was used to determine whether AF4 induced cell death by apoptosis and/or necrosis. Annexin-V-488 is cell impermeable and has a high affinity for phosphotidylserine, a membrane phospholipid that is normally present only in the inner leaflet of healthy cells cytoplasmic membranes. During apoptosis, phosphotidylserine is also present in the outer leaflet of the cell membrane as a result of disruption during apoptosis (Meers and Mealy, 1993). Meanwhile, PI is a membrane impermeable dye that intercalates into DNA. Therefore, cells stained with only Annexin-V-488 represent cells in the early stages of apoptosis, while cells stained with both Annexin-V-488 and PI represent cells in the late stages of apoptosis or necrosis. Cells that are non-viable and have permeable membranes, such as during the later stages of apoptosis or necrosis, can be stained with PI. Cells were plated in 6-well plates and allowed to adhere for 24h. Cells were then treated with AF4 and cultured for 24, 48, or 72 h. Following culture, cells were harvested and stained with annexin-V-488 prepared according to the manufacturer's protocol (Roche Diagnostics, Laval, QC; (Rode, Eisel et al. 2009)) and PI (1 µg/ml) in staining buffer (10 mM HEPES, 10 mM NaCl, and 5 mM CaCl2) for 15 min at room temperature and analysed by flow cytometry using the FL1 and FL2 channels.

2.13.1 ROS involvement in AF4-induced cancer cell death

To determine ROS involvement in AF4-induced cell death, MDA-MB-231 and MDA-MB 468 cells were pre-treated with the antioxidant N-acetylcysteine (NAC) for 90 min prior to 24 h AF4 or control treatment. 20 mM of NAC in cDMEM was used to pre-treat the cells, AF4 treatments were then added, reducing the concentration of NAC to 10 mM. Cells were then cultured for an addition 24 h, harvested, and stained with Annexin-V-488/PI and analyzed as described above.

2.13.2 Effect of decreased iron on AF4-induced cancer cell death

To investigate the importance of iron in AF4-induced cancer cell death, cells were pre-treated with the iron chelator deferiprone (DFE) for 90 min prior to 24 h AF4 treatment. 25 μg/mL of DFE in cDMEM was used to pre-treat the cells, AF4 or control treatments were then added reducing the final concentration of DFE to 12.5 μg/mL. Cells were then cultured for an additional 24 h, harvested, and stained with Annexin 488/PI and analyzed as described above.

2.14 DIOC6 staining for Mitochondrial Membrane Stability

To determine if AF4 treatment affects mitochondrial membrane stability, breast cancer cells were stained with 3,3'-dihexyloxacarbocyanine iodide (DiOC6) following AF4 or control treatment. DiOC6 is a cell-permeable dye that is selective for the mitochondrial membrane at low concentrations. As such, a decrease in cell fluorescence signifies a loss in mitochondrial membrane stability. Following culture, cells and their culture

supernatants were harvested and incubated with 40 nM DiOC6 in cDMEM for 15 min at room temperature. The samples were then analyzed with flow cytometry using the FL1.

2.14.1 ROS involvement in AF4-induced Changes in Mitochondrial Membrane Stability.

To determine if ROS play a role in AF4-induced changes in mitochondrial membrane stability, breast cancer cells were pre-treated with NAC. 20 mM of NAC in cDMEM was used to pre-treat the cells for 90 min, after which an equal volume of AF4 treatments or controls was added, reducing the final concentration of NAC to 10 mM. Samples were then harvested, stained DiOC6 and analyzed as described above.

2.14.2 Effect of decreased iron on AF4-induced Changes in Mitochondrial Membrane Stability.

To determine whether iron is involved in AF4-induced changes in mitochondrial membrane stability, cells were pre-treated with the 25 µg/mL DFE for 90 min. Following pre-treatment, AF4 or control treatments were added, reducing the DFE concentration of to 12.5 µg/mL. Samples were then harvested, stained with DiOC6, and analyzed as described above.

2.15 Amplex Red® Assay

The Amplex Red® assay was performed to further investigate the type of ROS produced by AF4 treatment. Cells were seeded in 96-well plates and allowed to adhere for 24 h prior to AF4 or control treatment. 100 µL of AF4 treatment made at 2x in phenol red free

cDMEM and 100 uL of staining solution (25 μM Amplex Red®, 0.005 U/mL HRP in phenol red free cDMEM) was added to each well and incubated at 37°C. Plates were incubated for 2 or 24 h following which the absorbance values of each well were determined at 570 nm on an Expert 96 microplate reader (Biochrom ASYS, Cambridge, UK). Increased fluorescence indicated the presence of peroxide radicals.

2.16 DCFDA Assay

To confirm the findings of the Amplex Red® assay as well as investigate the ability of AF4 to produce other reactive oxygen species in addition to peroxide radicals, a 5-(and-6)-chloromethyl-2',7'-dichlorodihydrofluorescein diacetate, acetyl ester (CM-H2DCFDA, or DCFDA) assay was performed. Cells were plated in a 96-well plate and allowed to adhere for 24 h. The cell supernatants were then remove and each well was washed with warm PBS then stained with 100 μL of staining solution containing 5 μM of DCFDA in serum and phenol-red free DMEM. For unstained controls, only serum and phenol-red free DMEM was added. The plates were then incubated for 30 min at 37°C in 10% CO2. After incubation, the stain was removed, and wells were washed with 1 mL of warm 1X PBS. AF4 and control treatments were added in 1% HI FBS and phenol-red free DMEM and cells were cultured for 2 or 24 h at 37°C. Fluorescence at 529 nm was measured with a Spectramax M2 microplate reader (Molecular Devices, San Jose, US).

2.17 Oregon Green 488® Proliferation Assay

The Oregon Green 488® cell proliferation assay was used to determine the effect of AF4 on cancer cell proliferation. Oregon Green 488® is a fluorescent dye that binds to

proteins in the cell and cell membrane. When these cells undergo cell division, the dye is equally distributed in both daughter cells, decreasing the dye in each cell by half. This decrease in fluorescence can then be used to calculate the number of cell divisions a cell has undergone (Wallace et al., 2008). Prior to seeding, flasks of MDA-MB-231 and MDA-MB 468 cells were serum starved for 20 h to synchronize the cell cycles in each population. The cells were then seeded into 6-well plates and allowed to adhere for 24 h. After the cells had adhered, they were washed with 2 mL of warm PBS. Oregon Green 488® dye in serum-free cDMEM was then added to a final concentration of 1.25 μM Oregon Green 488® and incubated at 37°C for 45 min. Following incubation, the dye was removed, cells were washed three times with 2 mL of warm cDMEM and allowed to recover for 2 h in 2 mL of warm cDMEM at 37°C. Subsequently, the non-proliferative cell control was harvested, fixed with 1% paraformaldehyde in PBS, and stored at 4°C until use. Remaining wells were then treated with control or subcytotoxic concentrations of AF4 for 72 h. Following culture, cells were harvested, resuspended in 0.5 mL PBS and analyzed by flow cytometry using the FL1 channel. The fluorescence of control and AF4-treated cells was compared to that of the non-proliferative control and the number of cells divisions (n) was calculated as follows: $MCF_{baseline} = (2^n)(MCF_{sample})$; where "n" stands for the number of cell divisions and "MCF" stands for mean channel fluorescence.

2.18 Cell Cycle Analysis

The effect of AF4 on cell cycle progression was investigated by cell cycle analysis. This assay utilizes PI to bind to the nucleic acids of cells to determine the amounts of cellular DNA content. This can then be used to differentiate between cells at different stages of

the cell cycle, as cells in G_0/G_1 stage possess 1 copy of DNA, 2 copies in the G_2 stage, and an intermediate amount in the S stage (Pozarowski and Darzynkiewicz, 2004). Breast cancer cells were serum-starved for 20 h to synchronize the cell cycles of the cells at G_0. The cells were then plated, allowed to adhere for 24h, and treated with AF4 for 72 h. Following treatment, cells were harvested and washed with 5 ml of ice cold PBS. The cells were then resuspended in 500 µL of ice cold PBS, and ice-cold ethanol (70%) was slowly added to the cells while vortexing to a final volume of 5 mL. The cells were then stored at -20°C for a minimum of 24 h. After storage, the cells were washed with 5 ml of PBS, centrifuged at 500 x g, and resuspended in PI staining solution containing 0.02 mg/mL PI, 0.1% v/v Triton X-100, and 0.2 mg/ml DNase-free RNase A in PBS. The cells were then incubated for 30 min at room temperature in the dark. Cellular fluorescence was determined by flow cytometry on the FL2 channel. Cellular events were limited to 50 cells per second due to the likelihood of cell doublets, which could confound the results. The data was analyzed using ModFitLT V2.0 software (Becton Dickson, CA) to determine percentage of cells in each phase of the cell cycle.

2.19 Western Blotting

2.19.1 Preparation of Total Cell Lysates

To determine if AF4 could affect the levels of proteins involved in a variety of cellular processes, western blotting was performed. Cell lysates were prepared for western blotting by first seeding cells into T75 flasks, with cell density being dependant on the timepoint as described above in section 2.3. Cells were then treated with AF4 and cultured for the desired time. Cells and supernatant were then harvested, washed with 1

mL of ice-cold PBS and centrifuged at 500 x g for 5 min at 4°C. The supernatants were then removed and the pellet was resuspended in 30 µL RIPA lysis buffer solution (0.1% Nonidet P-40; 0.5% sodium deoxycholate; 0.1% sodium dodecylsulphate (SDS); 20 mM Tris-HCl; 150 mM sodium chloride (NaCl); 1mM ethylenediaminetetraacetic acid (EDTA), 1mM ethylene glycol tetraacetic acid (EGTA) pH 7.5 with 5 µg/mL pepstatin, 10 µg/mL aprotinin, 5 µg/mL leupeptin, 1mM phenylmethyl sulfonyl fluoride (PMSF); 100 µM sodium orthovanadate (Na3VO4), 1mM dithiothreitol (DTT), 10 mM sodium fluoride (NaF) and 10 µM phenylarsine oxide (PAO)). Cells were lysed on ice for 15 min then centrifuged at 14,000 x g for 10 min at 4°C. Cell lysate was then removed and stored at -80°C.

2.19.2 Protein Quantification

A Bradford assay was used to determine the total protein concentrations of cellular lysates. Bovine serum albumin (BSA) protein standard or 2.5 µL of each lysate was diluted in 1 mL of diluted Bio-Rad protein assay dye (1:5 with dH2O). BSA was used to generate a protein standard curve with concentrations ranging from 0.5 µg/mL to 30 µg/mL. The standards and samples were plated in triplicate onto a 96-well flat bottom plate, and the absorbance values of each well was measured at 570 nm using an Expert 96 microplate reader. The concentration of each sample was then calculated using the standard curve. Additional lysis buffer was used to equalise protein concentrations for different treatments. 3X SDS-PAGE buffer (6% w/v SDS, 30% v/v glycerol, 15% v/v β-mercaptoethanol, 0.01% v/v bromophenol blue, and 200 mM Tris-HCl [pH 6.8]), was

then added and samples were heated at 95 °C for 5 minutes to denature the proteins. Samples were then stored at -80 °C.

2.19.3 Western Blot Analysis

Equal amounts of protein (10-40 μg) were loaded into the wells of an SDS-polyacrylamide gel (10, 12, or 15% polyacrylamide). The amount of protein added was dependant on an estimate of cellular protein levels, while the polyacrylamide percentage was selected based on the size of the proteins of interest. Proteins were resolved by electrophoresis for 2 h at 100 V in SDS running buffer (0.1% w/v SDS, 200 mM glycine, and 200 mM Tris-HCl [pH 8.3]). The proteins present within the gel were then transferred to a nitrocellulose membrane using an iBlot™ dry transfer system (Invitrogen, Burlington, ON) according to the manufacturer's protocol. Following transfer, the membrane was blocked in 5% skim milk powder (w/v) in Tris-buffered saline (200 mM Tris, 1.5 M NaCl (pH 7.6)) containing 0.05%Tween-20 (TTBS). In cases where phosphorylated proteins were being probed, membranes were blocked with 5% BSA (w/v) in TTBS. After blocking, the membrane was rinsed with TTBS to remove excess blocking solution, and then incubated overnight at 4°C with the primary antibody of interest (antibodies were typically diluted 1:1000 v/v in 5% skim milk (w/v) or BSA, depending on manufacturer's instructions). Following antibody staining, membranes were repeatedly washed by TTBS (6x 5 min). Membranes were then stained with the appropriate HRP-conjugated secondary antibody (1:5000 v/v in 5% skim milk (w/v) or BSA, depending on manufacturer's instructions) for 1 h at room temperature. Protein bands were detected after using Luminata™ Forte Western HRP substrate in a Bio-Rad

ChemiDoc Imaging System (Bio-Rad Laboratories Inc., Hercules, CA). The blots were then probed for β-actin and detected as described above. Protein levels were determined using densitometry with the Image Lab software (version 5.2, Bio-Rad, Hercules, CA). β-actin levels were used to control for differences in protein loading.

2.20 Statistical Analysis

Statistical analysis was conducted using GraphPad Prism 5 (GraphPad Software Inc., San Diego, CA). Statistical comparisons were performed using Student's t-test when comparing two groups, or by a one-way analysis of variance (ANOVA) when comparing multiple groups. With ANOVA, the Tukey-Kramer multiple comparisons post-test was used to compare all groups with each other, while the Bonferroni post-test was used to compare select groups. For all tests, $p < 0.05$ was considered statistically significant and was denoted by *. In cases where the p-value is ≤ 0.01, the difference was denoted by **; and in cases where the p-value is ≤ 0.001 the difference was denoted by ***.

CHAPTER 3: RESULTS

3.1 AF4 Induces Morphological Changes in MDA-MB 231 and MDA-MB-468 Triple-Negative Breast Cancer Cells but Not MCF10A Epithelial Cells.

The effects of AF4 on the appearance of MDA-MB-231 and MDA-MB-468 triple-negative breast cancer cells and MCF10A epithelial cells were first investigated to see if any differences were apparent between cancerous and healthy cells after treatment. Both triple-negative breast cancer cell lines displayed changes in morphology induced by AF4 (Figure 5). This change was the most prominent in the MDA-MB-231 cells, which lost their characteristic elongated shape and became rounder. As MDA-MB-468 cells are round to begin with, the effects of AF4 on these cells were less apparent. However, after AF4 treatment the cells lost their characteristic cobblestone pattern, became more spread out, and appeared slightly smaller in size. The MCF10A cells, on the other hand, did not seem to be affected by AF4 treatment. These cells appeared elongated without AF4 treatment, similar to MDA-MB-231 cells, but did not display any changes to morphology after AF4 treatment.

3.2 AF4 Inhibits the Growth of Breast Cancer Cell Lines in a Dose- and Time-Dependent Manner and is Less Potent but More Selective than Quercetin

An MTT assay was used to determine if AF4 can inhibit the growth of breast cancer cells better than quercetin, the aglycone of the major flavonoid components of AF4, as well as to determine the relative toxicity of AF4 and quercetin to healthy cells. Both AF4 and quercetin inhibited the growth of multiple breast cancer cell lines, including human triple-negative MDA-MB-231 cells (Figure 6A), MDA-MB-468 cells (Figure 6B), estrogen and

progesterone receptor positive MCF-7 cells (Figure 6C), HER2-overexpressing SKBR3 cellss (Figure 6D) and the MCF10A healthy epithelial cell line (Figure 6E). Murine 4T1 triple-negative mammary carcinoma cells (Figure 6F) and HC11 normal epithelial cells (Figure 6G) were also compared in terms of response to AF4. In both cancerous and non-cancerous human cell lines, AF4 exerted a dose-dependent but not a time-dependent effect. The human cancer cell lines also did not vary much in terms of AF4 concentrations needed to elicit a significant decrease in cell growth. For these breast cancer cell lines, AF4 produced a significant reduction in cell growth at 100 µg/mL after 24 h of treatment. In comparison, MCF10A cells only displayed a significant reduction in cell growth at 100 µg/mL AF4 after 72 h of treatment. Quercetin displayed both time and dose-dependent growth inhibition in the human cell lines. Differences between the AF4 concentration needed to produce a response in breast cancer cell lines and MCF10A cells were also not as obvious with quercetin. Quercetin also produced significant reductions in growth at lower concentrations than AF4.

As for the murine cell lines, although the MCF10A human epithelial cell line seemed to be more refractory to AF4 in comparison to their cancerous counterparts, the HC1 mouse epithelial cell line and 4T1 mouse triple-negative mammary carcinoma cells had a similar response to AF4, which produced a time-dependent inhibitory effect on these cells. The comparison of the effects of quercetin versus AF4 on these murine cell lines also showed that there is not much of a difference between the two compounds. It should be noted, however, that both quercetin and AF4 react with the MTT reagent in the absence of cells to produce significant increases in absorbance at higher concentrations (Figure 7), which is a potential confounding factor.

Given the challenges of using MTT assays to determine the effects of AF4 and quercetin on cell growth, the acid phosphatase assay was used to confirm the MTT assay results using the same cell lines and treatment conditions (Figure 8). Similar results were found in terms of concentrations of AF4 and quercetin required to cause a significant decrease in cell growth as well as a time-dependent effect. Human breast cancer cells treated with AF4 displayed significant decreases in cell growth with concentrations as low as 50 μg/ml of AF4, while MCF10A cells required 100 μg/ml of AF4 and 72 h of treatment to show a significant inhibitory effect. In many cases, time-dependent inhibitory effects of AF4 were also seen. Once again, quercetin inhibited the growth of human cells at a lower concentration than AF4 and produced time-dependent inhibition in more cases than AF4. The murine cell lines also showed similar responses to AF4 and quercetin, with similar growth inhibitory patterns observed between the 4T1 and HC11 cell lines.

To determine if AF4 or quercetin was more selective for cancerous or healthy cells, the data obtained from the MTT and acid phosphatase assays were compared (Figure 9). Breast cancer cells treated with 100 μg/mL of AF4 for 72 h in the MTT assay showed a significant decrease in growth compared to the MCF10A cells (Figure 9A). However, quercetin at the same dose and time point showed no differences between growth inhibition of the healthy and cancerous cell lines. These differences were even more apparent when comparing the effects of AF4 and quercetin directly from the MTT (Figure 9C) and acid phosphatase assays (Figure 9D). At lower doses of AF4 or quercetin, the differences in cell growth between AF4 and quercetin increased with concentration

until around 50% reduction in cell growth. After this point, the difference between AF4 and quercetin decreases until about 90% reductions in cell growth.

3.3 AF4 Induces Dose- and Time-Dependent Cell Death in Triple-Negative Breast Cancer Cells

MTT and acid phosphatase assays test for relative cell number after treatment, but these assays do not allow for the determination of whether treated cells are being reduced in number as a result of increased cytotoxicity or decreased cell proliferation. AF4-induced cytotoxicity was first examined using the trypan blue assay to differentiate between dead and live cells (Figure 10). The trypan blue assay showed that AF4 and quercetin were both cytotoxic to MDA-MB-231 cells (Figure 10A) and MDA-MB-468 cells (Figure 10B). Similar to the cell growth inhibition assays, quercetin was more potent than AF4, and both AF4 and quercetin exerted dose- and time-dependent responses cytotoxic action. When breast cancer cells were compared to MCF10A cells, once again AF4 was more selective for cancer cells than quercetin, as the minimum dose of AF4 required to kill the triple-negative breast cancer cell lines did not kill the MCF10A cells even after 72 h of treatment. This was not the case for quercetin.

To confirm these findings, FACs analysis was utilized. Since AF4 and quercetin show colour in solution, the inherent fluorescence of each compound was tested in each channel by briefly exposing cells to AF4 or quercetin (Figure 11). Both compounds seemed to fluoresce, however, quercetin was much more fluorescent than AF4 in the FL1 and FL2 channels. Therefore, quercetin was not used for further experimentation as this fluorescence would confound the results.

Flow cytometric analysis of 7-AAD stained cells was used to confirm the cytotoxic effect of AF4 (Figure 12). MDA-MB-231 cells treated with AF4 displayed significant cell death after treatment with 100 µg/mL of AF4 (Figure 12A). Meanwhile, MDA-MB-468 cells displayed significant cell death following treatment with 50 µg/mL of treatment (Figure 12B). In both breast cancer cell lines, a time-dependent response was seen with 100 µg/mL of AF4.

To further confirm these findings, as well as to determine the cell death pathway by which AF4 killed breast cancer cells, flow cytometric analysis of Annexin-V 488/PI-stained cells was performed. This assay allows for the differentiation of live cells, cells in the early stages of apoptosis, and cells in the late stages of apoptosis or necrosis (Figure 13). MDA-MB-231 cells (Figure 13A) and MDA-MB-468 cells (Figure 13B) displayed significant cell death after treatment with 50 µg/mL of AF4, although there were no apparent time-dependent effects. In addition, there were no clear trends in terms of the fraction of cells entering the early stages of apoptosis versus those in late stages of apoptosis or necrosis. When these findings were compared to the effect of AF4 on MCF10A cells (Figure 13C), once again MCF10A cells were more resistant to AF4. For the MCF10A cells, cell death as determined by Annexin-V 488/PI staining with the subtraction of cell death from the medium control from experimental conditions can be found in Supplementary Figure 1.

3.4 AF4-Induced Cell Death Is ROS-Dependent but Not Dependent on Caspase or PARP1 Cleavage

To determine the mechanism by which AF4 induces cell death in breast cancer cells, the ability of AF4 to cause the production of peroxide radicals was investigated

with the Amplex Red assay (Figure 14). AF4 at 100 μg/mL induced production of ROS in both MDA-MB-231 cells (Figure 14A) and MDA-MB-468 cells (Figure 14B). No significant time-dependent effects of AF4 on ROS production were seen. In addition, it should be noted that AF4 caused significant amounts of ROS to accumulate in cell-free medium (Figure 14C). To confirm that AF4 was in fact causing intracellular ROS accumulation, a DCFDA assay was used with similar results (Figure 15). AF4 only caused significant production of ROS after 100 μg/mL of treatment, and there was no significant time-dependent effect.

To see if the ROS production caused by AF4 had a significant impact on AF4-induced cytotoxicity, Annexin-V 488/PI staining of cells was performed following pre-treatment with the antioxidant NAC followed by AF4 treatment (Figure 16). In both MDA-MB-231 cells and MDA-MB-468 cells, NAC significantly decreased the number of dead cells in cultures treated with 100 μg/mL of AF4. To determine if the ROS production caused by AF4 resulted in ferroptosis, Annexin-V 488/PI staining of breast cancer cells was performed following AF4 treatment with or without the iron chelator DFE (Figure 17). In contrast to the findings with NAC pre-treatment, DFE pre-treatment exacerbated AF4-induced cell death in both MDA-MB-231 cells (Figure 17A) and MDA-MB-468 cells (Figure 17B).

$DIOC_6$ staining of MDA-MB-231 and MDA-MB-468 cells was performed to determine whether mitochondrial membrane integrity was affected by treatment with AF4 with or without NAC or DFE pre-treatment. AF4 caused damage to the mitochondrial membrane at a dose of 50 μg/mL, and this effect was ROS-dependent and iron-independent. ROS-dependence of the effect of mitochondria was consistent with the

ROS dependent cytotoxicity findings seen with Annexin-V 488/PI stained cells. However, the lack of an effect of iron chelation was not consistent with the observation that iron chelation exacerbated AF4-mediated cytotoxicity.

Given the role that ROS plays in AF4-mediated cytotoxic effects as well as the selectivity of AF4 towards cancer cells, MTT assays were used to compare the growth inhibitory effects of H_2O_2 on MDA-MB-231 cells, MDA-MB-468 cells, and MCF10A cells to determine if these cell lines responded differently to a high concentration of ROS (Figure 19). Under each treatment condition, there was a significant difference between growth inhibition of the triple-negative breast cancer cell lines versus the MCF10A cells, indicating that MCF10A cells were more resistant than breast cancer cells to ROS exposure.

Further investigation of the mechanism behind AF4-mediated cytotoxicity was carried out by western blotting. Neither caspase nor PARP1 cleavage was required for AF4-induced cell death (Figure 20). In both MDA-MB-231 and MDA-MB-468 triple-negative breast cancer cell lines, AF4 concentrations that caused significant cell death in these cell lines did not induce caspase 3, 7, 8, or PARP1 cleavage. To confirm AF4 did not affect the levels of housekeeping genes used for normalization of western blot data, the effect of AF4 on the levels of the proteins tubulin and GAPDH was determined (Figure 21). These western blots indicate that AF4 had no effect on β-actin, tubulin, or GAPDH levels.

3.5 AF4 Inhibits the Proliferation of Triple-Negative Breast Cancer Cells Via G_1 Cell Cycle Arrest

The ability of AF4 to inhibit breast cancer cell proliferation was examined with the Oregon Green flow cytometric assay. A dose-dependent increase in the fluorescence of AF4 treated cells, which translates into fewer cell divisions was observed (Figure 22). This inhibitory effect on cell proliferation was only significant at 40 µg/mL of AF4 in MDA-MB-231 cells (Figure 22A) and starting from 30 µg/mL of AF4 in MDA-MB-468 cells (Figure 22B). Cell cycle analysis was performed to determine the mechanism by which this inhibition of breast cancer cell proliferation was occurring (Figure 23). Breast cancer cells accumulated in the G_1 stage of the cell cycle after AF4 treatment, in a dose-dependent manner. Similar to the Oregon Green staining assay, a significant effect was only found after treatment with 40 µg/mL of AF4. To confirm the observations with cell cycle analysis, western blotting was performed to determine the effect of AF4 on the protein levels of cyclins and CDKs involved in cell cycle progression (Figure 24). In both MDA-MB-231 and MDA-MB-468 cell lines, cyclin D3, CDK4, and CDK6 levels were downregulated after treatment with 40 µg/mL of AF4, however, no effects were found at lower doses. Depending on the cell line, these effects occurred at different time-points. The levels of the other cyclins and CDKs were not affected by AF4.

3.6 AF4 Affects Signalling Through the PI3K/AKT and ERK Pathways

Western blotting was used to investigate the mechanism behind AF4-mediated decreases in the proliferation of MDA-MB-231 cells and MDA-MB-468 cells. Both the PI3K/AKT (Figure 25) and ERK/MAPK (Figure 26) signalling pathways were investigated. In both

breast cancer cell lines, treatment with AF4 only affected the phosphorylated Akt as well and PTEN. AF4 treatment decreased Akt phosphorylation in MDA-MB-231 cells (Figure 25A) and MDA-MB-468 cells (Figure 25B), and this effect was reversed with the pre-treatment of cells with NAC. In addition, PTEN phosphorylation was decreased in both breast cancer cell lines following AF4 treatment, and this effect was also reversed with NAC pre-treatment.

The effect of AF4 on the ERK/MAPK pathway depended on the cell line. In MDA-MB-231 cells, AF4 treatment increased the phosphorylation of ERK 1 and 2, which was partially reversed with NAC pre-treatment (Figure 26A). However, in MDA-MB-468 cells, AF4 decreased the phosphorylation of ERK 1 and 2 (Figure 26B). With the MDA-MB-468 cells, it seemed that even with NAC pre-treatment ERK phosphorylation levels did not return to baseline. No effects of AF4 on RAF phosphorylation were seen with either breast cancer cell line. Western blots were also performed to investigate possible effects of AF4 on proteins upstream and downstream of Akt (PP2A, p38, JNK, GSK3β, and β-catenin) which are involved in ROS signalling (Figure 27). However, none of these proteins were affected by AF4 treatment.

3.7 AF4 Induces Changes in Protein Levels of Epigenetic Enzymes

Western blot analysis of enzymes involved in epigenetic modulation showed that AF4 altered the levels of these enzymes in MDA-MB-231 and MDA-MB-468 triple-negative breast cancer cell lines, and in the MCF10A epithelial cell line (Figure 28). For the most part, these effects of AF4 were not time-dependent and were consistent across all cell lines. DNMT1 levels were inhibited by AF4 while DNMT3A was upregulated following

exposure to AF4 at concentrations as low as 20 μg/mL. No effects of AF4 on DNMT3B were observed. Protein levels of the DNA demethylation enzyme TET2 were increased with AF4 treatment. Significant inhibition of HDAC2 protein levels in both breast cancer cell lines as well as MCF10A cells were seen after only 20 μg/mL of AF4 treatment. The only other HDACs significantly affected by AF4 treatment were HDAC1 after 72 h of treatment in MDA-MB-231 cells (Figure 28A) and HDAC3 after 48 h of treatment in MCF10A cells (Figure 28C). As for the HATs, only GCN5 was inhibited by AF4 treatment at 40 μg/mL of AF4 treatment. Lastly, the acetylation of H3K27 was inhibited by AF4 treatment, while there was no effect on H3K9 acetylation.

CHAPTER 4: DICUSSION

4.1 AF4 Induces Morphological Changes in Triple-Negative Breast Cancer Cells but Not Healthy Epithelial Cells

Both triple-negative cell lines exhibited morphological changes after AF4 treatment. In contrast, the healthy cell line was left unaffected. Morphological changes in cells are a result of biochemical changes, such as when apoptosis is triggered (Saraste and Pulkki, 2000). As such, the lack of morphological change in healthy cells upon AF4 exposure shows that AF4 may be selective towards cancer cells. However, AF4 has shown to have effects on healthy cells at higher doses. Although 50 μg/mL of AF4 may not produce cytotoxic effects in MCF10A cells to the point where morphological changes can be seen after 24 h, at different time points and concentrations of AF4 there would most likely be similar effects as seen with the triple-negative breast cancer cell lines in the treatment conditions used here.

4.2 AF4 Inhibits the Growth of Triple-Negative Breast Cancer Cells More Selectively Than Quercetin

From MTT and acid phosphatase assays, it seems that AF4 is less potent than quercetin in terms of breast cancer cell growth inhibition. In every cell line tested, quercetin shoed significant growth inhibition at a lower concentration than AF4. Note, however, that concentrations used in this study were based on weight per unit volume, rather than moles per unit volume. This was done because it was not possible to determine the molarity of AF4 as it contains multiple components. Therefore, quercetin is only more potent than AF4 in this regard. Moreover, potency does not necessarily

correlate with efficacy. Both AF4 and quercetin killed more than 90% of cancer cells at the highest concentration and longest time of exposure, suggesting that AF4 and quercetin are comparable in efficacy at least when comparing growth inhibitory effects. The fact that AF4 is composed of multiple phytochemicals may affect its potency. Although the components of AF4 may work together to inhibit the growth of the breast cancer cells, the individual components may affect different pathways, and thus may not be capable of producing any significant changes within these pathways until a certain concentration is reached.

Although the acid phosphatase assay suggested that AF4 inhibited the growth of cancer cells in a time-dependent manner, the MTT assay suggested otherwise. The lack of a time-dependent response seen with the MTT assay could be due to AF4 reacting with MTT and increasing the absorbance values obtained. Although cell-free controls were put in place to allow for the subtraction of the absorbance of the cell-free control from the treatment conditions, absorbance values are not linear as suggested by the Beer-Lambert law at higher absorbance values (Reule, 1976). Another possibility is that AF4 either degrades more easily than quercetin or is metabolized more easily. However, none of the data obtained from this study can support these claims. It is more likely that the trend observed was a result of the limitations of the MTT assay.

From MTT and acid phosphatase assays, it seems that AF4 was slightly selective more for human breast cancer cells relative to human epithelial cells, which supports the hypothesis that the multiple components of AF4 work together to allow for a more selective effect. In each assay, MCF10A cells required either more time or a higher dose of AF4 to produce growth inhibitory effects. This was not seen with quercetin, in which

the lowest concentration and exposure time that inhibited the growth of breast cancer cells also inhibited the growth of MCF10A cells. This suggests that AF4 could be used in humans at concentrations that would inhibit the growth of cancer cells while remaining relatively non-toxic to healthy cells. Interestingly, this difference was not observed in the murine cell lines. Although the triple-negative 4T1 mouse mammary carcinoma cell line was much more sensitive to AF4 in comparison to the human breast cancer cell lines, the HC11 epithelial cells had a similar response to AF4. This suggests that AF4 may not be selective in murine cell lines and/or may be more potent in mice due to differences in cell physiology. One major difference observed between the human and murine cell lines was the doubling time. Murine cell lines had a much shorter doubling time in comparison to human cell lines, which may affect AF4 efficacy. Another possibility is related to the fact that these cells were seeded at lower numbers to avoid an overabundance of cells at the end of culture because murine cell lines have such a short doubling time. As a result, even though the concentrations of AF4 used were consistent across cell lines, the ratio of AF4 to cells was much higher for the murine cell lines, which means that each murine cell had many more units of AF4 to react with, and thus AF4 could overwhelm the cellular defenses present within HC11 cells. Lastly, only one healthy cell line was used for the comparison with human and murine mammary cancer cells. It is possible that other healthy cell lines might have had different sensitivity to AF4, whether or not it was the same cell type. As such, the selectivity of AF4 depends on whether AF4 can inhibit the growth of other healthy cell lines or not.

4.3 AF4 Induces ROS-Dependent Breast Cancer Cell Death Through an Unknown Mechanism

The ability of phytochemicals to kill cancer cells while remaining relatively non-toxic to healthy cells has been documented in a variety of cases (Cheng et al., 2010; Sudan and Rupasinghe, 2014). In this project, AF4 produced similar results, which seem to be at least partially due to the ability of AF4 to cause ROS production as NAC pre-treatment reduced cell death. Peroxide radicals were found to be produced by AF4 treated breast cancer cells, which could possibly be produced by the mitochondria upon AF4-induced damage to the mitochondria. It is also possible that H_2O_2produced by AF4 in cell-free cultures entered the cells to play a role in AF4-mediated cytotoxicity as was seen with myricetin in triple-negative breast cancer cells (Knickle et al., 2018). The production of H_2O_2 by AF4 in cell-free medium has been observed with other phytochemicals such as EGCG and quercetin, and is thought to be the product of polyphenol autooxidation due to the presence of bicarbonate in tissue culture media (Long et al., 2000; Odiatou et al., 2013). Although H_2O_2 is poorly reactive on its own, it can be converted to highly reactive hydroxide radicals via the Fenton reaction (Halliwell and Gutteridge, 1990). This suggests that AF4 may require the presence of bicarbonate to produce ROS-dependent cytotoxic effects. Given that human fluids such as blood utilize bicarbonate buffer systems, AF4 should be able to produce ROS in the human body to destroy cancer cells, albeit at the cost of exposing normal cells to ROS (Hasan, 2013). As triple-negative breast cancer cells were more susceptible to death after being treated with H_2O_2 than healthy epithelial cells, AF4 may be exploiting the increased capability of healthy cells to defend against ROS. The ability of AF4 to induce ROS also means that AF4 is acting as a

pro-oxidant rather than antioxidant at the doses given to the cells. Although the antioxidant capabilities of AF4 have not been tested, its components have been shown to possess antioxidant capabilities (Iacopini et al., 2008; Rice-Evans et al., 1996). Since some antioxidants at high doses are capable of causing ROS production (Lambert and Elias, 2010; Pan et al., 2008; Polyakov et al., 2001), the involvement of ROS in AF4-mediated cytotoxicity is not surprising. It is possible that the difference in ROS sensitivity between cancerous and non-cancerous cells is due to the aberrant expression of survival and proliferation genes in the cancer cells. While normal cells with dysregulated survival and proliferation signals would undergo apoptosis to avoid forming a cancer, cancer cell lines are capable of downregulating intracellular signals that would otherwise cause the cells to kill themselves. However, this does not mean that these cancer cells are able to completely overcome these signals. Studies have shown that treating cancer cells with antioxidants allows them to grow faster, which is likely due to the scavenging of mitochondrial ROS released by the cell in an attempt to undergo apoptosis (Jiang et al., 2017; Sayin et al., 2014). As such, doses of AF4 that can kill cancer cells, but not healthy epithelial cells, are likely just able to push these cancer cells over the edge in terms of pro-apoptotic and pro-survival signals. Meanwhile, healthy cells are able to compensate for increased ROS, and thus are not as affected. This may also explain why the less-aggressive hormone receptor positive cell line MCF-7 breast cancer cells seemed to be less sensitive to AF4 compared to the triple-negative breast cancer cell lines.

The involvement of ROS in AF4-mediated cytotoxicity also helps to explain why the cytotoxic effects of AF4 seem to be more dose-dependent than time-dependent. It is

possible that cellular levels of antioxidants are upregulated via various mechanisms in response to AF4 (Nguyen et al., 2009; Ray et al., 2012). Alternatively, it is possible that AF4 does not remain stable in culture for periods over 24 h under the conditions at which the cells were treated. An understanding of the stability of phytochemicals, and especially glycosylated phytochemicals, is lacking. Given their roles as both antioxidants and prooxidants, depending on the circumstances, it is likely that these compounds easily oxidize when exposed to air, such as during cell culture.

The importance of ROS in the AF4-mediated cytotoxic effects on breast cancer cells also brings up the question as to possible combination actions of the phytochemicals within AF4. As many of the components of AF4 are known to be antioxidants at low concentrations, the cytotoxic effects of these phytochemicals are likely due at least in part to their prooxidant activity at high doses. If all the components of AF4 work to produce ROS in triple-negative breast cancer cells, then they may not be targeting multiple pathways. However, given the data obtained, it is clear that the combination of phytochemicals in AF4 seemed to produce more selective effects when breast cancer cells were compared with healthy cell. Since components of AF4 have distinct properties that are not shared with the other components, such as the ability of EGCG to directly bind to DNMT1 (Lee et al., 2005), it is possible that smaller effects combine to produce the observed anti-cancer effects. However, it is also possible that the components of AF4 caused production of different types of ROS, which could then affect several different but related pathways that affect cell proliferation (Soheila et al., 2001; Thorpe et al., 2004).

Lastly, the ability of AF4 to induce ROS production raises concerns about its safety within the human body. It is possible that excessive amounts of AF4 in the human

body could induce oxidative stress in multiple systems, or at smaller doses affect processes such as immune signalling through it's production of ROS. Indeed, a study showed that AF4 reduced neuroinflammation in a mouse model of autoimmune encephalomyelitis, though this effect is likely due to AF4's antioxidant effects instead and/or ROS-independent immune suppressive effects (Warford et al., 2014). Although in this study AF4 seemed to produce beneficial effects via the reduction of inflammation, this may be an unwanted side effect in cancer patients given that the immune system plays a critical role in controlling cancer progression. Alternatively, since AF4 acts as both an antioxidant and pro-oxidant, AF4 may increase inflammation at doses that kill cancer cells. If AF4 is able to induce systemic inflammation *in vivo*, it could promote cancer development and progression as described by Hanahan and Weinberg (2011) or cause autoimmune diseases. These potential side-effects could be circumvented via localized treatments rather than systemic treatments, which may limit the use of AF4 to solid tumors that have not yet metastasized. Alternatively, delivery systems such as the use of nanoparticles that selectively bind to cancer cells to release the drug of interest directly into the cell could be used, as has been done with drugs such as doxorubicin (Shafei et al., 2017).

Currently, the mechanism by which AF4 induces cell death is not clear. Although the data obtained from Annexin-V 488/PI flow cytometry experiments confirmed that AF4 was cytotoxic to breast cancer cells, it is not clear which cell death pathways was being activated. Despite ROS-dependent cell death and ROS-dependent damage to the mitochondrial membranes of AF4-treated cells, investigation into the cleavage and activation of caspases revealed that no caspases were cleaved after exposure to

concentrations of AF4 that killed breast cancer cells. This, combined with the fact that no discernable PARP1 cleavage was observed, suggested that AF4 did not induce cell death via apoptosis. This was in contrast to the pro-apoptotic effect of AF4 on HepG2 liver cancer cells, in which caspase-3 was cleaved (Sudan and Rupasinghe, 2014).

The studies on AF4 with an iron chelator also ruled out ferroptosis, as AF4-induced mitochondrial damage was not iron-dependent. This was an interesting finding as the production of H_2O_2 in medium by AF4 should require iron to produce more reactive hydroxyl radicals in cells (Halliwell and Gutteridge, 1990). In addition, iron chelation with AF4 killed more cells than AF4 or iron chelation alone. This is not surprising, as iron chelation is known to kill cancer cells (Richardson, 2002). Although the dose of DFE used in these experiments was low enough that there was no significant effect when used alone the dosage used may have been sufficient to synergize with AF4 to induce increased cytotoxicity. It is interesting however, that there was no difference in mitochondrial membrane damage in cells treated with AF4 or AF4 with DFE. This may have been due to problems with the $DIOC_6$ assay, which showed three peaks rather than two, making it difficult to distinguish between cells that had intact mitochondria versus those with damaged mitochondria. It is currently unknown why three peaks were observed; however, ROS may play a role since NAC-pretreated breast cancer cells that were stained with $DIOC_6$ displayed two peaks whereas cells pre-treated with DFE for the most part did not. It may be that iron-chelation also exacerbates AF4-induced mitochondrial damage, given the synergistic effects seen in cytotoxicity.

No other data presented from project support the idea that AF4 can even induce mitochondrial membrane damage. Studies with other dyes that allow for the

differentiation of live and damaged mitochondria as well as western blotting for proteins normally sequestered within the mitochondria, such as cytochrome c or apoptosis inducing factor 1 (AIF) could be performed to refute an effect of AF4 on mitochondria (Candé et al., 2004; Ow et al., 2008).

One alternative cell death mechanism that could be induced by AF4 is necroptosis, which can be induced by ROS and could therefore be induced directly by ROS that accumulated in AF4-treated cells (Vandenabeele et al., 2010). This is supported by the fact that caspase 8, which is not activated by AF4, is an inhibitor of necroptosis (Yuan et al., 2016). Another possibility is that the large amounts of ROS that were introduced into the breast cancer cells damaged the cell faster than the cells could signal for apoptosis induction, which can occur with high doses of H_2O_2 (Saito et al., 2006). Since caspase and PARP1 cleavage was only investigated 24 h after AF4 treatment, it is hard to say whether or not this is the case. However, given that the dose of AF4 used to treat the cells killed a little less than half the cells whereas all cancer cells were killed after 72 h treatment, it is possible that AF4 is directly signalling for necroptosis rather than using this pathway as an alternative to apoptosis.

One other concern is that the concentration of AF4 may not have been sufficient to induce caspase activation. The concentration of AF4 that was selected for use was based on amounts that would induce some cell death after a longer period of exposure, however, it may be that a higher concentration of AF4 for a shorter amount of time would induce caspase cleavage. Nonetheless, the mechanism behind AF4-induced cell death needs to be further investigated.

4.4 AF4 Inhibits Cell Proliferation

Both MDA-MB-231 and MDA-MB-468 triple-negative breast cancer cells showed decreased proliferation after AF4 exposure, with MDA-MB-468 cells being most sensitive to this effect. The inhibition of cell proliferation was only statistically significant when higher concentrations of AF4 were used, though there was a trend to inhibition at even the lowest concentration of AF4. It is important to note that the increased fluorescence of AF4-treated cells in the Oregon Green assay could partially be due to AF4 itself rather than its effects since AF4 is inherently fluorescent. However, the results obtained from cell cycle analysis confirms the results from the Oregon Green assay since triple-negative breast cancer cells treated with AF4 were arrested at the G1 stage. Again, this effect was only significant when the highest concentrations of AF4 were used. This effect on breast cancer cells also differed from the effect seen in AF4-treated liver cancer cells, in which AF4 induced cell cycle arrest at the G_2/M phase (Sudan and Rupasinghe, 2014).

The results obtained from cell proliferation and cell cycle analyses were confirmed by western blotting for cell cycle proteins, which showed a decrease in the protein levels of cyclin D3, CDK4, and CDK6, all of which are involved in pushing the cell past the G1 stage (Satyanarayana and Kaldis, 2009). Although E cyclins and CDK2 are also involved in this process, AF4 did not seem to affect the levels of these proteins. These effects of AF4 on cell cycle proteins were seen in both MDA-MB-231 and MDA-MB-468 cell lines, albeit with some differences. The decreased protein levels of cyclin D3, CDK4, and CDK6 seemed to be affected by the length of AF4 exposure, since all three proteins did not display decreased protein levels at both 24 h and 48 h post-

treatment. In some cases, one of these three proteins were downregulated after 24 h of treatment, but not after 48 h, implying that there may be an attempt by the cell to counteract the anti-proliferation effects of AF4. As for the other cyclins and CDKs, the levels of these proteins by either cell line were not affected by AF4.Given that the concentrations at which AF4 had inhibitory effects on proliferation were close to the concentrations at which AF4 can induce cytotoxicity, it seems that AF4's main anti-cancer effect is its ability to kill these cancers.

Although AF4 is composed mostly of quercetin and quercetin glycosides, the mechanism by which AF4 induces cell cycle arrest differs from that of quercetin. While AF4 downregulates the protein levels of cyclin D3, CDK4, and CDK6 to induce G_1/M cell cycle arrest, quercetin induces G_2 cell cycle arrest in breast cancer cells and ovarian cancer cells (Priyadarsini et al., 2010; Rivera Rivera et al., 2016). Quercetin glycosides may have a different effect than their parent compound, although currently there is little evidence to suggest that quercetin glycosides have a different effect on the cell cycle. Other studies that investigated phytochemical combination treatments found similar results, in that the combined effect of multiple phytochemicals differs from that of different phytochemicals alone. In one study that used a combination of quercetin, resveratrol, and catechin at equimolar concentrations, it was found that this mixture induced G_1/M cell cycle arrest while quercetin alone induced G_2 arrest (Rivera Rivera et al., 2016). Thus, different effects of AF4 and quercetin on the cell cycle are likely due to the interaction of multiple phytochemicals.

ROS was likely involved in AF4-induced cell cycle arrest, since treatment of cells with ROS causes cell cycle arrest at both G_1 and G_2 stages of the cell cycle (Boonstra and

Post, 2004). Studies with other phytochemicals that induce ROS also show induction of cell cycle arrest, although in these cases cell cycle arrest occurs at G_2 (Hseu et al., 2012; Kuo et al., 2007; Yogosawa et al., 2012). Although ROS seem to play a large role in the anti-cancer effects of AF4, it is not known whether AF4 inhibited cell proliferation independent of ROS. This could easily be determined by pre-treating breast cancer cells with NAC prior to analysis by flow cytometry and western blotting.

4.5 AF4 Inhibits Akt Activation Through an Unknown Mechanism

AF4 induced cytotoxicity and inhibited breast cancer cell proliferation, but the signalling mechanism that leads up to these effects is not known. Although the PI3K/Akt pathway seems to be downregulated by many phytochemicals (Dhar et al., 2015; Hseu et al., 2012; Rivera Rivera et al., 2016), this pathway is for the most part unaffected by AF4. Moreover, phosphorylated PTEN, which is a tumor suppressor protein that downregulates signalling through the PI3K/Akt pathway (Gang et al., 2007), was downregulated in this pathway. Paradoxically, decreased phosphorylation and activation of PTEN suggests that the Akt pathway was upregulated or not affected by AF4. However, AF4 decreased Akt phosphorylation. Decreased phosphorylation of PTEN in the presence of AF4 is also consistent with the idea that ROS plays a major role in AF4-mediated anti-cancer effects since phosphatases such as PTEN are deactivated by ROS (Leslie et al., 2003). The only other protein in the PI3K/Akt pathway that was significantly affected by AF4 was Akt itself. Akt phosphorylation was inhibited following AF4 treatment, even though PTEN was deactivated. Since phosphorylated mTOR, which lies downstream of Akt, was not affected, Akt must have been deactivated through another mechanism. AF4 also did not

affect the protein levels of PP2A subunit C, the regulatory subunit of PP2A that unlike other phosphatases is activated by ROS (Jiang et al., 2017). In addition, AF4 did not affect GSK3β phosphorylation or β-catenin activation.

AF4 likely affects other targets of Akt to produce its anticancer effects since Akt is involved in many cell processes. Proteins of interest include FOXO3A, and NF-κB, both of which are inhibited by ROS. Studies into indole compounds, a group of phytochemical compounds found in cruciferous vegetables, have found that these compounds inhibit NF-κB signalling through the PI3K/Akt pathway (Ahmad et al., 2013). Although a ROS independent mechanism is suggested for indoles, it is likely that inhibition of Akt phosphorylation by AF4-induced ROS affected NF-κB signalling, as changes in NF-κB protein levels have been seen in response to ROS in normal cells (Chandel et al., 2000). Alterations in NF-κB protein levels would also support the idea that AF4 induces necroptosis as a mechanism for cell death, as NF-κB has been shown to be capable of activating RIPK1 to induce necroptosis (Oberst, 2016).

Some studies suggest that ROS can directly inhibit Akt via the phosphorylation of thiol groups within the protein, which would explain why proteins upstream of Akt signalling were unaffected (Cross and Templeton, 2004; Tan et al., 2015; Trachootham et al., 2009). Another possible explanation is that the multiple phytochemicals present within AF4 cause Akt inhibition through different pathways in such a way that detection of Akt inhibition via western blotting produces significant results, nut proteins upstream or downstream of Akt signalling seem to be unaffected by AF4. However, more work needs to be done to eliminate all possible targets of Akt within these pathways to support this claim.

RAS activation was not affected by AF4, however, the phosphorylation of ERK 1/2 was affected by AF4, indicating that the ERK/MAPK pathway was partially affected by AF4 treatment. In AF4-treated MDA-MB-468 cells, ERK 1/2 phosphorylation was downregulated, indicating that AF4 affected multiple pathways involved in cancer cell proliferation. On the other hand, for AF4 treatment of MDA-MB-231 cells caused ERK 1/2 phosphorylation to be increased. This effect was likely due to some compensatory mechanisms present within MDA-MB-231 cells, since these breast cancer cells are more aggressive than MDA-MB-468 cells and have different mutations. However, this pathway was not investigated intensively. Multiple other proteins are present in this pathway that may or may not be affected by AF4 which could lead to the observed effects (McCubrey et al., 2007). Further research is needed to determine the exact mechanisms behind AF4-mediated anticancer effects.

4.6 AF4 Exhibits Epigenetic Effects

Since changes in diet can elicit epigenetic changes (McKay J. A. and Mathers J. C., 2011), it is not surprising that the mixture of dietary phytochemicals in induced changes in enzymes involved in epigenetic regulation. AF4 affected the protein levels of epigenetic enzymes in both triple-negative breast cancer cell lines, as well as healthy MCF10A epithelial cells, to a similar extent. However, the meaning of AF4-induced changes in protein levels in epigenetic enzymes in terms of cellular pathways that are affected are unknown. Current techniques to investigate the downstream effects of epigenetic enzyme modulation are currently limited. As such, it is not known whether there are significant changes in global DNA methylation or histone acetylation after AF4 treatment of cells.

Given that AF4 inhibited DNMT1 while upregulating DNMT3A, it seems possible that AF4 could reverse promoter hypermethylation and global hypomethylation commonly seen in cancers. The downregulation of DNMT1 could lead to the demethylation of tumour suppressor genes, since DNMT1 is responsible for maintaining the methylation profile of cells undergoing division. The upregulation in protein levels of TET2 by AF4 treatment supports the idea of the demethylating effect of AF4, which could occur actively through the activity of TET2 rather than passively through the absence of DNMT1. Whether demethylation from these processes would be specific or not is unknown. The ability of DNMT3A to methylate DNA at new sites in the genome may help restore genomic stability. However, as research into the signalling mechanisms for DNA methylation are lacking, the significance of this change cannot be known for certain. Because of the AF4-mediated inhibition of one DNMT and the upregulation of another, its also hard to say whether AF4 has the potential to induce the viral mimicry state as described by Roulois et al. (2015), which could possibly give it the potential to recruit immune cells for cancer cell elimination. Given the ability of AF4 to impact inflammation (Warford et al., 2014), however, it is not known how this effect might play out within a living system even if it occurs.

A similar conclusion can be drawn regarding the histone acetylation modifying effects of AF4. One study has suggested that HDAC2 is directly involved in the inhibition of Akt and inhibition of downstream targets mTOR and NF-κB in hepatocarcinoma cells (Noh et al., 2014). Although my findings suggest that mTOR was not activated in response to AF4, it is still unknown whether AF4 can affect NF-κB signalling in breast cancer cells. Such an effect may explain why HDAC2 inhibition is

seen with so many phytochemicals that exhibit anticancer activities (Dhar et al., 2015; Lee et al., 2011; Park et al., 2017).

Studies into the effects of phytochemicals on HATs are currently limited, and as such not many comparisons can be made. Curcumin induces proteasome-dependent degradation of CBP while having no effect on GCN5 or PCAF (Thakur et al., 2014). However, studies on the phytochemicals present within AF4 have produced conflicting results. Quercetin increases histone acetylation through HAT activation, while EGCG is a potent HAT inhibitor (Gianfredi et al., 2017; Thakur et al., 2014). However, AF4 only downregulates GCN5 protein levels, with a decrease in histone acetylation. This, despite the fact that AF4 contains mainly quercetin glycosides, suggesting that these glycosides either do not have any HAT inhibitory effects and that the other components of AF4 are inhibited GCN5, or that these glycosides have an effect opposite to that of their parent compound. It is also possible that the small amount of catechins present in AF4 are more potent modulators of HAT activity than quercetin. Since H3K27 acetylation was downregulated upon AF4 treatment, HAT inhibition may have overcome HDAC inhibition to alter histone acetylation, however, only two acetylation sites were investigated in this study.

Although interesting, my findings do not show causality between epigenetic changes induced by AF4 and its anti-cancer effects. At this time, it is not known whether these changes in protein levels of epigenetic machinery were an indirect result of AF4 exposure. In this case, rather than AF4 directly affecting the protein expression of these epigenetic enzymes, the levels of these enzymes could be altered by the cell in order to upregulate cellular defenses in response to AF4. Moreover, it is not known whether AF4

can affect the enzymatic activity of these proteins. Nevertheless, it is possible that the changes in the levels of epigenetic proteins were a direct result of phytochemical treatment, as is seen with other phytochemicals such as EGCG and PEITC (Fang et al., 2003; Park et al., 2017). Since AF4 contains catechins, its likely that DNMT1 inhibition was a direct consequence of AF4 exposure. HATs usually have protein targets that are not epigenetic related, such as p53 (Glozak et al., 2005; Linares et al., 2007). As such, it is unclear whether the inhibition of these HATs serves the purpose of epigenetic modulation or for modulation of other proteins within the cell, although AF4 seemed to affect histone acetylation. As for DNMTs, it is uncertain if changes in protein levels caused by AF4 lead to downstream global changes in the epigenome. Nonetheless, AF4-mediated epigenetic changes should be investigated further as it may provide novel targets for cancer prevention and treatment.

4.7 Study Limitations

Although the results of this project highlight the potential of using phytochemicals as anti-cancer agents, certain limitations exist. First, as AF4 is a plant extract, the exact composition of AF4 may vary from batch to batch. Although the use of LC/MS allowed for the determination of the abundance of each compound in each stock, no two batches are likely to be exactly the same, which poses a problem in terms of reproducibility of data, i.e., the trends may be the same, but the required dose to attain such an effect may differ from batch to batch. In addition, the colour of AF4 influences the data obtained from a number of the techniques used in this project. For example, MTT assays, the dark colour of AF4 at high concentrations has a significant impact on the absorbance obtained

from each well. Although cell-free controls were used to allow for the subtraction of the background absorbance from AF4-containing cell cultures, this is not a perfect solution to the problem. The inherent fluorescence of AF4 also affects data obtained from flow cytometry. Although cells were washed after AF4 treatment, it is possible that residual AF4 present in the cells was a confounding factor. Lastly, the stability of AF4 is not known but may be an issue. For example, acylated anthocyanins found in acai berries are less temperature-stable than their non-acylated counterparts (Del Pozo-Insfran et al., 2004). Given that the majority of AF4 is composed of quercetin glycosides, the activity of AF4 may change depending on how AF4 is handled and the length of culture of AF4-treated cells. The issue of AF4 stability may not be as important in *in vivo* models due to metabolism and excretion; however, there would be a much larger number of metabolites resulting from AF4 than with single phytochemical treatments. This makes it even more likely that *in vivo* and *in vitro* effects of AF4 may differ.

4.8 Future Directions

As previously mentioned, the mechanism by which AF4 produces its anti-cancer effects is still not known. To confirm that apoptosis is not the pathway induced by AF4, terminal deoxynucleotidyl transferase dUTP nick end labeling (TUNEL) assays could be used to detect DNA fragmentation, which is seen in apoptosis. The cytoplasmic levels of cytochrome c and apoptosis-inducing factor could also be probed with western blots to confirm apoptosis-independent cell death as well as to determine the involvement of the mitochondria damage in AF4 cytotoxicity. In terms of cell death pathways, the utilization of a necroptosis inhibitor as well as probing for activated components in the signalling

pathway for necroptosis may determine whether AF4 induces necroptosis in breast cancer cells. As for cell proliferation pathways, IKB kinase ε should be investigated as a potential Akt activator, along with downstream NF-κB activation to explain the inhibitory effect of AF4 on cell proliferation and survival signals. AF4-mediated inhibition of NF-κB would support the idea that AF4 induces cell death by necroptosis, as NF-κB seems to play a role in the induction of necroptosis (Oberst, 2016). Alternatively, the ROS produced by AF4 could induce oncosis, a form of cell death that results from excess ROS (Zheng et al., 2017). These results would allow for the better understanding of how AF4 affects cancerous and non-cancerous cells.

Since AF4 exhibited some epigenetic modulatory capabilities, the significance of these findings should be further investigated. In particular, the mechanism by which AF4 induces epigenetic changes, as well as how these effects are involved in the anti-cancer effects of AF4. The use of lower doses of AF4 and longer exposure may yield improved understanding of these epigenetic effects. It is possible that the short and long term epigenetic effects of AF4 may be different, as seen in one study of the epigenetic effects of the phytochemical phenethyl isothiocyanate (PEITC) (Park et al., 2017). In this study, high-dose PEITC treatment for 72 h has little effect on the binding of most HDACs and HATs to chromatin, however, lower dose treatment for 6 weeks produced a much greater effect, and in some cases modulated HDAC and HAT chromatin binding differently than was seen with short-term treatment (Park et al., 2017). In addition, the epigenetic effects of AF4 can be investigated further with chromatin immunoprecipitation (ChIP)-sequencing to investigate any differences in DNA binding of epigenetic enzymes whose protein levels were affected by AF4 treatment.

Drug resistance studies could also be conducted with AF4 given its ability to inhibit Akt signalling and affect protein levels of epigenetic enzymes. Akt playd a role in drug resistance through the PI3K/Akt pathway, and it has been suggested that downstream activation of mTOR by this pathway activates DNMTs to increase the expression of proteins involved in cellular drug efflux (Martin et al., 2014). Although AF4 did not seem to affect Akt signalling through the PI3K/Akt pathway, studies with the Akt inhibitor perisofine in drug-resistant MCF-7 breast cancer cells have shown that Akt inhibition improved the cytotoxic response to doxorubicin (Lin et al., 2012). Perisofine reduces signalling through the Akt/NF-κB pathway, along with partial downregulation of P-glycoprotein (P-gp), a well-studied drug export protein implicated in chemoresistance of many cancers (Lin et al., 2012). It is also possible that AF4 may inhibit drug export mechanisms, as has already been seen with a variety of phytochemicals, including 6-gingerol, capsaicin, curcumin, and resveratrol, all of which inhibit the function of the drug efflux protein P-glycoprotein (Nabekura et al., 2005). ROS synergizes with conventional therapeutics to overcome drug resistance by overwhelming endogenous antioxidants (Trachootham et al., 2009). Since radiation therapies and some chemotherapy drugs either directly or indirectly cause ROS production in cancer cells that results in apoptosis, it is likely that an increase in tolerance to ROS by cancer cells plays a role in drug resistance that could be overcome via synergy of AF4-induced ROS and radio- or chemotherapy-induced ROS (Trachootham et al., 2009). AF4 inhibited DNMT1 protein expression, but increased DNMT3A protein expression, leading to the question as to whether this modification in levels of epigenetic proteins leads to any changes in promoter methylation for these export proteins.

Studies on the metabolites of AF4 produced by the liver would also allow for better predictions of the effects of AF4 in the human body. As foreign compounds are subject to metabolism by the liver in preparation for excretion, the bioactivity of these compounds may provide some clues as to how AF4 would behave *in vivo*. The bioactivity of these metabolites would also allow for the prediction of the efficacy of orally-ingested AF4, as AF4 would be subject to first-pass metabolism after absorption in the intestine.

4.9 Summary and Conclusions

This study shows that AF4 possesses numerous anti-cancer effects, some of which differ from the compounds that comprise AF4 (Figure 29). The combined effects of the components of AF4 may contribute to its selectivity towards cancer cells. AF4 induced morphological changes in triple-negative breast cancer cells without affecting healthy epithelial cells and inhibited the growth of breast cancer cells in a time- and dose-dependent manner. Although AF4 was less potent than its main component, quercetin, AF4 was more for breast cancer cells in terms of growth inhibition and cytotoxicity. Although AF4 induced ROS-dependent cytotoxicity and mitochondrial membrane damage in breast cancer cells, the mechanism for this effect is currently unknown as AF4 did not activate caspases or PARP1, which are indicators of apoptosis. AF4 inhibited the proliferation of breast cancer cells via the induction of G_1 cell cycle arrest, which was accompanied by the decreased protein levels of cyclin D3, CDK4, and CDK6, involved in the progression of the cell from the G_1 phase of the cell cycle to the S phase. Although the mechanism behind the anti-survival and antiproliferative effects of AF4 are currently unknown, AF4 caused the inhibition of Akt through a ROS-dependent mechanism that

did not affect other components of the PI3K/Akt pathway. Downstream targets of Akt that were not affected by AF4 included mTOR and β-catenin. The ERK/MAPK pathway was also affected by AF4, but the effect was cell line-dependent. Lastly, AF4 affected the protein levels of several enzymes involved in epigenetic modulation in both triple-negative breast cancer and healthy cells. These effects included inhibition of DNMT1, upregulation of DNMT3A, upregulation of TET2, inhibition of HDAC2, and inhibition of GCN5. Although HDAC2 was strongly inhibited by AF4, there seemed to be no effect on H3K9 acetylation, whereas H3K27 acetylation was downregulated.

Together, these findings indicate that AF4 shows promise as a selective therapeutic for triple-negative breast cancer that could possibly be used to improve the effect of current therapeutics based on its ability to produce ROS. The addition of ROS to cancer cells could cause hard to treat breast cancers to become more sensitive to anti-survival signals that initiate cell death pathways. Although not currently well understood, the epigenetic effects could also have anti-cancer or chemopreventative effects, which could assist in the anti-cancer effects of ROS or prevent cancers from forming in the first place.

Despite the potential of AF4, more work needs to be done to confirm its safety in a living organism. The major role that ROS plays in AF4-mediated cytotoxicity implies potential side effects, including decreased wound healing, modulation of inflammation, and the risk of oxidative stress. Together, these effects could have lifelong effects in patients or even promote the formation of new cancers. However, research into novel drug delivery systems such as targeted nanoparticles may help circumvent these effects. Further studies into the mechanism of AF4-mediated cytotoxicity anti-proliferative effect

are also needed to better understand how AF4 interacts with both cancerous and non-cancerous cells. Nonetheless, the findings of this study have laid the groundwork for future pre-clinical studies of AF4, which determine whether AF4 might benefit patients with triple-negative breast cancer.

REFERENCES

Abal, M., Andreu, J.M., and Barasoain, I. (2003). Taxanes: microtubule and centrosome targets, and cell cycle dependent mechanisms of action. Curr. Cancer Drug Targets *3*, 193–203.

Alli, E., Sharma, V.B., Sunderesakumar, P., and Ford, J.M. (2009). Defective repair of oxidative DNA damage in triple-negative breast cancer confers sensitivity to inhibition of poly(ADP-ribose) polymerase. Cancer Res. *69*, 3589–3596.

Bannister, A.J., and Kouzarides, T. (2011). Regulation of chromatin by histone modifications. Cell Res. *21*, 381.

Bishayee, K., Khuda-Bukhsh, A.R., and Huh, S.O. (2015). PLGA-loaded gold-nanoparticles precipitated with quercetin downregulate HDAC-Akt activities controlling proliferation and activate p53-ROS crosstalk to induce apoptosis in hepatocarcinoma cells. Mol. Cells *38*, 518–527.

Boonstra, J., and Post, J.A. (2004). Molecular events associated with reactive oxygen species and cell cycle progression in mammalian cells. Gene *337*, 1–13.

Bouayed, J., and Bohn, T. (2010). Exogenous antioxidants—double-edged swords in cellular redox state: health beneficial effects at physiologic doses versus deleterious effects at high doses. Oxid. Med. Cell. Longev. *3*, 228–237.

Boyle, P. (2012). Triple-negative breast cancer: epidemiological considerations and recommendations. Ann. Oncol. *23*, vi7–vi12.

Brait, M., and Sidransky, D. (2011). Cancer epigenetics: above and beyond. Toxicol. Mech. Methods *21*, 275–288.

Brill, A., Torchinsky, A., Carp, H., and Toder, V. (1999). The role of apoptosis in normal and abnormal embryonic development. J. Assist. Reprod. Genet. *16*, 512–519.

Brisken, C. (2013). Progesterone signalling in breast cancer: a neglected hormone coming into the limelight. Nat. Rev. Cancer *13*, 385–396.

Bryant, H.E., Schultz, N., Thomas, H.D., Parker, K.M., Flower, D., Lopez, E., Kyle, S., Meuth, M., Curtin, N.J., and Helleday, T. (2005). Specific killing of BRCA2-deficient tumours with inhibitors of poly(ADP-ribose) polymerase. Nature *434*, 913–917.

Canadian Cancer Society (2017). Canadian Cancer Statistics.

Candé, C., Vahsen, N., Garrido, C., and Kroemer, G. (2004). Apoptosis-inducing factor (AIF): caspase-independent after all. Cell Death Differ. *11*, 591–594.

Carracedo, A., and Pandolfi, P.P. (2008). The PTEN–PI3K pathway: of feedbacks and cross-talks. Oncogene *27*, 5527–5541.

Cheng, S., Gao, N., Zhang, Z., Chen, G., Budhraja, A., Ke, Z., Son, Y.O., Wang, X., Luo, J., and Shi, X. (2010). Quercetin induces tumor-selective apoptosis through downregulation of Mcl-1 and activation of Bax. Clin. Cancer Res. *16*.

Chinnaiyan, A.M. (1999). The apoptosome: heart and soul of the cell death machine. Neoplasia *1*, 5–15.

Choi, K.C., Jung, M.G., Lee, Y.H., Yoon, J.C., Kwon, S.H., Kang, H.B., Kim, M.J., Cha, J.H., Kim, Y.J., Jun, W.J., et al. (2009). Epigallocatechin-3-gallate, a histone acetyltransferase inhibitor, inhibits EBV-induced B lymphocyte transformation via duppression of RelA acetylation. Cancer Res. *69*, 583–592.

Chrun, E.S., Modolo, F., and Daniel, F.I. (2017). Histone modifications: a review about the presence of this epigenetic phenomenon in carcinogenesis. Pathol. - Res. Pract. *213*, 1329–1339.

Collins, J.A., Schandl, C.A., Young, K.K., Vesely, J., and Willingham, M.C. (1997). Major DNA fragmentation is a late event in apoptosis. J. Histochem. Cytochem. *45*, 923–934.

Dai, X., Li, T., Bai, Z., Yang, Y., Liu, X., Zhan, J., and Shi, B. (2015). Breast cancer intrinsic subtype classification, clinical use and future trends. Am. J. Cancer Res. *5*, 2929–2943.

Davies, M.A. (2011). Regulation, role, and targeting of Akt in cancer. J. Clin. Oncol. *29*, 4715–4717.

Decker, P., and Muller, S. (2002). Modulating poly (ADP-ribose) polymerase activity: potential for the prevention and therapy of pathogenic situations involving DNA damage and oxidative stress. Curr. Pharm. Biotechnol. *3*, 275–283.

Del Pozo-Insfran, D., Brenes, C.H., and Talcott, S.T. (2004). Phytochemical composition and pigment stability of açai (Euterpe oleracea Mart.). J. Agric. Food Chem. *52*, 1539–1545.

Dent, R., Trudeau, M., Pritchard, K.I., Hanna, W.M., Kahn, H.K., Sawka, C.A., Lickley, L.A., Rawlinson, E., Sun, P., and Narod, S.A. (2007). Triple-negative breast cancer: clinical features and patterns of recurrence. Clin. Cancer Res. *13*, 4429–4434.

Dhanasekaran, D.N., and Reddy, E.P. (2008). JNK signaling in apoptosis. Oncogene *27*, 6245–6251.

Dhar, S., Kumar, A., Li, K., Tzivion, G., and Levenson, A.S. (2015). Resveratrol regulates PTEN/Akt pathway through inhibition of MTA1/HDAC unit of the NuRD complex in prostate cancer. Biochim. Biophys. Acta - Mol. Cell Res. *1853*, 265–275.

Ding, R., Jin, Y., Liu, X., Zhu, Z., Zhang, Y., Wang, T., and Xu, Y. (2016). H3K9 acetylation change patterns in rats after exposure to traffic-related air pollution. Environ. Toxicol. Pharmacol. *42*, 170–175.

Downward, J. (2003). Targeting RAS signalling pathways in cancer therapy. Nat. Rev. Cancer *3*, 11–22.

Eling, N., Reuter, L., Hazin, J., Hamacher-Brady, A., and Brady, N.R. (2015). Identification of artesunate as a specific activator of ferroptosis in pancreatic cancer cells. Oncoscience *2*, 517–532.

Elmore, S. (2007). Apoptosis: a review of programmed cell death. Toxicol. Pathol. *35*, 495–516.

Esteller, M. (2007). Cancer epigenomics: DNA methylomes and histone-modification maps. Nat. Rev. Genet. *8*, 286–298.

Fang, M.Z., Wang, Y., Ai, N., Hou, Z., Sun, Y., Lu, H., Welsh, W., and Yang, C.S. (2003). Tea polyphenol (−)-epigallocatechin-3-gallate inhibits DNA methyltransferase and reactivates methylation-silenced genes in cancer cell lines. Cancer Res. *63*, 7563–7570.

Ferlay, J., Shin, H.-R., Bray, F., Forman, D., Mathers, C., and Parkin, D.M. (2010). Estimates of worldwide burden of cancer in 2008: GLOBOCAN 2008. Int. J. Cancer *127*, 2893–2917.

Fernando, W., Coombs, M.R.P., Hoskin, D.W., and Rupasinghe, H.P.V. (2016). Docosahexaenoic acid-acylated phloridzin, a novel polyphenol fatty acid ester derivative, is cytotoxic to breast cancer cells. Carcinogenesis *37*, 1004–1013.

Foulkes, W.D., Stefansson, I.M., Chappuis, P.O., Bégin, L.R., Goffin, J.R., Wong, N., Trudel, M., and Akslen, L.A. (2003). Germline BRCA1 mutations and a basal epithelial phenotype in breast cancer. J. Natl. Cancer Inst. *95*, 1482–1485.

Füllgrabe, J., Kavanagh, E., and Joseph, B. (2011). Histone onco-modifications. Oncogene *30*, 3391–3403.

Galluzzi, L., Buqué, A., Kepp, O., Zitvogel, L., and Kroemer, G. (2016). Immunogenic cell death in cancer and infectious disease. Nat. Rev. Immunol. *17*, 97–111.

Gama-Sosa, M.A., Slagel, V.A., Trewyn, R.W., Oxenhandler, R., Kuo, K.C., Gehrke, C.W., and Ehrlich, M. (1983). The 5-methylcytosine content of DNA from human tumors. Nucleic Acids Res. *11*, 6883–6894.

Gang, S., Gaoliang, O., and Shideng, B. (2007). The activation of Akt/PKB signaling pathway and cell survival. J. Cell. Mol. Med. *9*, 59–71.

Garg, A.D., Nowis, D., Golab, J., Vandenabeele, P., Krysko, D.V., and Agostinis, P. (2010). Immunogenic cell death, DAMPs and anticancer therapeutics: an emerging amalgamation. Biochim. Biophys. Acta - Rev. Cancer *1805*, 53–71.

Garg, A.D., Krysko, D.V., Verfaillie, T., Kaczmarek, A., Ferreira, G.B., Marysael, T., Rubio, N., Firczuk, M., Mathieu, C., Roebroek, A.J.M., et al. (2012). A novel pathway combining calreticulin exposure and ATP secretion in immunogenic cancer cell death. EMBO J. *31*, 1062–1079.

Gianfredi, V., Nucci, D., Vannini, S., Villarini, M., and Moretti, M. (2017). In vitro biological effects of sulforaphane (SFN), epigallocatechin-3-gallate (EGCG), and curcumin on breast cancer cells: a systematic review of the literature. Nutr. Cancer *69*, 969–978.

Goossens, V., Stangé, G., Moens, K., Pipeleers, D., and Grooten, J. (1999). Regulation of tumor necrosis factor-induced, mitochondria- and reactive oxygen species-dependent cell death by the electron flux through the electron transport chain complex I. Antioxid. Redox Signal. *1*, 285–295.

Greenwell, M., and Rahman, P. (2015). Medicinal plants: their use in anticancer treatment. Int. J. Pharm. Sci. Res. *6*, 4103–4112.

Gu, J.W., Makey, K.L., Tucker, K.B., Chinchar, E., Mao, X., Pei, I., Thomas, E.Y., and Miele, L. (2013). EGCG, a major green tea catechin suppresses breast tumor angiogenesis and growth via inhibiting the activation of HIF-1α and NFκB, and VEGF expression. Vasc. Cell *5*, 9–19.

Halliwell, B., and Gutteridge, J.M.C. (1990). Role of free radicals and catalytic metal ions in human disease: An overview. In Methods in Enzymology, (Academic Press), pp. 1–85.

Hanahan, D., and Weinberg, R.A. (2011). Hallmarks of cancer: the next generation. Cell *144*, 646–674.

Hasan, A. (2013). Handbook of Blood Gas/Acid-base Interpretation (London: Springer-Verlag).

Hemmings, B.A., and Restuccia, D.F. (2012). PI3K-PKB/Akt pathway. Cold Spring Harb. Perspect. Biol. *4*, a011189.

Hseu, Y.-C., Lee, M.-S., Wu, C.-R., Cho, H.-J., Lin, K.-Y., Lai, G.-H., Wang, S.-Y., Kuo, Y.-H., Senthil Kumar, K.J., and Yang, H.-L. (2012). The chalcone flavokawain B induces G2/M cell-cycle arrest and apoptosis in human oral carcinoma HSC-3 cells through the intracellular ROS generation and downregulation of the Akt/p38 MAPK signaling pathway. J. Agric. Food Chem. *60*, 2385–2397.

Hudis, C.A. (2007). Trastuzumab — mechanism of action and use in clinical practice. N. Engl. J. Med. *357*, 39–51.

Hudis, C.A., and Gianni, L. (2011). Triple-Negative Breast Cancer: An Unmet Medical Need. The Oncologist *16*, 1–11.

Iacopini, P., Baldi, M., Storchi, P., and Sebastiani, L. (2008). Catechin, epicatechin, quercetin, rutin and resveratrol in red grape: content, in vitro antioxidant activity and interactions. Wine Nutr. Bioact. Non-Nutr. More *21*, 589–598.

Issa, J.-P.J., and Kantarjian, H.M. (2009). Targeting DNA methylation. Clin. Cancer Res. *15*, 3938–3946.

Jemal, A., Bray, F., Center, M.M., Ferlay, J., Ward, E., and Forman, D. (2011). Global cancer statistics. CA. Cancer J. Clin. *61*, 69–90.

Jiang, Y., Cao, Y., Wang, Y., Li, W., Liu, X., Lv, Y., Li, X., and Mi, J. (2017). Cysteine transporter SLC3A1 promotes breast cancer tumorigenesis. Theranostics *7*, 1036–1046.

Kale, A., Gawande, S., and Kotwal, S. (2008). Cancer phytotherapeutics: role for flavonoids at the cellular level. Phytother. Res. *22*, 567–577.

Kalle, A.M., Mallika, A., Badiger, J., Alinakhi, Talukdar, P., and Sachchidanand (2010). Inhibition of SIRT1 by a small molecule induces apoptosis in breast cancer cells. Biochem. Biophys. Res. Commun. *401*, 13–19.

Kane, L.P., Shapiro, V.S., Stokoe, D., and Weiss, A. (1999). Induction of NF-κB by the Akt/PKB kinase. Curr. Biol. *9*, 601–604.

Keating, G.M., and Santoro, A. (2009). Sorafenib. Drugs *69*, 223–240.

Keddy, P.G.W., Dunlop, K., Warford, J., Samson, M.L., Jones, Q.R.D., Rupasinghe, H.P.V., and Robertson, G.S. (2012). Neuroprotective and anti-inflammatory effects of the flavonoid-enriched fraction AF4 in a mouse model of hypoxic-ischemic brain injury. PLoS ONE *7*, e51324.

Kelly, T.K., De Carvalho, D.D., and Jones, P.A. (2010). Epigenetic modifications as therapeutic targets. Nat. Biotechnol. *28*, 1069–1078.

Khorsandi, L., Orazizadeh, M., Niazvand, F., Abbaspour, M.R., Mansouri, E., and Khodadadi, A. (2017). Quercetin induces apoptosis and necroptosis in MCF-7 breast cancer cells. Bratisl. Lek. Listy *118*, 123.

Kim, Y.-S., Morgan, M.J., Choksi, S., and Liu, Z. (2007). TNF-induced activation of the Nox1 NADPH oxidase and its role in the induction of necrotic cell death. Mol. Cell *26*, 675–687.

Knickle, A., Fernando, W., Greenshields, A., Rupasinghe, H.P.V., and Hoskin, D. (2018). Myricetin-induced apoptosis of triple-negative breast cancer cells is mediated by the iron-dependent generation of reactive oxygen species from hydrogen peroxide. Food Chem Toxicol *118*, 154–167.

Kohli, R.M., and Zhang, Y. (2013). TET enzymes, TDG and the dynamics of DNA demethylation. Nature *502*, 472–479.

Kopelovich, L., Crowell, J.A., and Fay, J.R. (2003). The epigenome as a target for cancer chemoprevention. J. Natl. Cancer Inst. *95*, 1747–1757.

Korsmeyer, S., Shutter, J., Veis, D., Merry, D., and Oltvai, Z. (1993). Bcl-2/Bax: a rheostat that regulates an anti-oxidant pathway and cell death. Semin. Cancer Biol. *4*, 327–332.

Kroemer, G., Galluzzi, L., Vandenabeele, P., Abrams, J., Alnemri, E., Baehrecke, E., Blagosklonny, M., El-Deiry, W., Golstein, P., Green, D., et al. (2009). Classification of cell death: recommendations of the Nomenclature Committee on Cell Death 2009. Cell Death Differ. *16*, 3–11.

Kryston, T.B., Georgiev, A.B., Pissis, P., and Georgakilas, A.G. (2011). Role of oxidative stress and DNA damage in human carcinogenesis. Mutat. Res. Mol. Mech. Mutagen. *711*, 193–201.

Kuo, P.L., Chen, C.Y., and Hsu, Y.L. (2007). Isoobtusilactone A induces cell cycle arrest and apoptosis through reactive oxygen species/apoptosis signal-regulating kinase 1 signaling pathway in human breast cancer cells. Cancer Res. *67*, 7406–7420.

Lakhani, S.R., Reis-Filho, J.S., Fulford, L., Penault-Llorca, F., van der Vijver, M., Parry, S., Bishop, T., Benitez, J., Rivas, C., Bignon, Y.-J., et al. (2005). Prediction of BRCA1 status in patients with breast cancer using estrogen receptor and basal phenotype. Clin. Cancer Res. *11*, 5175–5180.

Lambert, J.D., and Elias, R.J. (2010). The antioxidant and pro-oxidant activities of green tea polyphenols: a role in cancer prevention. Polyphenols Health *501*, 65–72.

Lee, S.H., Meng, X.W., Flatten, K.S., Loegering, D.A., and Kaufmann, S.H. (2013). Phosphatidylserine exposure during apoptosis reflects bidirectional trafficking between plasma membrane and cytoplasm. Cell Death Differ. *20*, 64–76.

Lee, S.J., Krauthauser, C., Maduskuie, V., Fawcett, P.T., Olson, J.M., and Rajasekaran, S.A. (2011). Curcumin-induced HDAC inhibition and attenuation of medulloblastoma growth in vitro and in vivo. BMC Cancer *11*, 144–157.

Lee, W.J., Shim, J.Y., and Zhu, B.T. (2005). Mechanisms for the inhibition of DNA methyltransferases by tea catechins and bioflavonoids. Mol. Pharmacol. *68*, 1018–1030.

Lee, Y.H., Kwak, J., Choi, H.K., Choi, K.-C., Kim, S., Lee, J., Jun, W., Park, H.J., and Yoon, H.G. (2012). EGCG suppresses prostate cancer cell growth modulating acetylation of androgen receptor by anti-histone acetyltransferase activity. Int. J. Mol. Med. *30*, 69–74.

Leslie, N.R., Bennett, D., Lindsay, Y.E., Stewart, H., Gray, A., and Downes, C.P. (2003). Redox regulation of PI 3-kinase signalling via inactivation of PTEN. EMBO J. *22*, 5501–5510.

Lim, E., Metzger-Filho, O., and Winer, E.P. (2012). The natural history of hormone receptor-positive breast cancer. Oncology *26*, 688–694, 696.

Lin, X., Zhang, X., Wang, Q., Li, J., Zhang, P., Zhao, M., and Li, X. (2012). Perifosine downregulates MDR1 gene expression and reverses multidrug-resistant phenotype by inhibiting PI3K/Akt/NF-κB signaling pathway in a human breast cancer cell line. Neoplasma *59*, 248–256.

Long, J.S., and Ryan, K.M. (2012). New frontiers in promoting tumour cell death: targeting apoptosis, necroptosis and autophagy. Oncogene *31*, 5045–5060.

Long, L.H., Clement, M.V., and Halliwell, B. (2000). Artifacts in cell culture: rapid generation of hydrogen peroxide on addition of (−)-epigallocatechin, (−)-epigallocatechin gallate, (+)-catechin, and quercetin to commonly used cell culture media. Biochem. Biophys. Res. Commun. *273*, 50–53.

Malumbres, M. (2014). Cyclin-dependent kinases. Genome Biol. *15*, 122–132.

Manning, B.D., and Toker, A. (2017). AKT/PKB signaling: navigating the network. Cell *169*, 381–405.

Martin, H.L., Smith, L., and Tomlinson, D.C. (2014). Multidrug-resistant breast cancer: current perspectives. Breast Cancer Targets Ther. *6*, 1–13.

McCubrey, J.A., Steelman, L.S., Chappell, W.H., Abrams, S.L., Wong, E.W.T., Chang, F., Lehmann, B., Terrian, D.M., Milella, M., Tafuri, A., et al. (2007). Roles of the Raf/MEK/ERK pathway in cell growth, malignant transformation and drug resistance. Biochim. Biophys. Acta - Mol. Cell Res. *1773*, 1263–1284.

McKay J. A., and Mathers J. C. (2011). Diet induced epigenetic changes and their implications for health. Acta Physiol. *202*, 103–118.

Meers, P., and Mealy, T. (1993). Calcium-dependent annexin V binding to phospholipids: stoichiometry, specificity, and the role of negative charge. Biochemistry (Mosc.) *32*, 11711–11721.

Michailidis, Y., Karagounis, L.G., Terzis, G., Jamurtas, A.Z., Spengos, K., Tsoukas, D., Chatzinikolaou, A., Mandalidis, D., Stefanetti, R.J., Papassotiriou, I., et al. (2013). Thiol-based antioxidant supplementation alters human skeletal muscle signaling and attenuates its inflammatory response and recovery after intense eccentric exercise. Am. J. Clin. Nutr. *98*, 233–245.

Moore, L.D., Le, T., and Fan, G. (2012). DNA methylation and its basic function. Neuropsychopharmacology *38*, 23–38.

Mosmann, T. (1983). Rapid colorimetric assay for cellular growth and survival: application to proliferation and cytotoxicity assays. J. Immunol. Methods *65*, 55–63.

Mottet, D., and Castronovo, V. (2008). Histone deacetylases: target enzymes for cancer therapy. Clin. Exp. Metastasis *25*, 183–189.

Müller, A., and Florek, M. (2010). 5-Azacytidine/azacitidine. Cancer Res *184*, 159–170.

Nabekura, T., Kamiyama, S., and Kitagawa, S. (2005). Effects of dietary chemopreventive phytochemicals on P-glycoprotein function. Biochem. Biophys. Res. Commun. *327*, 866–870.

Nair, S.V.G., Ziaullah, and Rupasinghe, H.P.V. (2014). Fatty acid esters of phloridzin induce apoptosis of human liver cancer cells through altered gene expression. PLoS ONE *9*, e107149.

Nelson, J., and Falk, R. (1993a). Phloridzin and phloretin inhibition of 2-deoxy-D-glucose uptake by tumor cells in vitro and in vivo. Anticancer Res *13*, 2293–2299.

Nelson, J., and Falk, R. (1993b). The efficacy of phloridzin and phloretin on tumor cell growth. Anticancer Res *13*, 2287-92.

Nevins, J.R. (2001). The Rb/E2F pathway and cancer. Hum. Mol. Genet. *10*, 699–703.

Nicholson, D. (1999). Caspase structure, proteolytic substrates, and function during apoptotic cell death. Cell Death Differ. *6*, 1028–1042.

Nicholson, K.M., and Anderson, N.G. (2002). The protein kinase B/Akt signalling pathway in human malignancy. Cell. Signal. *14*, 381–395.

Nidai Ozes, O., Mayo, L.D., Gustin, J.A., Pfeffer, S.R., Pfeffer, L.M., and Donner, D.B. (1999). NF-κB activation by tumour necrosis factor requires the Akt serine–threonine kinase. Nature *401*, 82–85.

Noh, J.H., Bae, H.J., Eun, J.W., Shen, Q., Park, S.J., Kim, H.S., Nam, B., Shin, W.C., Lee, E.K., Lee, K., et al. (2014). HDAC2 provides a critical support to malignant progression of hepatocellular carcinoma through feedback control of mTORC1 and AKT. Cancer Res. *74*, 1728–1738.

Oakman, C., Viale, G., and Di Leo, A. (2010). Management of triple negative breast cancer. The Breast *19*, 312–321.

Odiatou, E.M., Skaltsounis, A.L., and Constantinou, A.I. (2013). Identification of the factors responsible for the in vitro pro-oxidant and cytotoxic activities of the olive polyphenols oleuropein and hydroxytyrosol. Cancer Lett. *330*, 113–121.

O'Shaughnessy, J., Osborne, C., Pippen, J.E., Yoffe, M., Patt, D., Rocha, C., Koo, I.C., Sherman, B.M., and Bradley, C. (2011). Iniparib plus chemotherapy in metastatic triple-negative breast cancer. N. Engl. J. Med. *364*, 205–214.

O'Shaughnessy, J., Schwartzberg, L., Danso, M.A., Miller, K.D., Rugo, H.S., Neubauer, M., Robert, N., Hellerstedt, B., Saleh, M., Richards, P., et al. (2014). Phase III study of iniparib plus gemcitabine and carboplatin versus gemcitabine and carboplatin in patients with metastatic triple-negative breast cancer. J. Clin. Oncol. *32*, 3840–3847.

Ow, Y.-L.P., Green, D.R., Hao, Z., and Mak, T.W. (2008). Cytochrome c: functions beyond respiration. Nat. Rev. Mol. Cell Biol. *9*, 532–542.

Pan, M.H., Hsieh, M.C., Kuo, J.M., Lai, C.S., Wu, H., Sang, S., and Ho, C.T. (2008). 6-Shogaol induces apoptosis in human colorectal carcinoma cells via ROS production, caspase activation, and GADD 153 expression. Mol Nutr Food Res *52*, 527–537.

Park, J.E., Sun, Y., Lim, S.K., Tam, J.P., Dekker, M., Chen, H., and Sze, S.K. (2017). Dietary phytochemical PEITC restricts tumor development via modulation of epigenetic writers and erasers. Sci. Rep. *7*, 40569.

Petrelli, F., Coinu, A., Borgonovo, K., Cabiddu, M., Ghilardi, M., Lonati, V., and Barni, S. (2014). The value of platinum agents as neoadjuvant chemotherapy in triple-negative breast cancers: a systematic review and meta-analysis. Breast Cancer Res. Treat. *144*, 223–232.

Peyressatre, M., Prével, C., Pellerano, M., and Morris, M.C. (2015). Targeting cyclin-dependent kinases in human cancers: from small molecules to peptide inhibitors. Cancers *7*, 179–237.

Plimack, E.R., Kantarjian, H.M., and Issa, J.-P. (2007). Decitabine and its role in the treatment of hematopoietic malignancies. Leuk. Lymphoma *48*, 1472–1481.

Polyakov, N.E., Leshina, T.V., Konovalova, T.A., and Kispert, L.D. (2001). Carotenoids as scavengers of free radicals in a fenton reaction: antioxidants or pro-oxidants? Free Radic. Biol. Med. *31*, 398–404.

Pop, C., Timmer, J., Sperandio, S., and Salvesen, G.S. (2006). The apoptosome activates caspase-9 by dimerization. Mol. Cell *22*, 269–275.

Pozarowski, P., and Darzynkiewicz, Z. (2004). Analysis of cell cycle by flow cytometry. In Checkpoint Controls and Cancer: Volume 2: Activation and Regulation Protocols, A.H. Schönthal, ed. (Totowa, NJ: Humana Press), pp. 301–311.

Prat, A., Parker, J.S., Karginova, O., Fan, C., Livasy, C., Herschkowitz, J.I., He, X., and Perou, C.M. (2010). Phenotypic and molecular characterization of the claudin-low intrinsic subtype of breast cancer. Breast Cancer Res. *12*, R68.

Priyadarsini, R.V., Senthil Murugan, R., Maitreyi, S., Ramalingam, K., Karunagaran, D., and Nagini, S. (2010). The flavonoid quercetin induces cell cycle arrest and mitochondria-mediated apoptosis in human cervical cancer (HeLa) cells through p53 induction and NF-κB inhibition. Eur. J. Pharmacol. *649*, 84–91.

Raisova, M., Hossini, A.M., Eberle, J., Riebeling, C., Orfanos, C.E., Geilen, C.C., Wieder, T., Sturm, I., and Daniel, P.T. (2001). The Bax/Bcl-2 ratio determines the susceptibility of human melanoma cells to CD95/Fas-mediated apoptosis. J. Invest. Dermatol. *117*, 333–340.

Reis-Filho, J.S., and Pusztai, L. (2011). Gene expression profiling in breast cancer: classification, prognostication, and prediction. The Lancet *378*, 1812–1823.

Reule, A. (1976). Errors in spectrophotometry and calibration procedures to avoid them. J. Res. Natl. Bur. Stand. *80A*, 609–624.

Rice-Evans, C.A., Miller, N.J., and Paganga, G. (1996). Structure-antioxidant activity relationships of flavonoids and phenolic acids. Free Radic. Biol. Med. *20*, 933–956.

Richardson, D.R. (2002). Iron chelators as therapeutic agents for the treatment of cancer. Crit. Rev. Oncol. Hematol. *42*, 267–281.

Ristow, M., and Zarse, K. (2010). How increased oxidative stress promotes longevity and metabolic health: The concept of mitochondrial hormesis (mitohormesis). Exp. Gerontol. *45*, 410–418.

Rivera Rivera, A., Castillo-Pichardo, L., Gerena, Y., and Dharmawardhane, S. (2016). Anti-breast cancer potential of quercetin via the Akt/AMPK/mammalian target of rapamycin (mTOR) signaling cascade. PLOS ONE *11*, e0157251.

Roche, J., Nasarre, P., Gemmill, R., Baldys, A., Pontis, J., Korch, C., Guilhot, J., Ait-Si-Ali, S., and Drabkin, H. (2013). Global Decrease of Histone H3K27 Acetylation in ZEB1-Induced Epithelial to Mesenchymal Transition in Lung Cancer Cells. Cancers *5*, 334–356.

Roulois, D., Loo Yau, H., Singhania, R., Wang, Y., Danesh, A., Shen, S.Y., Han, H., Liang, G., Jones, P.A., Pugh, T.J., et al. (2015). DNA-demethylating agents target colorectal cancer cells by inducing viral mimicry by endogenous transcripts. Cell *162*, 961–973.

Saito, Y., Nishio, K., Ogawa, Y., Kimata, J., Kinumi, T., Yoshida, Y., Noguchi, N., and Niki, E. (2006). Turning point in apoptosis/necrosis induced by hydrogen peroxide. Free Radic. Res. *40*, 619–630.

Saraste, A., and Pulkki, K. (2000). Morphologic and biochemical hallmarks of apoptosis. Cardiovasc. Res. *45*, 528–537.

Satyanarayana, A., and Kaldis, P. (2009). Mammalian cell-cycle regulation: several Cdks, numerous cyclins and diverse compensatory mechanisms. Oncogene *28*, 2925–2939.

Sauve, A.A., Wolberger, C., Schramm, V.L., and Boeke, J.D. (2006). The biochemistry of sirtuins. Annu. Rev. Biochem. *75*, 435–465.

Sayin, V.I., Ibrahim, M.X., Larsson, E., Nilsson, J.A., Lindahl, P., and Bergo, M.O. (2014). Antioxidants accelerate lung cancer progression in mice. Sci. Transl. Med. *6*, 221ra15.

Shafei, A., El-Bakly, W., Sobhy, A., Wagdy, O., Reda, A., Aboelenin, O., Marzouk, A., El Habak, K., Mostafa, R., Ali, M.A., et al. (2017). A review on the efficacy and toxicity of different doxorubicin nanoparticles for targeted therapy in metastatic breast cancer. Biomed. Pharmacother. *95*, 1209–1218.

Shapiro, C.L., and Recht, A. (2001). Side Effects of Adjuvant Treatment of Breast Cancer. N. Engl. J. Med. *344*, 1997–2008.

Sharma, S., Kelly, T.K., and Jones, P.A. (2010). Epigenetics in cancer. Carcinogenesis *31*, 27–36.

Shen, H.-M., and Liu, Z. (2006). JNK signaling pathway is a key modulator in cell death mediated by reactive oxygen and nitrogen species. Free Radic. Biol. Med. *40*, 928–939.

Siegel, R.L., Miller, K.D., and Jemal, A. (2018). Cancer statistics, 2018. CA. Cancer J. Clin. *68*, 7–30.

Slee, E.A., Adrain, C., and Martin, S.J. (2001). Executioner caspase-3, -6, and -7 perform distinct, non-redundant roles during the demolition phase of apoptosis. J. Biol. Chem. *276*, 7320–7326.

Soheila, A.-H.-M., Fred, J.C., Brian, J., and Brian, T. (2001). Early signaling components in ultraviolet-B responses: distinct roles for different reactive oxygen species and nitric oxide. FEBS Lett. *489*, 237–242.

Sudan, S., and Rupasinghe, H.P.V. (2014). Flavonoid-enriched apple fraction AF4 induces cell cycle arrest, DNA topoisomerase II inhibition, and apoptosis in human liver cancer HepG2 cells. Nutr. Cancer *66*, 1–10.

Tetsuo, K., Akira, M., and Takashi, K. (1990). The role of the vimentin intermediate filaments in rat 3Y1 cells elucidated by immunoelectron microscopy and computer-graphic reconstruction. Biol. Cell *68*, 139–146.

Thakur, V.S., Deb, G., Babcook, M.A., and Gupta, S. (2014). Plant phytochemicals as epigenetic modulators: role in cancer chemoprevention. AAPS J. *16*, 151–163.

Thorn, C.F., Oshiro, C., Marsh, S., Hernandez-Boussard, T., McLeod, H., Klein, T.E., and Altman, R.B. (2011). Doxorubicin pathways: pharmacodynamics and adverse effects. Pharmacogenet. Genomics *21*, 440–446.

Thornberry, N.A., and Lazebnik, Y. (1998). Caspases: enemies within. Science *281*, 1312–1316.

Thorpe, G.W., Fong, C.S., Alic, N., Higgins, V.J., and Dawes, I.W. (2004). Cells have distinct mechanisms to maintain protection against different reactive oxygen species: oxidative-stress-response genes. Proc. Natl. Acad. Sci. U. S. A. *101*, 6564–6569.

Trachootham, D., Alexandre, J., and Huang, P. (2009). Targeting cancer cells by ROS-mediated mechanisms: a radical therapeutic approach? Nat. Rev. Drug Discov. *8*, 579–591.

Vandenabeele, P., Galluzzi, L., Vanden Berghe, T., and Kroemer, G. (2010). Molecular mechanisms of necroptosis: an ordered cellular explosion. Nat. Rev. Mol. Cell Biol. *11*, 700–714.

Verhelst, K., Verstrepen, L., Carpentier, I., and Beyaert, R. (2013). IκB kinase ε (IKKε): A therapeutic target in inflammation and cancer. Biochem. Pharmacol. *85*, 873–880.

Wallace, P.K., Tario, J.D., Fisher, J.L., Wallace, S.S., Ernstoff, M.S., and Muirhead, K.A. (2008). Tracking antigen-driven responses by flow cytometry: Monitoring proliferation by dye dilution. Cytometry A *73A*, 1019–1034.

Wang, J.C. (2002). Cellular roles of DNA topoisomerases: a molecular perspective. Nat. Rev. Mol. Cell Biol. *3*, 430–440.

Wang, L.-S., and Stoner, G.D. (2008). Anthocyanins and their role in cancer prevention. Cancer Lett. *269*, 281–290.

Warford, J., Jones, Q.R.D., Nichols, M., Sullivan, V., Rupasinghe, H.P.V., and Robertson, G.S. (2014). The flavonoid-enriched fraction AF4 suppresses neuroinflammation and promotes restorative gene expression in a mouse model of experimental autoimmune encephalomyelitis. J. Neuroimmunol. *268*, 71–83.

Warren, S. (2001). Trypan blue exclusion test of cell viability. Curr. Protoc. Immunol. *21*, A.3B.1-A.3B.2.

Wilhelm, S.M., Adnane, L., Newell, P., Villanueva, A., Llovet, J.M., and Lynch, M. (2008). Preclinical overview of sorafenib, a multikinase inhibitor that targets both Raf and VEGF and PDGF receptor tyrosine kinase signaling. Mol. Cancer Ther. *7*, 3129–3140.

Xie, X., Zhang, D., Zhao, B., Lu, M.K., You, M., Condorelli, G., Wang, C.Y., and Guan, K.-L. (2011). IκB kinase ε and TANK-binding kinase 1 activate AKT by direct phosphorylation. Proc. Natl. Acad. Sci. U. S. A. *108*, 6474–6479.

Xie, Y., Hou, W., Song, X., Yu, Y., Huang, J., Sun, X., Kang, R., and Tang, D. (2016). Ferroptosis: process and function. Cell Death Differ. *23*, 369–379.

Yang, T., Sinai, P., and Kain, S. (1996). An acid phosphatase assay for quantifying the growth of adherent and nonadherent cells. Anal. Biochem. *241*, 103–108.

Yao, H., Xu, W., Shi, X., and Zhang, Z. (2011). Dietary flavonoids as cancer prevention agents. J. Environ. Sci. Health *29*, 1–31.

Yogosawa, S., Yamada, Y., Yasuda, S., Sun, Q., Takizawa, K., and Sakai, T. (2012). Dehydrozingerone, a structural analogue of curcumin, induces cell-cycle arrest at the G2/M Phase and accumulates intracellular ROS in HT-29 human colon cancer cells. J. Nat. Prod. *75*, 2088–2093.

Yu, H., Guo, P., Xie, X., Wang, Y., and Chen, G. (2017). Ferroptosis, a new form of cell death, and its relationships with tumourous diseases. J. Cell. Mol. Med. *21*, 648–657.

Yuan, J., Najafov, A., and Py, B. (2016). Roles of caspases in necrotic cell death. Cell *167*, 1693–1704.

Zembruski, N.C.L., Stache, V., Haefeli, W.E., and Weiss, J. (2012). 7-Aminoactinomycin D for apoptosis staining in flow cytometry. Anal. Biochem. *429*, 79–81.

Zhang, J., and Powell, S.N. (2005). The role of the BRCA1 tumor suppressor in DNA double-strand break repair. Mol. Cancer Res. *3*, 531.

Zhang, E., Han, L., Yin, D., He, X., Hong, L., Si, X., Qiu, M., Xu, T., De, W., Xu, L., et al. (2017). H3K27 acetylation activated-long non-coding RNA CCAT1 affects cell proliferation and migration by regulating SPRY4 and HOXB13 expression in esophageal squamous cell carcinoma. Nucleic Acids Res. *45*, 3086–3101.

Zheng, J.Y., Tan, H.L., Matsudaira, P.T., and Choo, A. (2017). Excess reactive oxygen species production mediates monoclonal antibody-induced human embryonic stem cell death via oncosis. Cell Death Differ. *24*, 546.

APPENDIX A: TABLES

Table 1. Concentration of AF4 Components. Adapted from Sudan and Rupasinghe, (2014).

Compound	Concentration (mg/mL)
Flavonols	**8770.7**
Quercetin	9.9 ± 0.3
Quercetin-3-*O*-paltoside	63.8 ± 2.4
Quercetin-3-*O*-rutinoside	1535.7 ± 46.2
Quercetin-3-*O*-galactoside	2914.9± 72.8
Quercetin-3-*O*-glucoside	1474.8 ± 58.9
Quercetin-3-*O*-rhamnoside	2771.6 ± 77.5
Phenolic acids	**1264.7**
Chlorogenic acid	1221.1 ± 31.2
Cafeic acid	43.6 ± 2.0
Flavan-3-ols	**1151.1**
Catechin	106.8 ± 3.7
Epicatechin	1044.3 ± 36.8
Anthocyanins	**559.4**
Cyanidin-3-*O*-galactoside	559.4 ± 16.7
Dihydrochalcones phloridzin	**386.8 ± 13.6**
Total phenolics	**12132.7**

Table 2. Anti-Cancer Effects of Widely Studied Phytochemicals Also Found in AF4

Phytochemical	Cell cycle inhibition	Anti-proliferation mechanism	Cell death mechanism	Epigenetic effects
Quercetin	G2 (Rivera Rivera et al., 2016)	PI3K/Akt (Rivera Rivera et al., 2016)	Apoptosis (Khorsandi et al., 2017)	DNMT1, HDAC 1 and 2 inhibition (Bishayee et al., 2015)
EGCG	G2 (Gianfredi et al., 2017)	NFκB (Gu et al., 2013)	Caspase-dependent apoptosis (Gianfredi et al., 2017)	DNMT1, HAT inhibition (Choi et al., 2009; Lee et al., 2012)
Cyanidin-3-*O*-galactoside	Unknown	Unknown	Unknown	Unknown
Phloridzin	No effect (Fernando et al., 2016)	No effect (Nair et al., 2014)	No effect (Fernando et al., 2016)	Unknown

APPENDIX B: FIGURES

Figure 1. Overview of the Cell Cycle. Progression through the cell cycle is controlled by the expression of cyclins and CDKs. Progression through the G1 stage of the cell cycle is partially mediated by the D cyclins, which couple to CDK4 and CDK6. This results in phosphorylation and inactivation of Rb. The coupling of E cyclins with CDK2 also contribute to the progression from the G1 stage to the S phase. Progression from the S phase to the G2 phase is mediated by the coupling of CDK2 with the A cyclins. Lastly, CDK1 activation by both A and C cyclins is required for the progression from the G2 phase into the M phase.

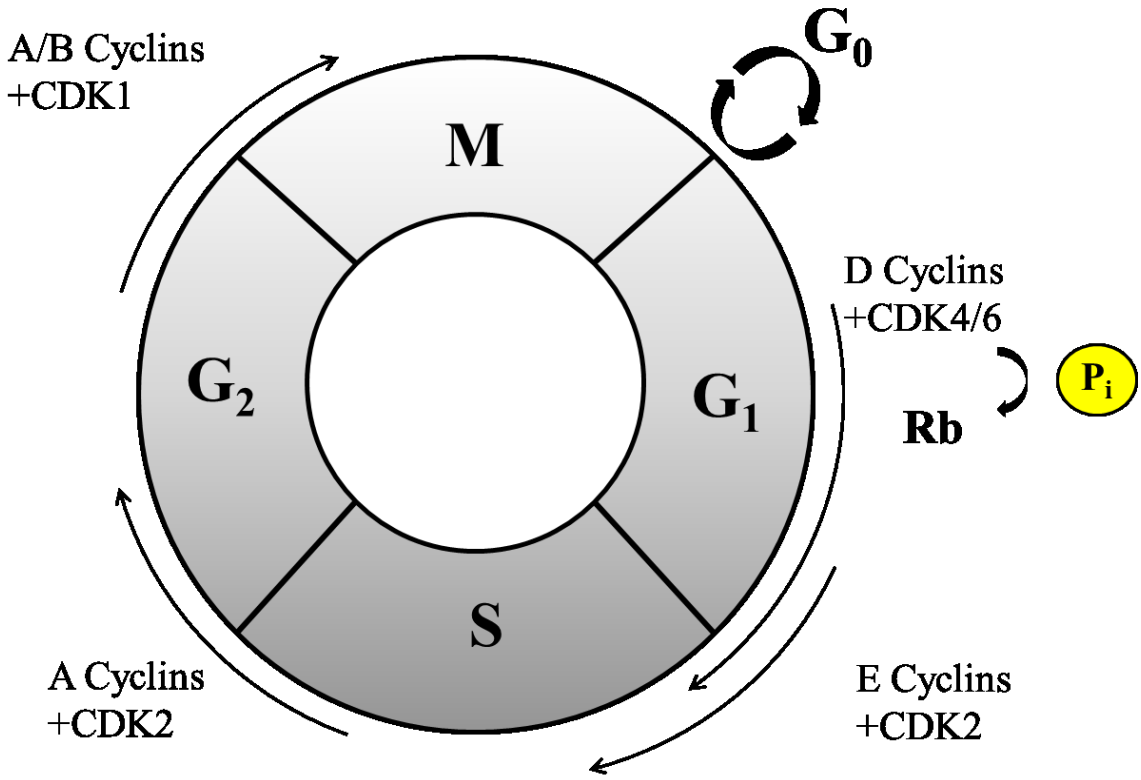

Figure 1. Overview of the Cell Cycle

Figure 2. PI3K/Akt and MAPK/ERK Signalling Pathways. The PI3K/Akt and MAPK/ERK pathways are two extensively studied signalling pathways involved in cancer initiation and progression. The binding of external growth factors signals for the phosphorylation and activation of numerous proteins in both pathways, which ultimately lead to increased cell survival and cell proliferation signals. This is accomplished via the upregulation of pro-survival gene expression and downregulation of pro-apoptotic gene expression to prevent cell death, and the dysregulation of the cell cycle, leading to uncontrolled cell proliferation. Dysregulation of the PI3K/Akt and MAPK/ERK pathways can occur through a variety of mechanisms, including the over-expression of extracellular receptors, over-expression of genes within these signalling pathways, or gene mutations in tumor suppressor genes that would otherwise inhibit the increase in survival and proliferation signals.

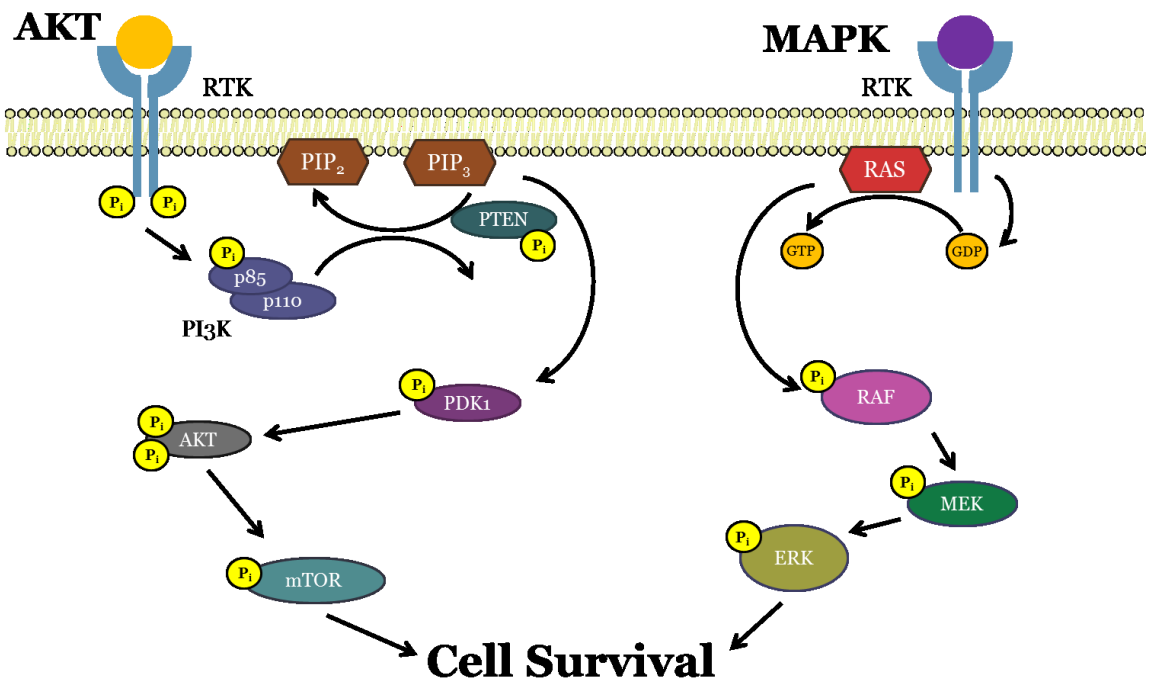

Figure 2. PI3K/Akt and MAPK/ERK Signalling Pathways

Figure 3. Structures of Major AF4 Components. A variety of phytochemicals are present in AF4, some of which are shown here. The anti-cancer effects of some of these phytochemicals have been intensively studied in numerous cancers and show potential to serve as selective cancer treatment agents.

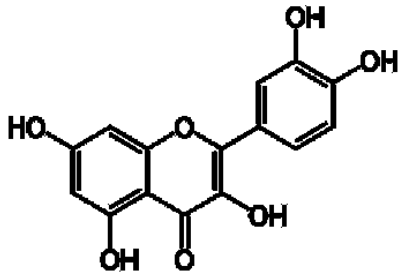

Quercetin

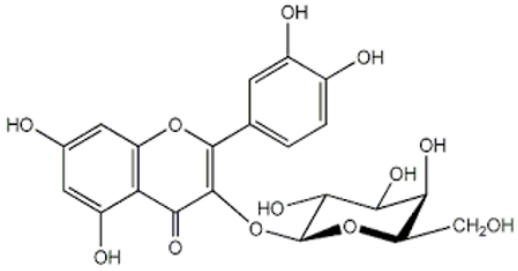

Quercetin-3-O-glucoside

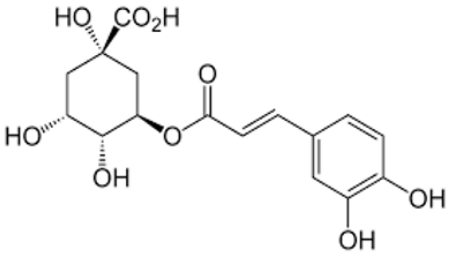

Chlorogenic acid

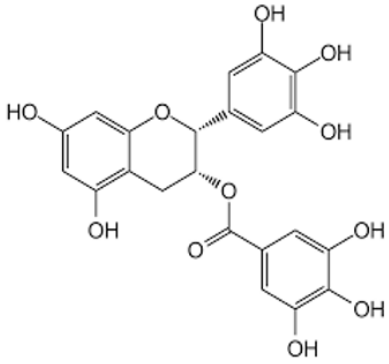

Epicatechin

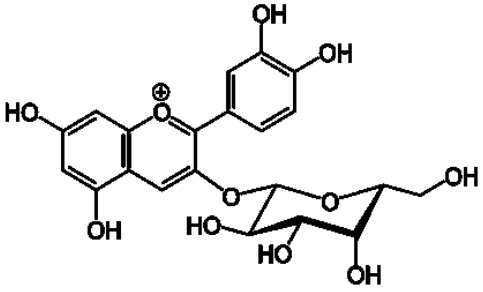

Cyanidin-3-O-galactoside

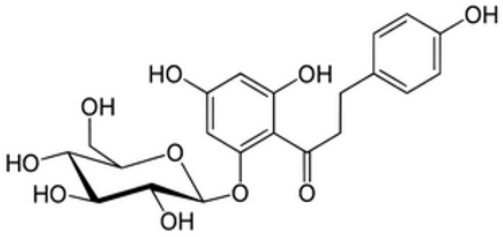

Phloridzin

Figure 3. Structures of Major AF4 Components

Figure 4. ROS-Mediated Anti-Survival and Growth Inhibition Signalling Pathways. Numerous anti-growth pathways are thought to be induced by ROS-mediated effects in cells. These include ROS-mediated activation of PP2A, which in turn activates Akt, GSK3β, and β-catenin. Other pathways include p-38 and JNK MAPKs. These pathways all work to promote apoptosis and inhibit proliferation signals in the cell and can be activated by mitochondrial ROS that are released as a consequence of signals for apoptosis or damage to mitochondrial membranes

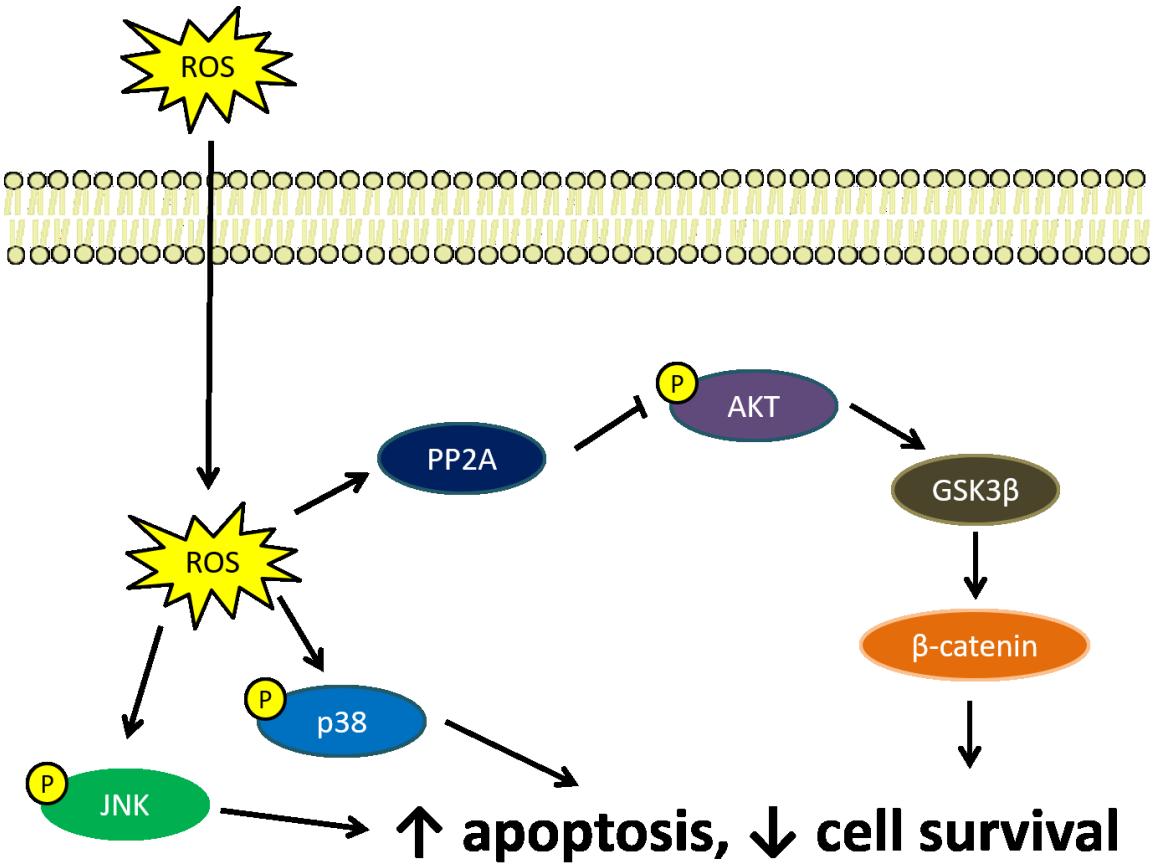

Figure 4. ROS-Mediated Anti-Survival and Growth Inhibition Signalling Pathways

Figure 5. AF4 Induces Morphological Changes in MDA-MB-231 and MDA-MB-468 Breast Cancer Cells but Not in MCF10A Epithelial Cells. MDA-MB-231 and MDA-MB-468 triple-negative breast cancer cells and transformed but non-malignant MCF10A epithelial cells were treated with 50 µg/mL of AF4 for 24 h to determine if AF4 induced any morphological changes. Arrows represent cells with changes in morphology that differ from the non-treated cells. Representative images shown from three independent trials. Images of cells were obtained with a phase contrast microscope at 200 x magnification.

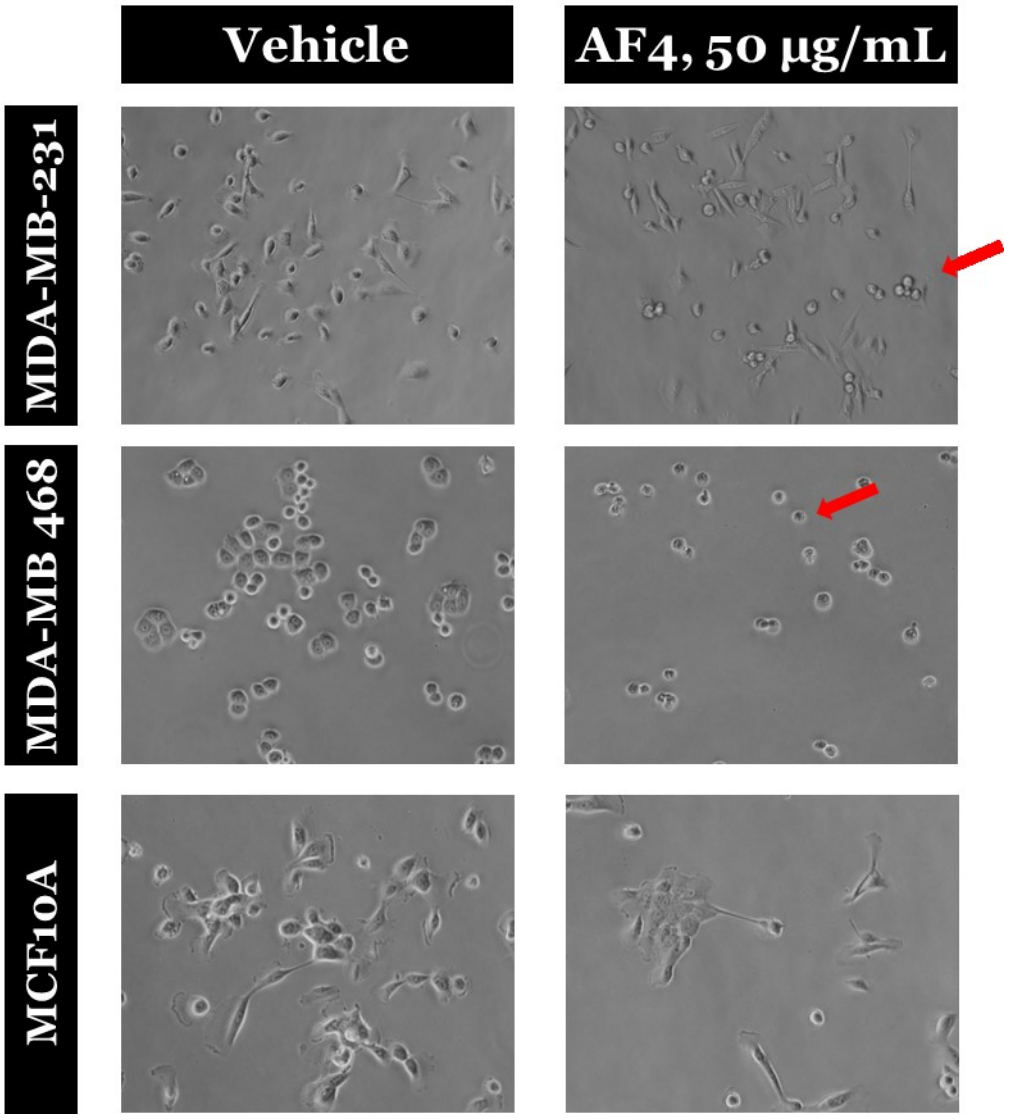

Figure 5. AF4 Induces Morphological Changes in MDA-MB-231 and MDA-MB-468 Breast Cells but Not in MCF10A Epithelial Cells

Figure 6. AF4 and Quercetin Inhibit the Growth of a Panel of Breast Cancer Cell Lines in a Dose- and Time-Dependent Manner in an MTT Assay. The growth inhibitory effects of AF4 were compared to those of quercetin against a panel of breast cancer cell lines as well as healthy cell lines in an MTT assay. These cell lines included human MDA-MB-231 triple-negative breast cancer cells (A), MDA-MB-468 triple-negative breast cancer cells (B), hormone receptor positive MCF-7 breast cancer cells (C), HER2-overexpressing SKBR breast cancer cells (D), and MCF10A transformed epithelial cells (E). Murine 4T1 triple-negative mammary carcinoma cells (F) and HC11 transformed epithelial cells (G) were also used. Cells were seeded at 5 x 10^3 cells per well in a flat-bottom 96-well plate and allowed to adhere overnight. After incubation, cells were treated with various concentrations (25 μg/mL -200 μg/mL) of AF4 and quercetin for 24, 48, and 72-h. After culture, MTT was added and solubilized with DMSO. Absorbance values were then read and normalized relative to the medium control. Data represented as mean values ± SEM of five independent trials. Significant reductions in growth were determined by ANOVA with the Tukey-Kramer multiple comparisons post-test, with * used to represent significant differences to the medium control, and # used to represent significant differences between timepoints; $p < 0.05$ denoted by * or #, < 0.01 denoted by ** or ##, and < 0.001 denoted by *** or ###.

A.

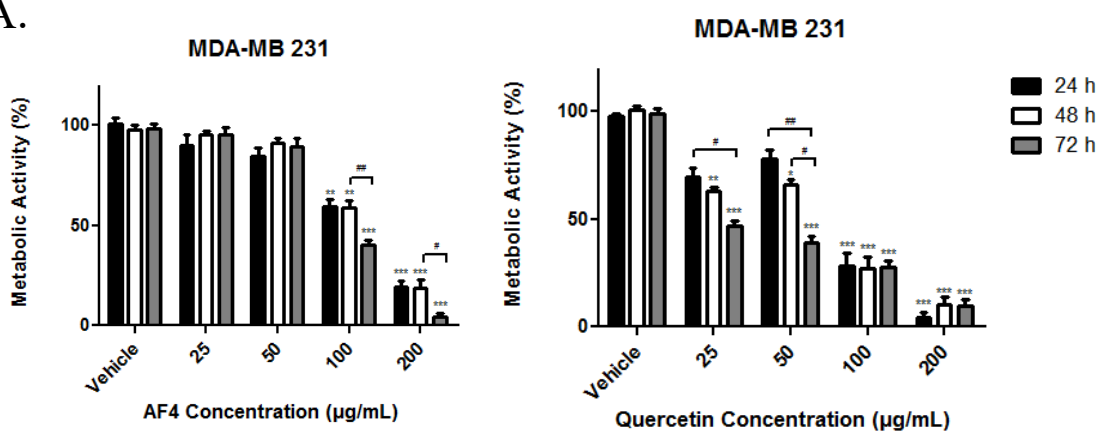
MDA-MB 231
Metabolic Activity (%)
100
50
0
Vehicle
25
50
100
200
AF4 Concentration (µg/mL)
MDA-MB 231
Metabolic Activity (%)
100
50
0
Vehicle
25
50
100
200
Quercetin Concentration (µg/mL)
24 h
48 h
72 h

B.

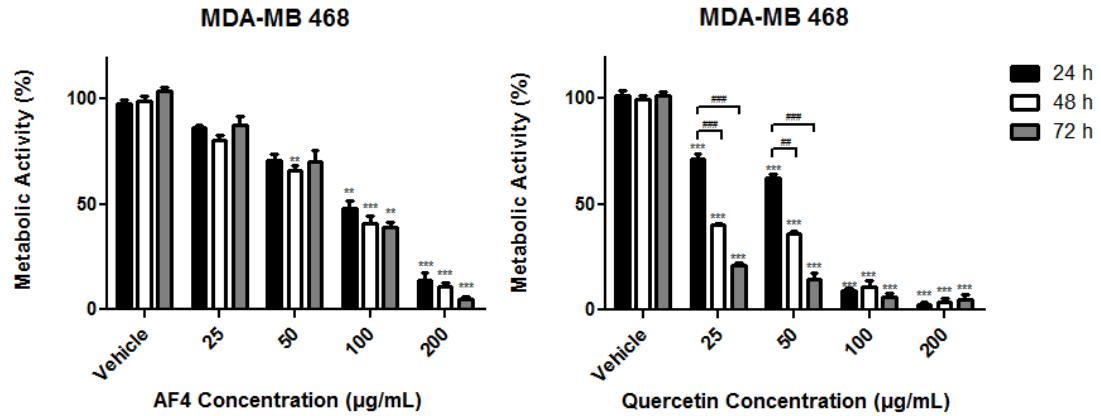
MDA-MB 468
Metabolic Activity (%)
100
50
0
Vehicle
25
50
100
200
AF4 Concentration (µg/mL)
MDA-MB 468
Metabolic Activity (%)
100
50
0
Vehicle
25
50
100
200
Quercetin Concentration (µg/mL)
24 h
48 h
72 h

C.

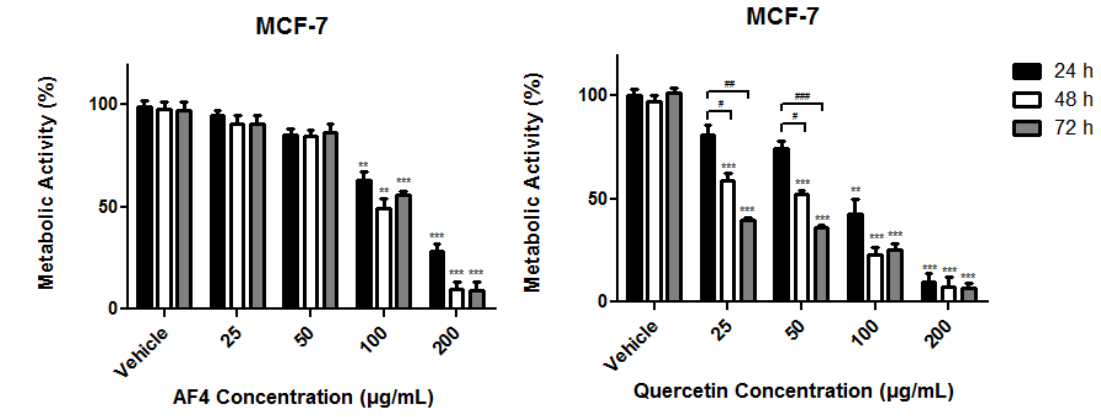
MCF-7
Metabolic Activity (%)
100
50
0
Vehicle
25
50
100
200
AF4 Concentration (µg/mL)
MCF-7
Metabolic Activity (%)
100
50
0
Vehicle
25
50
100
200
Quercetin Concentration (µg/mL)
24 h
48 h
72 h

D.

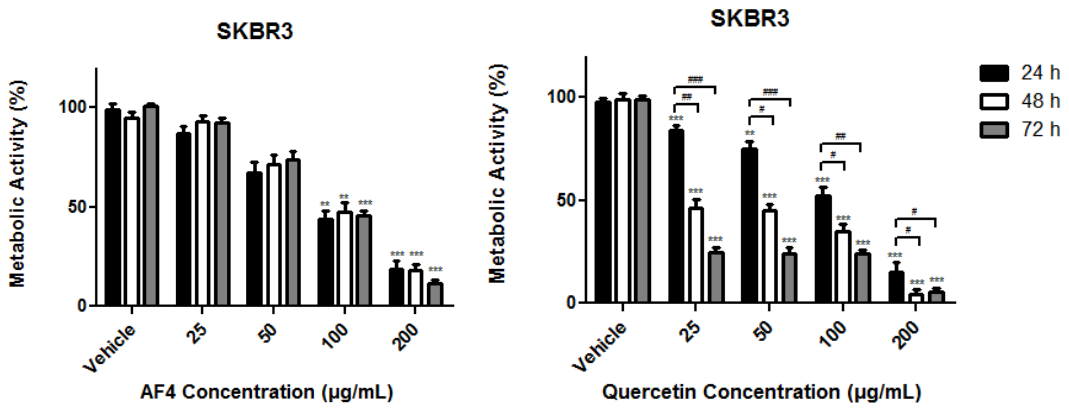
SKBR3
Metabolic Activity (%)
100
50
0
Vehicle
25
50
100
200
AF4 Concentration (µg/mL)
SKBR3
Metabolic Activity (%)
Quercetin Concentration (µg/mL)
24 h
48 h
72 h

E.

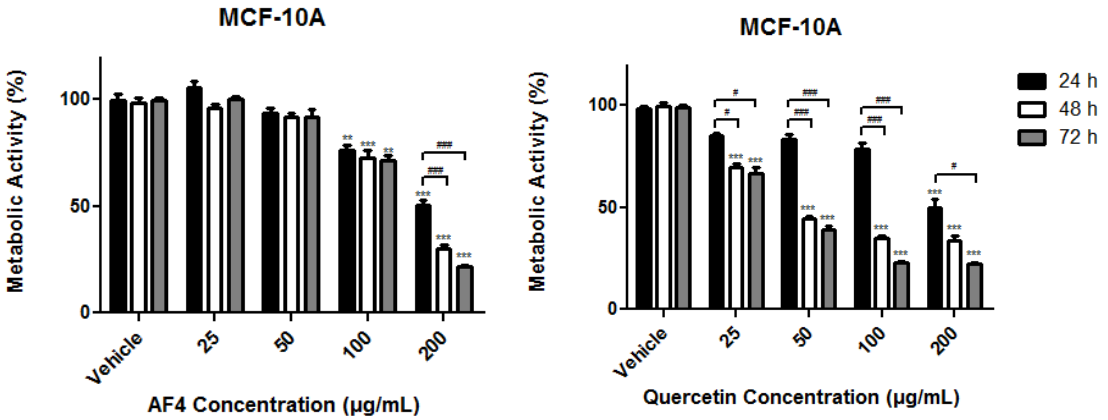
MCF-10A
Metabolic Activity (%)
100
50
0
Vehicle
25
50
100
200
AF4 Concentration (µg/mL)
MCF-10A
Metabolic Activity (%)
Quercetin Concentration (µg/mL)
24 h
48 h
72 h

F.

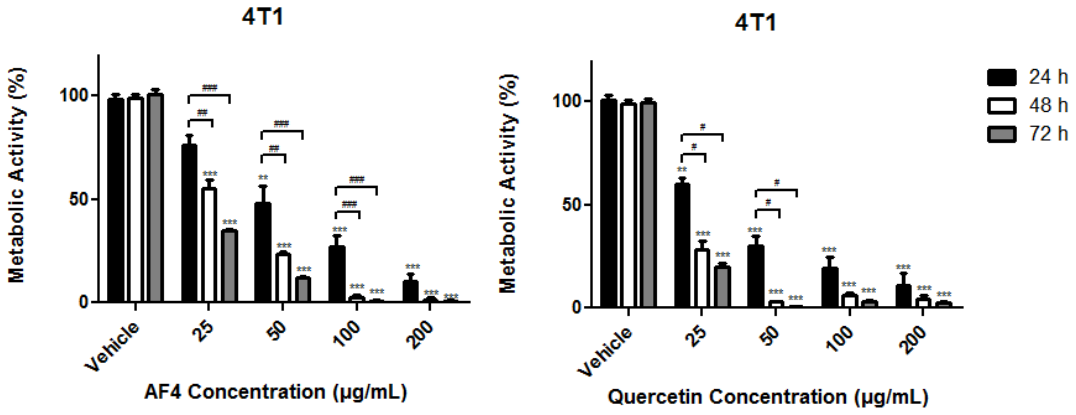

G.

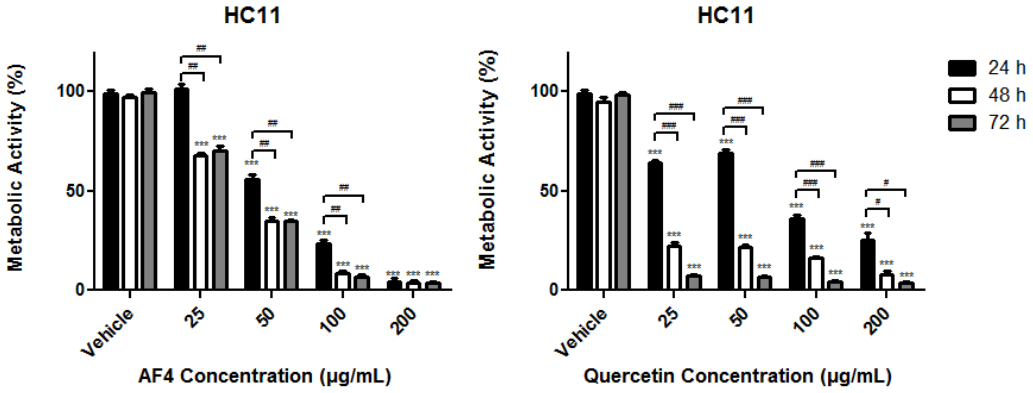

Figure 6. AF4 and Quercetin Inhibit the Growth of a Panel of Breast Cancer Cell Lines in a Dose- and Time-Dependent Manner in an MTT Assay

Figure 7. AF4 and Quercetin React with MTT. The absorbance values of AF4 and quercetin with MTT in the absence of cells was determined. AF4 and quercetin at various concentrations (25 µg/mL -200 µg/mL) was aliquoted into an empty flat-bottom 96-well plate and left to incubate for 24 h. These also served as cell-free controls for MTT. MTT was then added to each well and allowed to incubate for an addition 2 h. Formazan crystals were then dissolved in DMSO. Data shown as mean values ± SEM of three independent trials. Significance was determined by ANOVA with the Tukey-Kramer multiple comparisons post-test, and is denoted by * for $p < 0.05$, ** for $p < 0.01$, and *** for < 0.001.

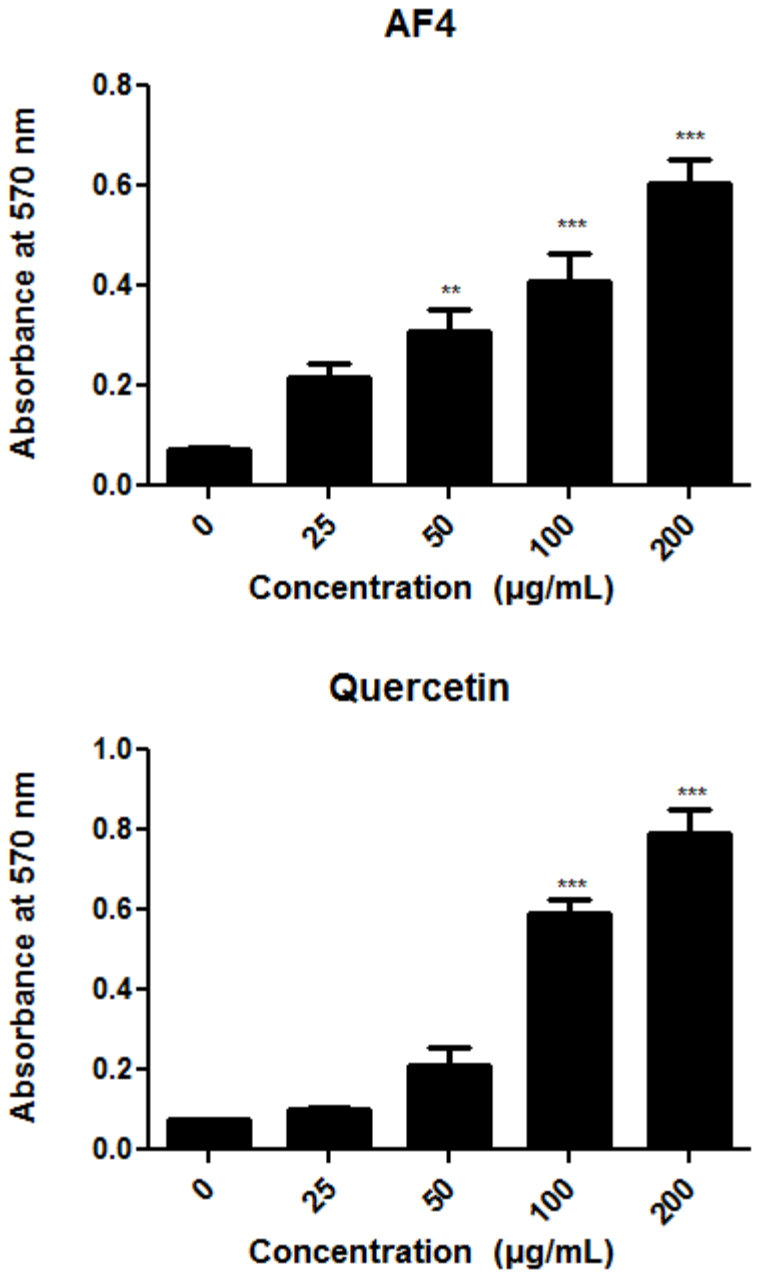

Figure 7. AF4 and Quercetin React with MTT.

Figure 8. AF4 and Quercetin Inhibit the Growth of Breast Cancer Cell Lines in a Dose- and Time-Dependent Manner in an Acid Phosphatase Assay. The growth inhibitory effects of AF4 and quercetin were confirmed with the acid phosphatase assay. These cell lines included human MDA-MB-231 triple-negative breast cancer cells (A), MDA-MB-468 triple-negative breast cancer cells (B), hormone receptor positive MCF-7 breast cancer cells (C), HER2-overexpressing SKBR breast cancer cells (D), and MCF10A transformed epithelial cells (E). Murine 4T1 triple-negative mammary cancer cells (F) and HC11 transformed epithelial cells (G) were also used. Cells were seeded at 5 x 10^3 cells per well in a flat-bottom 96-well plate and allowed to adhere overnight. After incubation, cells were treated with various concentrations (25 µg/mL -200 µg/mL) of AF4 or quercetin for 24, 48, and 72-hour time-points. After treatment, acid phosphatase substrate was added. Absorbance values were then read and normalized relative to the medium control. Data are shown as mean values ± SEM of three independent trials. Significance was determined by ANOVA with the Tukey-Kramer multiple comparisons post-test, and is denoted by * for $p < 0.05$, ** for $p < 0.01$, and *** for <0.001. Differences between time points are denoted by # for $p < 0.05$, ## for $p < 0.01$, and ### for < 0.001.

A.

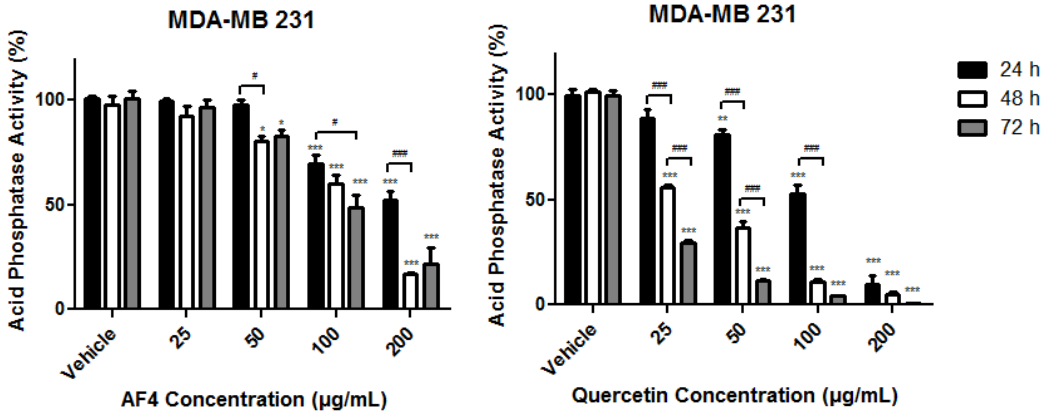
MDA-MB 231
Acid Phosphatase Activity (%)
AF4 Concentration (µg/mL)
Vehicle
25
50
100
200
MDA-MB 231
Quercetin Concentration (µg/mL)
24 h
48 h
72 h

B.

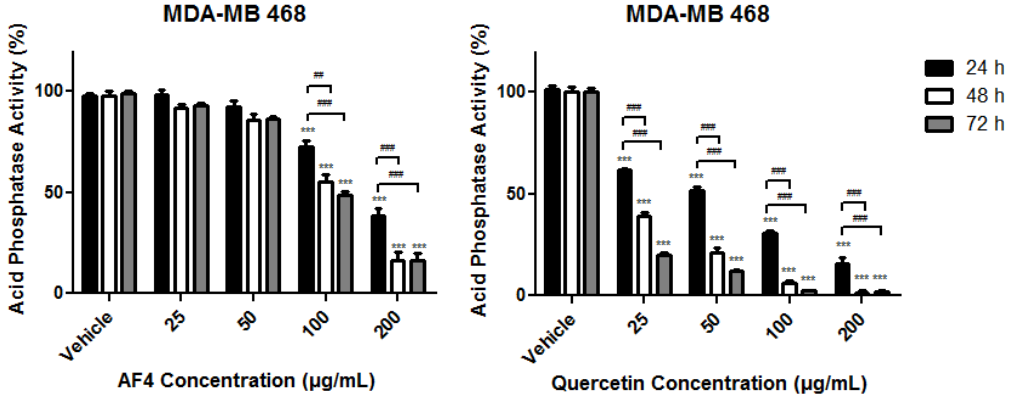
MDA-MB 468
Acid Phosphatase Activity (%)
AF4 Concentration (µg/mL)
Vehicle
25
50
100
200
MDA-MB 468
Quercetin Concentration (µg/mL)
24 h
48 h
72 h

C.

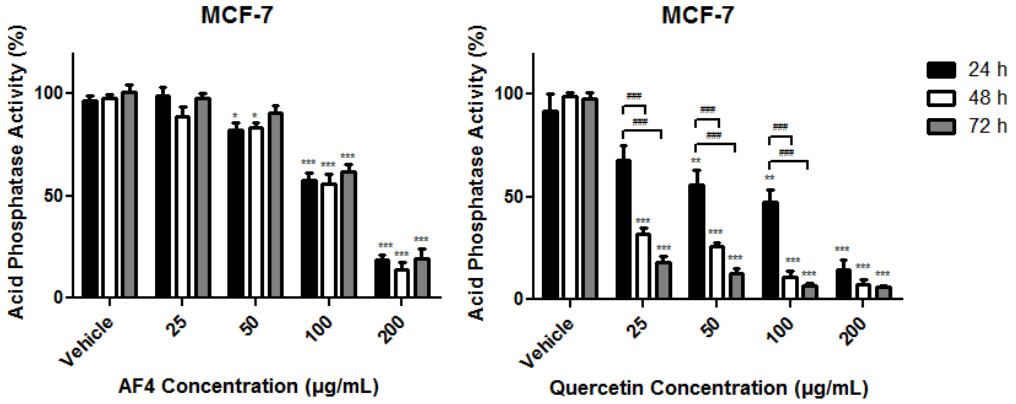
MCF-7
Acid Phosphatase Activity (%)
AF4 Concentration (µg/mL)
Vehicle
25
50
100
200
MCF-7
Quercetin Concentration (µg/mL)
24 h
48 h
72 h

D.

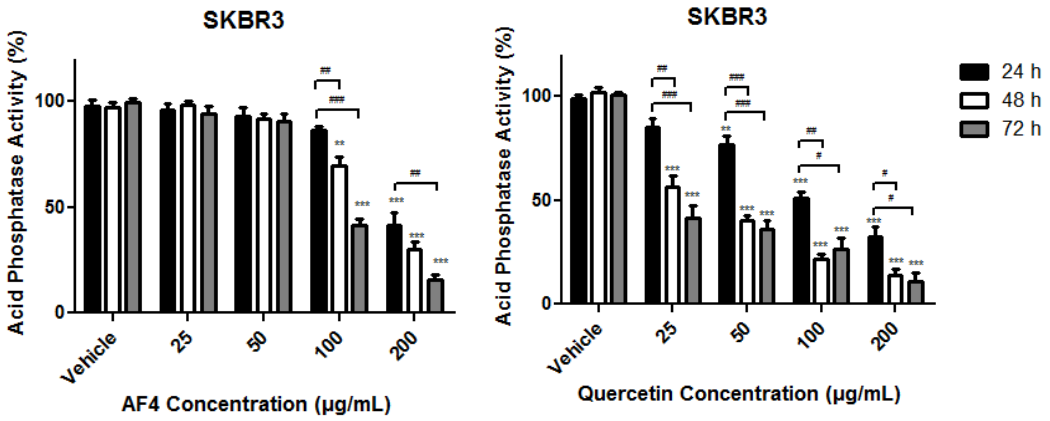
SKBR3
Acid Phosphatase Activity (%)
100
50
0
Vehicle
25
50
100
200
AF4 Concentration (µg/mL)
SKBR3
Acid Phosphatase Activity (%)
Quercetin Concentration (µg/mL)
24 h
48 h
72 h

E.

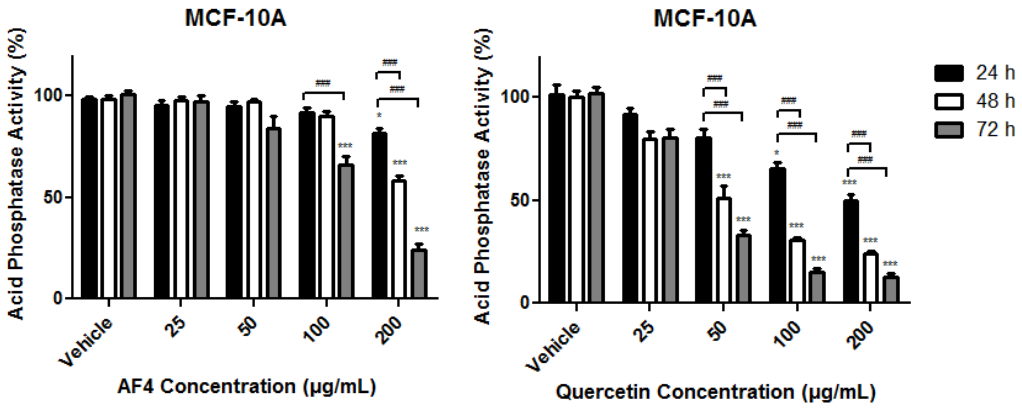
MCF-10A
Acid Phosphatase Activity (%)
100
50
0
Vehicle
25
50
100
200
AF4 Concentration (µg/mL)
MCF-10A
Acid Phosphatase Activity (%)
Quercetin Concentration (µg/mL)
24 h
48 h
72 h

F.

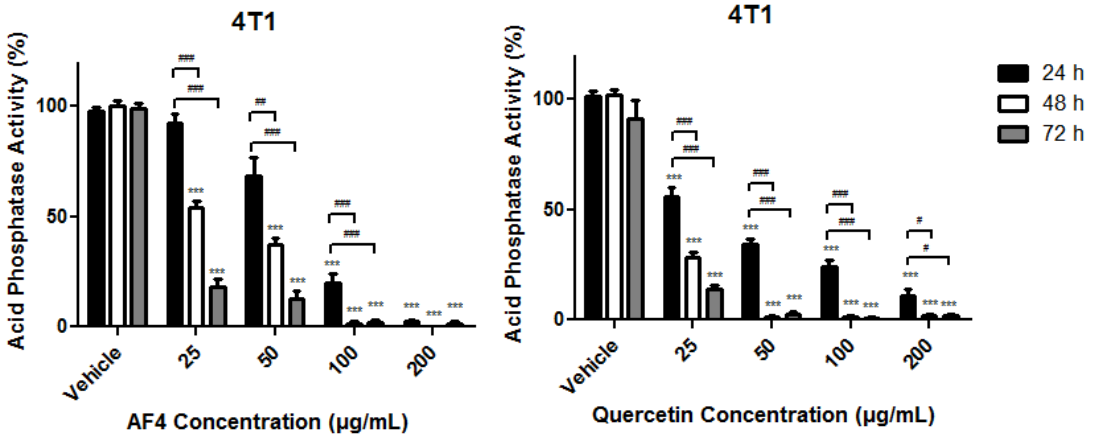

G.

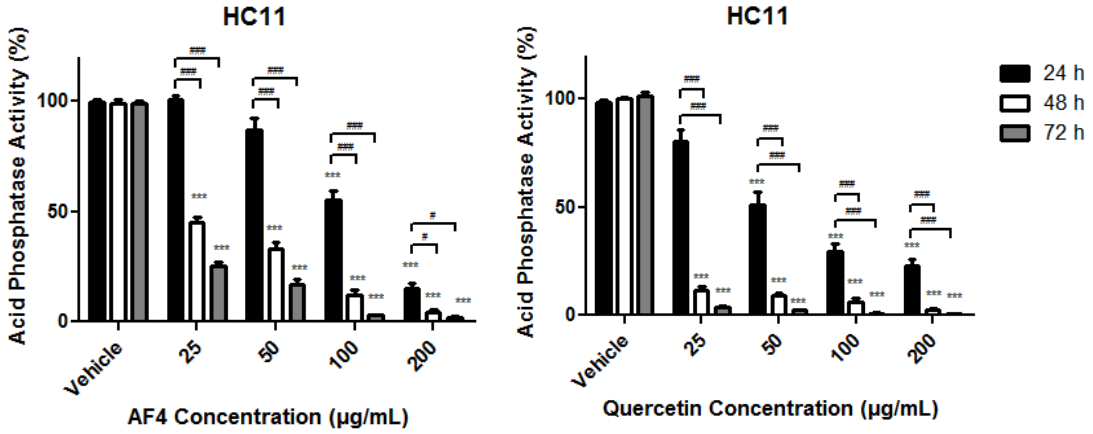

Figure 8. AF4 and Quercetin Inhibit the Growth Breast Cancer Cell Lines in a Dose- and Time-Dependent Manner in an Acid Phosphatase Assay

Figure 9. AF4 is a More Selective Inhibitor of Breast Cancer Cell Growth Than Quercetin in MTT and Acid Phosphatase Assays. The growth inhibitory effect of AF4 and quercetin were compared on breast cancer cells and healthy MCF10A cells with MTT and acid phosphatase assays. AF4 (A) and quercetin (B) at 100 µg/mL was used to treat a panel a breast cancer cell lines and the healthy epithelial cell line MCF10A for 72 h, and then the growth was measured with the MTT assay. Observations of growth inhibitory responses were compared to those of the MCF10A cells. The growth of MCF10A cells following exposure to AF4 or quercetin in MCF10A cells for 72 h was compared with MTT and acid phosphatase assays (C). Data shown as mean values ± SEM of five independent trials. Significance was determined by ANOVA with the Tukey-Kramer multiple comparisons post-test, and is denoted by * for $p < 0.05$, ** for $p < 0.01$, and *** for < 0.001. Differences between AF4 and quercetin are denoted by # for $p < 0.05$, ## for $p < 0.01$, and ### for < 0.001.

A. AF4

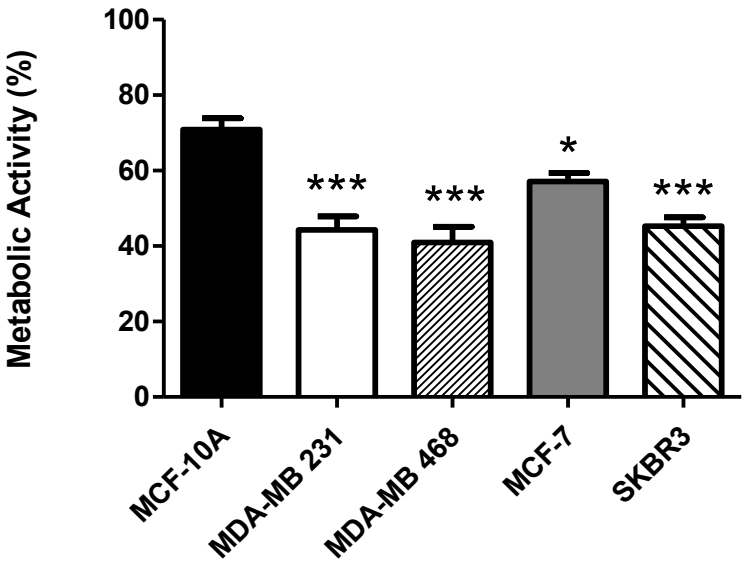

B. Quercetin

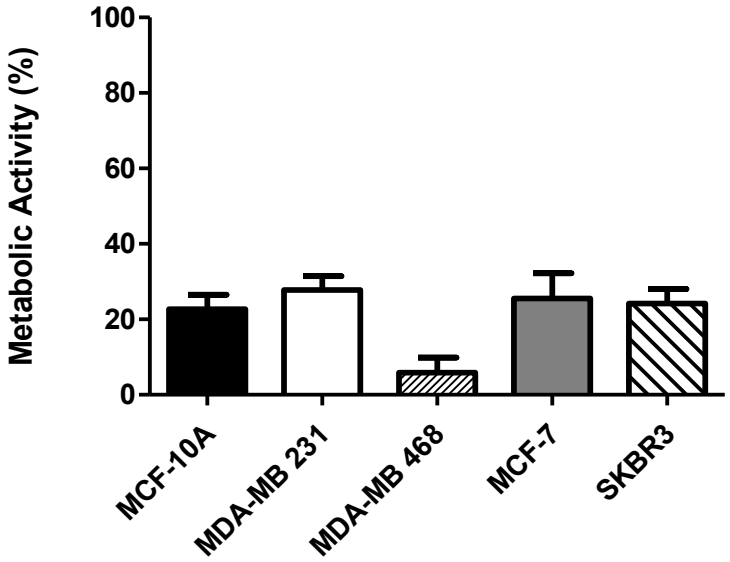

C.

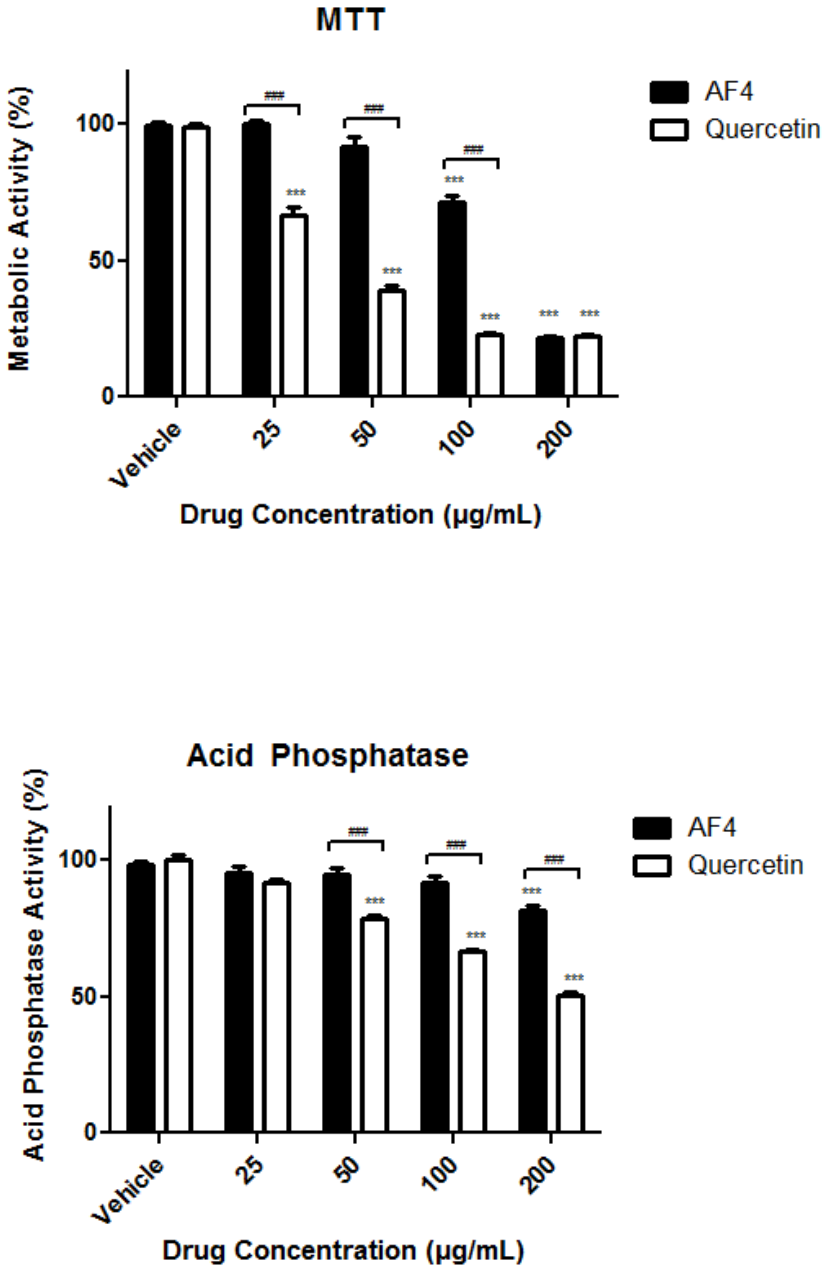

Figure 9. AF4 is a More Selective Inhibitor of Breast Cancer Cell Growth Than Quercetin in MTT and Acid Phosphatase Assays

Figure 10. AF4 and Quercetin Selectively Induce Cell Death in MDA-MB-231 and MDA-MB-468 Breast Cancer Cells in a Trypan Blue Assay. The ability of AF4 to kill breast cancer cells was determined with a trypan blue assay. MDA-MB-231 (A), and MDA-MB-468 (B) triple-negative breast cancer cells, and MCF10A epithelial cells (C) were seeded at a density of 20,000 cells per well for and allowed to adhere overnight prior to treatment with AF4 or quercetin at various concentrations (30 µg/mL -100 µg/mL) for 24 h, 48 h, and 72 h. Cells were then stained with trypan blue and the percentage of live cells found in the population was normalized to the medium control. Data are shown as mean values ± SEM of three independent trials. Significance was determined by ANOVA with the Tukey-Kramer multiple comparisons post-test, and is denoted by * for $p < 0.05$, ** for $p < 0.01$, and *** for < 0.001.

A. MDA-MB-231

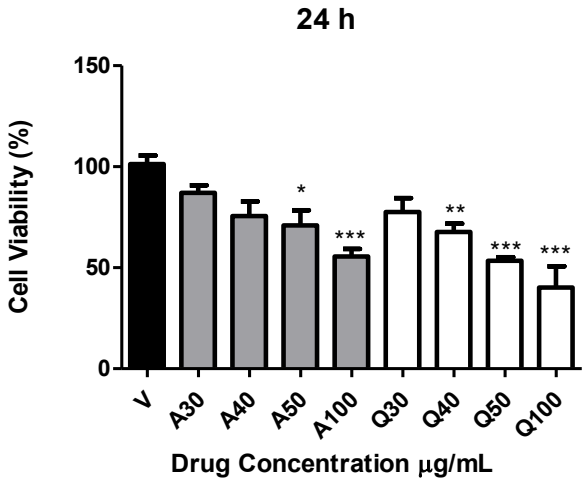

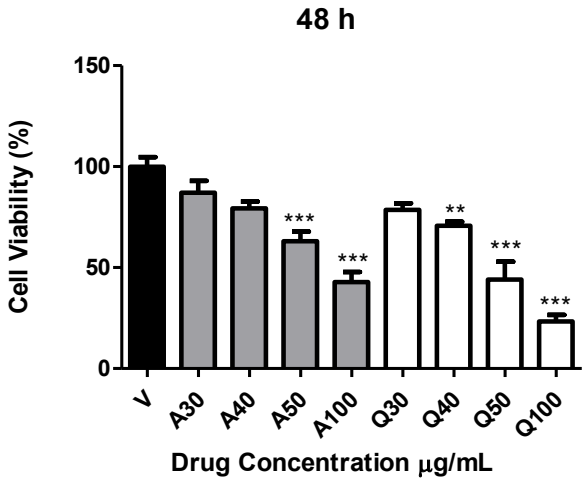

V – Vehicle

A – AF4

Q- Quercetin

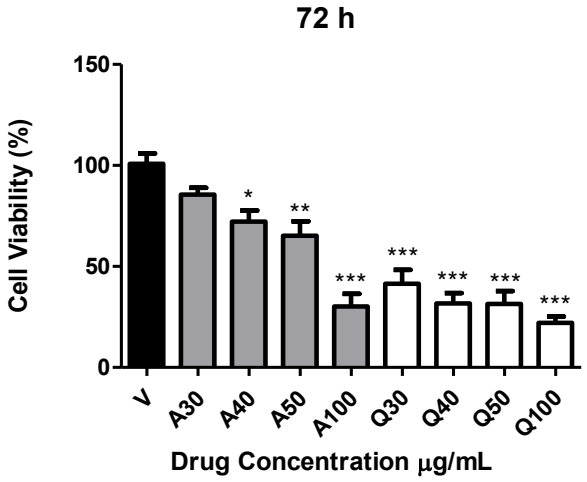

B. MDA-MB-468

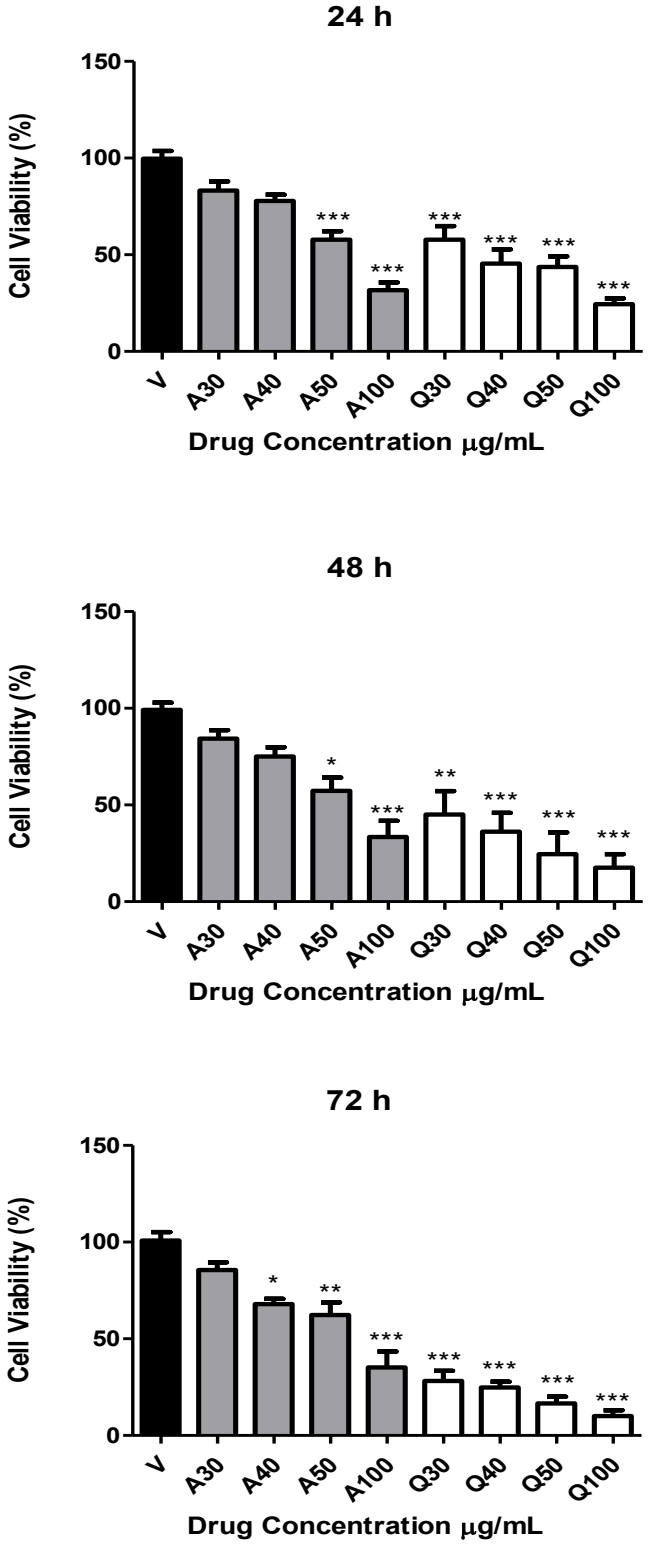

V – Vehicle

A – AF4

Q- Quercetin

C. MCF10A

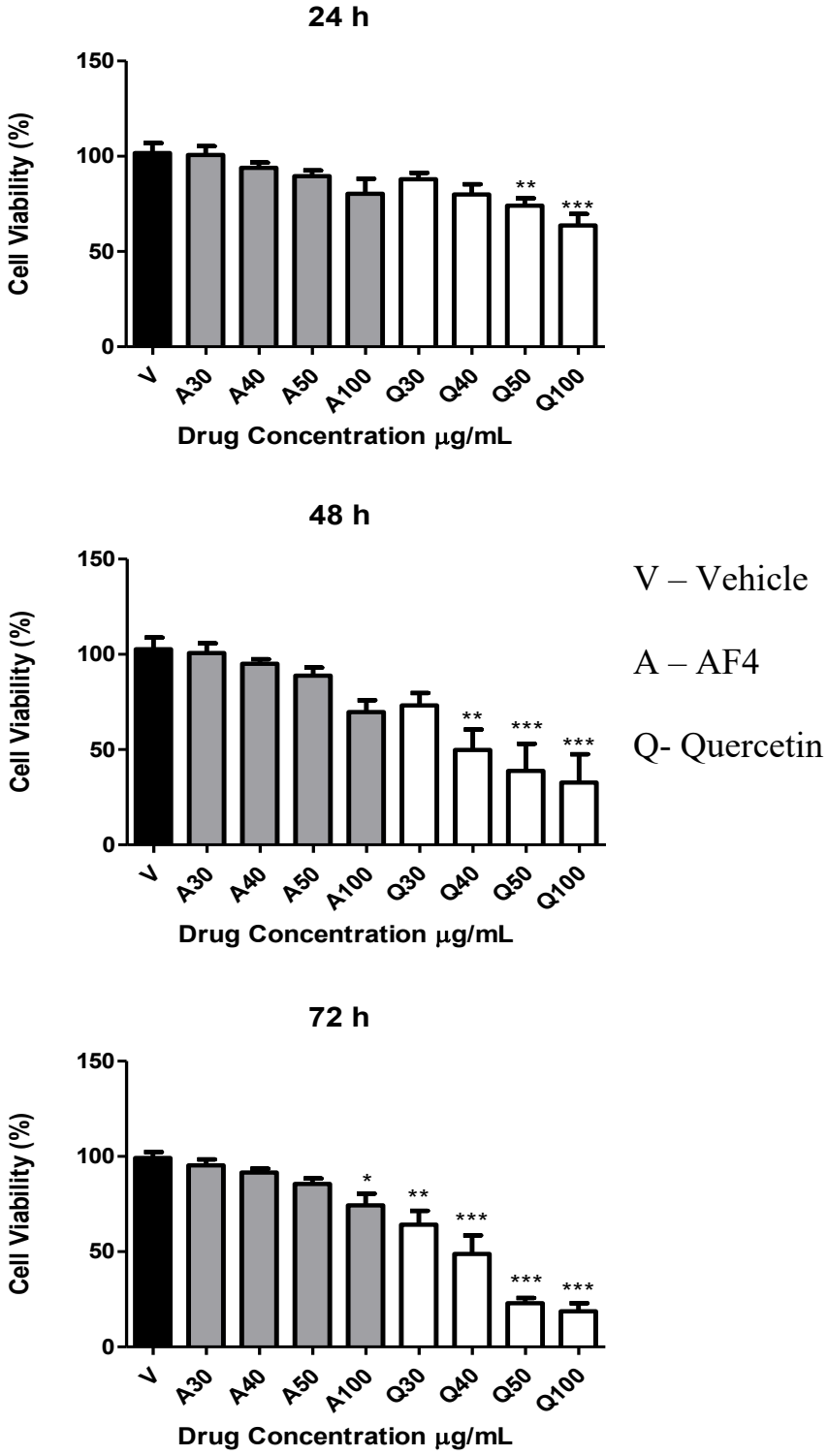

Figure 10. AF4 and Quercetin Selectively Induces Cell Death in MDA-MB-231 and MDA-MB-468 Cells Breast Cancer in a Trypan Blue Assay

Figure 11. AF4 and Quercetin Are Fluorescent. The fluorescence of cells exposed to AF4 (A) or quercetin (B) for a brief period of time was determined with flow cytometry. MDA-MB-231 cells were plated at a density of 50,000 cells per well in a 6-well plate and allowed to adhere overnight. Cells were then treated with 50 μg/mL of AF4 or quercetin for 15 min so that the compounds were taken into cells, which were then washed and read on the flow cytometer.

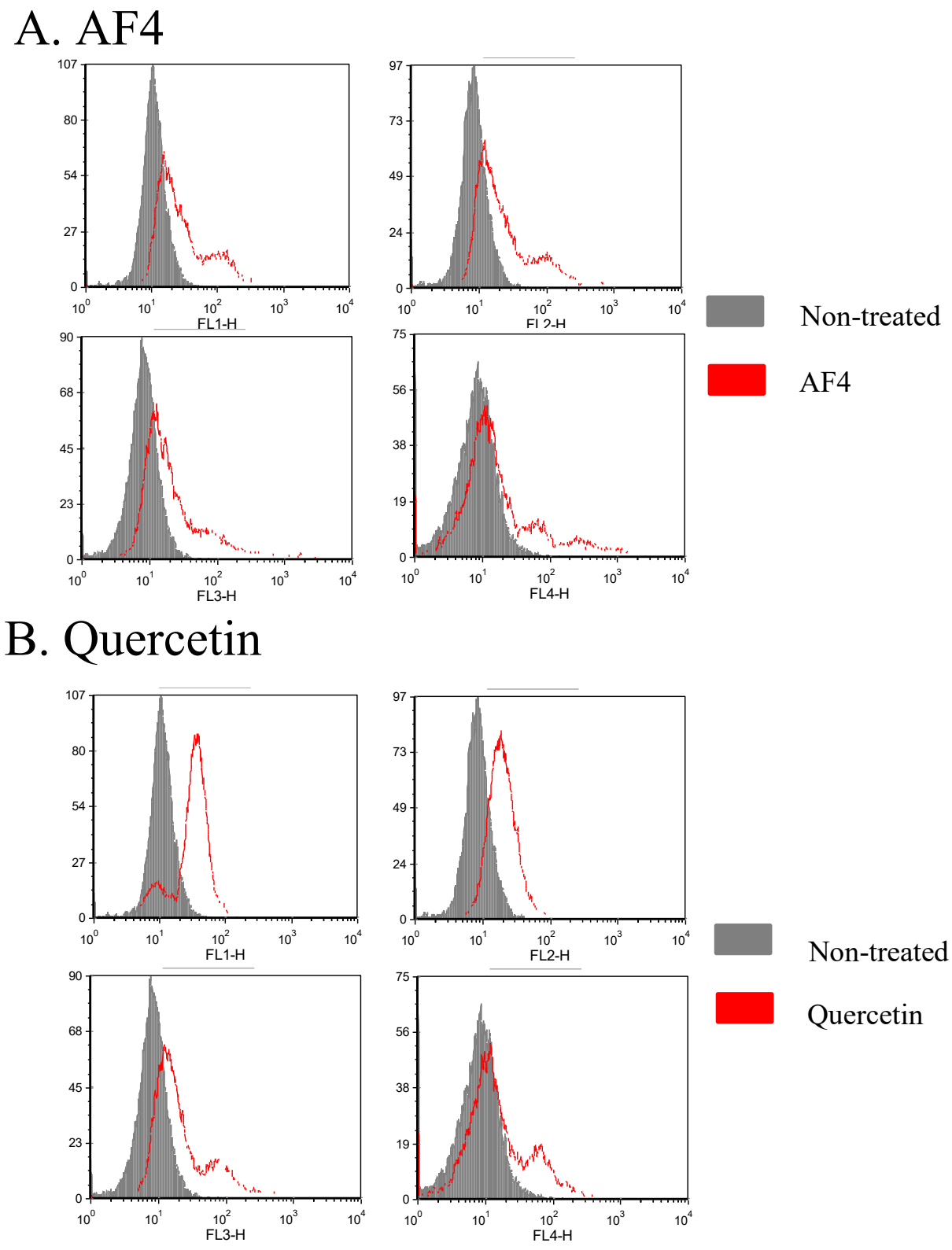

Figure 11. AF4 and Quercetin Are Fluorescent.

Figure 12. AF4 Causes Dose- and Time-Dependent Cell Death in MDA-MB-231 and MDA-MB-468 Breast Cancer Cells in a 7-AAD Assay. The cytotoxicity of AF4 was confirmed with 7-AAD staining and FACS. MDA-MB-231 (A) and MDA-MB-468 (B) triple-negative breast cancer cells were seeded at a density of 50,000 cells per well in a 6-well plate and allowed to adhere overnight. Cells were then treated with AF4 (30 μg/mL – 100 μg/mL) for 24, 48, and 72-h. Cells were stained with 7-AAD for 5 minutes prior to reading in a flow cytometer at FL3. Representative histograms are provided for vehicle and 100 μg/mL of AF4 treatment after 24 h and 72 h of treatment for each cell line. Marker 1 (M1) represents live cells while Marker 2 (M2) represents dead cells. Data are shown as mean values ± SEM of four independent trials. Significance was determined by ANOVA with the Tukey-Kramer multiple comparisons post-test, and is denoted by * for $p < 0.05$, ** for $p < 0.01$, and *** for $p < 0.001$. Differences between time points are denoted by # for $p < 0.05$, ## for $p < 0.01$, and ### for < 0.001.

A. MDA-MB-231

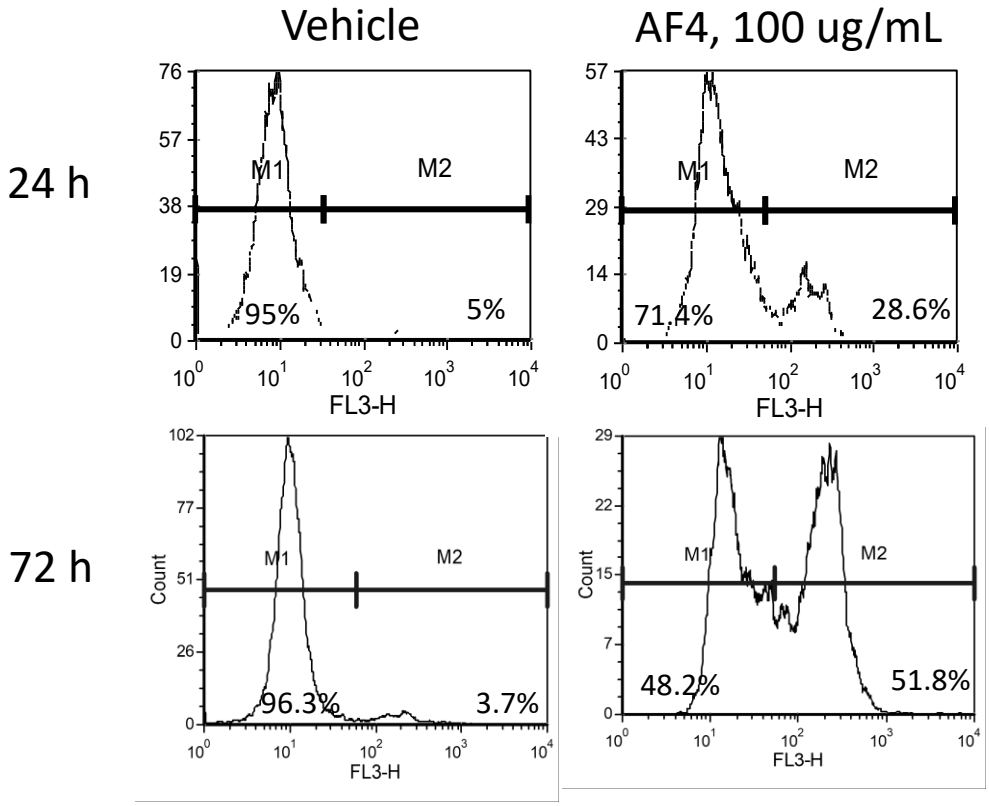
Vehicle
AF4, 100 ug/mL
24 h
72 h
M1
M2
95%
5%
71.4%
28.6%
96.3%
3.7%
48.2%
51.8%
FL3-H
Count

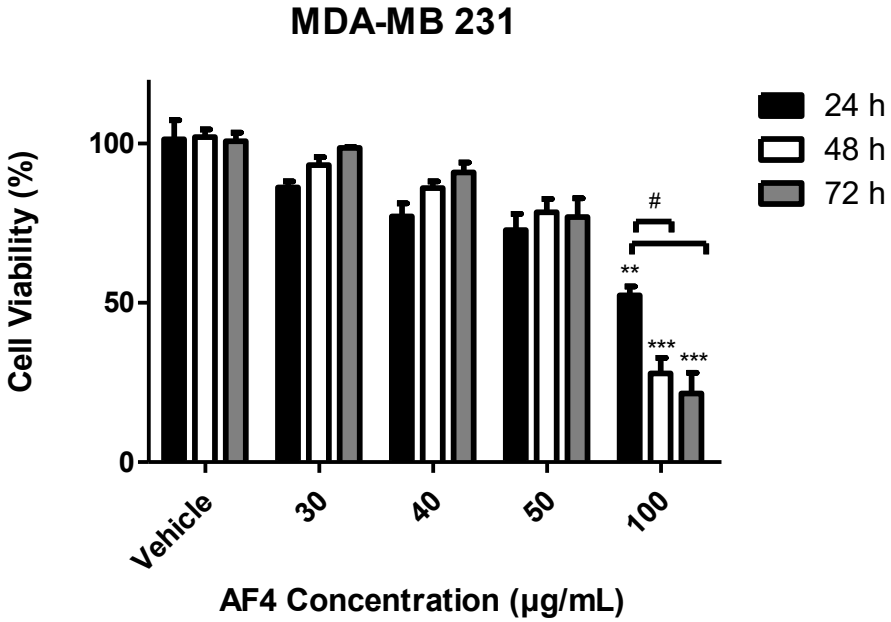
MDA-MB 231
Cell Viability (%)
AF4 Concentration (μg/mL)
24 h
48 h
72 h
Vehicle
30
40
50
100
#
**
***
***

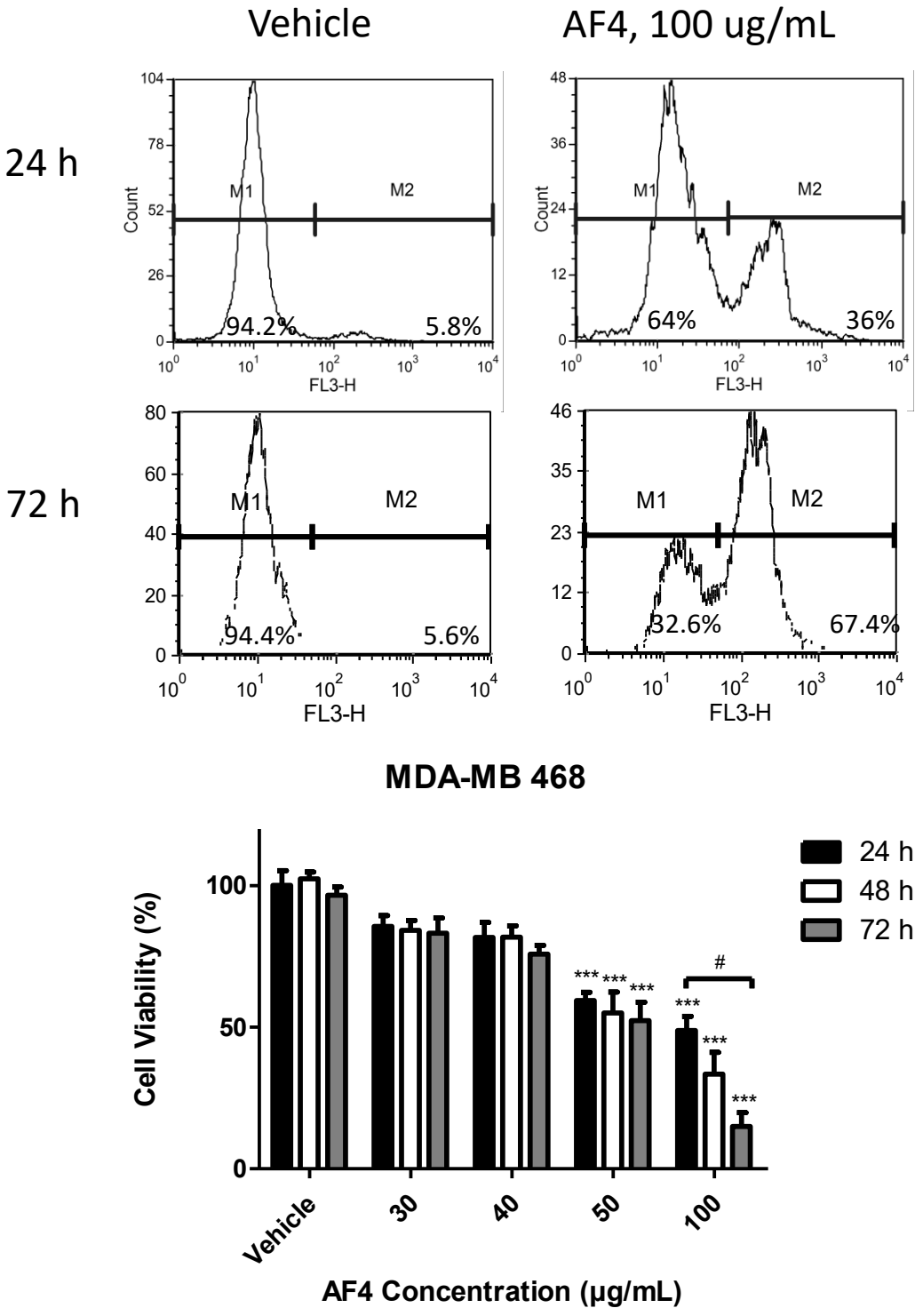

Figure 12. AF4 Causes Dose- and Time- Dependent Cell Death in MDA-MB-231 and MDA-MB-468 Breast Cancer Cells in a 7-AAD Assay

Figure 13. AF4 Causes Dose-Dependent Selective Cell Death in MDA-MB-231 and MDA-MB-468 Breast Cancer Cells in an Annexin-V 488/PI Flow Cytometry Assay. The cytotoxicity of AF4 was confirmed with Annexin-V 488/PI staining, which allows for the differentiation of live cells, cells in the early stages of apoptosis, and cells in the late stages of apoptosis or necrosis. MDA-MB-231 (A), MDA-MB-468 (B), and MCF10A (C) cells were seeded at a density of 50,000 cells per well in a 6-well plate and allowed to adhere overnight. Cells were then treated with AF4 (30 µg/mL – 100 µg/mL) for 24, 48, and 72-h. Cells were stained with Annexin-V 488 and PI 15 min prior to reading in a flow cytometer at FL1 (for Annexin-V 488) and FL2 (for PI). Representative dot plots are provided for each cell line after 72 h of treatment. Data are shown as mean values ± SEM of three independent trials. Significance was determined by ANOVA with the Tukey-Kramer multiple comparisons post-test, and is denoted by * for $p < 0.05$, ** for $p < 0.01$, and *** for < 0.001.

A. MDA-MB-231

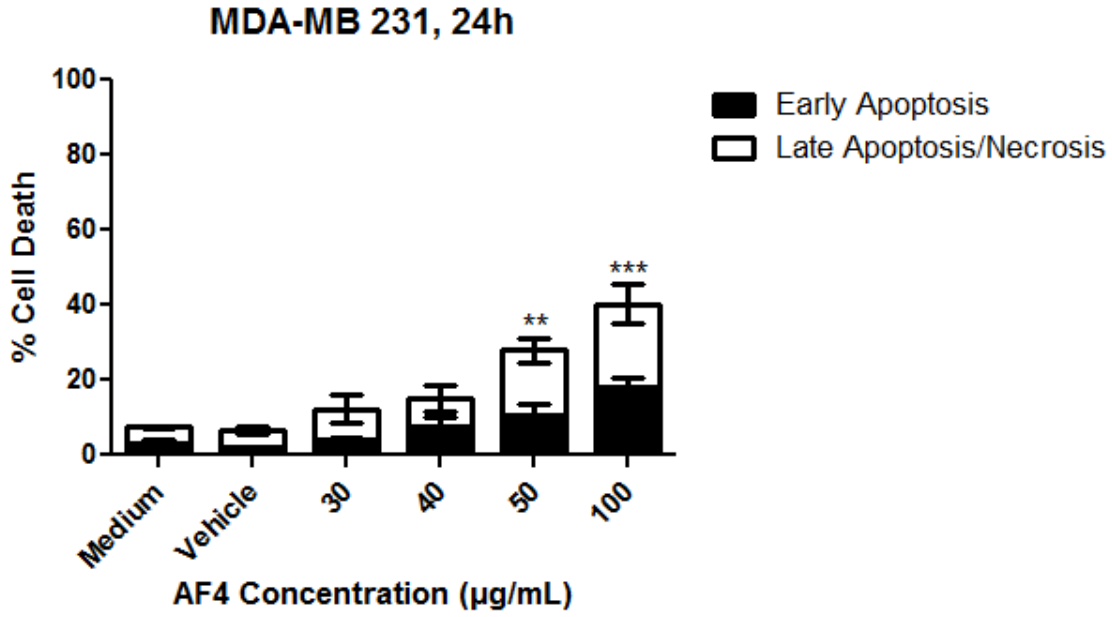
MDA-MB 231, 24h
% Cell Death
100
80
60
40
20
0
**
***
Medium
Vehicle
30
40
50
100
AF4 Concentration (µg/mL)
Early Apoptosis
Late Apoptosis/Necrosis

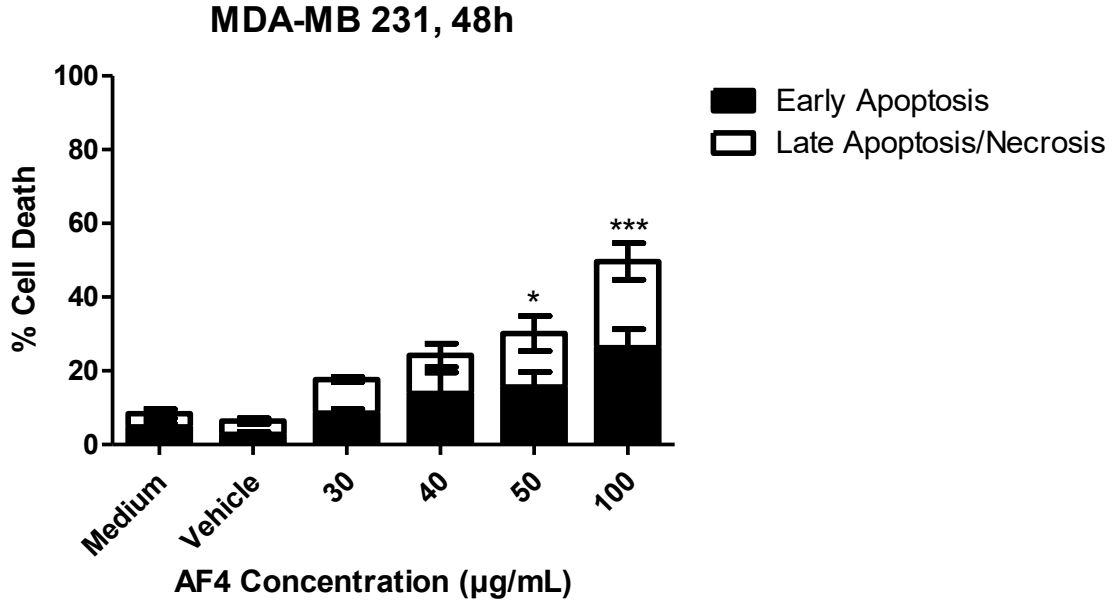
MDA-MB 231, 48h
% Cell Death
100
80
60
40
20
0
*
***
Medium
Vehicle
30
40
50
100
AF4 Concentration (µg/mL)
Early Apoptosis
Late Apoptosis/Necrosis

A. MDA-MB-231

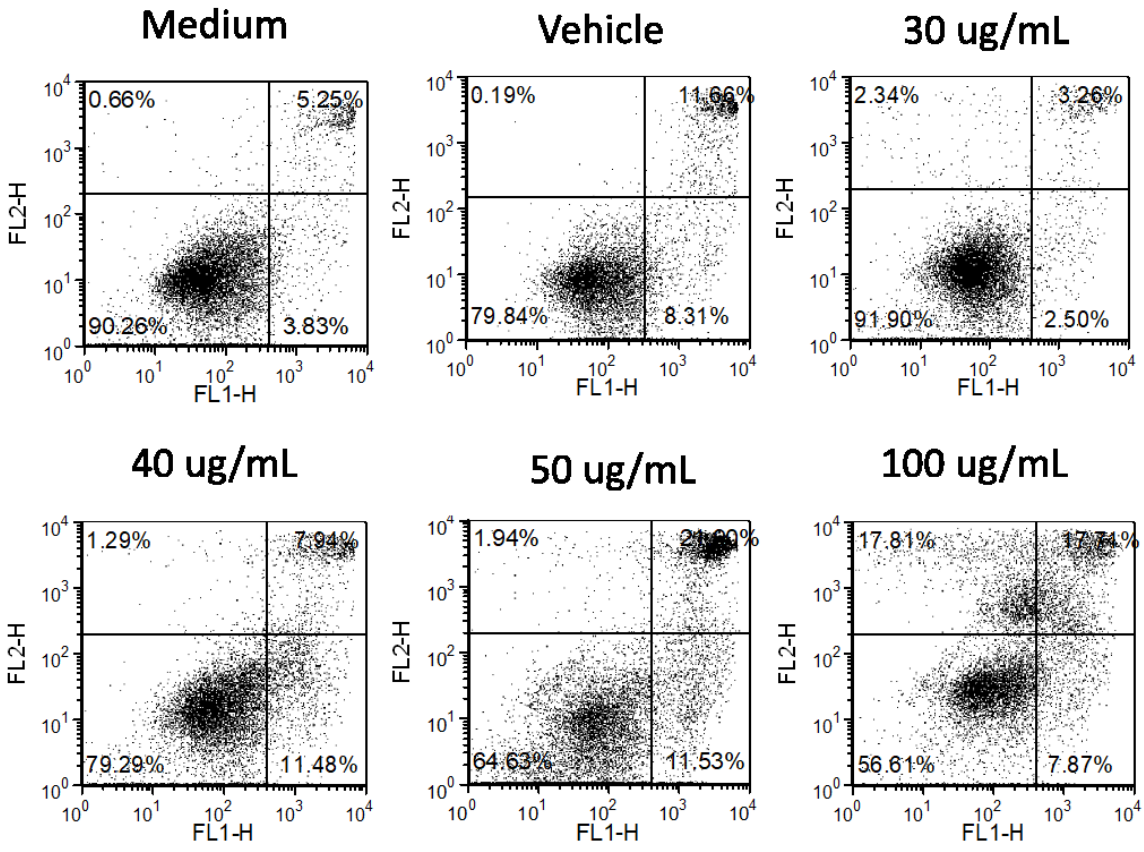
Medium
0.66%
5.25%
90.26%
3.83%
Vehicle
0.19%
11.66%
79.84%
8.31%
30 ug/mL
2.34%
3.26%
91.90%
2.50%
40 ug/mL
1.29%
7.94%
79.29%
11.48%
50 ug/mL
1.94%
64.63%
11.53%
100 ug/mL
17.81%
56.61%
7.87%
FL1-H
FL2-H

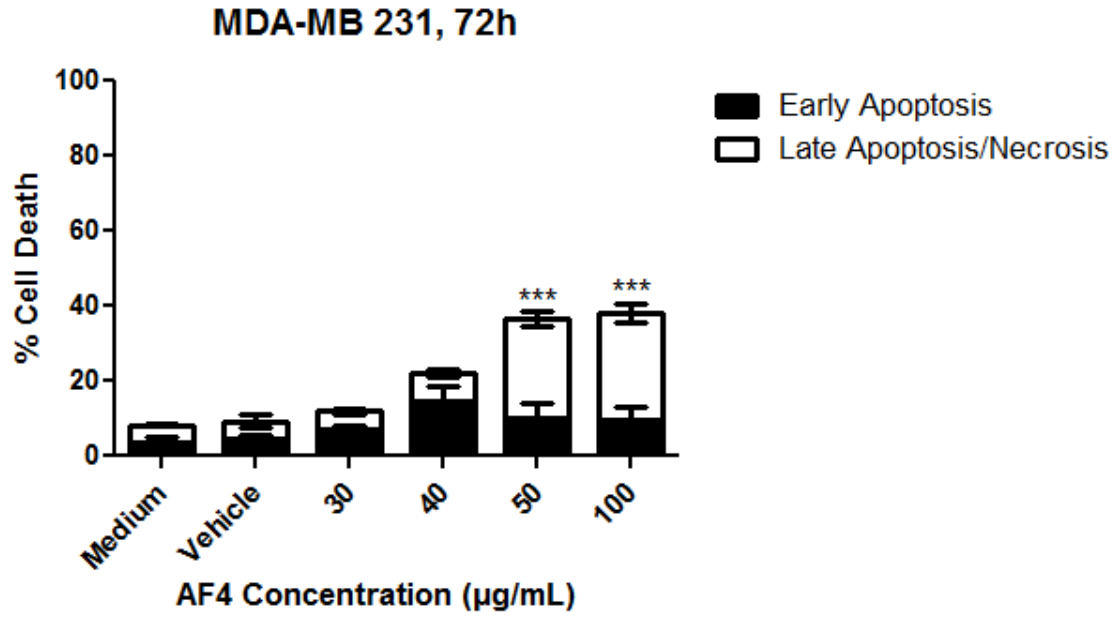
MDA-MB 231, 72h
Early Apoptosis
Late Apoptosis/Necrosis
% Cell Death
100
80
60
40
20
0
***
***
Medium
Vehicle
30
40
50
100
AF4 Concentration (µg/mL)

B. MDA-MB-468

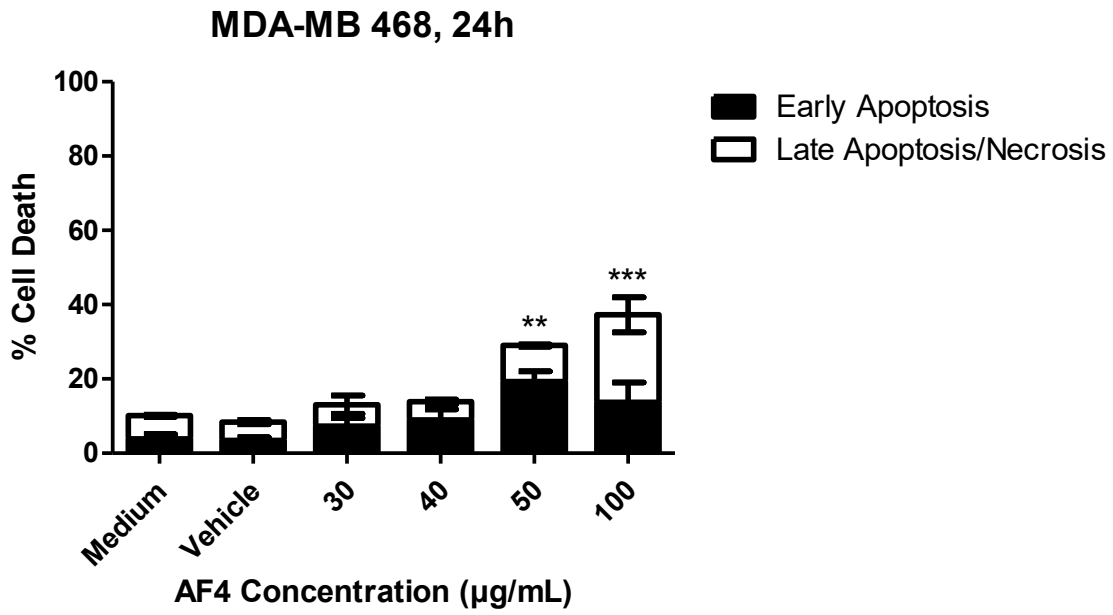
MDA-MB 468, 24h
% Cell Death
100
80
60
40
20
0
**
***
Medium
Vehicle
30
40
50
100
AF4 Concentration (µg/mL)
Early Apoptosis
Late Apoptosis/Necrosis

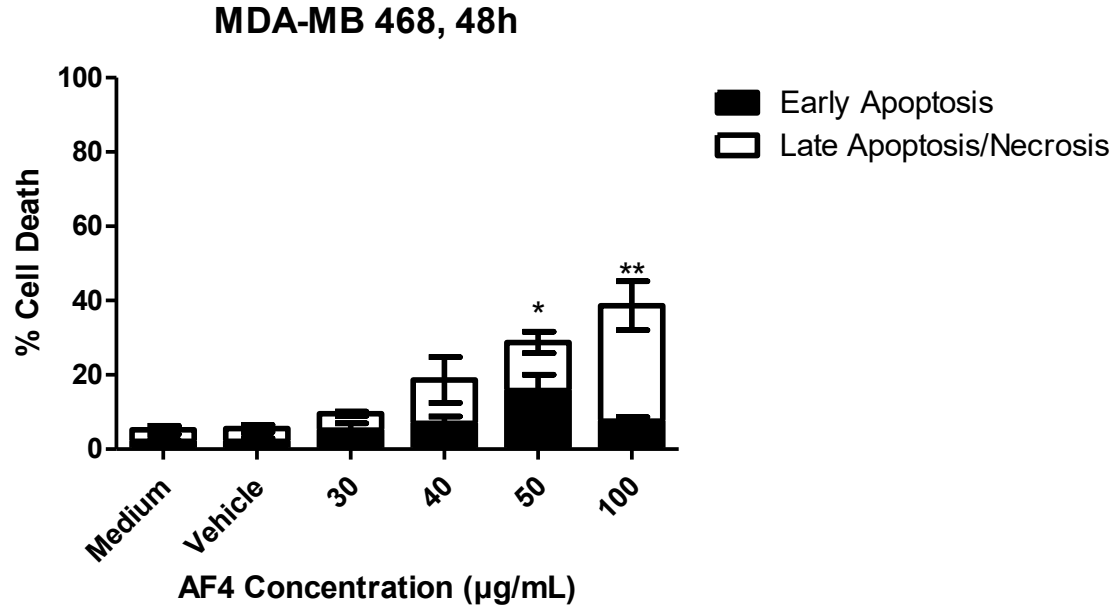
MDA-MB 468, 48h
% Cell Death
100
80
60
40
20
0
*
**
Medium
Vehicle
30
40
50
100
AF4 Concentration (µg/mL)
Early Apoptosis
Late Apoptosis/Necrosis

B. MDA-MB-468

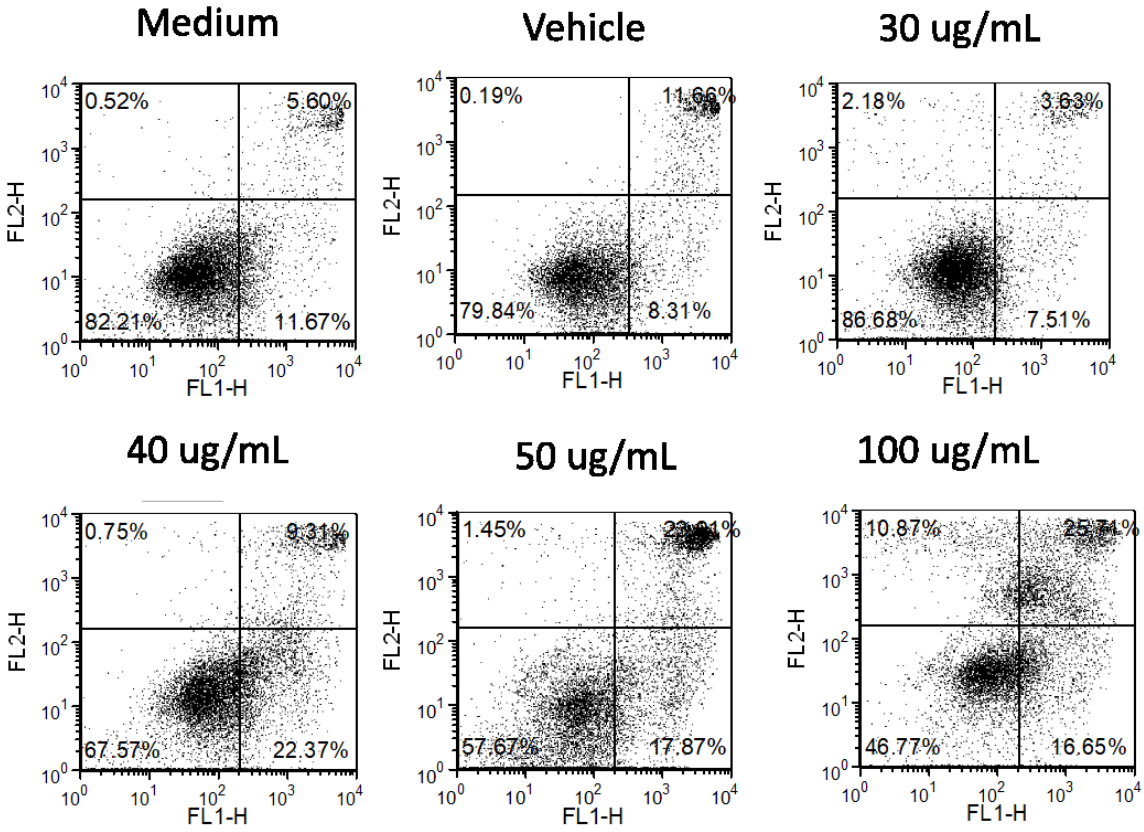
Medium
0.52%
5.60%
82.21%
11.67%
Vehicle
0.19%
11.66%
79.84%
8.31%
30 ug/mL
2.18%
3.63%
86.68%
7.51%
40 ug/mL
0.75%
9.31%
67.57%
22.37%
50 ug/mL
1.45%
23.91%
57.67%
17.87%
100 ug/mL
10.87%
25.71%
46.77%
16.65%
FL2-H
FL1-H

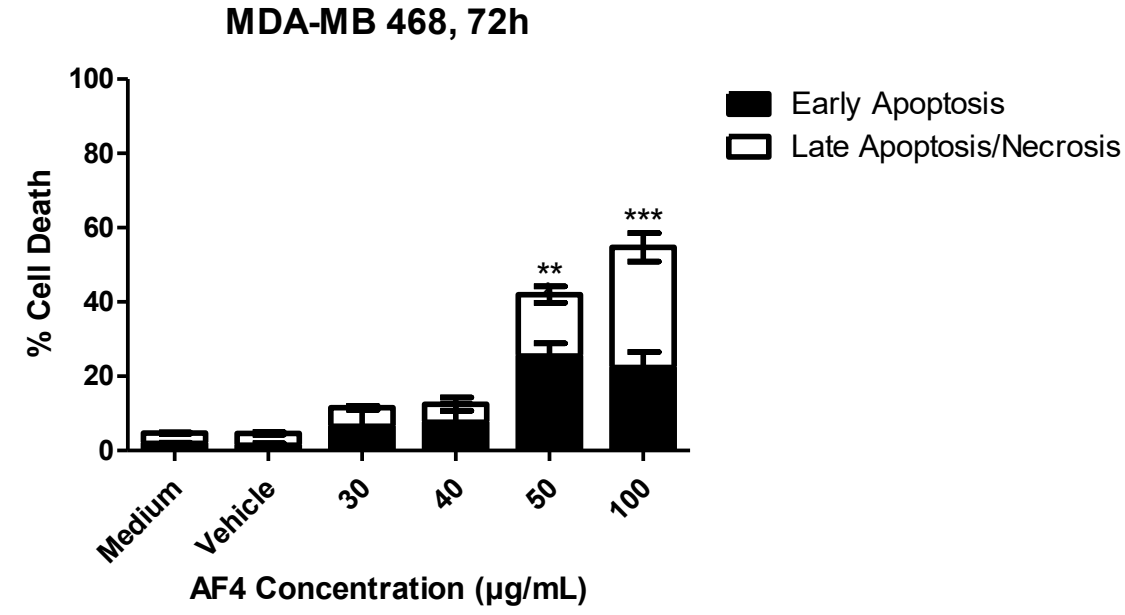
MDA-MB 468, 72h
Early Apoptosis
Late Apoptosis/Necrosis
% Cell Death
100
80
60
40
20
0
**
***
Medium
Vehicle
30
40
50
100
AF4 Concentration (µg/mL)

C. MCF10A

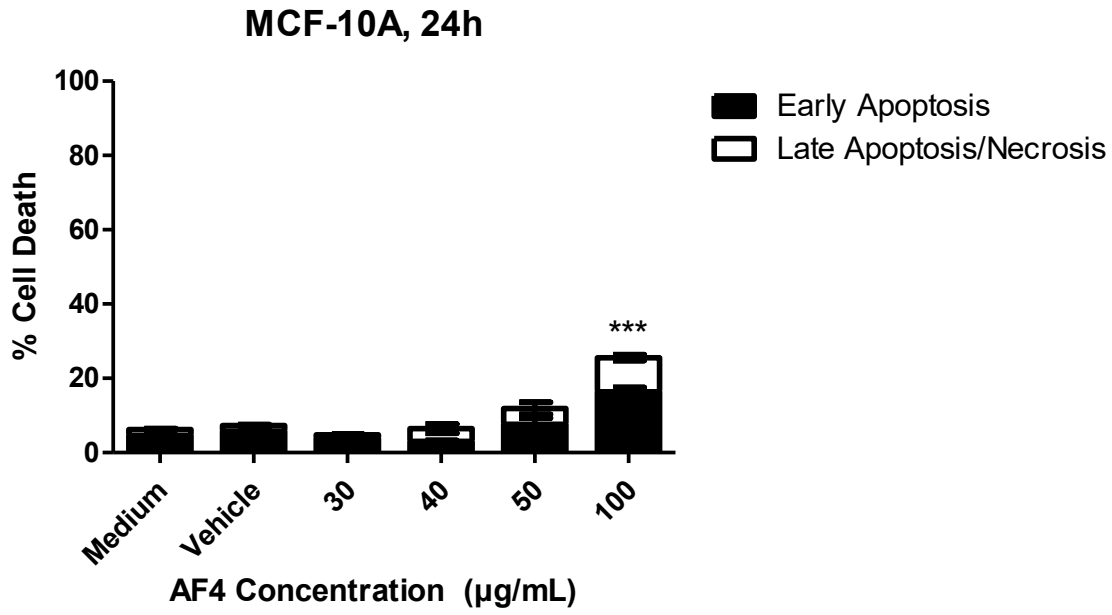
MCF-10A, 24h
Early Apoptosis
Late Apoptosis/Necrosis
% Cell Death
100
80
60
40
20
0
***
Medium
Vehicle
30
40
50
100
AF4 Concentration (µg/mL)

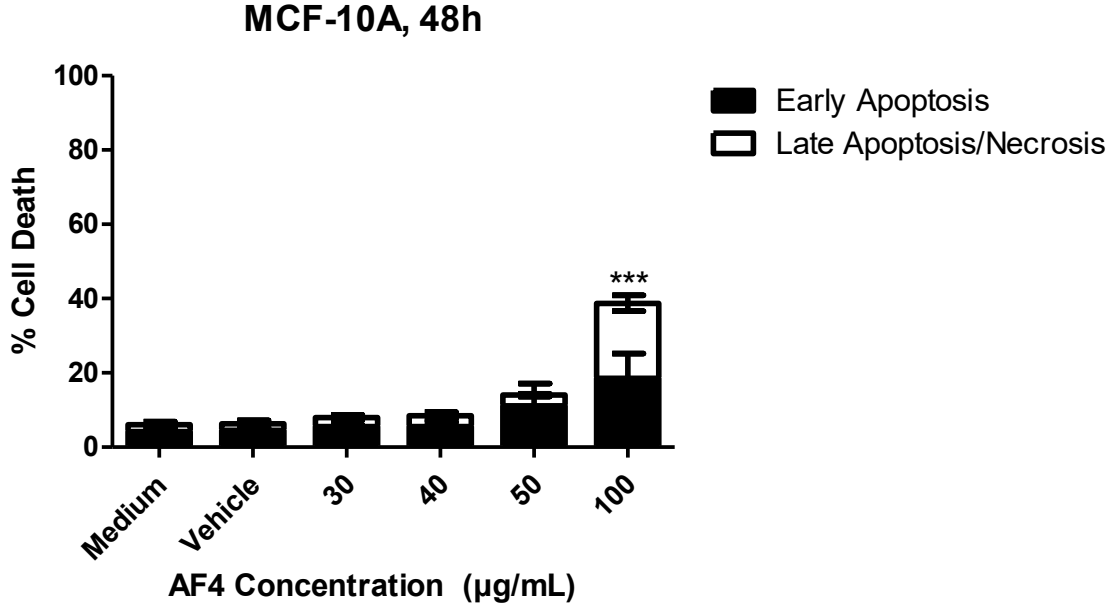
MCF-10A, 48h
Early Apoptosis
Late Apoptosis/Necrosis
% Cell Death
100
80
60
40
20
0
***
Medium
Vehicle
30
40
50
100
AF4 Concentration (µg/mL)

C. MCF10A

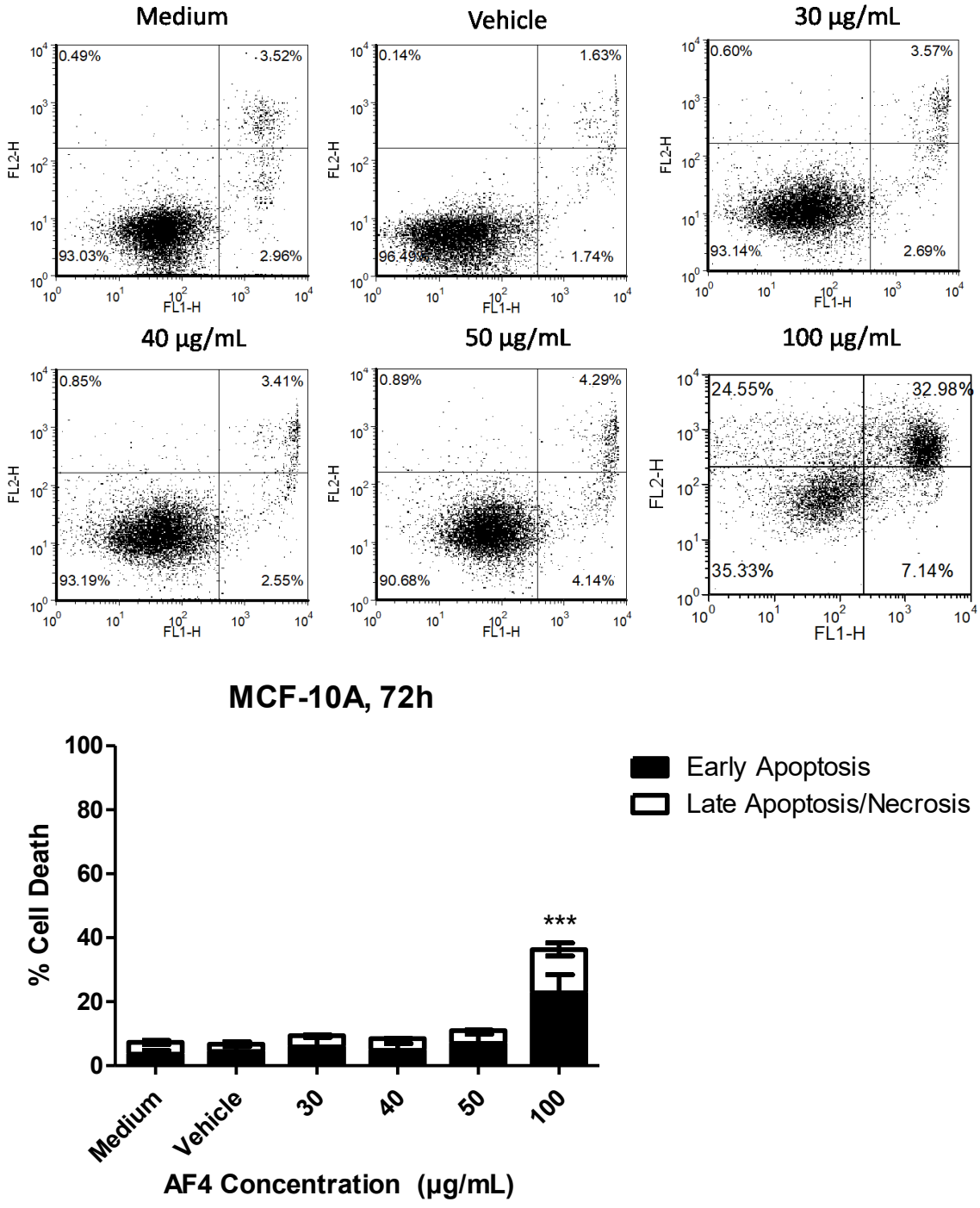

Figure 13. AF4 Causes Dose- Dependent Selective Cell Death in MDA-MB-231 and MDA-MB-468 Breast Cancer Cells in an Annexin-V 488/PI Flow Cytometric Assay

Figure 14. AF4 Produces Peroxide Radicals in MDA-MB-231 and MDA-MB-468 Breast Cancer Cells. The ability of AF4 to cause production of peroxide radicals in breast cancer cells was determined with an Amplex red assay. MDA-MB-231 (A) and MDA-MB-468 (B) breast cancer cells were seeded at a density of 5,000 cells per well in a flat-bottomed 96 well plate and allowed to adhere overnight. Cells were then treated with AF4 (50 µg/mL or 100 µg/mL) or the known peroxide radical inducer EGCG, which acted as the positive control. As AF4 is red in colour, as well as to control for the possibility that AF4 induces ROS in medium alone, a cell-free control was used (C). Data are shown as mean values ± SEM of three independent trials. Significance was determined by ANOVA with the Tukey-Kramer multiple comparisons post-test, and is denoted by * for $p < 0.05$, ** for $p < 0.01$, and *** for < 0.001.

A. MDA-MB-231

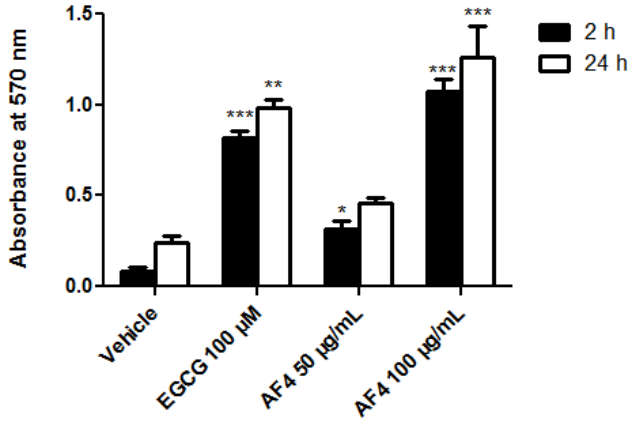

B. MDA-MB-468

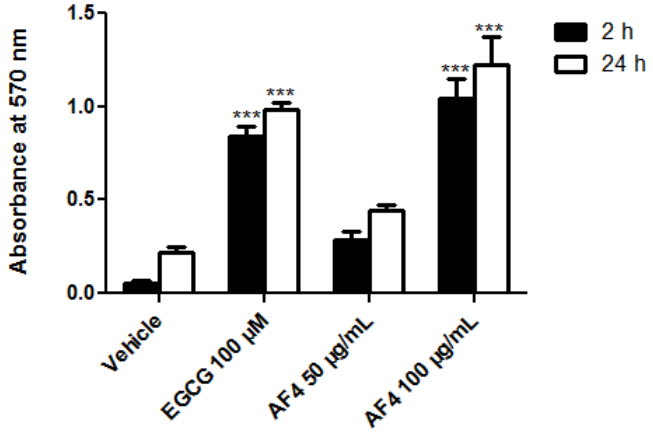

C. Cell-free

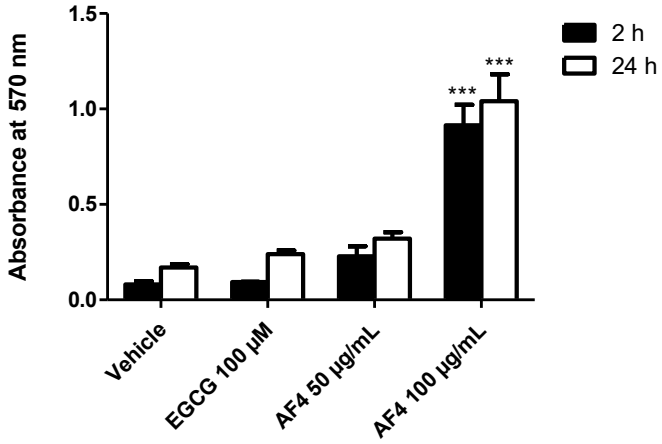

Figure 14. AF4 Produces Peroxide Radicals in MDA-MB-231 and MDA-MB-468 Breast Cancer Cells

Figure 15. AF4 Induces ROS Accumulation in MDA-MB-231 and MDA-MB-468 Breast Cancer Cells. The intracellular ROS-inducing effects of AF4 were confirmed with the DCFDA assay. MDA-MB-231 (A) and MDA-MB-468 (B) breast cancer cells were seeded at a density of 5,000 cells per well in an opaque flat-bottomed 96 well plate and allowed to adhere overnight. Cells were stained with DCFDA then treated with AF4 (50 µg/mL or 100 µg/mL) or EGCG, which acted as the positive control. Readings were obtained at 2 h and 24 h post-treatment. Data are shown as mean values ± SEM of three independent trials. Significance was determined by ANOVA with the Tukey-Kramer multiple comparisons post-test, and is denoted by * for $p < 0.05$, ** for $p < 0.01$, and *** for < 0.001. Differences between treatment groups is denoted by # for $p < 0.05$, ## for $p < 0.01$, and ### for < 0.001.

A. MDA-MB-231

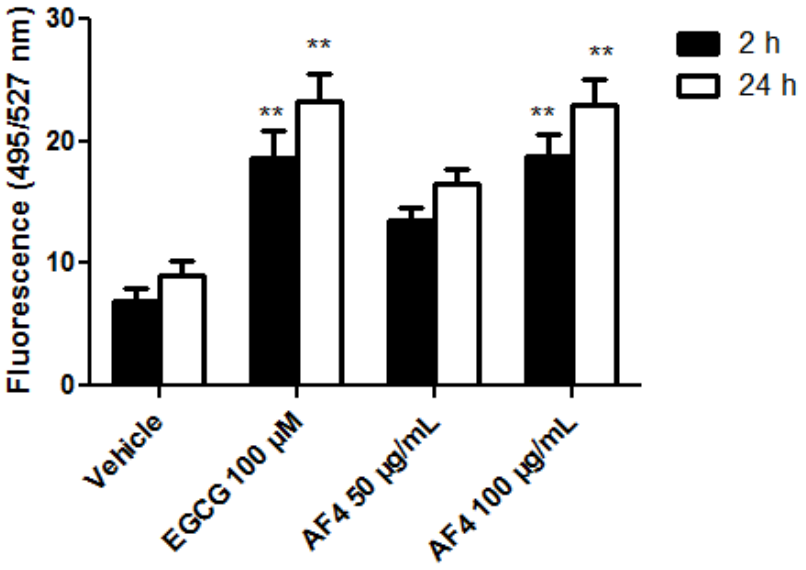

B. MDA-MB-468

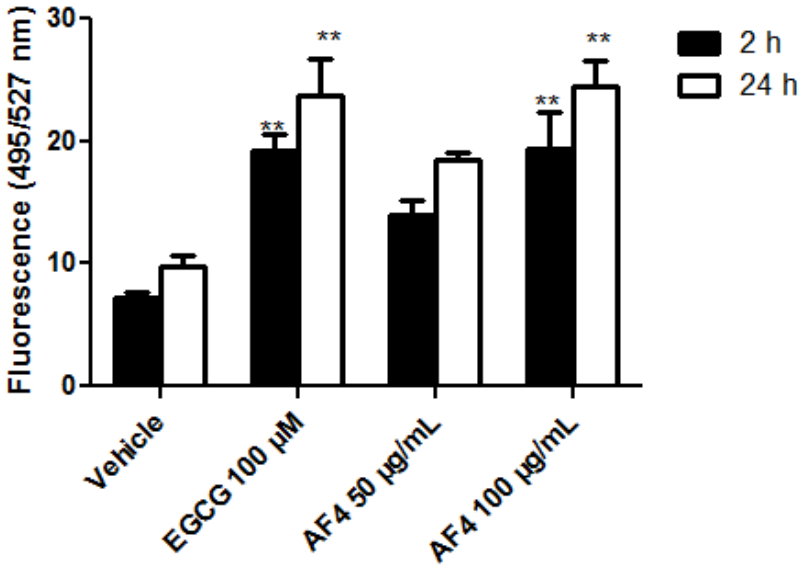

Figure 15. AF4 Induces ROS Accumulation in MDA-MB-231 and MDA-MB-468 Breast Cancer Cells.

Figure 16. AF4-Induced Cell Death is ROS-dependent. The involvement of ROS in AF4-mediated cell death was examined with an Annexin-V 488/PI flow cytometry assay. MDA-MB-231 (A) and MDA-MB-468 (B) breast cancer cells were seeded at a density of 50,000 cells per well in a 6-well plate and allowed to adhere overnight. Some cultures were then pre-treated with 20 mM NAC. Cells were then treated with AF4 (30 µg/mL – 100 µg/mL) for 24 h, and then stained with Annexin-V 488 and PI 15 min prior to reading in a flow cytometer at FL1 (for Annexin-V 488) and FL2 (for PI). Representative dot plots provided for MDA-MB-231 cells. Data are shown as mean values ± SEM of three independent trials. Significance was determined by ANOVA with the Tukey-Kramer multiple comparisons post-test, and is denoted by * for $p < 0.05$, ** for $p < 0.01$, and *** for < 0.001. Differences between treatment groups is denoted by # for $p < 0.05$, ## for $p < 0.01$, and ### for < 0.001.

A. MDA-MB-231

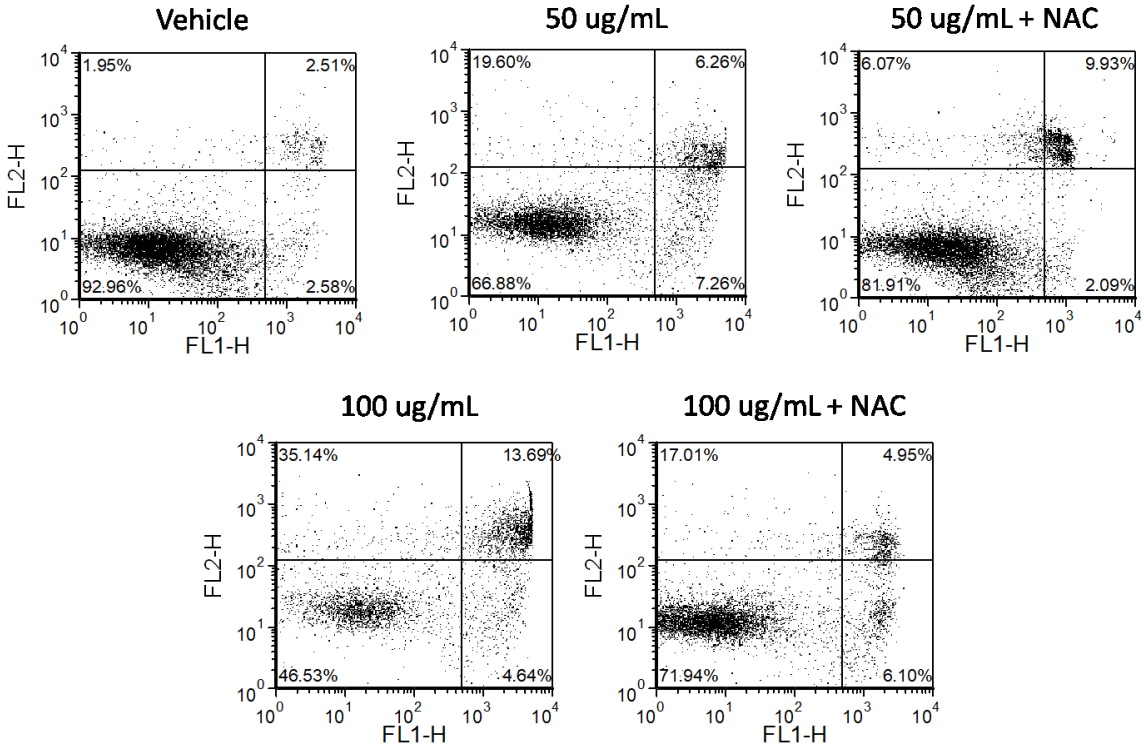
Vehicle
1.95%
2.51%
92.96%
2.58%
50 ug/mL
19.60%
6.26%
66.88%
7.26%
50 ug/mL + NAC
6.07%
9.93%
81.91%
2.09%
100 ug/mL
35.14%
13.69%
46.53%
4.64%
100 ug/mL + NAC
17.01%
4.95%
71.94%
6.10%
FL1-H
FL2-H

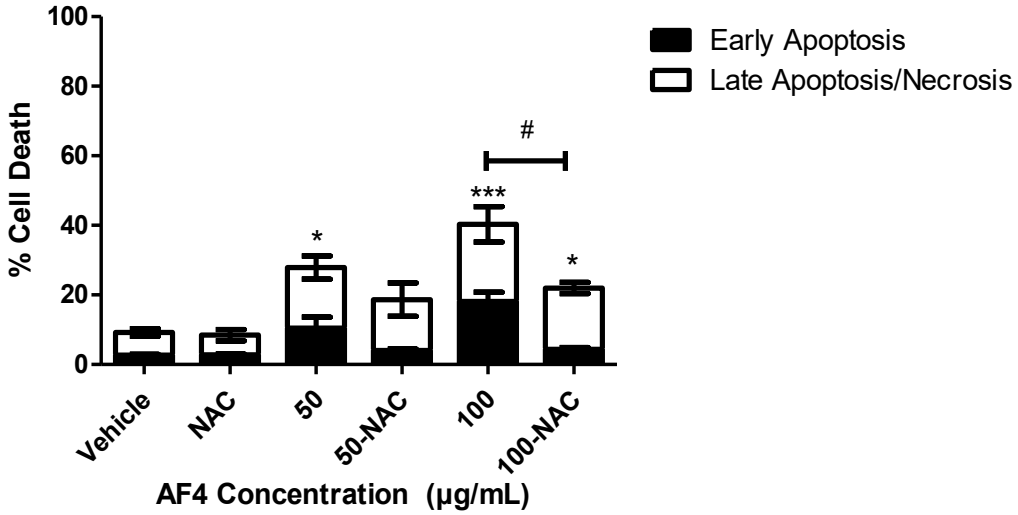
Early Apoptosis
Late Apoptosis/Necrosis
% Cell Death
100
80
60
40
20
0
*
***
#
*
Vehicle
NAC
50
50-NAC
100
100-NAC
AF4 Concentration (µg/mL)

B. MDA-MB-468

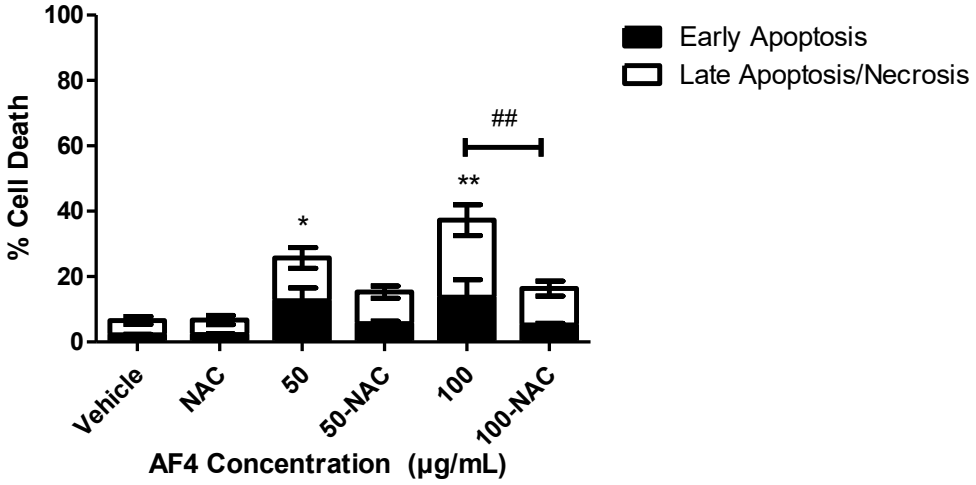

Figure 16. AF4-Induced Cell Death is ROS-dependent

Figure 17. AF4-Induced Breast Cancer Cell Death is Exacerbated by Iron Chelation. The involvement of iron in AF4-mediated cell death was examined with an Annexin-V 488/PI flow cytometry assay. MDA-MB-231 (A) and MDA-MB-468 (B) breast cancer cells were seeded at a density of 50,000 cells per well in a 6-well plate and allowed to adhere overnight. Some cultures were then pre-treated with 25 μg/mL DFE (iron chelator). Cells were then treated with AF4 (30 μg/mL – 100 μg/mL) for 24 h, and then stained with Annexin-V 488 and PI 15 min prior to reading in a flow cytometer at FL1 (for Annexin-V 488) and FL2 (for PI). Representative dot plots provided for MDA-MB-231 cells. Data are shown as mean values ± SEM of three independent trials. Significance was determined by ANOVA with the Tukey-Kramer multiple comparisons post-test, and is denoted by * for $p < 0.05$, ** for $p < 0.01$, and *** for < 0.001. Differences between treatment groups is denoted by # for $p < 0.05$, ## for $p < 0.01$, and ### for < 0.001.

A. MDA-MB-231

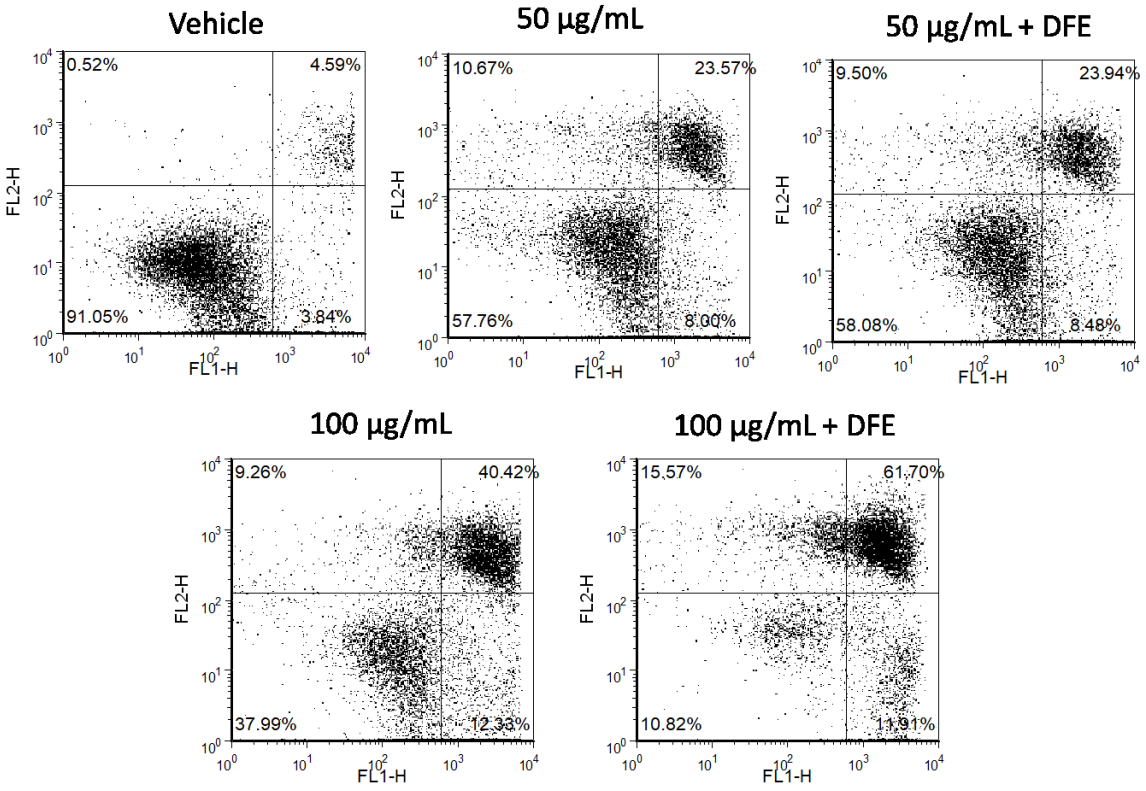
Vehicle
0.52%
4.59%
91.05%
3.84%
50 µg/mL
10.67%
23.57%
57.76%
8.00%
50 µg/mL + DFE
9.50%
23.94%
58.08%
8.48%
100 µg/mL
9.26%
40.42%
37.99%
12.33%
100 µg/mL + DFE
15.57%
61.70%
10.82%
11.91%
FL2-H
FL1-H

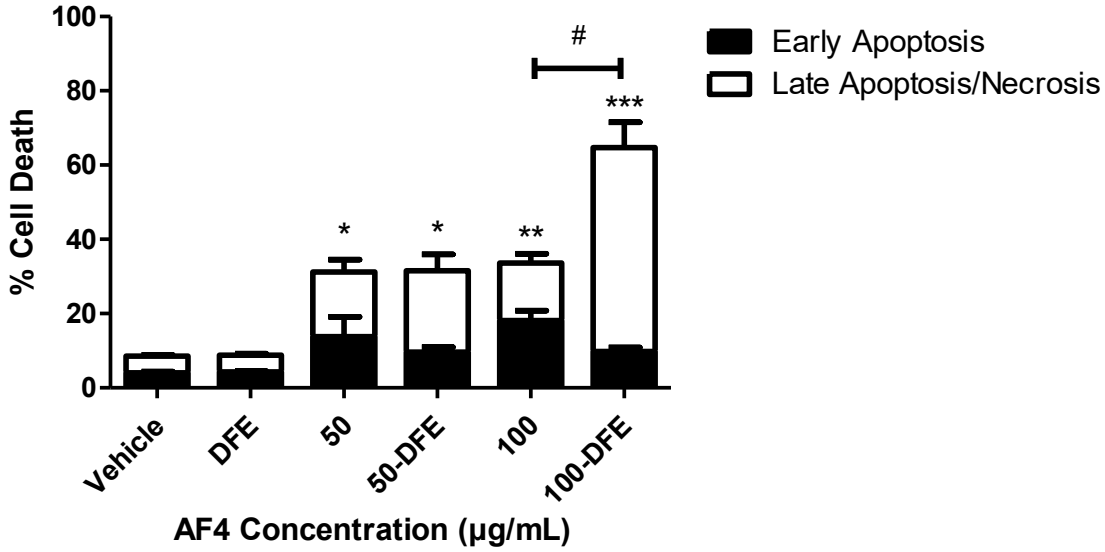
% Cell Death
100
80
60
40
20
0
#
***
*
*
**
Vehicle
DFE
50
50-DFE
100
100-DFE
AF4 Concentration (µg/mL)
Early Apoptosis
Late Apoptosis/Necrosis

B. MDA-MB-468

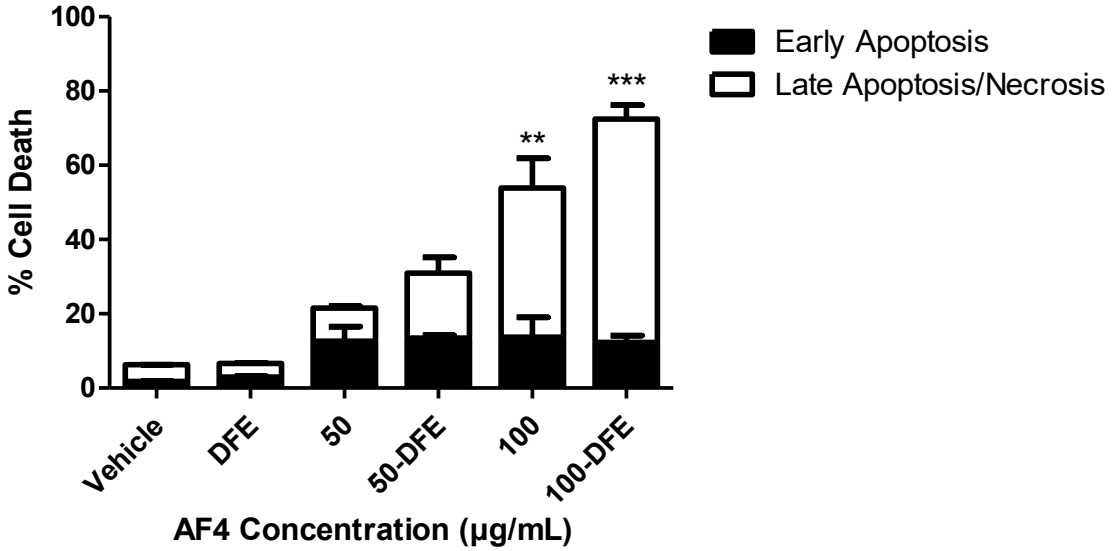

Figure 17. AF4-Induced Breast Cancer Cell Death is Exacerbated by Iron Chelation

Figure 18. AF4-Induced Mitochondrial Membrane Damage is ROS-dependent but Not Iron-dependent. The ability of AF4 to induce damage in mitochondrial membranes, as well as the involvement of ROS and iron in this process, was examined with a $DIOC_6$. MDA-MB-231 (A) and MDA-MB-468 (B) breast cancer cells were seeded at a density of 50,000 cells per well in a 6-well plate and allowed to adhere overnight. Certain cells were then pre-treated with 20 mM NAC or 25 μg/mL DFE. Cells were then treated with AF4 (50 μg/mL or 100 μg/mL) for 24 h. Cells were stained with DIOC6 15 min prior to reading in a flow cytometer at FL1. Cells within the first marker (M1) represent cells with damaged mitochondrial membranes. Representative histograms are provided for 48 h of AF4 treatment. Data are shown as mean values ± SEM of five independent trials. Significance was determined by ANOVA with the Tukey-Kramer multiple comparisons post-test, and is denoted by * for $p < 0.05$, ** for $p < 0.01$, and *** for < 0.001. Differences between treatment groups is denoted by # for $p < 0.05$, ## for $p < 0.01$, and ### for < 0.001.

A. MDA-MB-231, 24 h

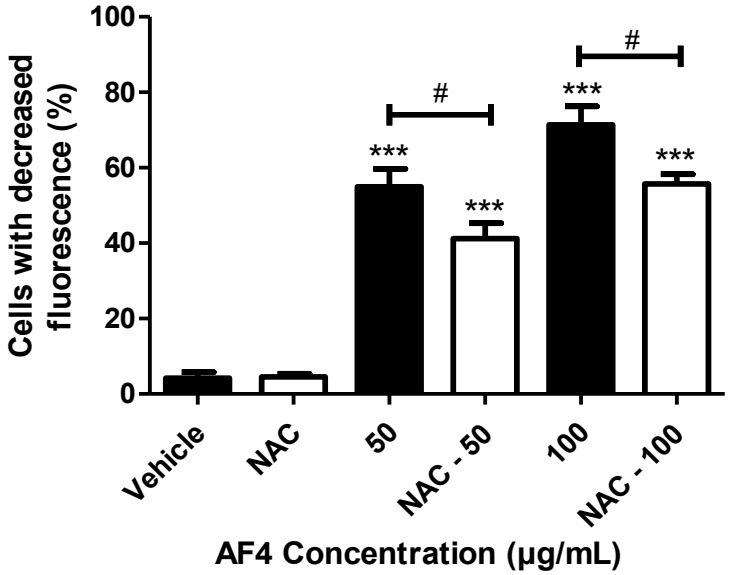

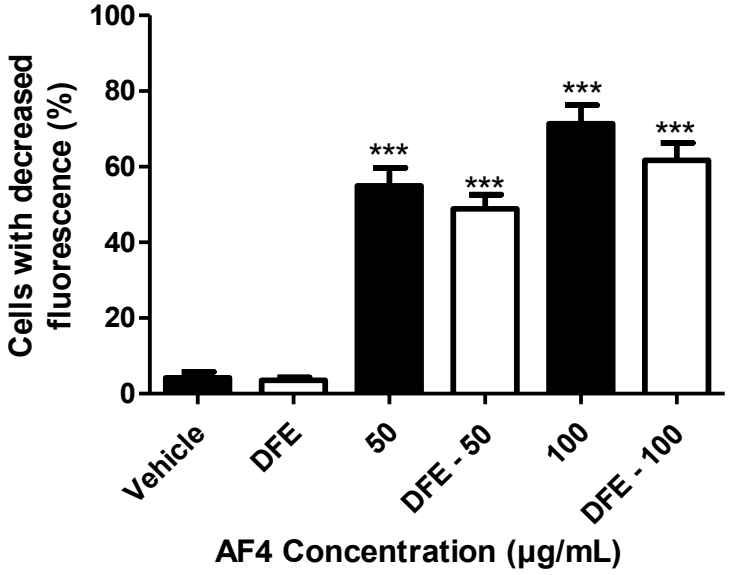

A. MDA-MB-231, 48 h

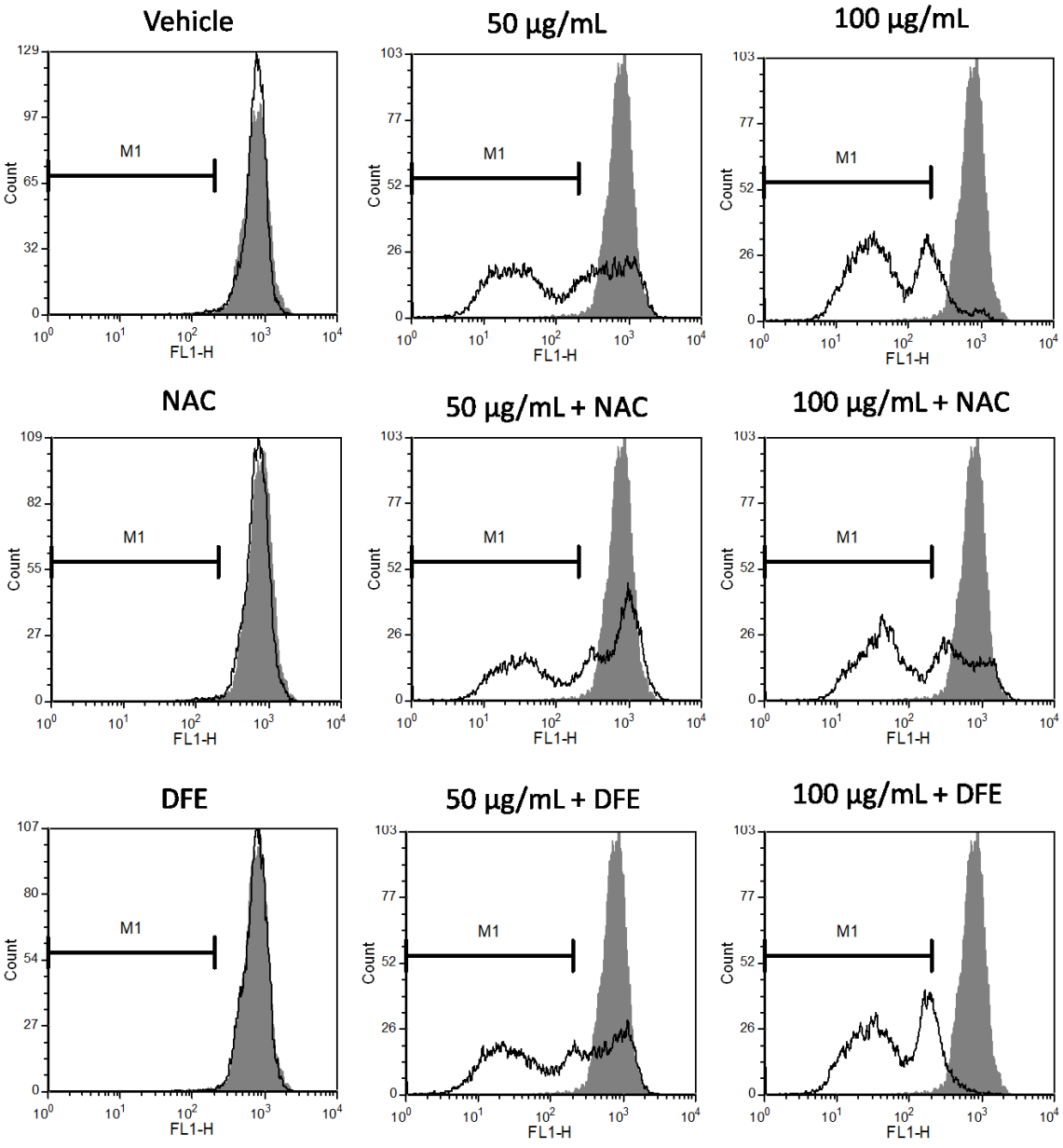

A. MDA-MB-231, 48 h

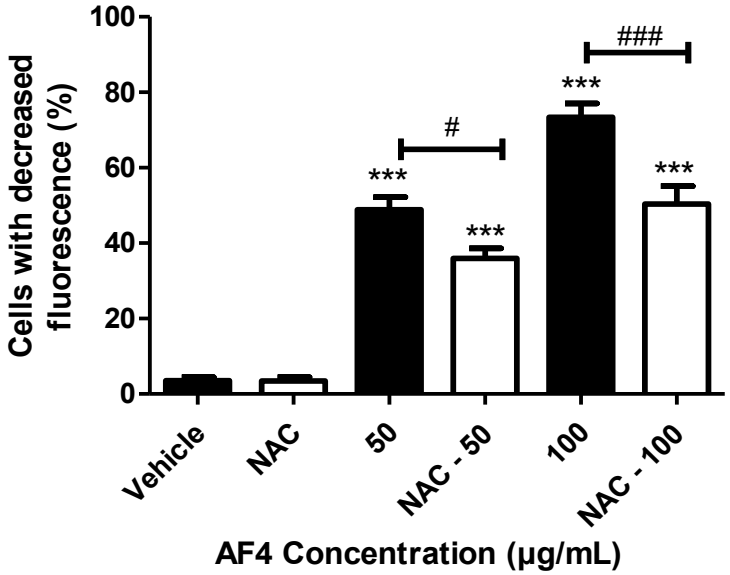

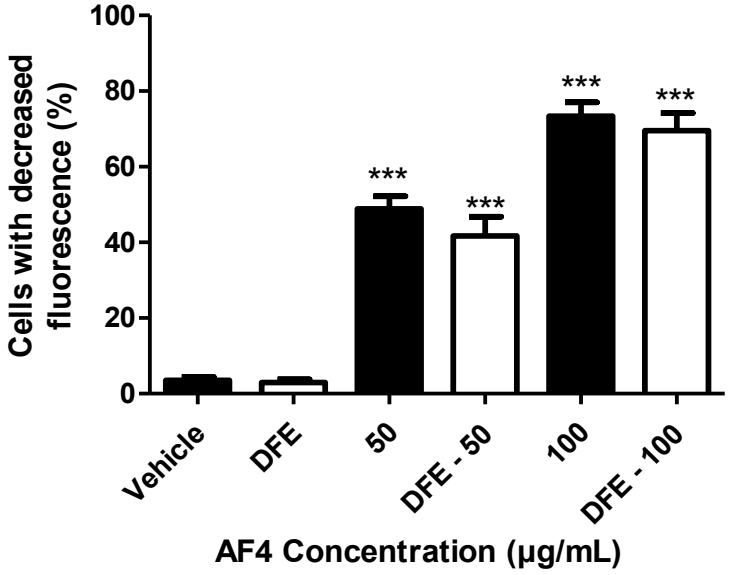

B. MDA-MB-468, 24 h

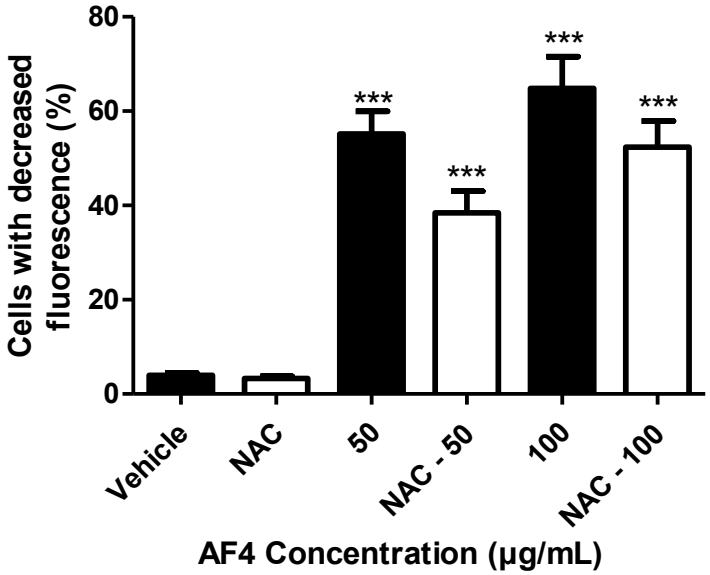

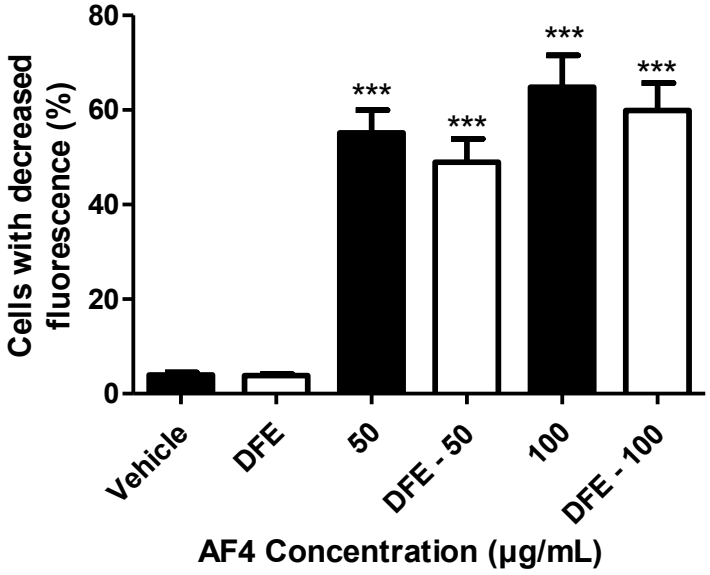

B. MDA-MB-468, 48 h

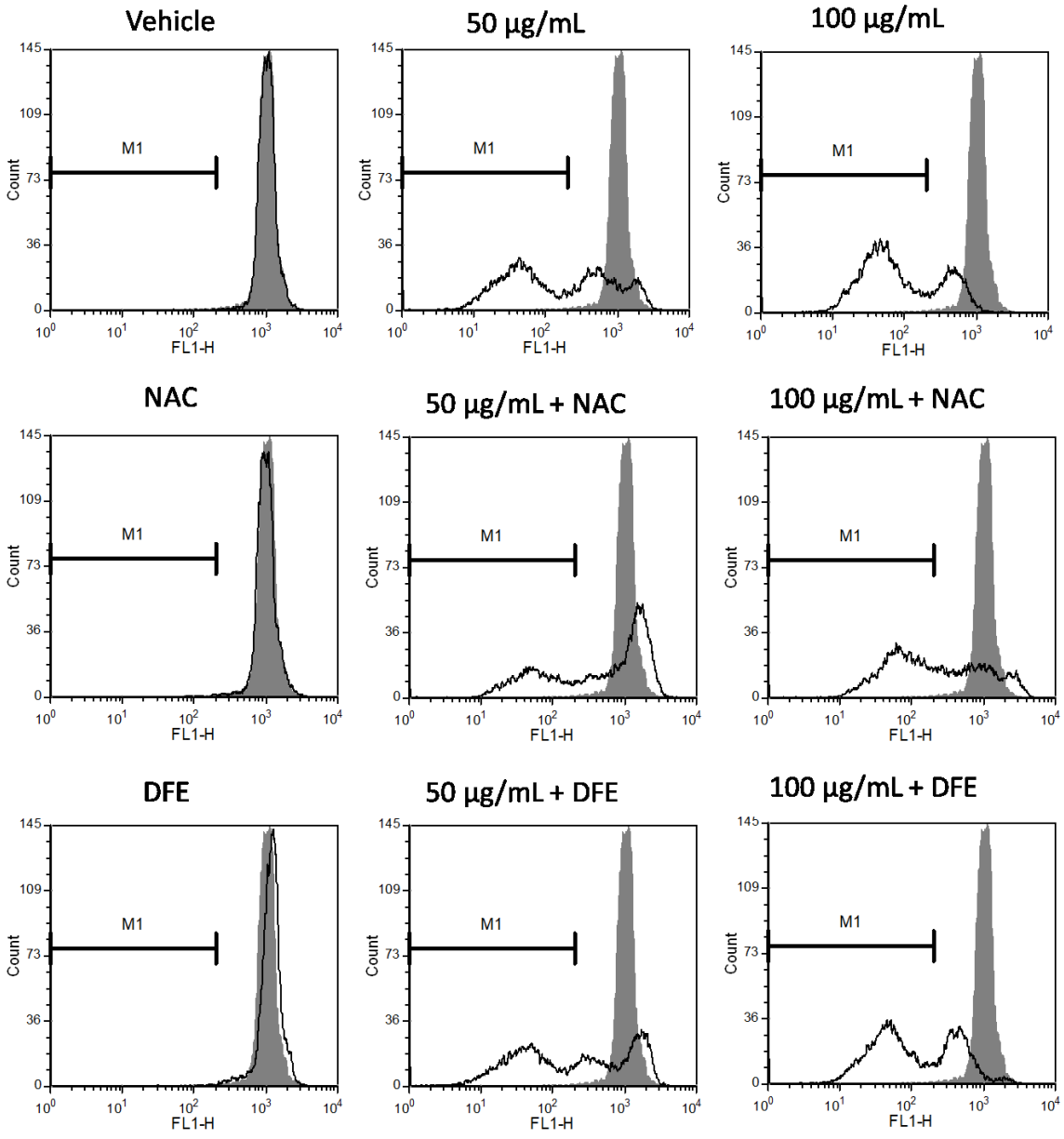

B. MDA-MB-468, 48 h

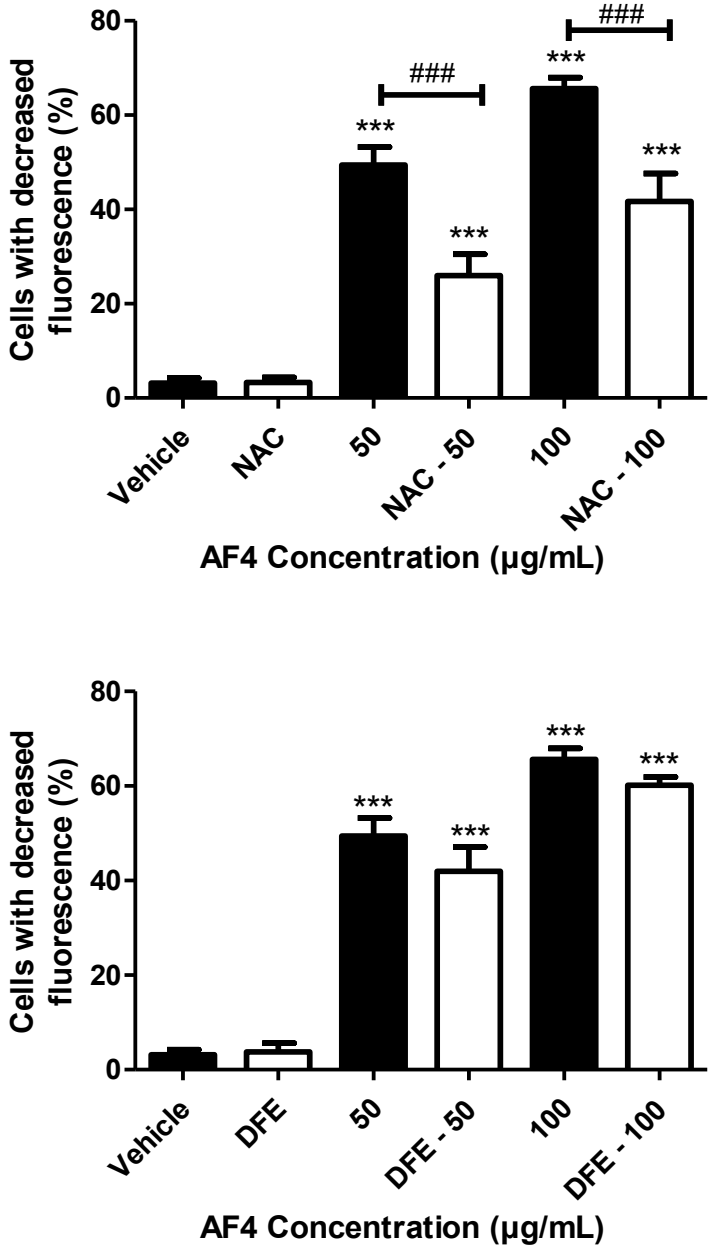

Figure 18. AF4-Induced Mitochondrial Membrane Damage is ROS-dependent but not Iron-dependent.

Figure 19. Breast Cancer Cells Are More Sensitive to Peroxide Treatment than MCF10A Epithelial Cells. The growth inhibitory effects of H_2O_2 on MDA-MB-231 (A) and MDA-MB-468 (B) triple-negative breast cancer cells were compared to MCF10A epithelial cells (C). Cells were seeded at 5 x 10^3 cells per well in a flat-bottom 96-well plate and allowed to adhere overnight. After incubation, cells were treated with various concentrations of H_2O_2 (25 μM -200 μM) for 24 h. After treatment, MTT was added and solubilized with DMSO. Absorbance values were then read and normalized relative to the medium control. Data are shown as mean values ± SEM of three independent trials. Significance was determined by ANOVA with the Tukey-Kramer multiple comparisons post-test, and is denoted by * for $p < 0.05$, ** for $p < 0.01$, and *** for < 0.001. Differences between treatment groups is denoted by # for $p < 0.05$, ## for $p < 0.01$, and ### for < 0.001.

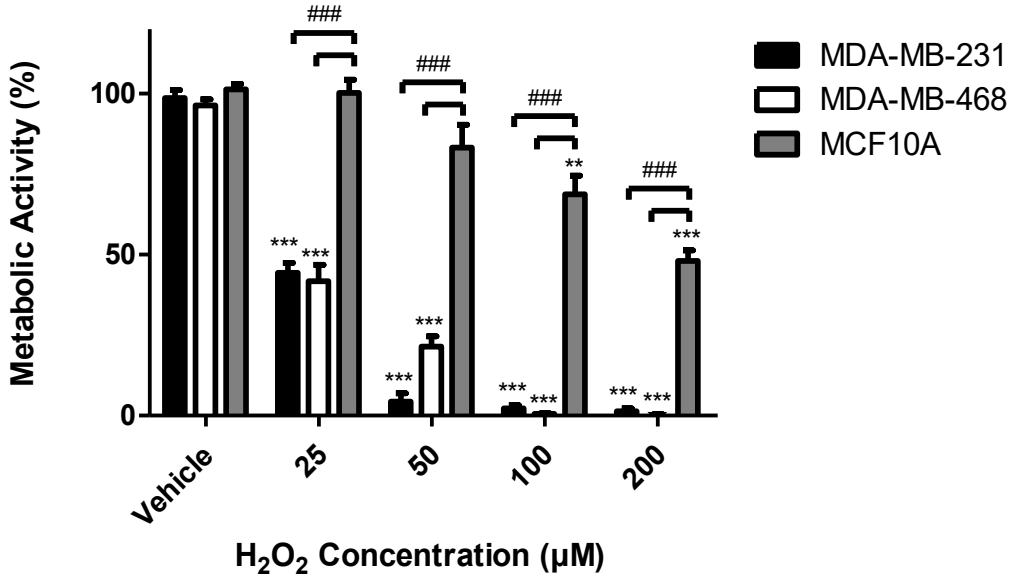

Figure 19. Breast Cancer Cells Are More Sensitive to Peroxide Treatment than MCF10A Epithelial Cells.

Figure 20. AF4-Induced Cell Death is Not Caspase-Dependent and Does Not Involve PARP1 Cleavage. The capability of AF4 to induce apoptosis in triple-negative breast cancer cells was investigated with western blotting for caspases and PARP1, which are involved in apoptosis. Protein isolates of MDA-MB-231 (A) and MDA-MB-468 (B) triple-negative breast cancer cells treated with AF4 (40 μg/mL and 50 μg/mL) with or without 20 mM NAC pre-treatment for 72 h were blotted and probed for total and cleaved caspases and PARP1. Histograms are shown only for uncleaved caspases and PARP1. Data are shown as mean values ± SEM of three independent trials. Significance was determined by ANOVA with the Tukey-Kramer multiple comparisons post-test, and is denoted by * for $p < 0.05$, ** for $p < 0.01$, and *** for $p < 0.001$.

A. MDA-MB-231

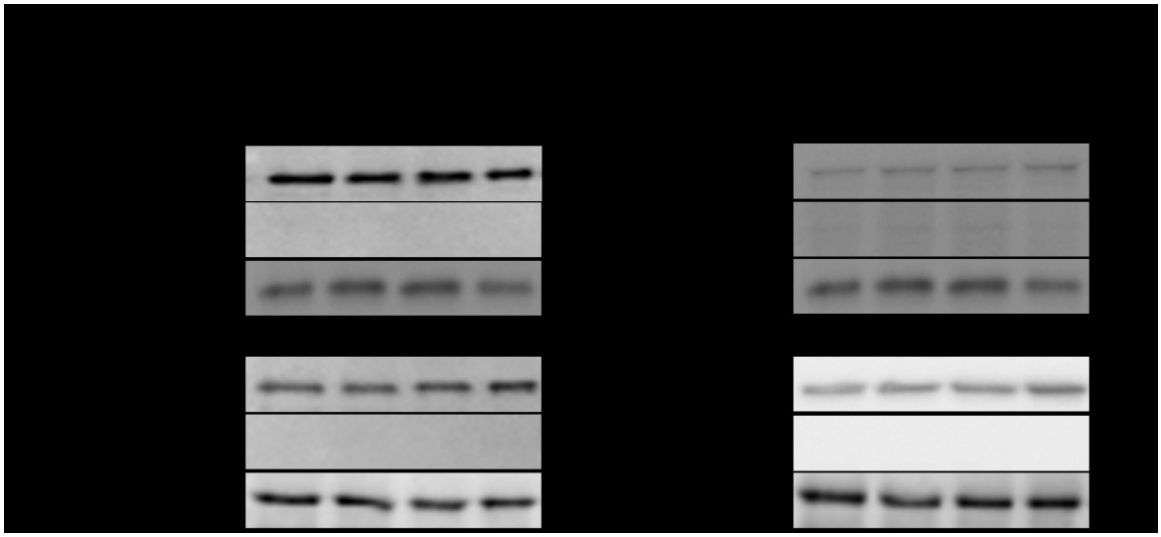

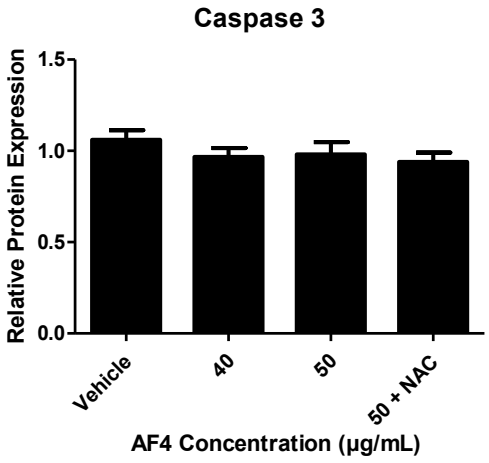
Caspase 3
Relative Protein Expression
1.5
1.0
0.5
0.0
Vehicle
40
50
50 + NAC
AF4 Concentration (µg/mL)

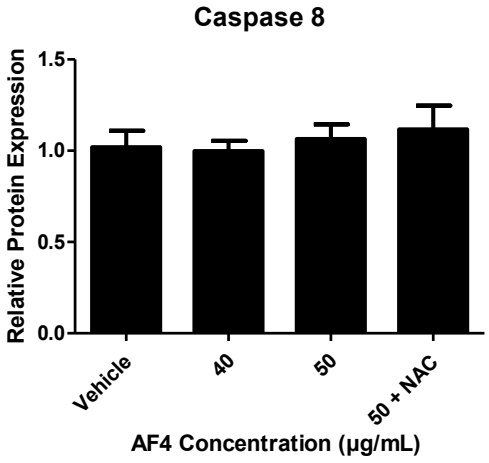
Caspase 8
Relative Protein Expression
1.5
1.0
0.5
0.0
Vehicle
40
50
50 + NAC
AF4 Concentration (µg/mL)

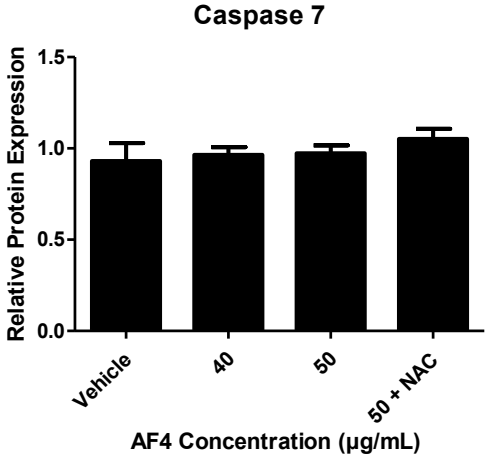
Caspase 7
Relative Protein Expression
1.5
1.0
0.5
0.0
Vehicle
40
50
50 + NAC
AF4 Concentration (µg/mL)

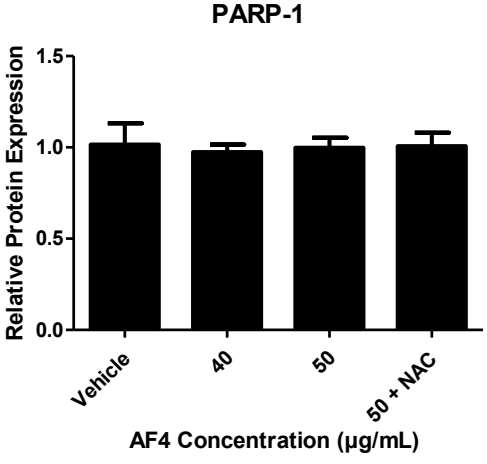
PARP-1
Relative Protein Expression
1.5
1.0
0.5
0.0
Vehicle
40
50
50 + NAC
AF4 Concentration (µg/mL)

B. MDA-MB-468

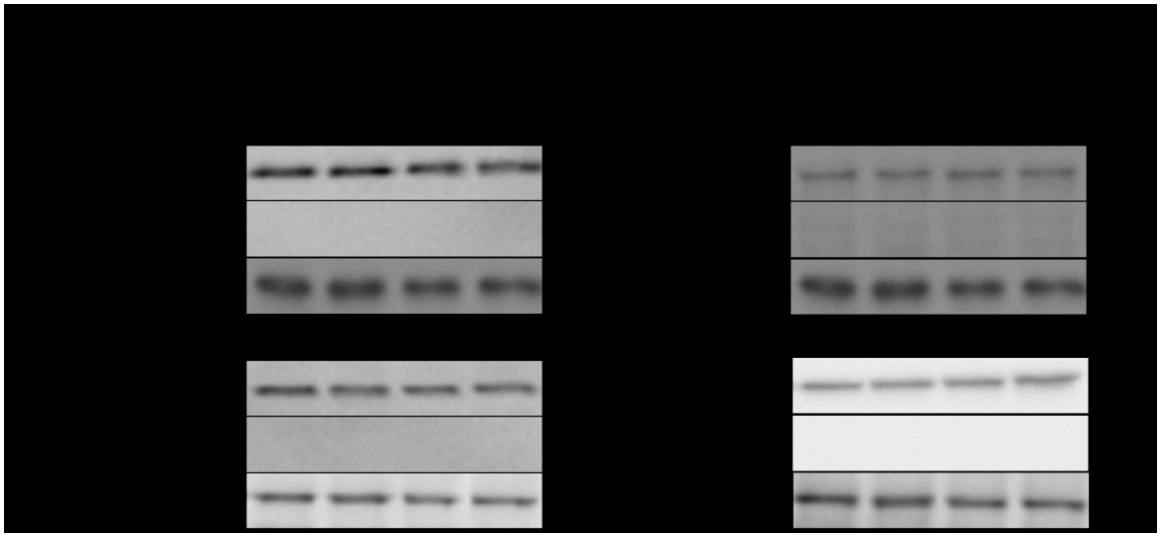

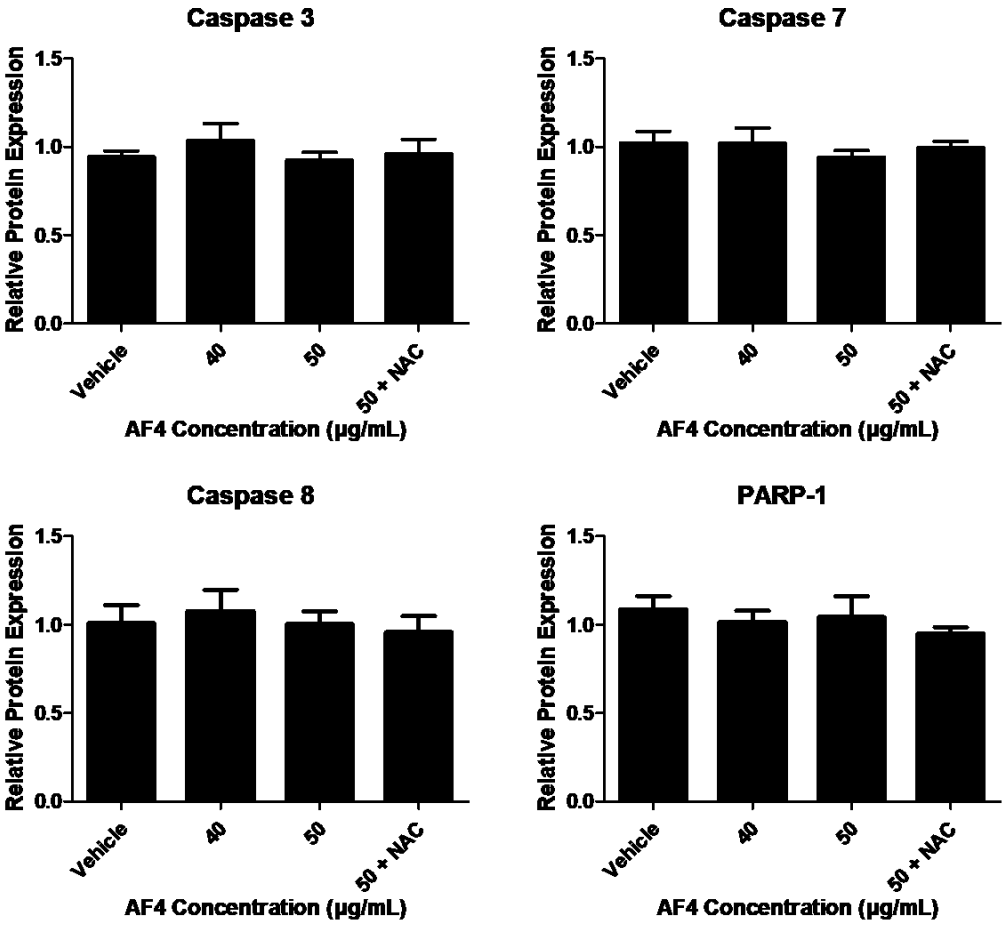

Figure 20. AF4-Induced Cell Death is Not Caspase-Dependant and Does Not Require PARP1 Cleavage

Figure 21. AF4 Does Not Affect the Protein Levels of the Housekeeping Genes GAPDH, Tubulin, and β-Actin. The effect of AF4 on the protein levels of housekeeping genes on MDA-MB-231 triple-negative breast cancer cells was determined by western blotting to ensure that normalization of western blot data was as accurate as possible. Data are shown as mean values ± SEM of three independent trials. Significance was determined by ANOVA with the Tukey-Kramer multiple comparisons post-test, and is denoted by * for $p < 0.05$, ** for $p < 0.01$, and *** for < 0.001. Differences between treatment groups is denoted by # for $p < 0.05$, ## for $p < 0.01$, and ### for < 0.001.

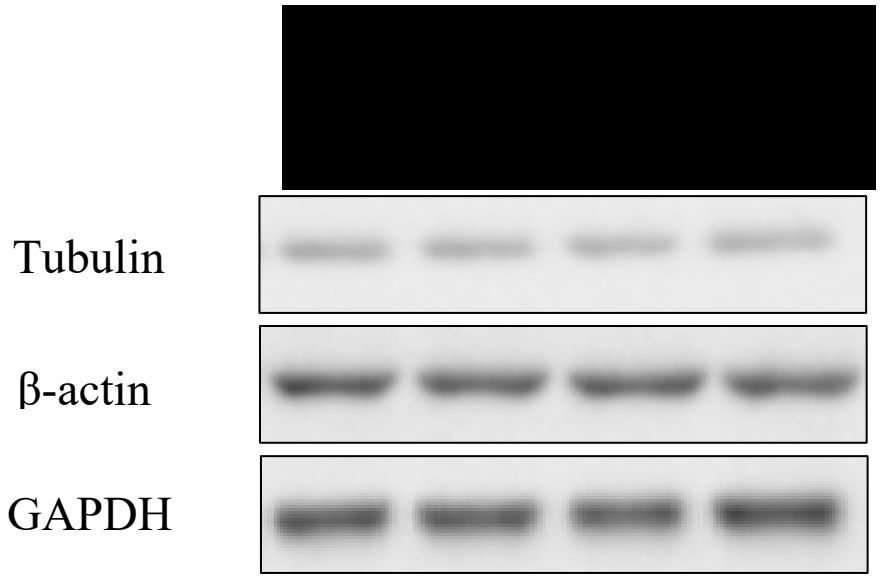

Figure 21. AF4 Does Not Affect the Protein Levels of the Housekeeping Genes GAPDH, Tubulin, and β-Actin.

Figure 22. AF4 Inhibits the Proliferation of MDA-MB-231 and MDA-MB-468 Breast Cancer Cells. The ability of AF4 to inhibit cell proliferation was examined with the Oregon Green flow cytometry assay. MDA-MB-231 (A) and MDA-MB-468 (B) cells were serum starved for 20 h then seeded at a density of 50,000 per well in a 6-well plate. Cells were allowed to adhere overnight then stained with Oregon Green prior to treating with AF4 at 20 µg/ mL, 30 µg/ mL, and 40 µg/ mL for 72 h. Representative histograms are shown. Data are shown as mean values ± SEM of four independent trials. Significance was determined by ANOVA with the Tukey-Kramer multiple comparisons post-test, and is denoted by * for $p < 0.05$, ** for $p < 0.01$, and *** for < 0.001.

A. MDA-MB-231

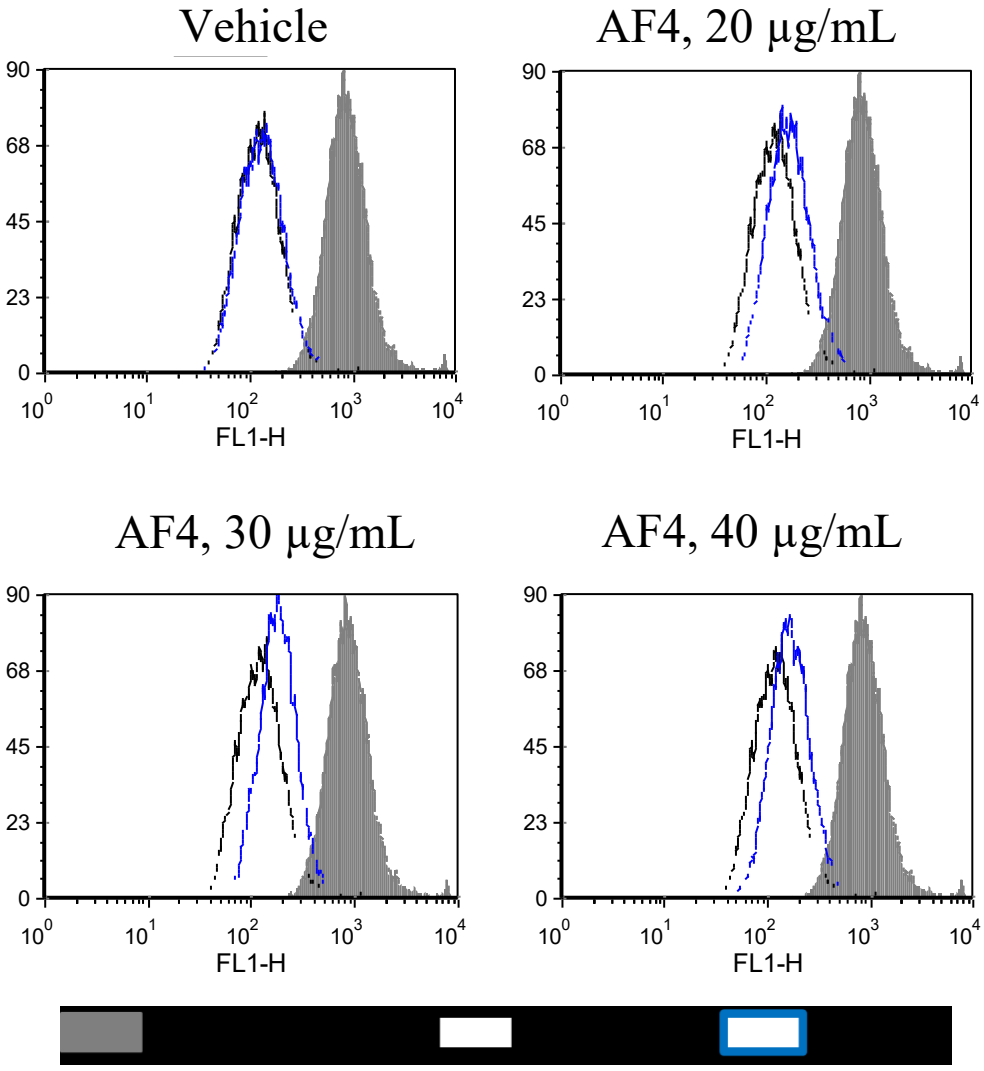
Vehicle
AF4, 20 µg/mL
AF4, 30 µg/mL
AF4, 40 µg/mL
90
68
45
23
0
10^0
10^1
10^2
10^3
10^4
FL1-H

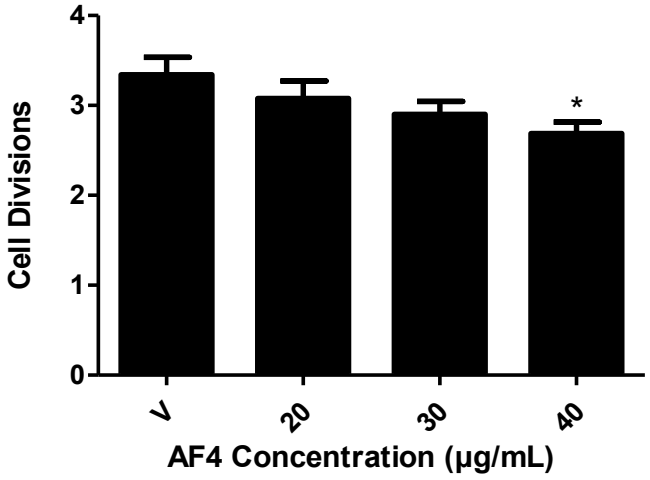
Cell Divisions
4
3
2
1
0
*
V
20
30
40
AF4 Concentration (µg/mL)

B. MDA-MB-468

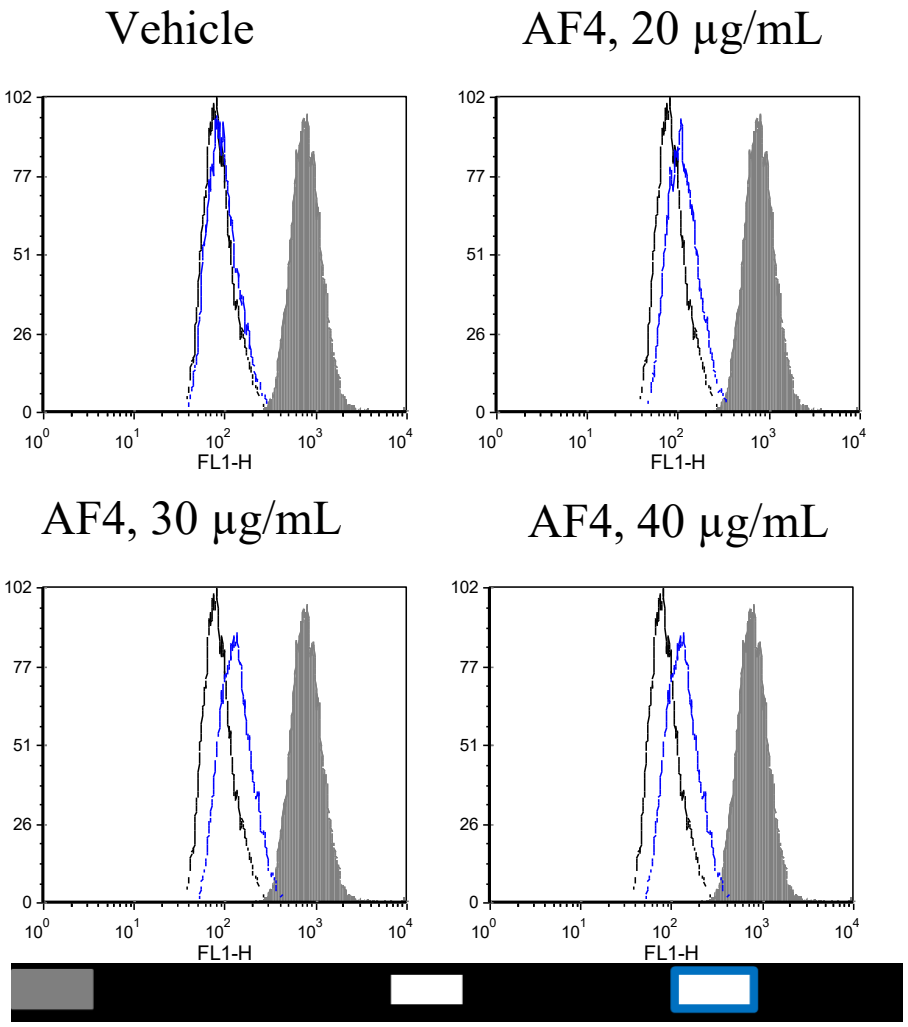
Vehicle
AF4, 20 µg/mL
AF4, 30 µg/mL
AF4, 40 µg/mL
102
77
51
26
0
FL1-H
Cell Divisions
AF4 Concentration (µg/mL)
V
20
30
40
*
**

Figure 22. AF4 Inhibits the Proliferation of MDA-MB-231 and MDA-MB-468 Breast Cancer Cells.

Figure 23. AF4 Induces G_0/G_1 Cell Cycle Arrest in MDA-MB-231 and MDA-MB-468 Breast Cancer Cells. The ability of AF4 to inhibit cell proliferation was examined further with cell cycle analysis. MDA-MB-231 (A) and MDA-MB-468 (B) cells were serum starved for 20 h then seeded at a density of 50,000 per well in a 6-well plate. Cells were allowed to adhere overnight prior to treating with AF4 at 20 µg/ mL, 30 µg/ mL, and 40 µg/ mL for 72h. Cells were then fixed, stained with PI, and read at FL2 at a rate of 50 cells per second. Representative histograms are shown. Data represented by mean values ± SEM of four independent trials. Significance was determined by ANOVA with the Tukey-Kramer multiple comparisons post-test, and is denoted by * for $p < 0.05$, ** for $p < 0.01$, and *** for $p < 0.001$.

A. MDA-MB-231

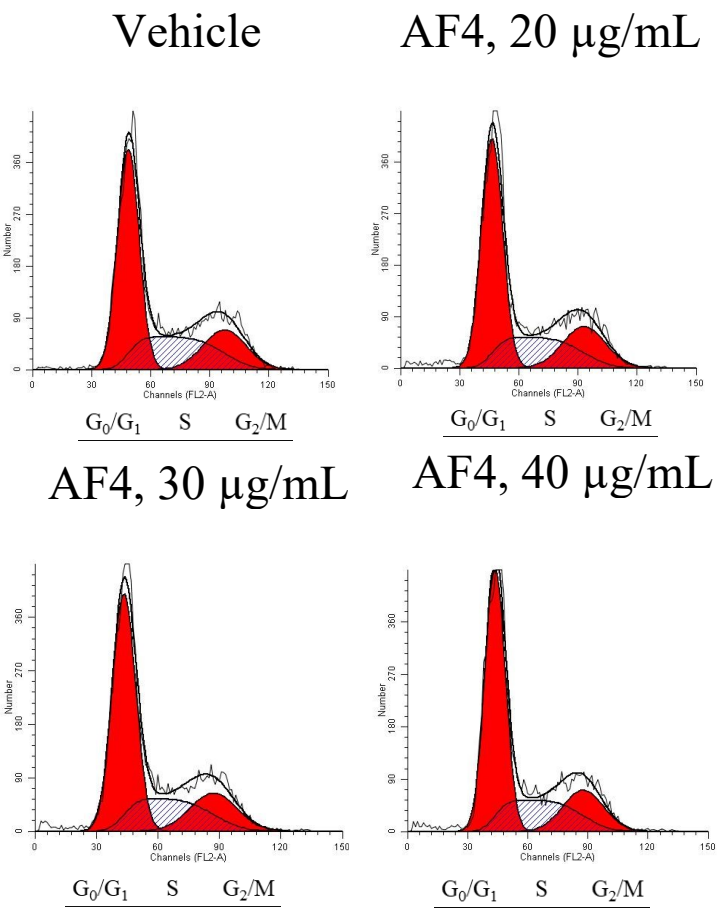
Vehicle
AF4, 20 µg/mL
AF4, 30 µg/mL
AF4, 40 µg/mL
Number
Channels (FL2-A)
G0/G1
S
G2/M

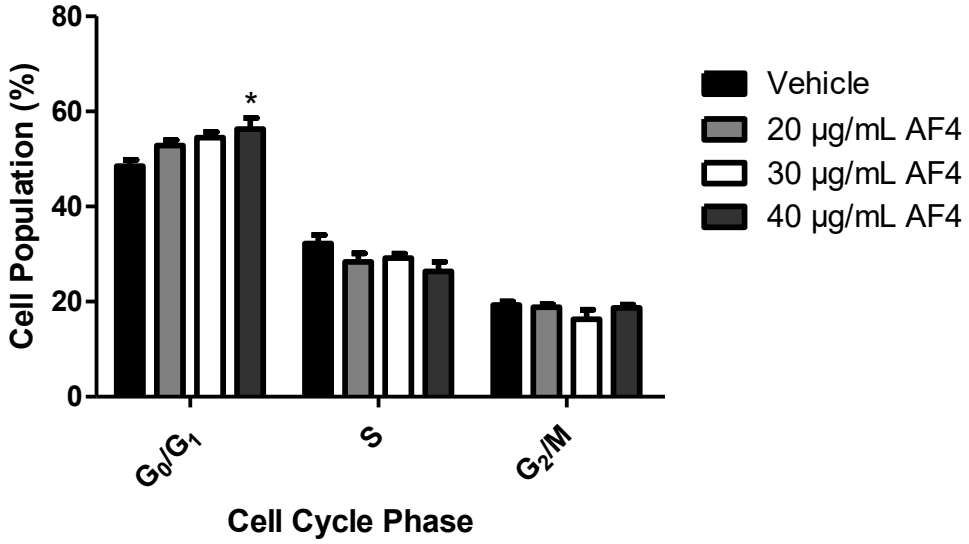
Cell Population (%)
80
60
40
20
0
*
G0/G1
S
G2/M
Cell Cycle Phase
Vehicle
20 µg/mL AF4
30 µg/mL AF4
40 µg/mL AF4

B. MDA-MB-468

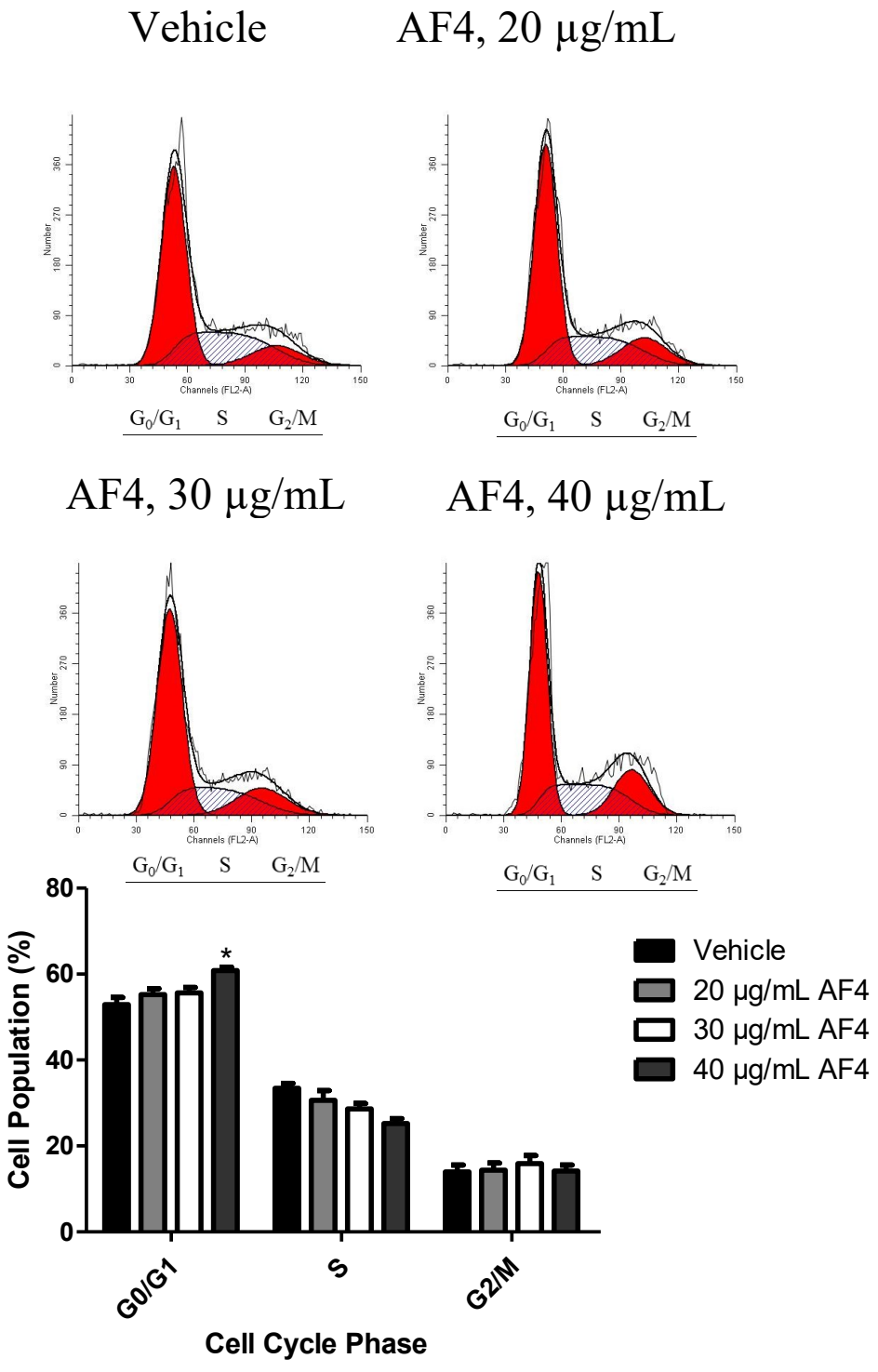

Figure 23. AF4 Induces G_0/G_1 Cell Cycle Arrest in MDA-MB-231 and MDA-MB-468 Breast Cancer Cells.

Figure 24.AF4 Downregulates the Protein Levels of G_1 Cell Cycle Proteins Cyclin D3, CDK4, and CDK6 in MDA-MB-231 and MDA-MB-468 Breast Cancer Cells. Protein isolates of MDA-MB-231 (A) and MDA-MB-468 (B) triple-negative breast cancer cells treated with AF4 (20 µg/mL and 40 µg/mL) for 24 h and 48 h were blotted and probed for the protein levels of cyclins and CDKs. Data are shown as mean values ± SEM of four independent trials. Significance was determined by ANOVA with the Tukey-Kramer multiple comparisons post-test, and is denoted by * for $p < 0.05$, ** for $p < 0.01$, and *** for $p < 0.001$.

A. MDA-MB-231, 24 h

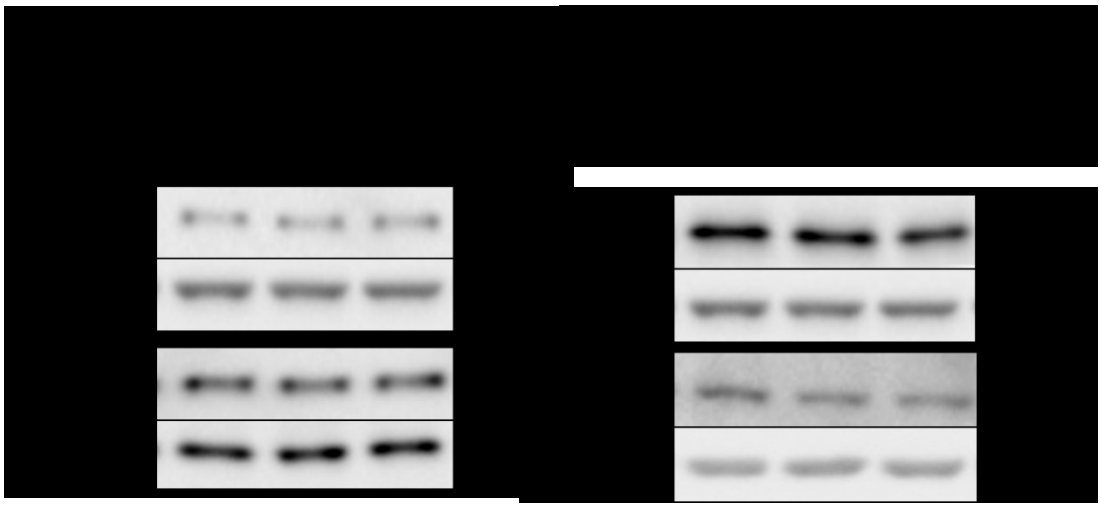

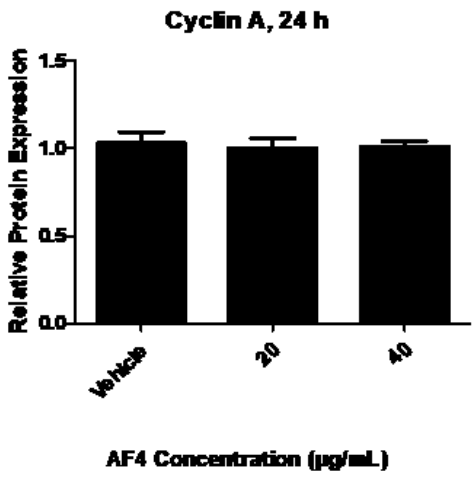

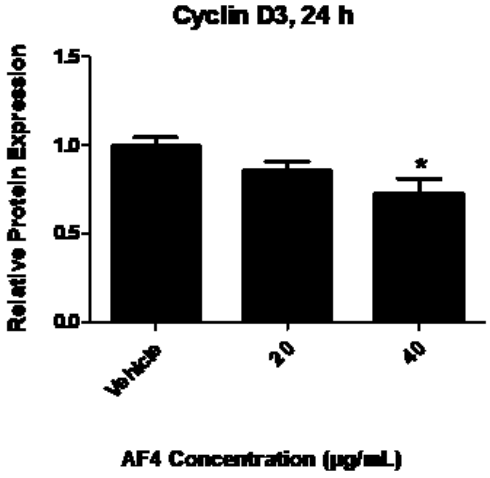

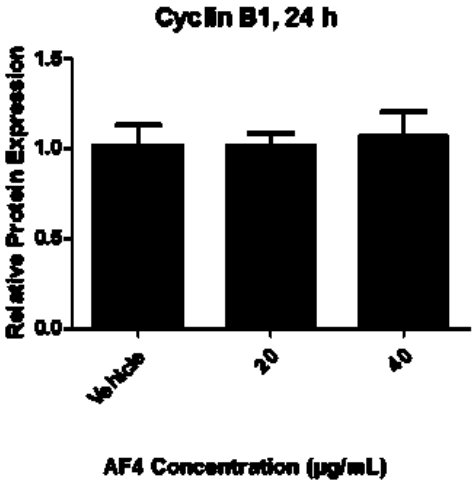

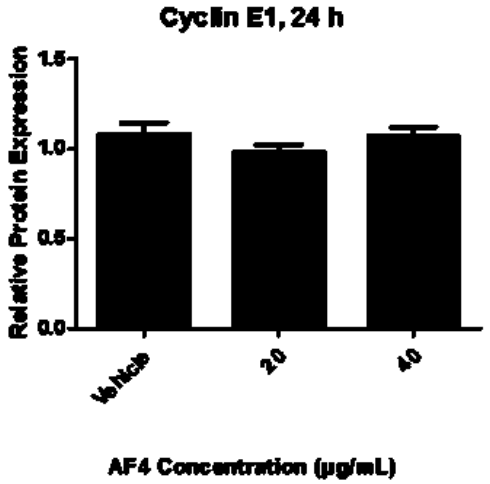

A. MDA-MB-231, 24 h

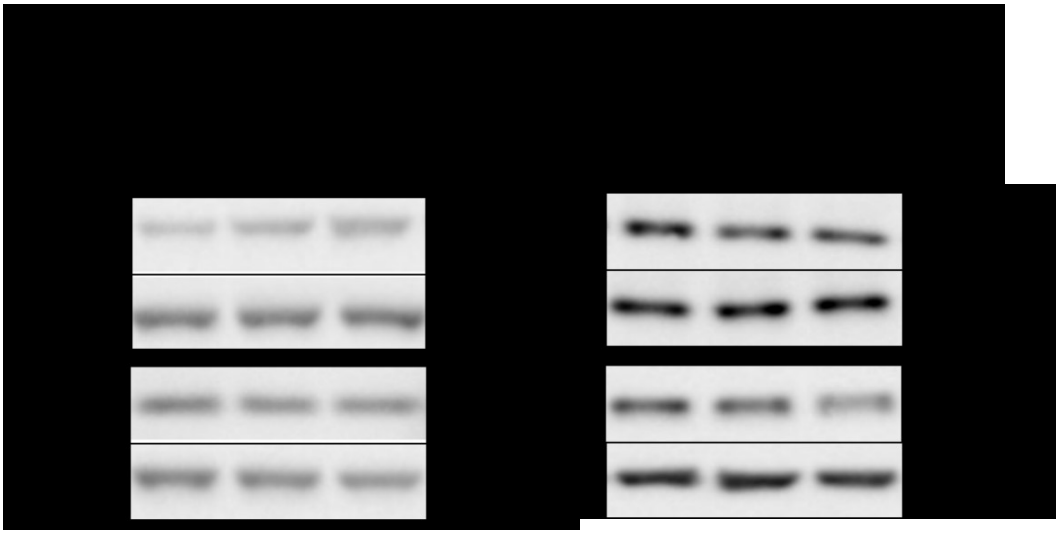

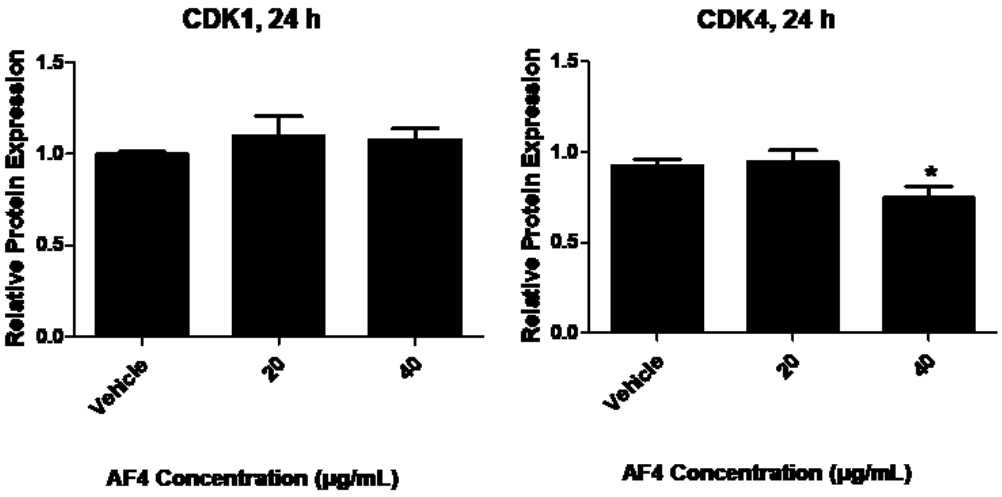

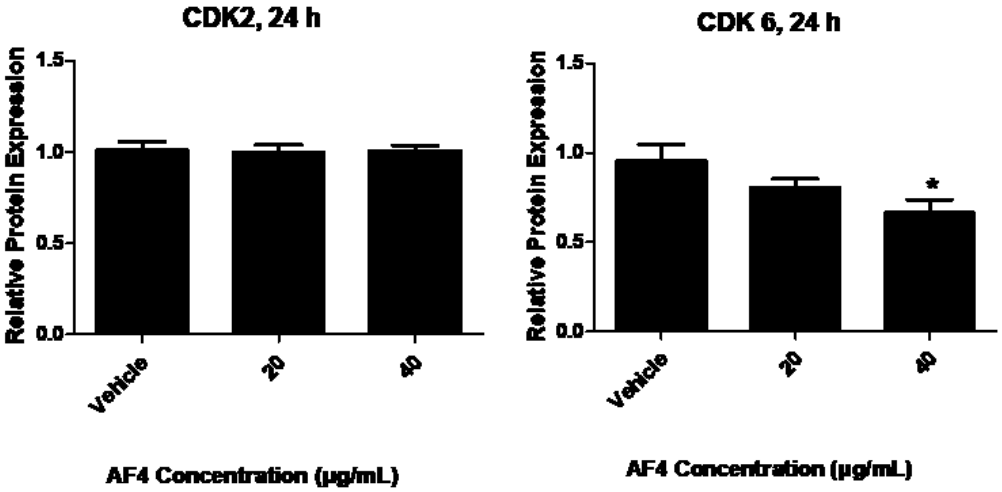

A. MDA-MB-231, 48 h

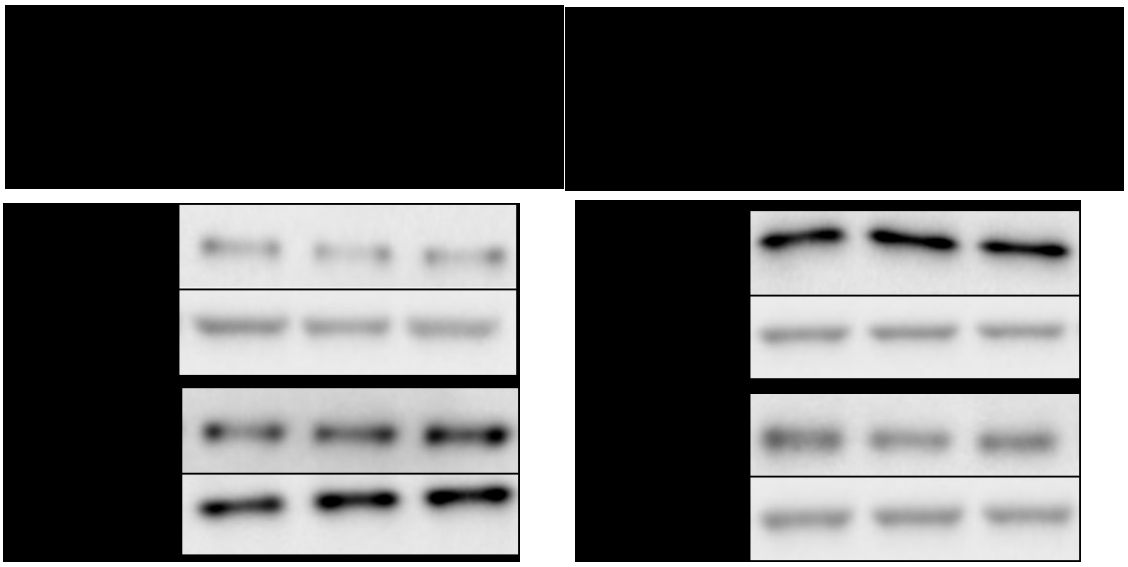

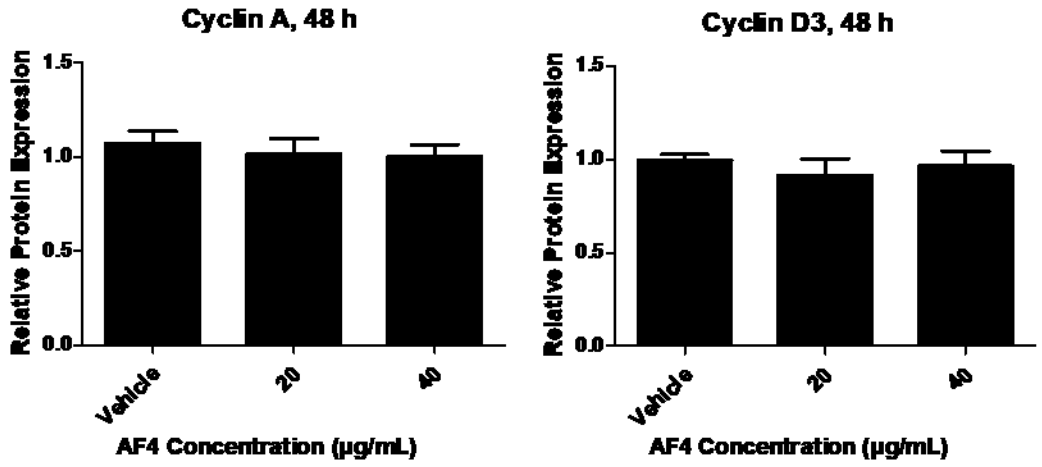

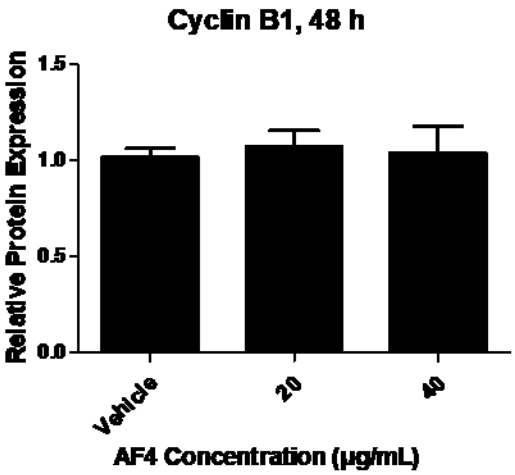

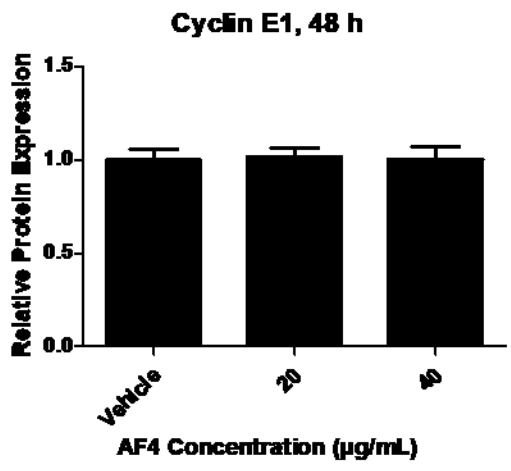

A. MDA-MB-231, 48 h

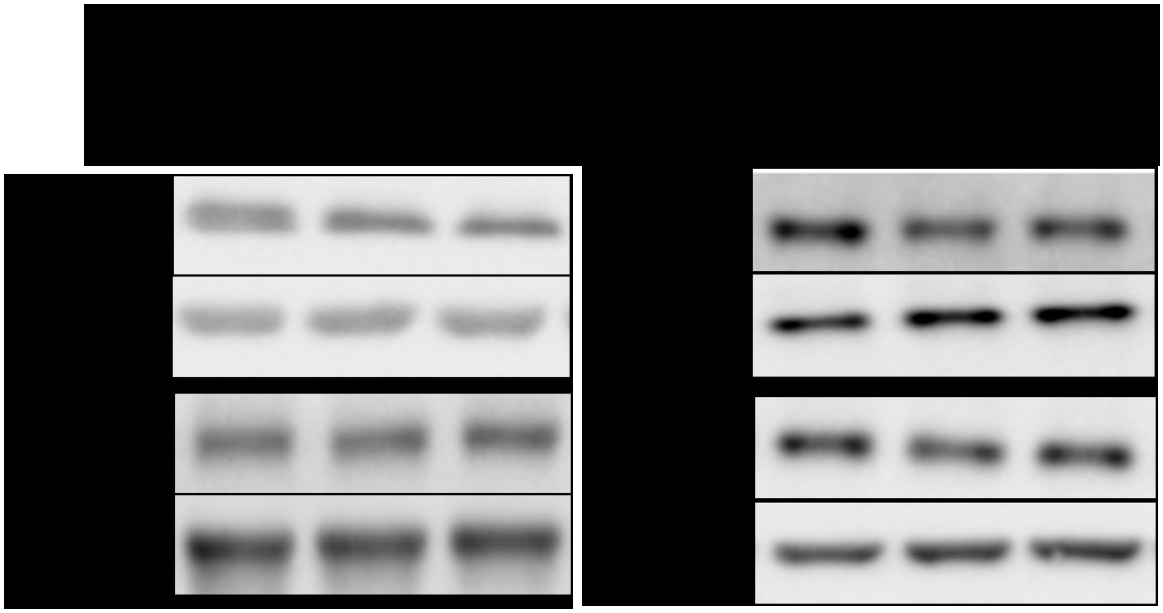

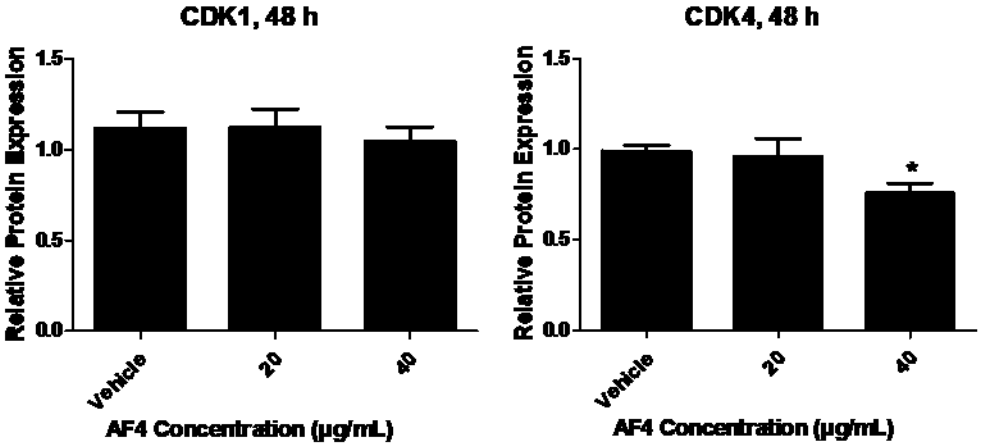

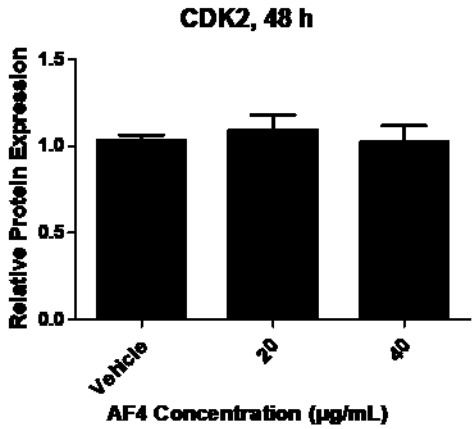

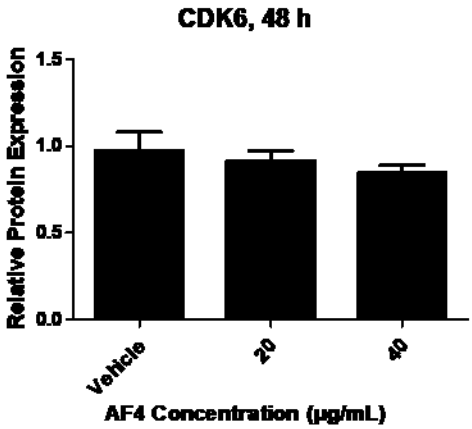

B. MDA-MB-468, 24 h

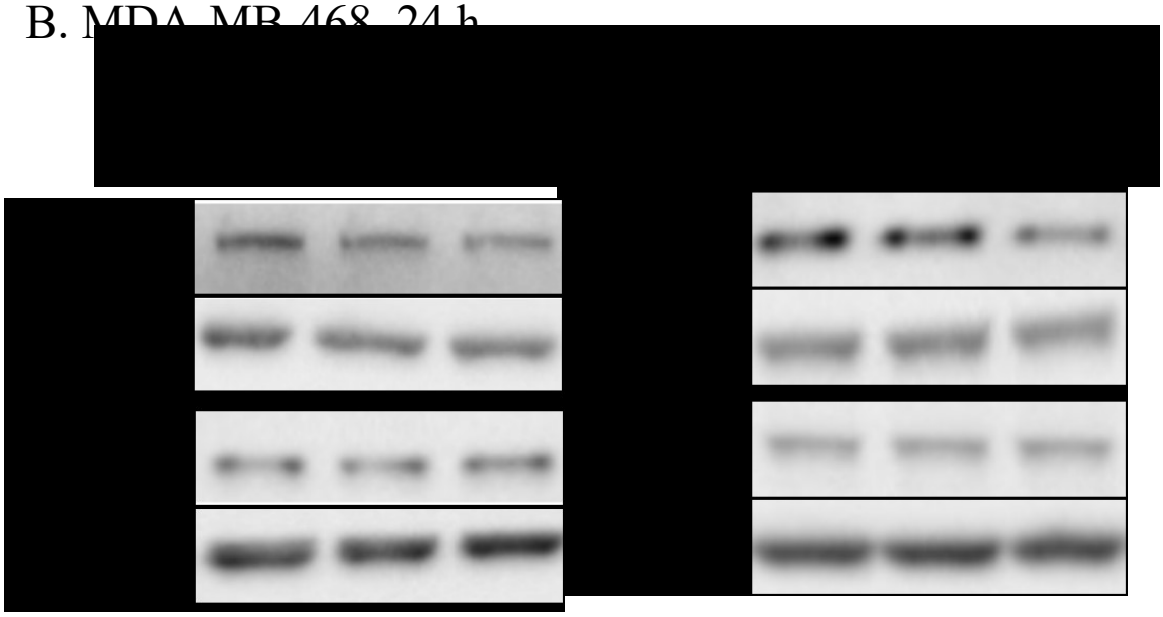

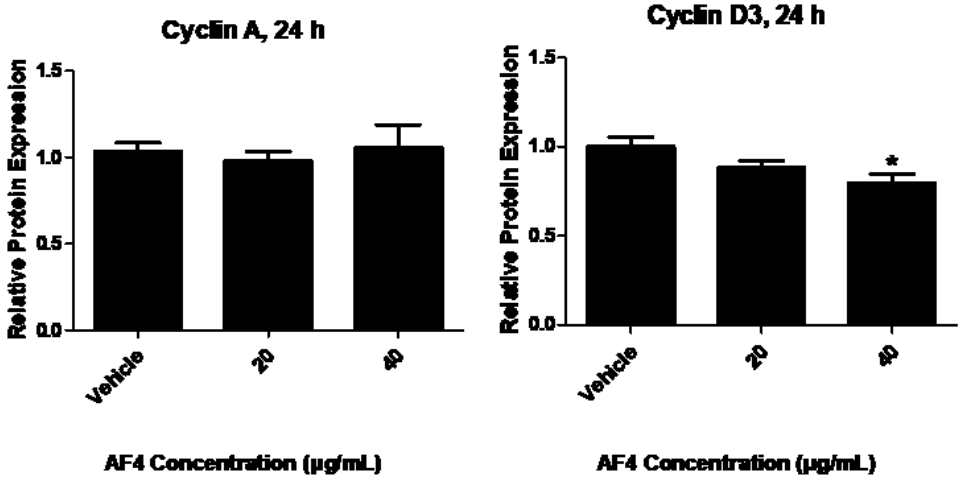

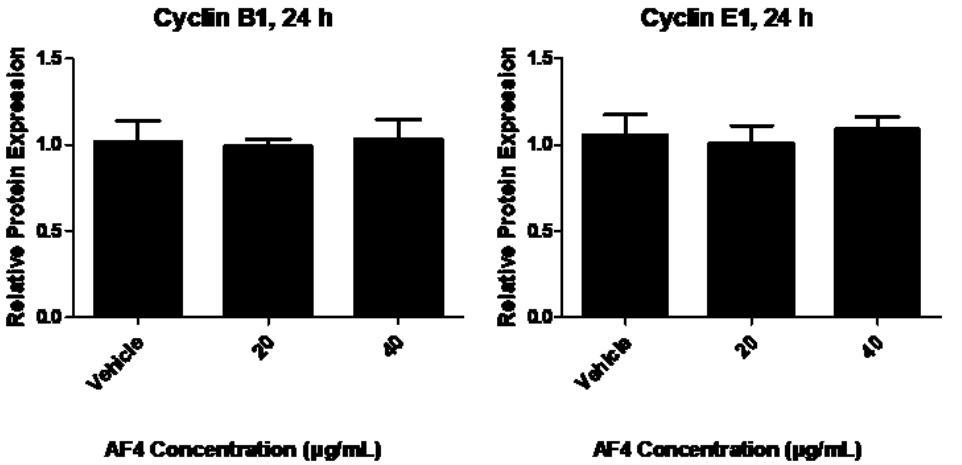

B. MDA-MB-468, 24 h

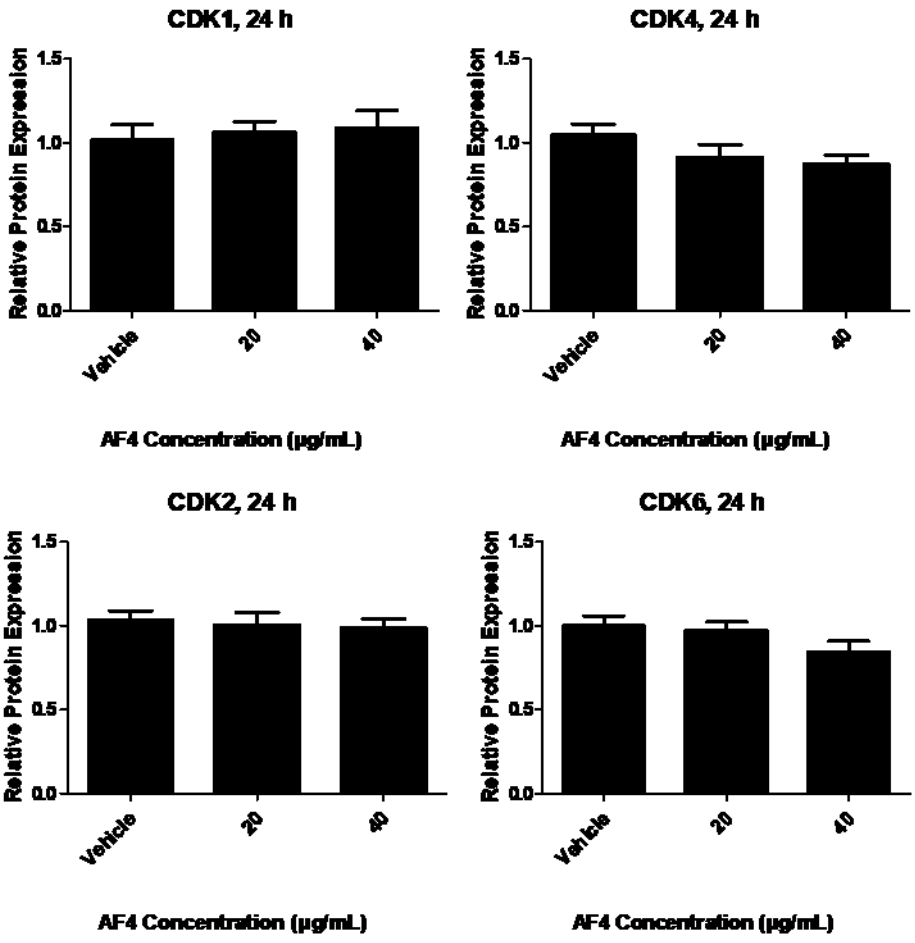

B. MDA-MB-468, 48 h

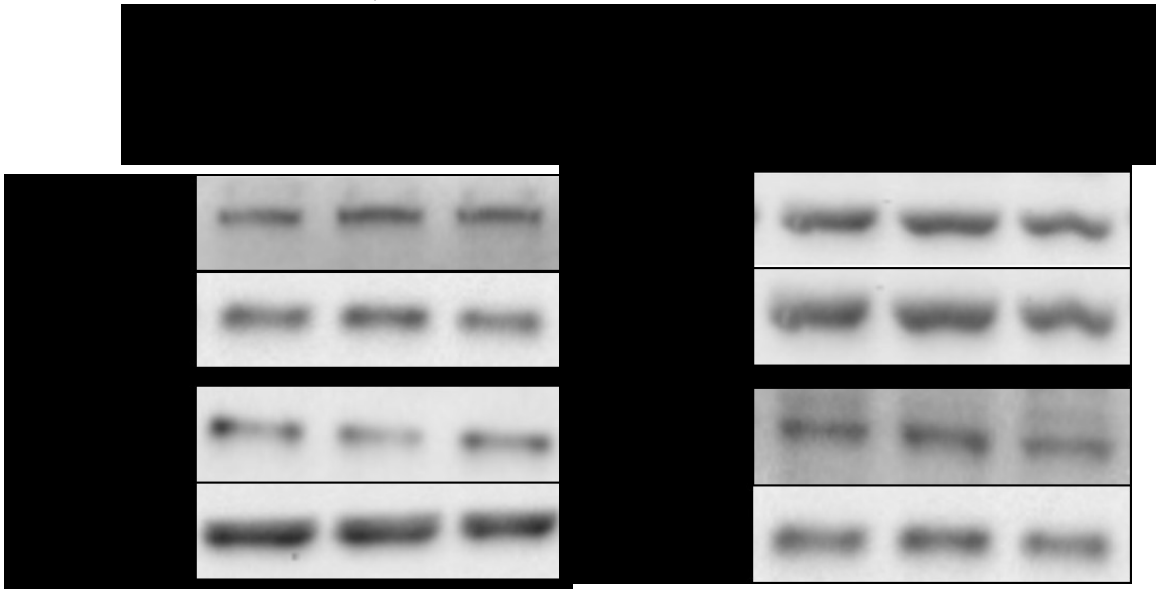

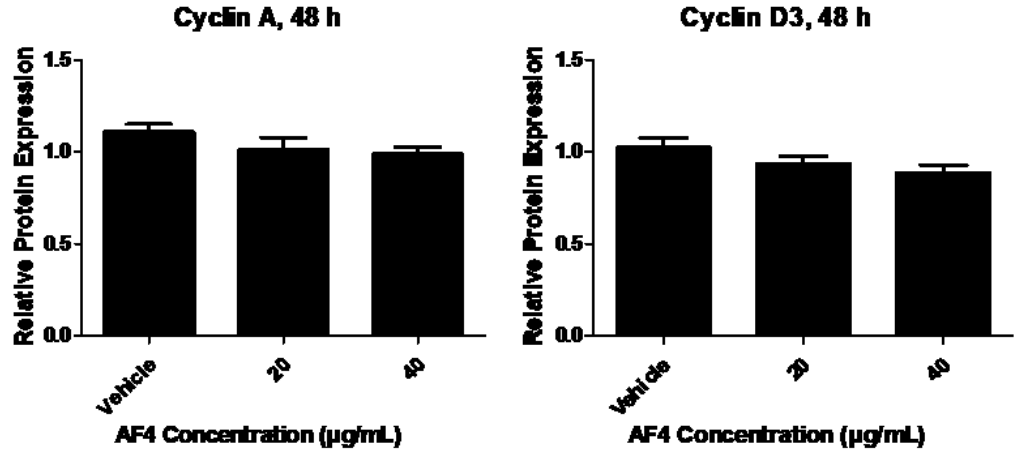

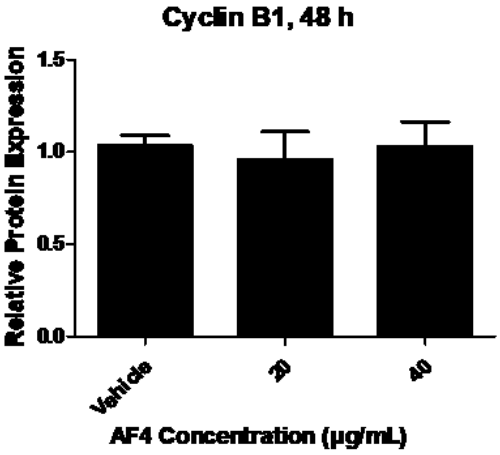

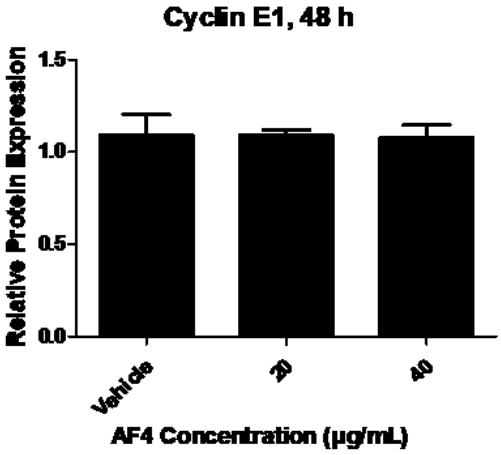

B. MDA-MB-468, 48 h

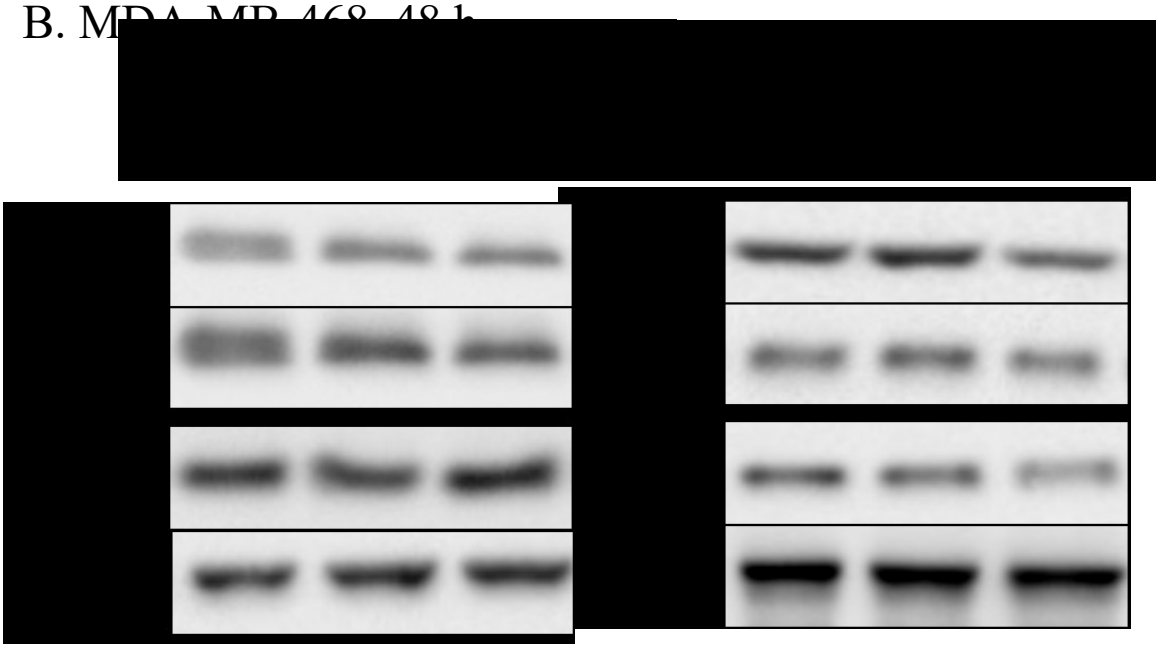

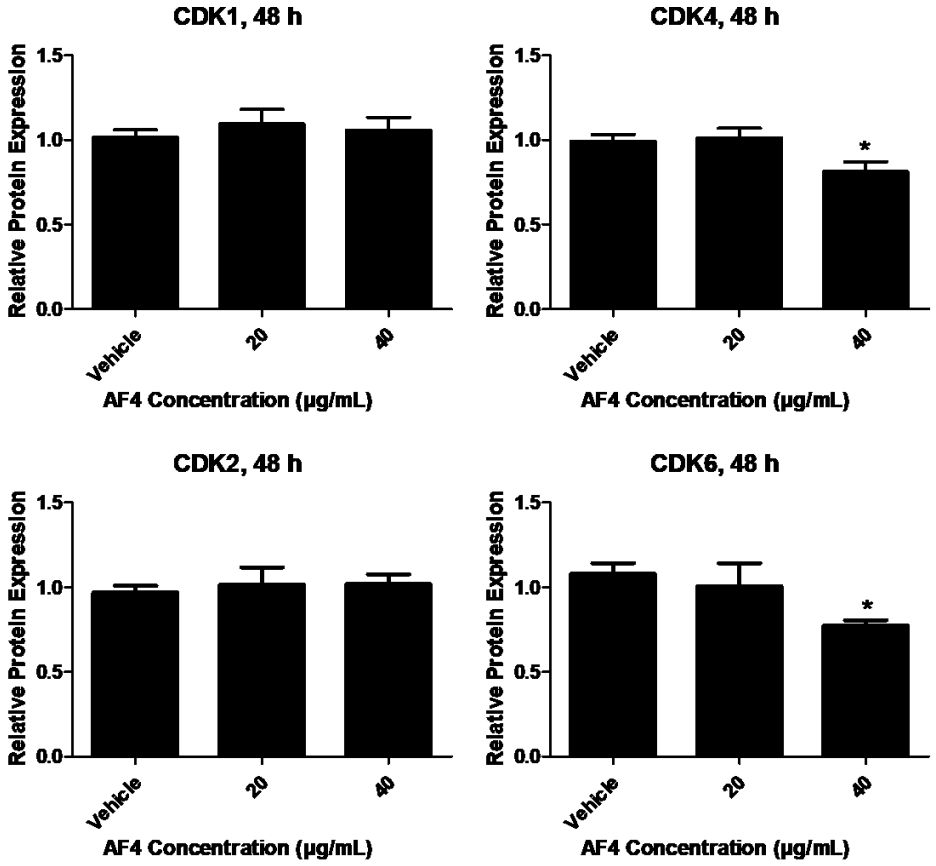

Figure 24.AF4 Downregulates the Protein Levels of G_1 Cell Cycle Proteins Cyclin D3, CDK4, and CDK6 in MDA-MB-231 and MDA-MB-468 Breast Cancer Cells.

Figure 25.AF4 Downregulates Akt Phosphorylation in a ROS-Dependent Manner. Protein isolates of MDA-MB-231cells (A) and MDA-MB-468 cells (B) treated with AF4 (20 µg/mL and 40 µg/mL) with or without 20 mM NAC pre-treatment for 72 h were blotted and probed for protein levels and phosphorylation of proteins in the PI3K/Akt pathway. Data are shown as mean values ± SEM of four independent trials. Significance was determined by ANOVA with the Tukey-Kramer multiple comparisons post-test, and is denoted by * for $p < 0.05$, ** for $p < 0.01$, and *** for < 0.001.

A. MDA-MB-231

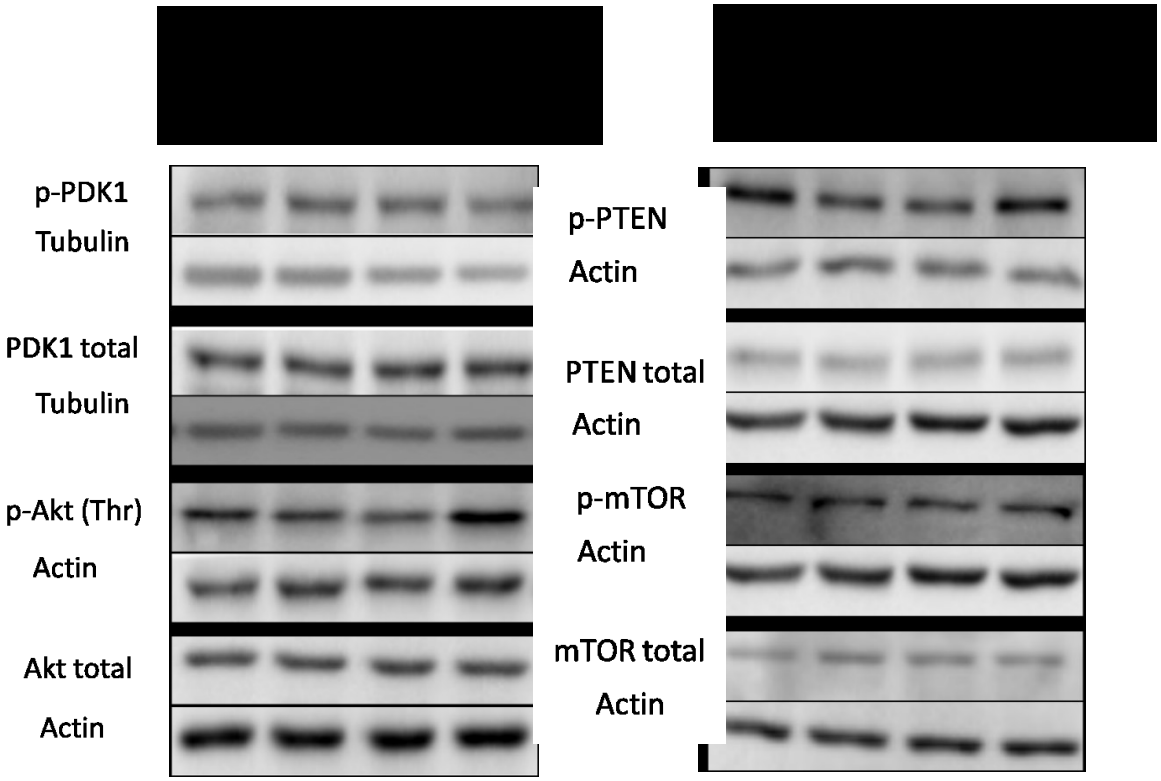
p-PDK1
Tubulin
PDK1 total
Tubulin
p-Akt (Thr)
Actin
Akt total
Actin
p-PTEN
Actin
PTEN total
Actin
p-mTOR
Actin
mTOR total
Actin

A. MDA-MB-231

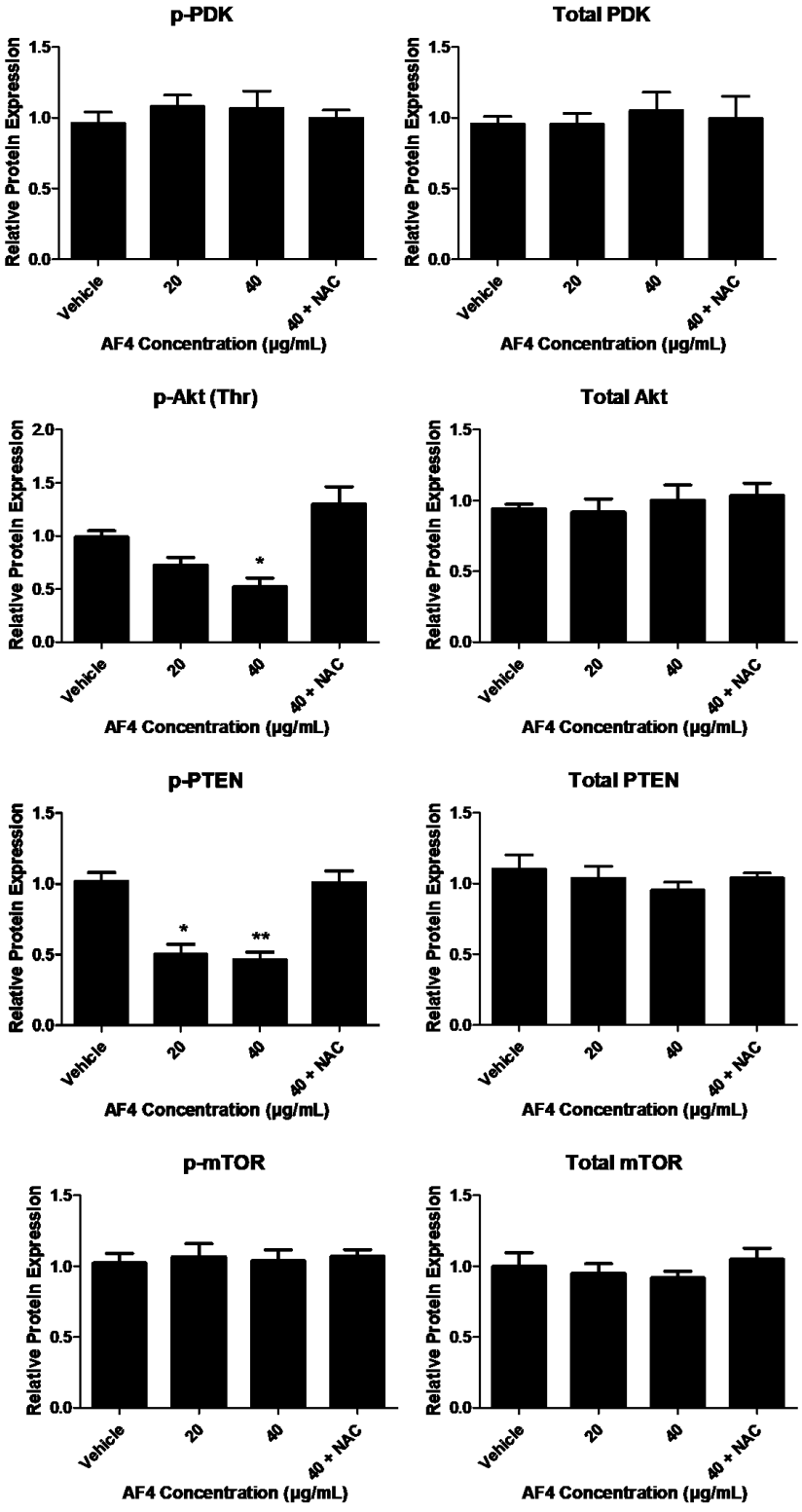
p-PDK
Total PDK
p-Akt (Thr)
Total Akt
p-PTEN
Total PTEN
p-mTOR
Total mTOR
Relative Protein Expression
AF4 Concentration (µg/mL)
Vehicle
20
40
40 + NAC
*
**

B. MDA-MB-468

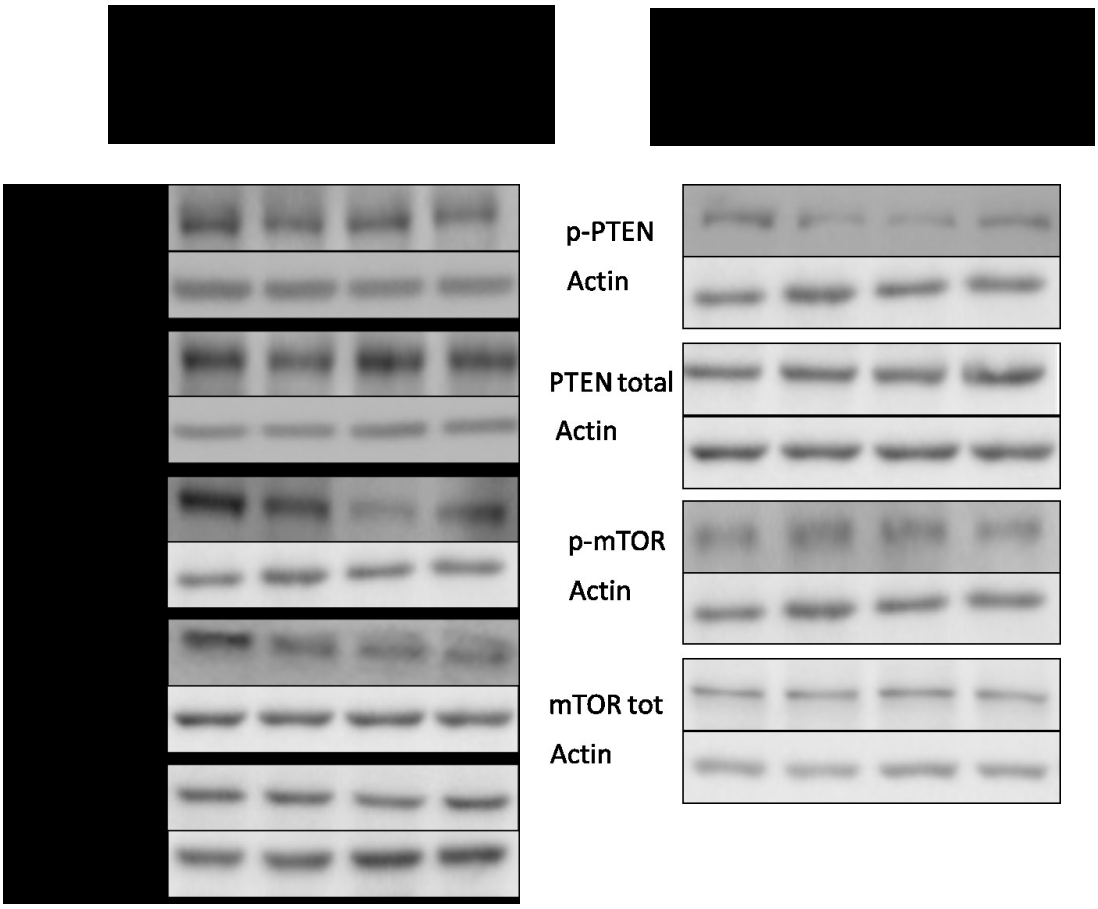

B. MDA-MB-468

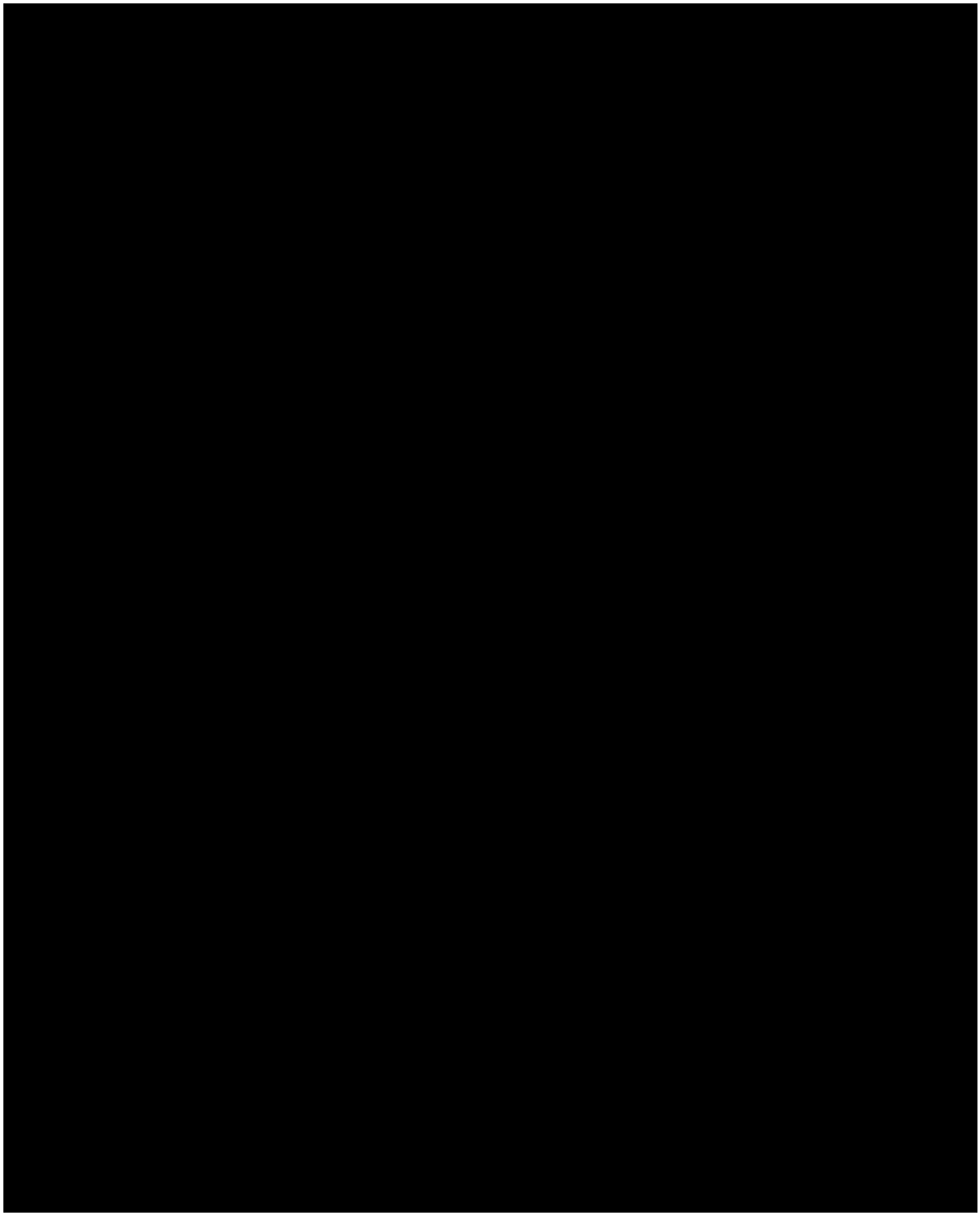

Figure 25. AF4 Downregulates Akt Phosphorylation in a ROS-Dependent Manner.

Figure 26. AF4 Affects Erk1/2 Phosphorylation in a ROS-Dependent Manner. Protein isolates of MDA-MB-231 cells (A) and MDA-MB-468 cells (B) treated with AF4 (20 μg/mL and 40 μg/mL) with or without 20 mM NAC pre-treatment for 72 h were blotted and probed for proteins in the ERK/MAPK pathway. Data are shown as mean values ± SEM of four independent trials. Significance was determined by ANOVA with the Tukey-Kramer multiple comparisons post-test, and is denoted by * for $p < 0.05$, ** for $p < 0.01$, and *** for < 0.001.

A. MDA-MB-231

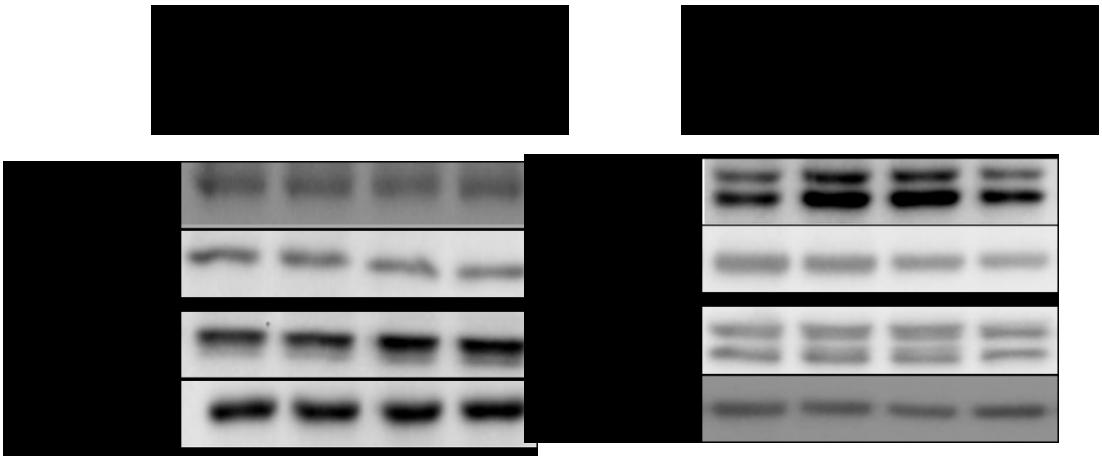

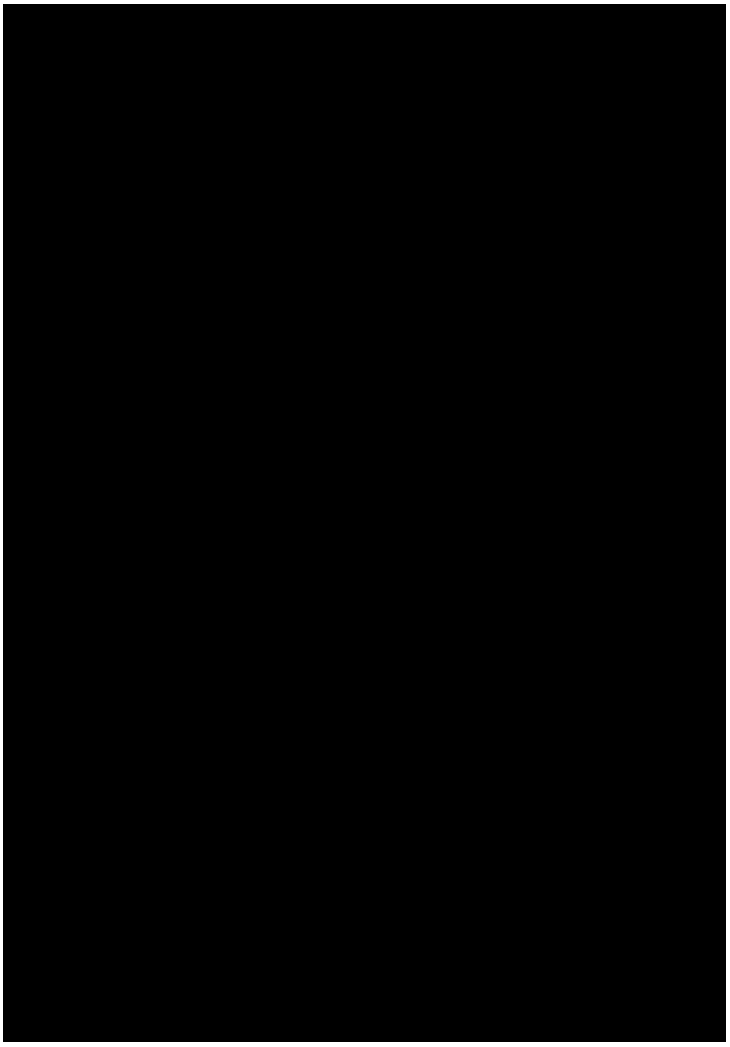

B. MDA-MB-468

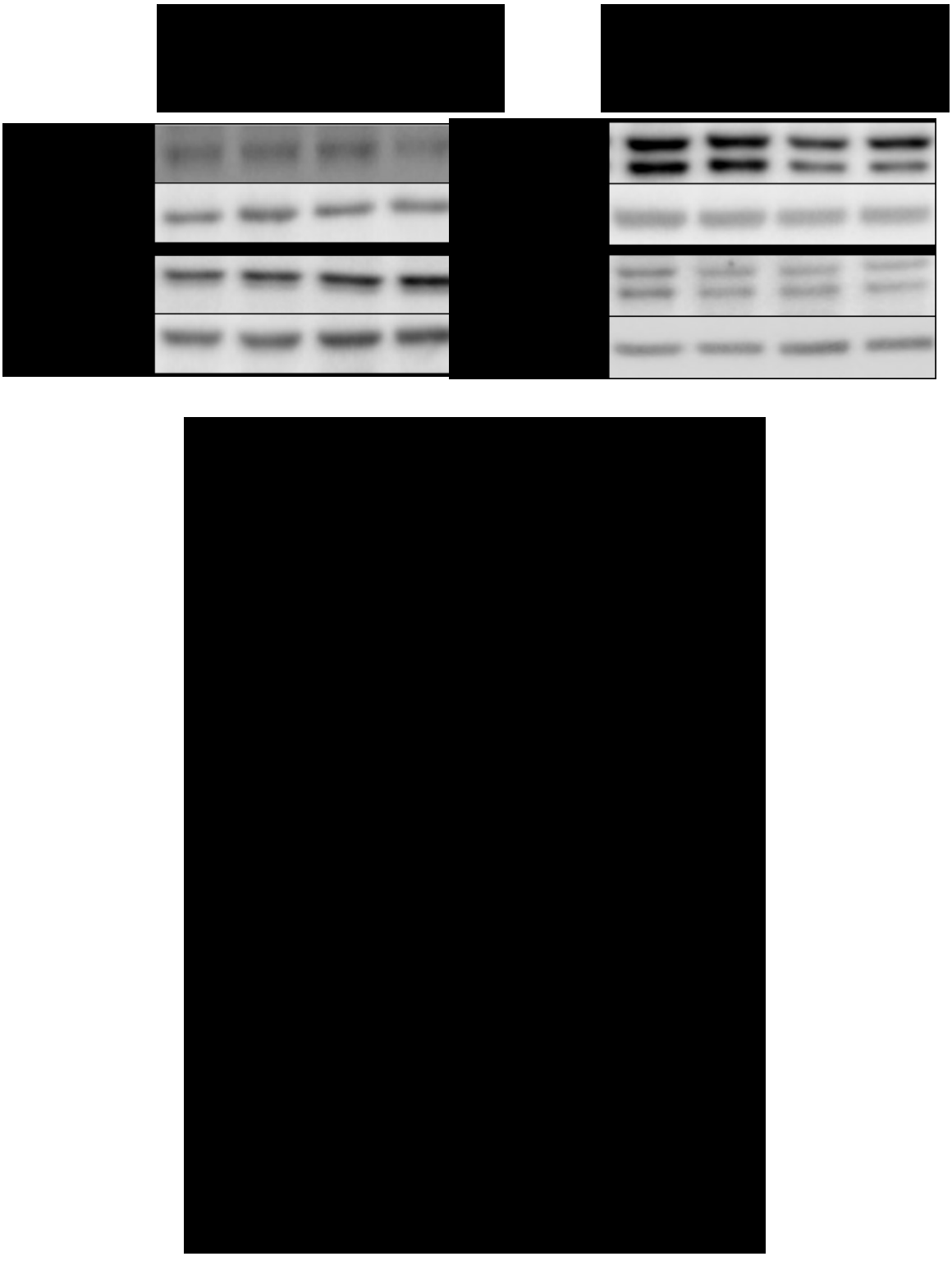

Figure 26. AF4 Affects Erk1/2 Phosphorylation in a ROS-Dependent Manner Independent of Independent of the MAPK/ERK Pathway.

Figure 27. AF4 Has No Effect on the Protein Levels of Proteins Involved in ROS Signalling. Protein isolates of MDA-MB-231 cells (A) and MDA-MB-468 cells (B) treated with AF4 (20 µg/mL and 40 µg/mL) with or without 20 mM NAC pre-treatment for 72 h were blotted and probed for proteins involved in ROS signalling. Data are shown as mean values ± SEM of four independent trials. Significance was determined by ANOVA with the Tukey-Kramer multiple comparisons post-test, and is denoted by * for $p < 0.05$, ** for $p < 0.01$, and *** for < 0.001.

A. MDA-MB-231

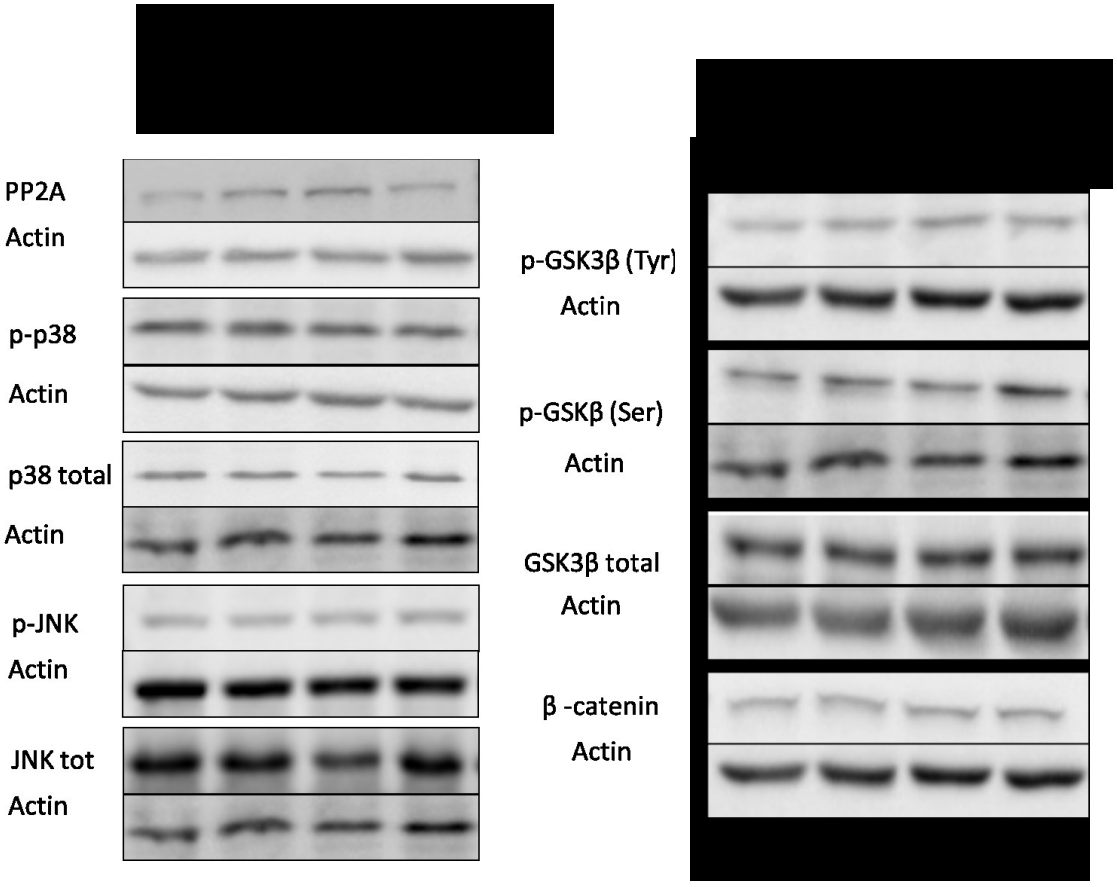
PP2A
Actin
p-p38
Actin
p38 total
Actin
p-JNK
Actin
JNK tot
Actin
p-GSK3β (Tyr)
Actin
p-GSKβ (Ser)
Actin
GSK3β total
Actin
β -catenin
Actin

A. MDA-MB-231

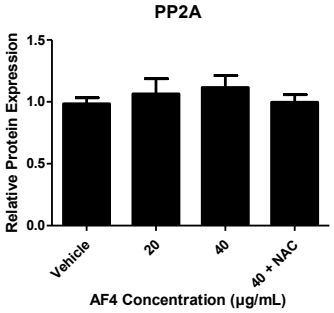
PP2A
Relative Protein Expression
1.5
1.0
0.5
0.0
Vehicle
20
40
40 + NAC
AF4 Concentration (µg/mL)

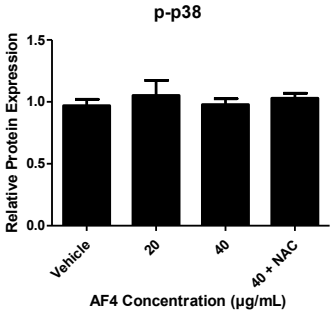
p-p38
Relative Protein Expression
1.5
1.0
0.5
0.0
Vehicle
20
40
40 + NAC
AF4 Concentration (µg/mL)

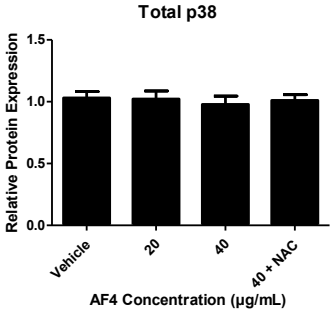
Total p38
Relative Protein Expression
1.5
1.0
0.5
0.0
Vehicle
20
40
40 + NAC
AF4 Concentration (µg/mL)

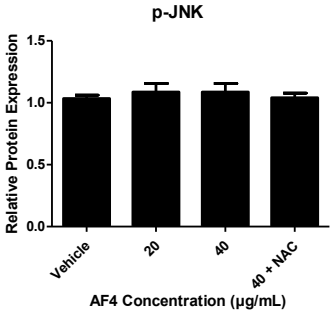
p-JNK
Relative Protein Expression
1.5
1.0
0.5
0.0
Vehicle
20
40
40 + NAC
AF4 Concentration (µg/mL)

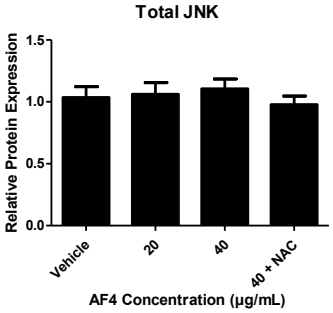
Total JNK
Relative Protein Expression
1.5
1.0
0.5
0.0
Vehicle
20
40
40 + NAC
AF4 Concentration (µg/mL)

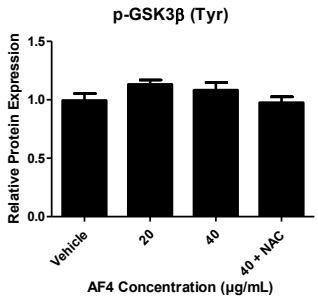
p-GSK3β (Tyr)
Relative Protein Expression
1.5
1.0
0.5
0.0
Vehicle
20
40
40 + NAC
AF4 Concentration (µg/mL)

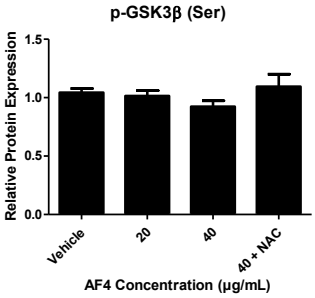
p-GSK3β (Ser)
Relative Protein Expression
1.5
1.0
0.5
0.0
Vehicle
20
40
40 + NAC
AF4 Concentration (µg/mL)

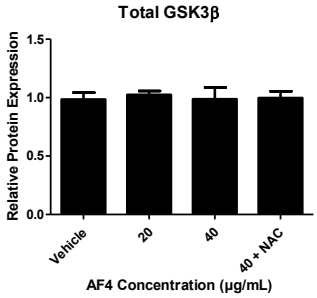
Total GSK3β
Relative Protein Expression
1.5
1.0
0.5
0.0
Vehicle
20
40
40 + NAC
AF4 Concentration (µg/mL)

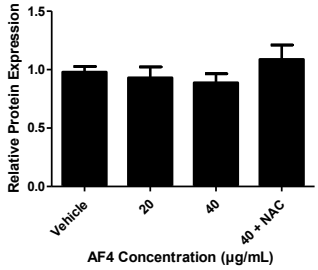
β-catenin
Relative Protein Expression
1.5
1.0
0.5
0.0
Vehicle
20
40
40 + NAC
AF4 Concentration (µg/mL)

B. MDA-MB-468

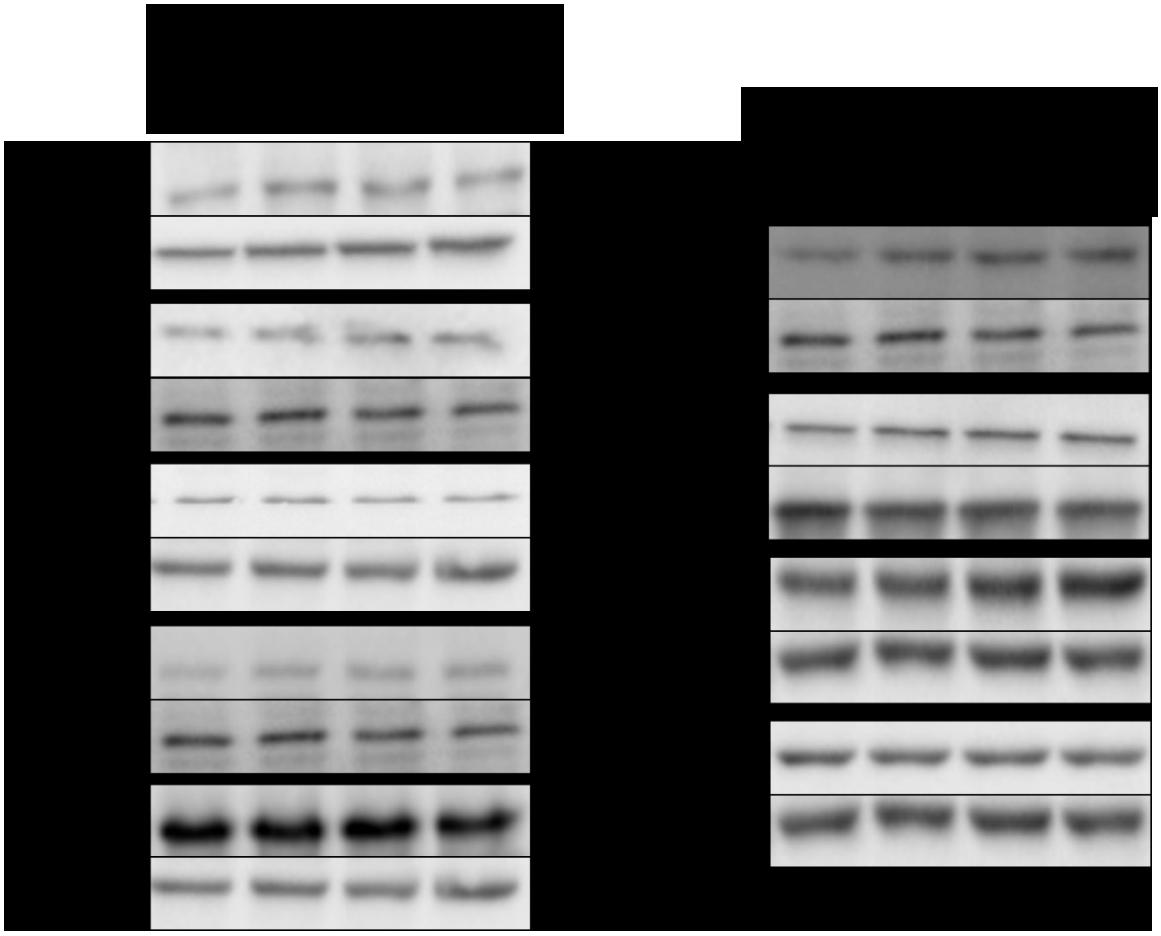

B. MDA-MB-468

Figure 27. AF4 Has No Effect on the Protein Levels of Cancer-Related Proteins Involved in ROS Signalling.

Figure 28.AF4 Affects the Protein Levels of Epigenetic Enzymes in MDA-MB-231 and MDA-MB-468 Breast Cancer Cells and MCF10A Epithelial Cells. Protein isolates of MDA-MB-231 cells (A), MDA-MB-468 cells (B), and MCF10A cells (C) treated with AF4 (20 µg/mL and 40 µg/mL) for 48 h and72 h were blotted and probed for the levels of proteins involved epigenetic remodelling. Data are shown as mean values ± SEM of four independent trials. Significance was determined by ANOVA with the Tukey-Kramer multiple comparisons post-test, and is denoted by * for $p < 0.05$, ** for $p < 0.01$, and *** for < 0.001.

A. MDA-MB-231, 48 h

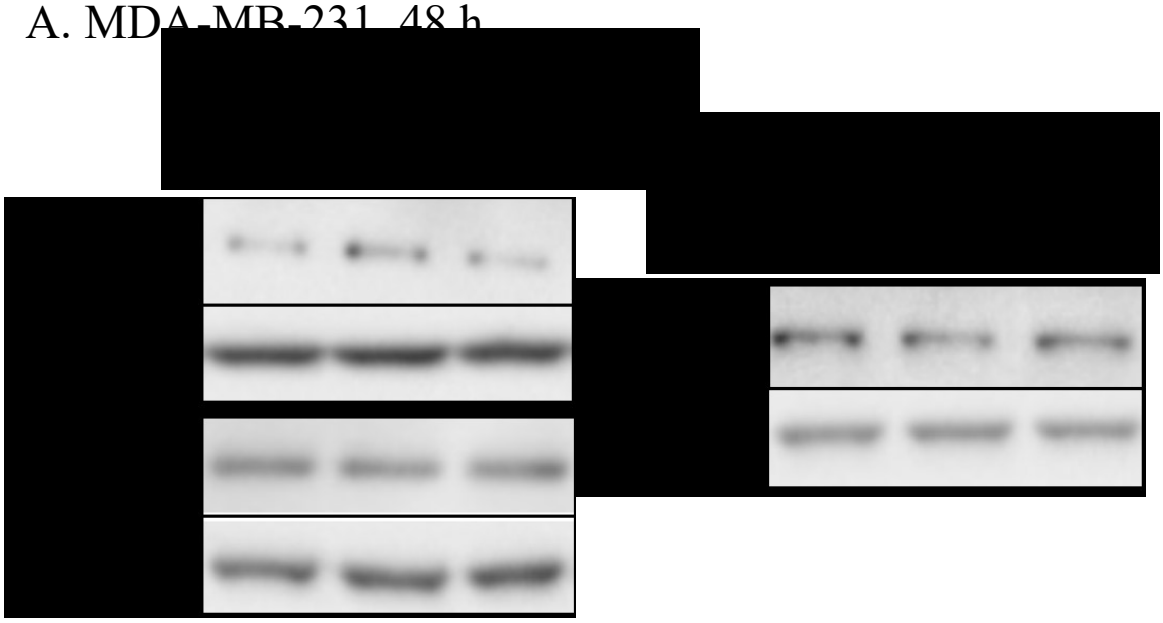

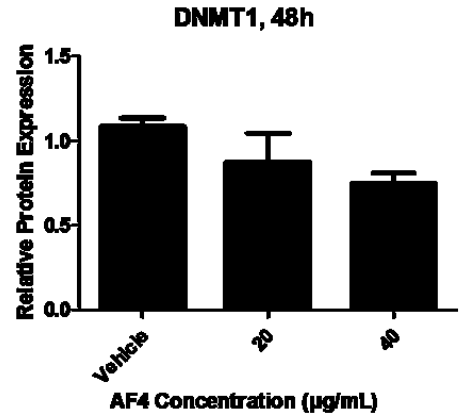

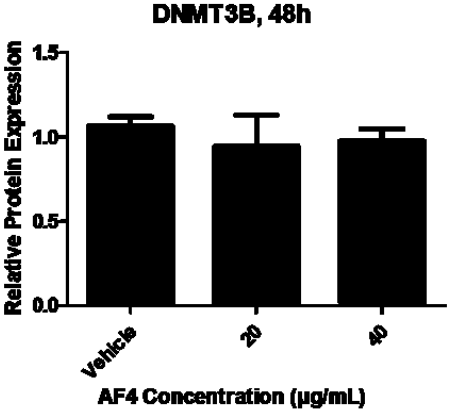

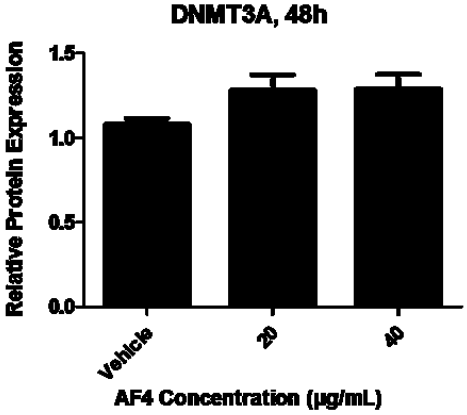

A. MDA-MB-231, 48 h

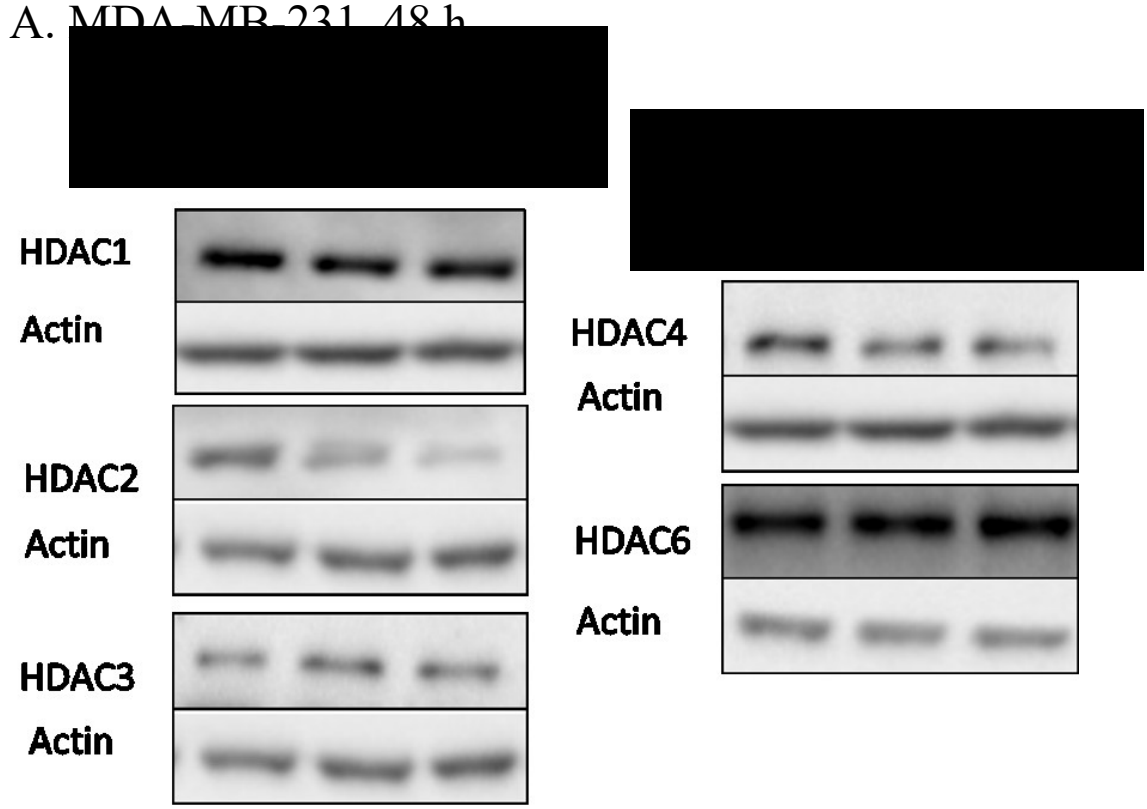

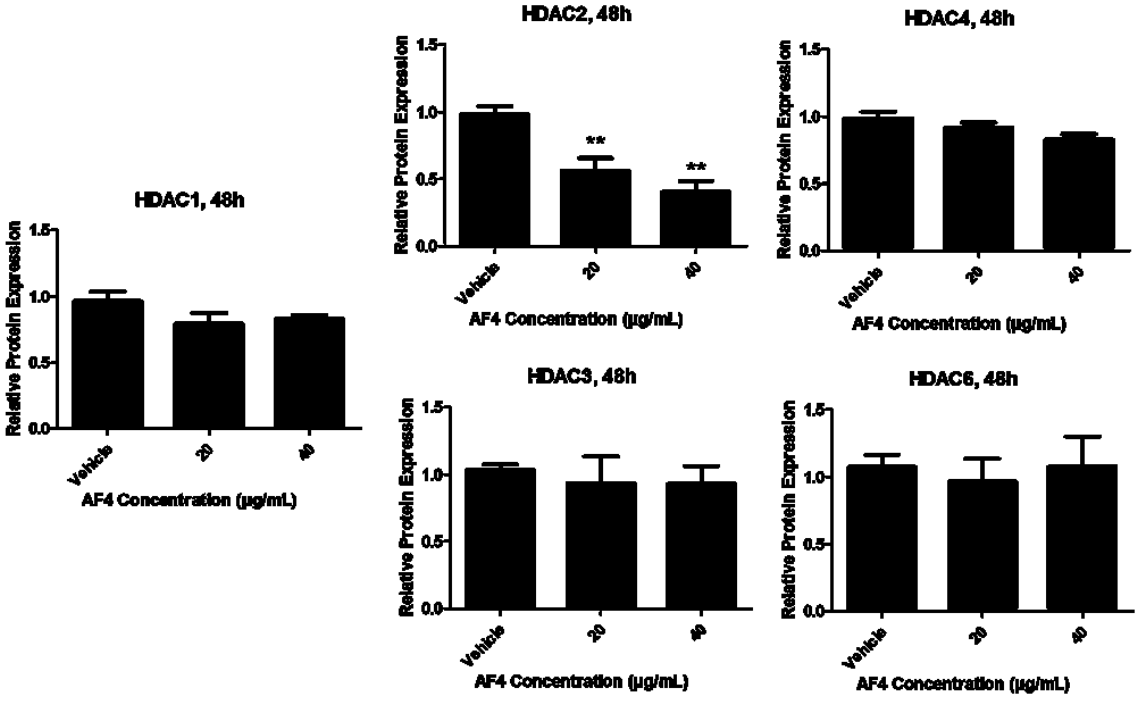

A. MDA-MB-231, 48 h

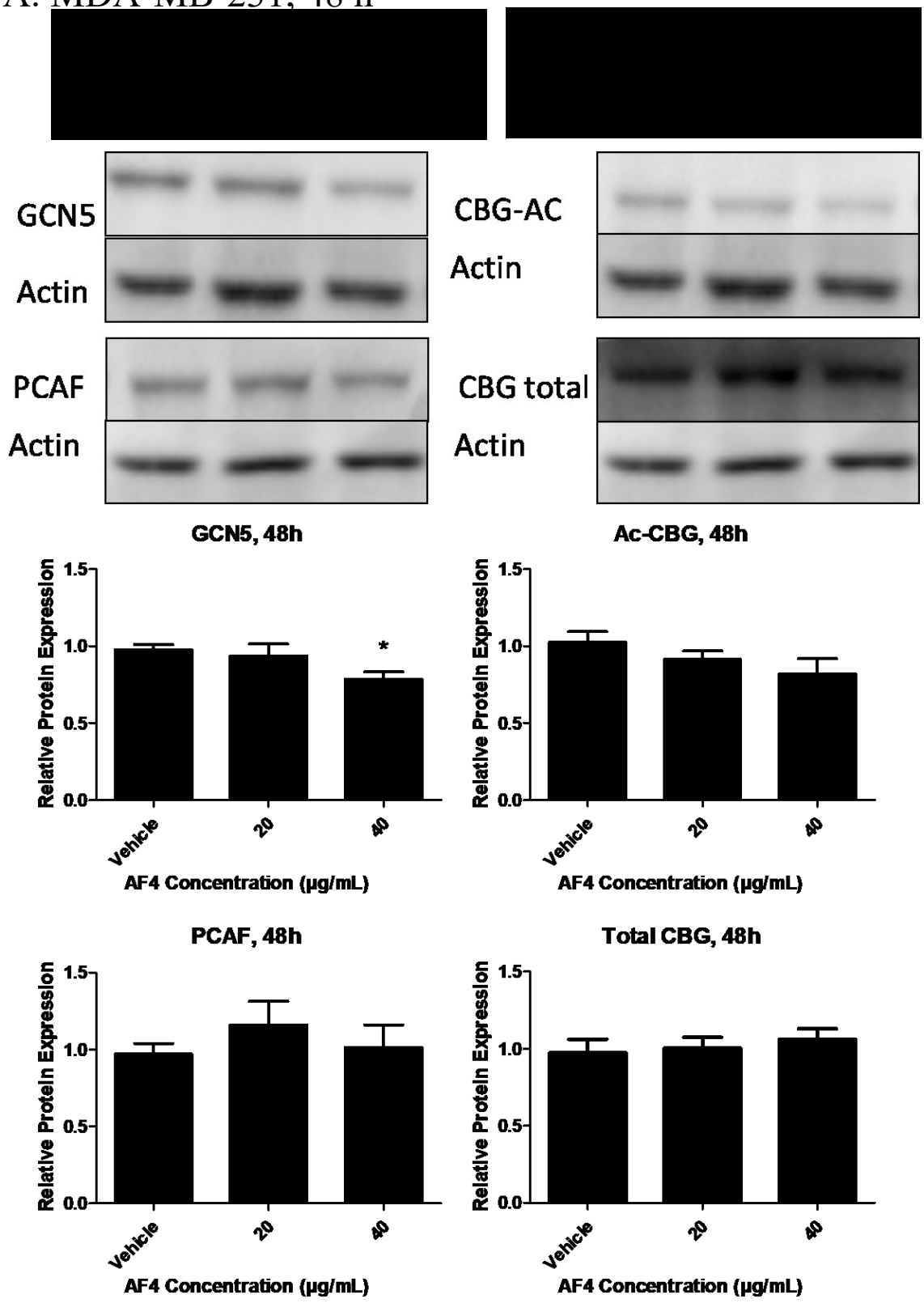

A. MDA-MB-231, 48 h

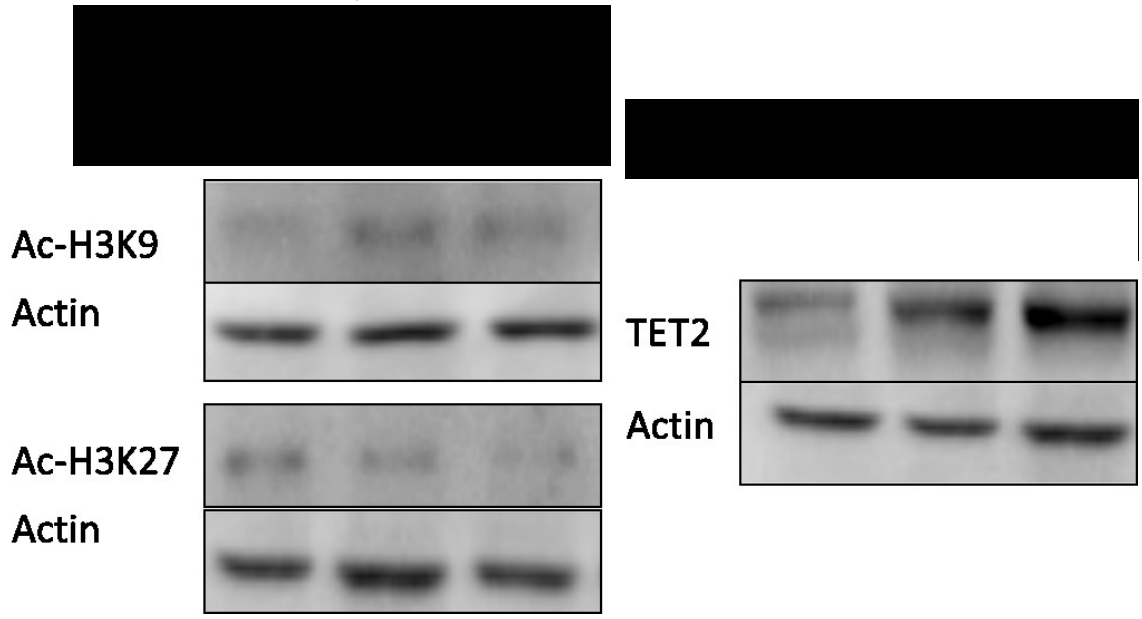

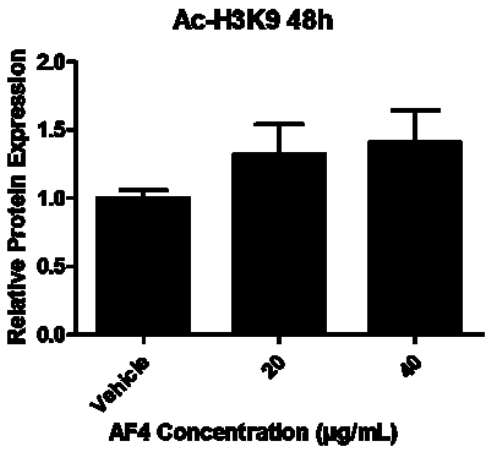

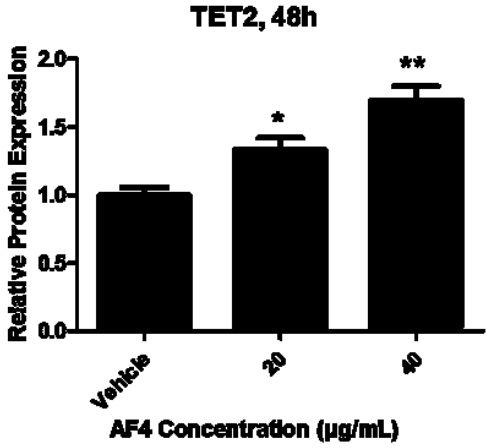

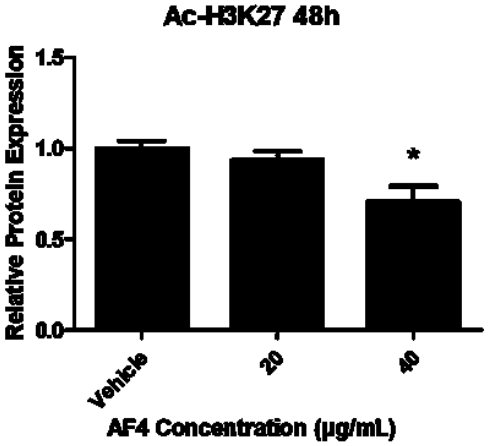

A. MDA-MB-231, 72 h

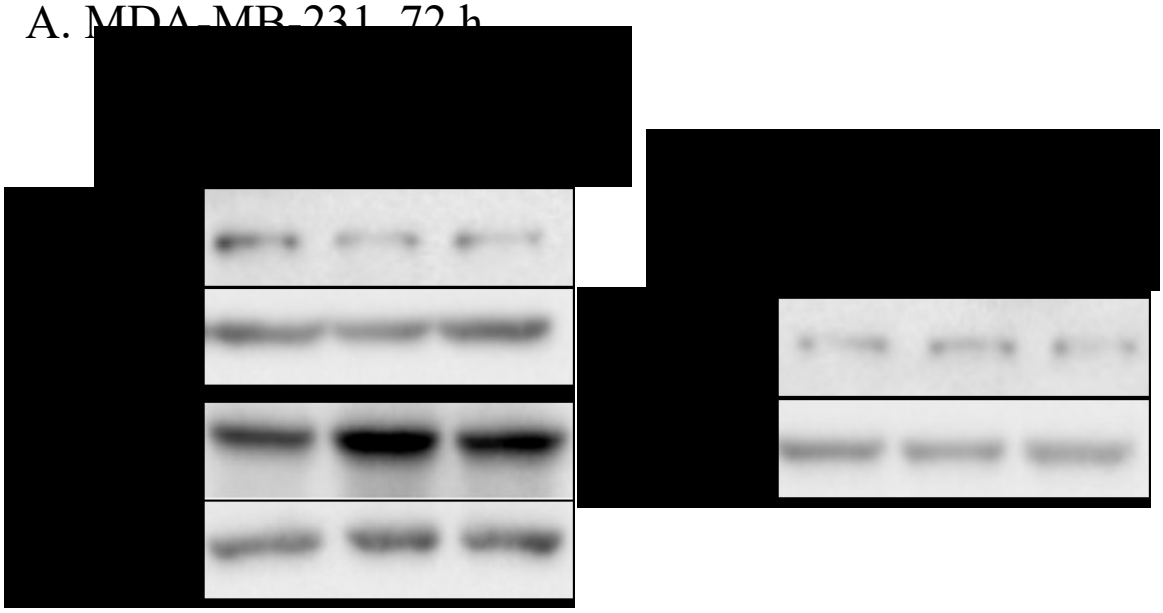

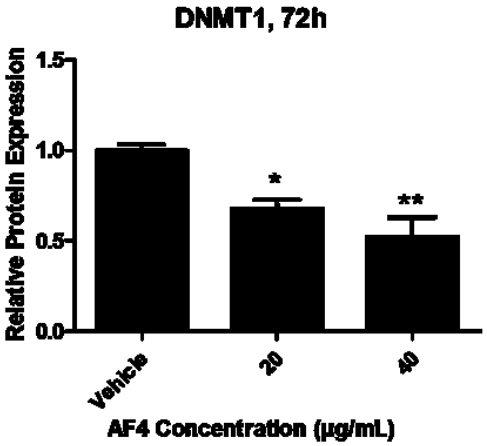

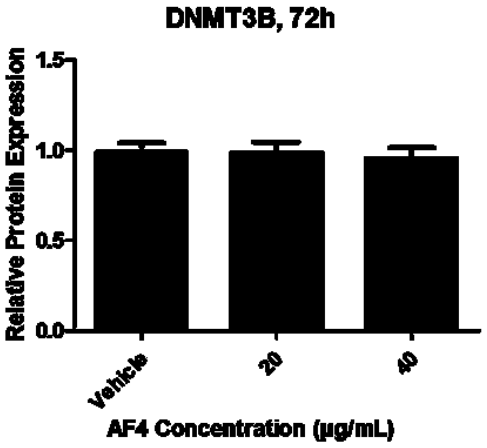

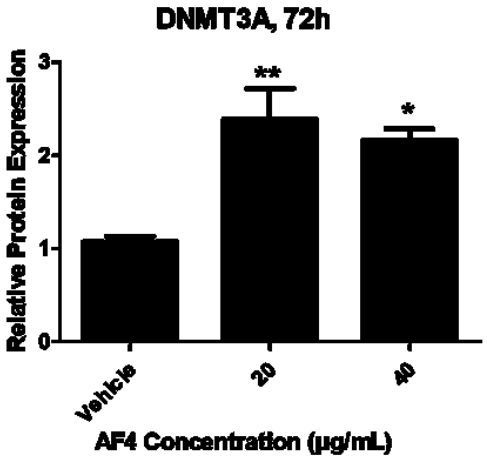

A. MDA-MB-231, 72 h

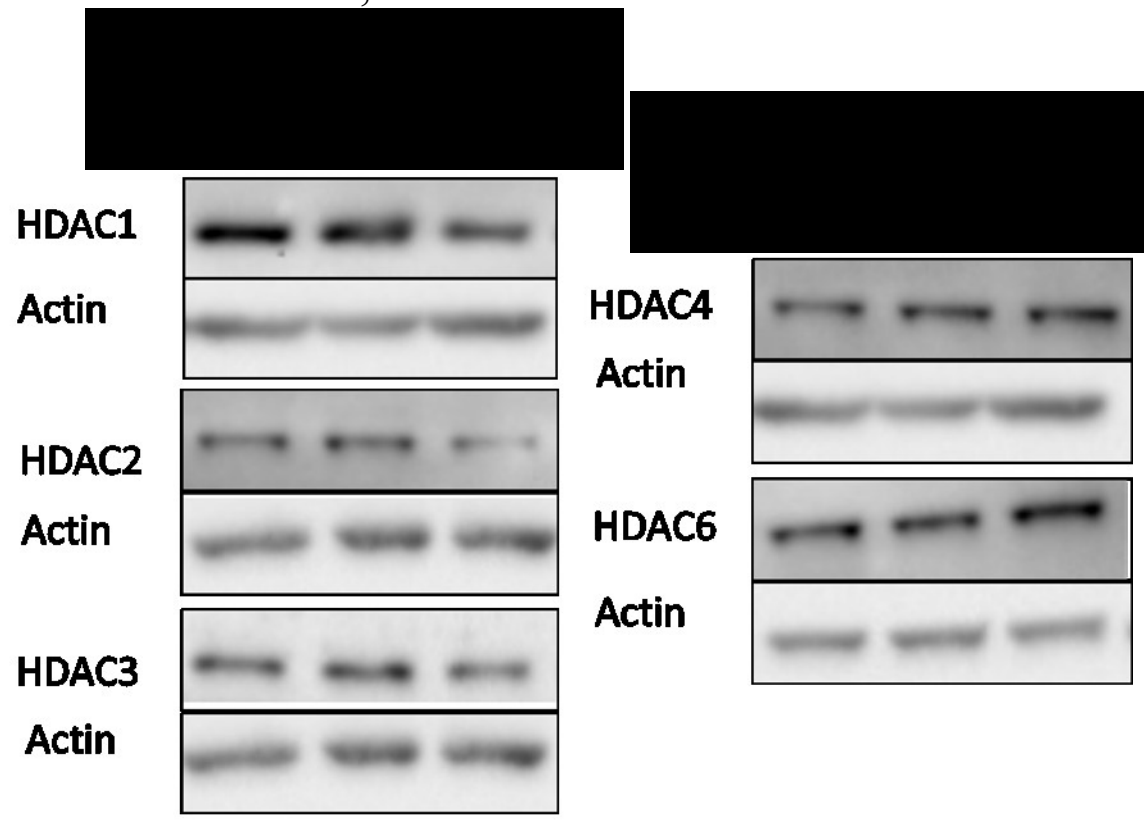

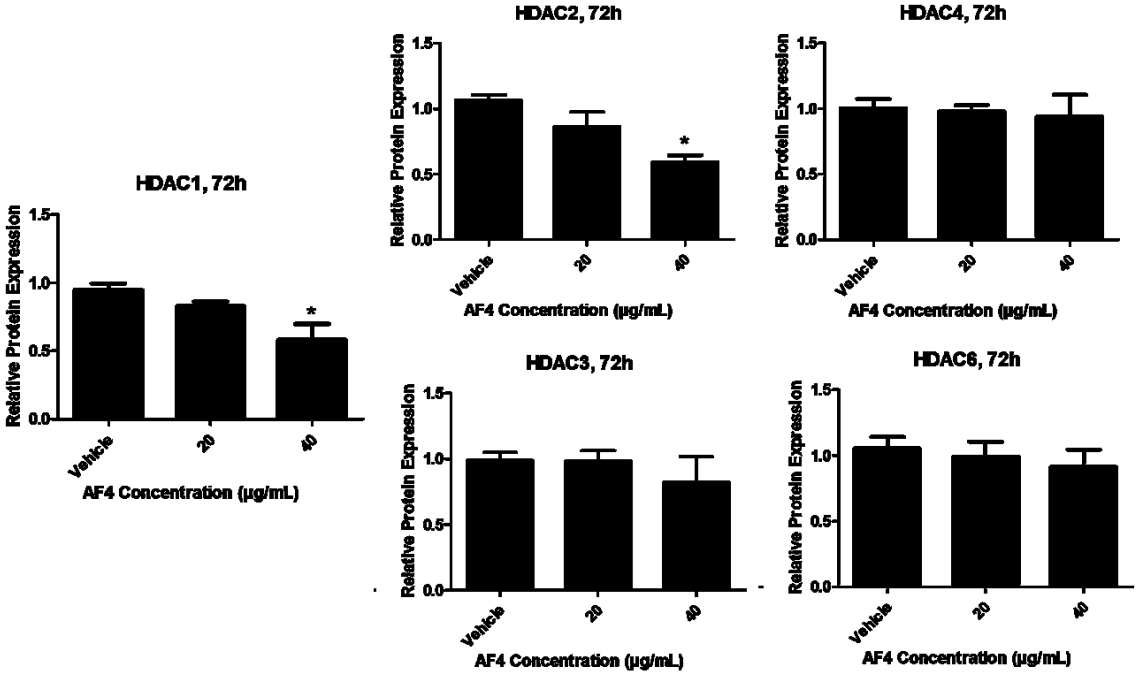

A. MDA-MB-231, 72 h

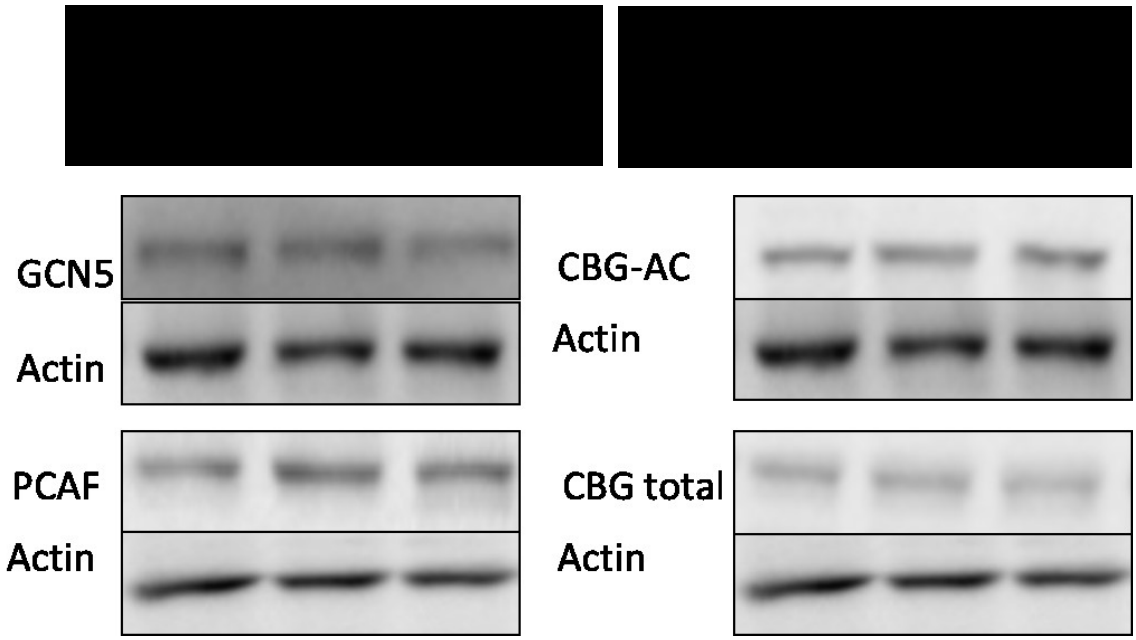

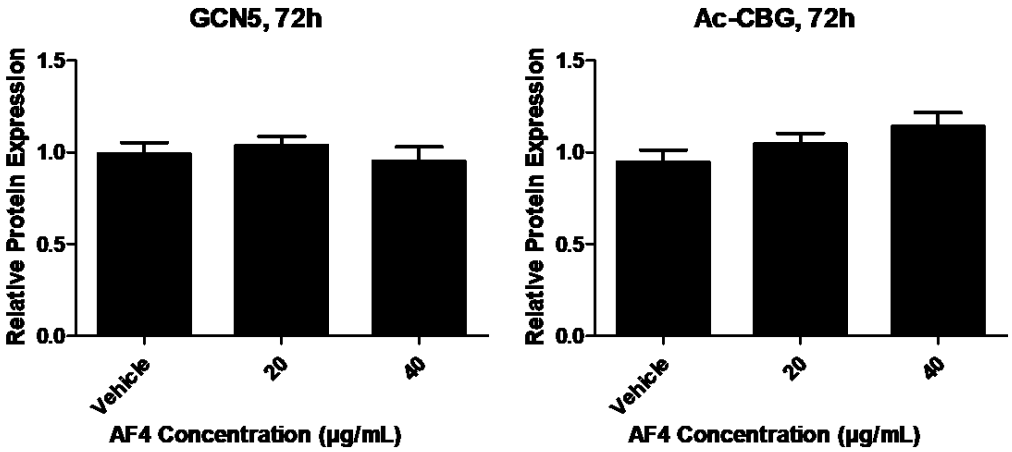

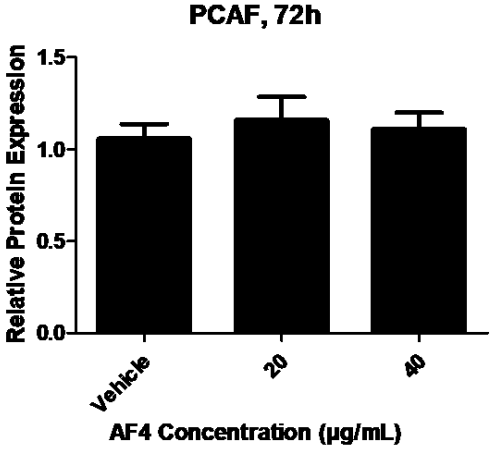

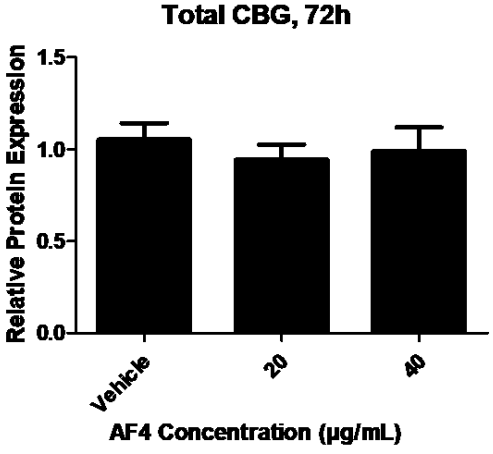

A. MDA-MB-231, 72 h

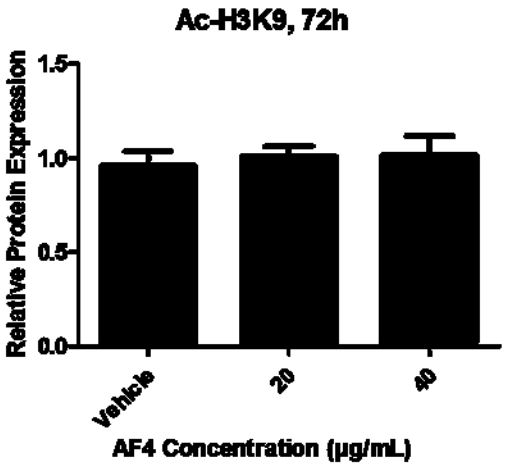

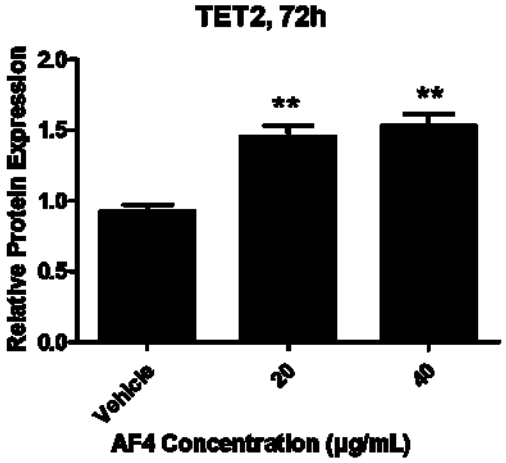

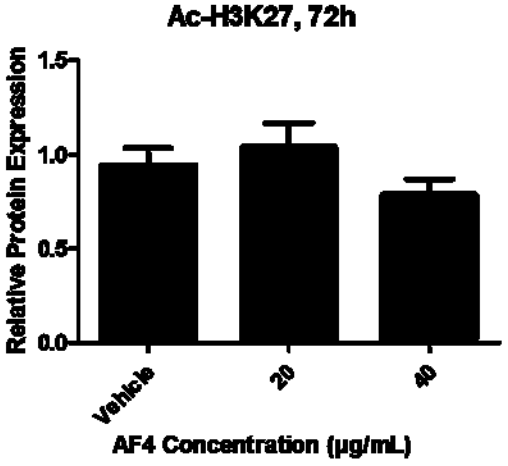

B. MDA-MB-468, 48 h

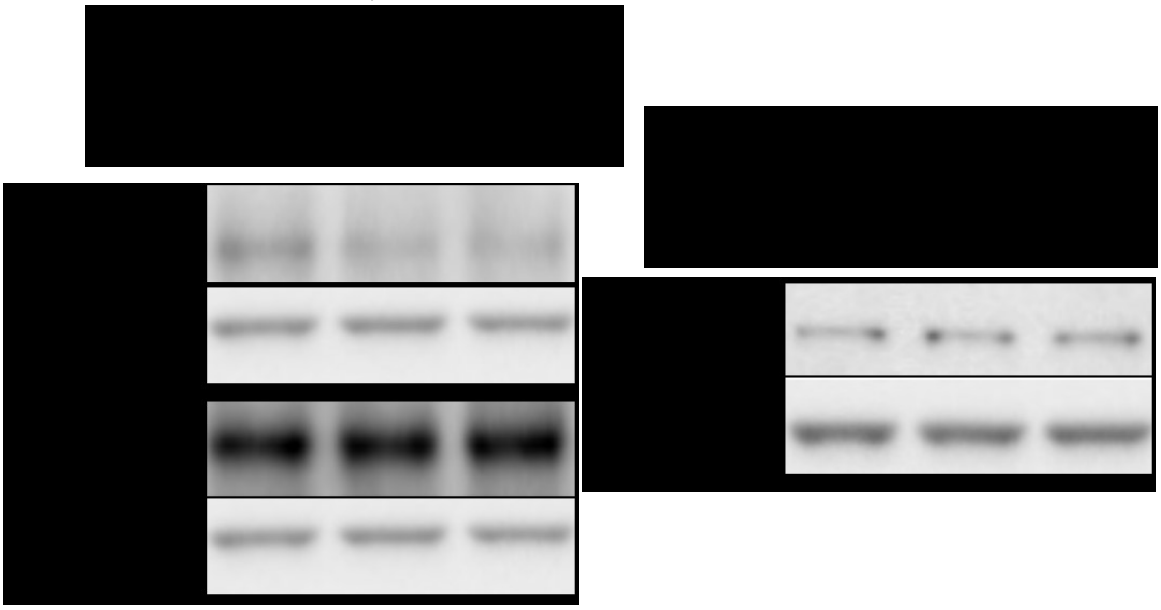

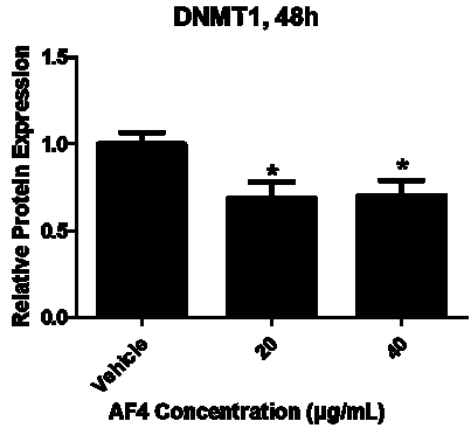

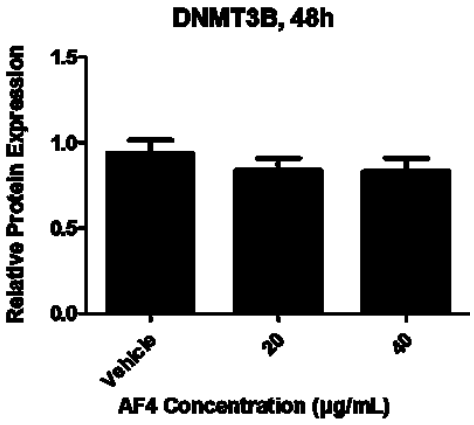

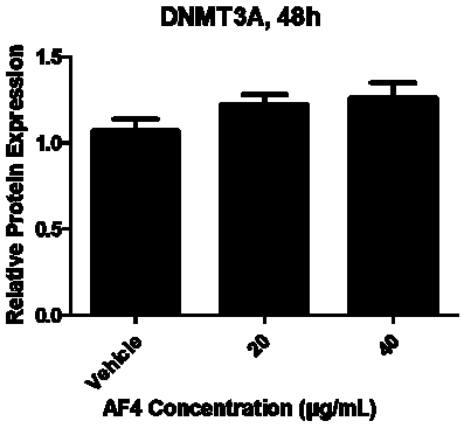

B. MDA-MB-468, 48 h

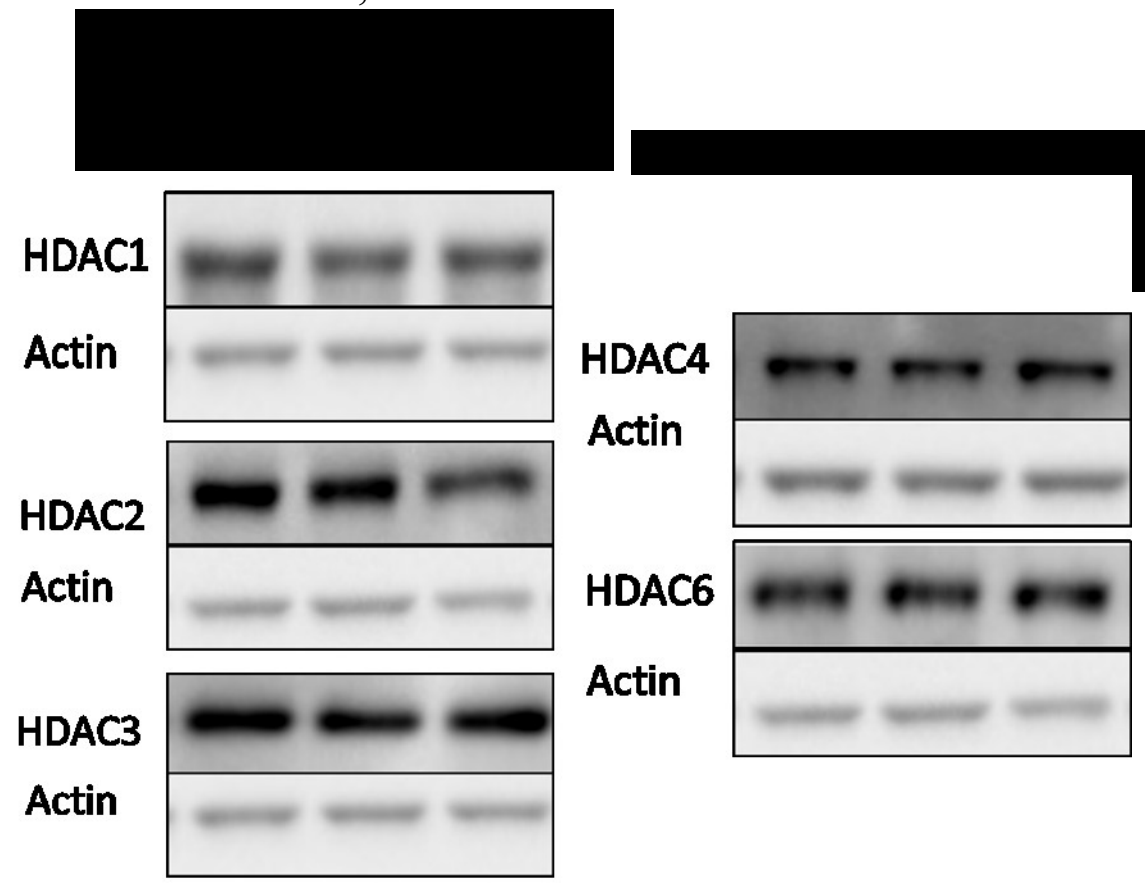

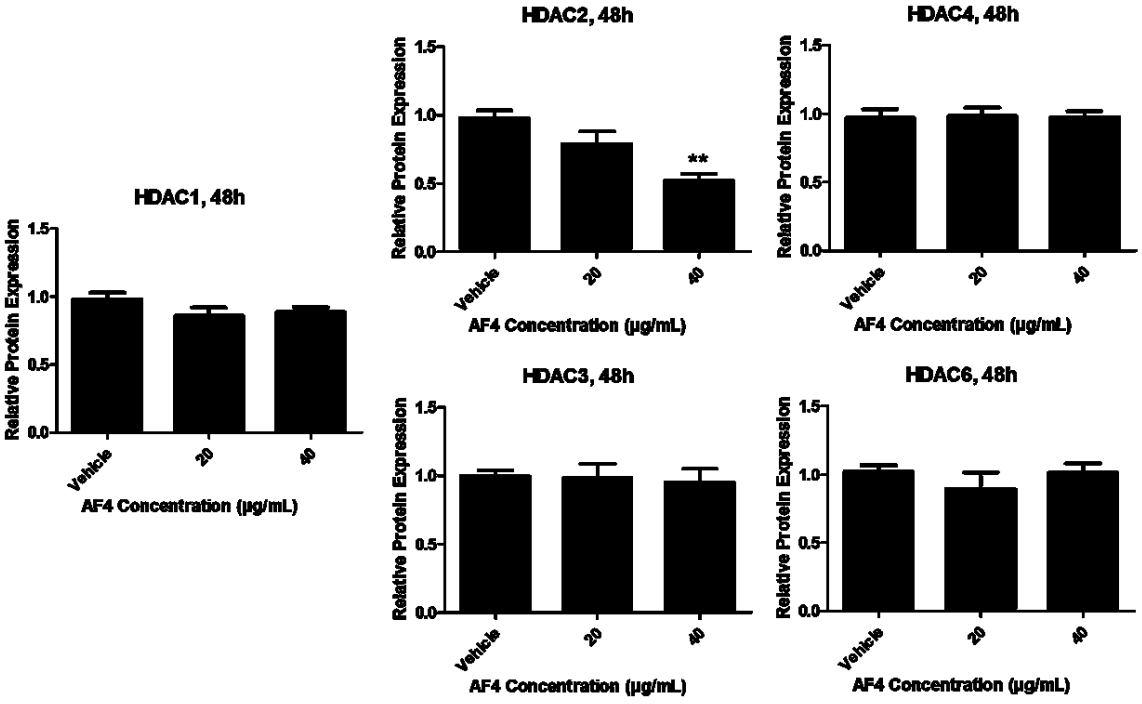

B. MDA-MB-468, 48 h

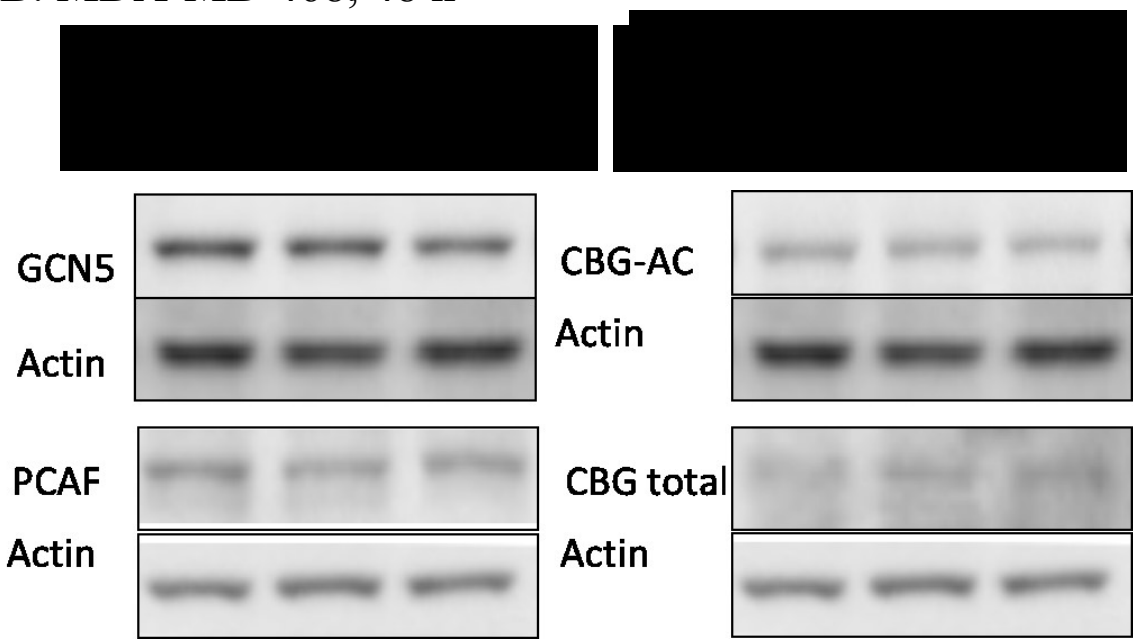

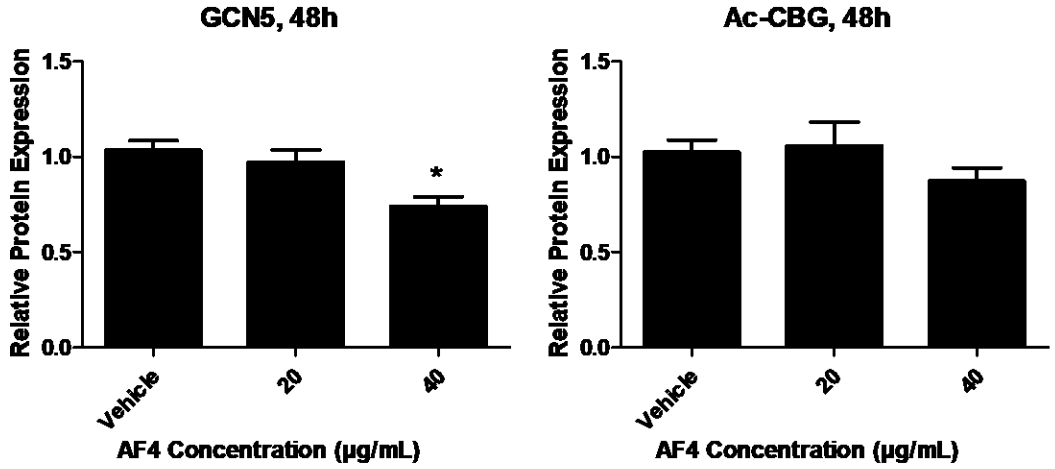

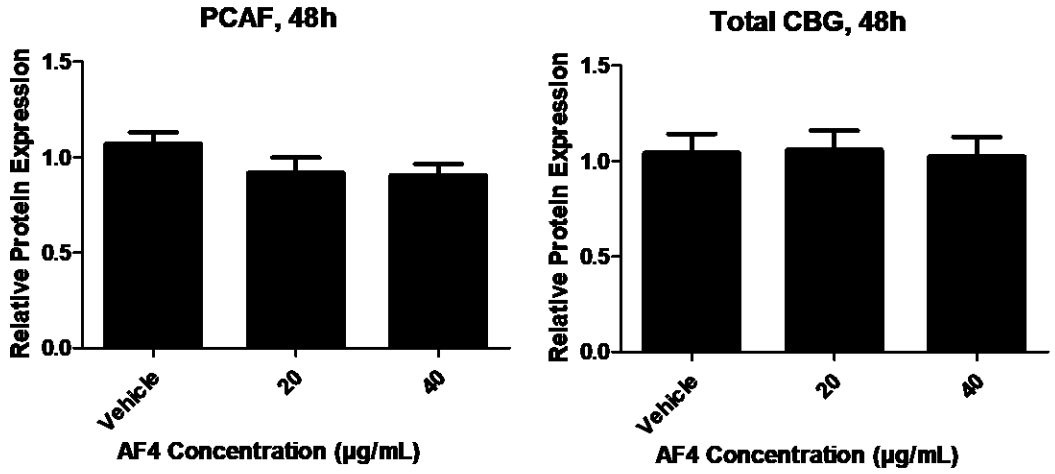

B. MDA-MB-468, 48 h

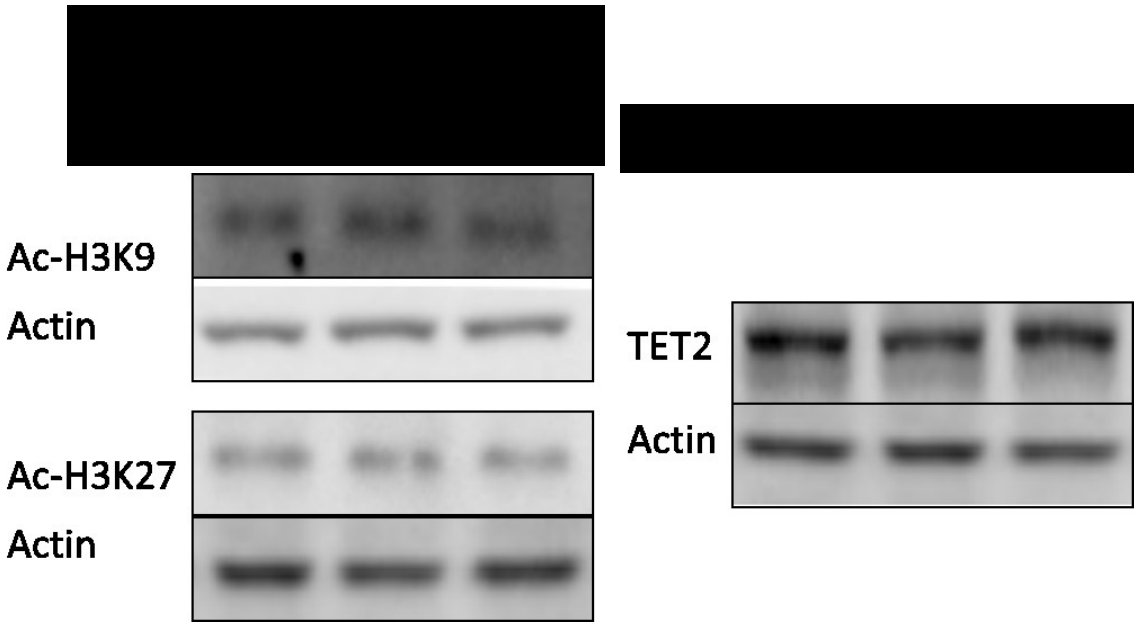

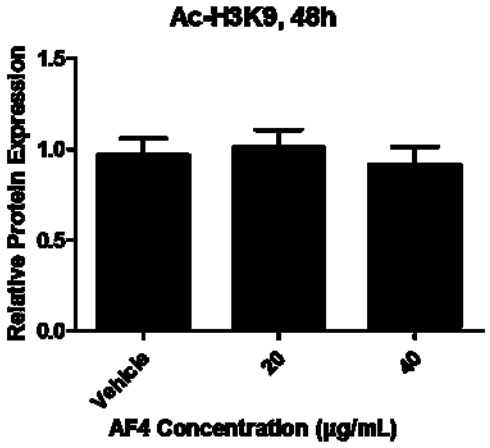

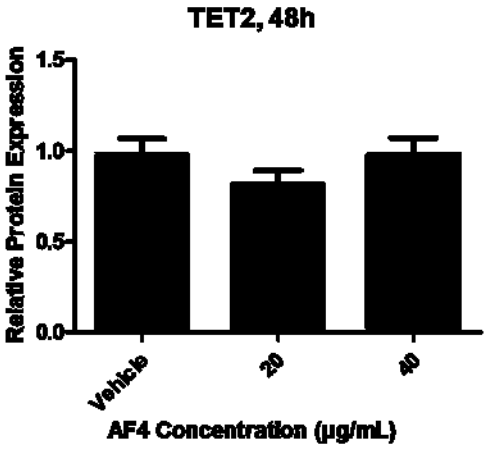

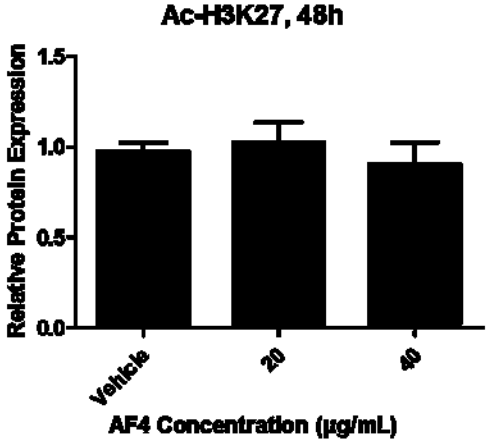

B. MDA-MB-468, 72 h

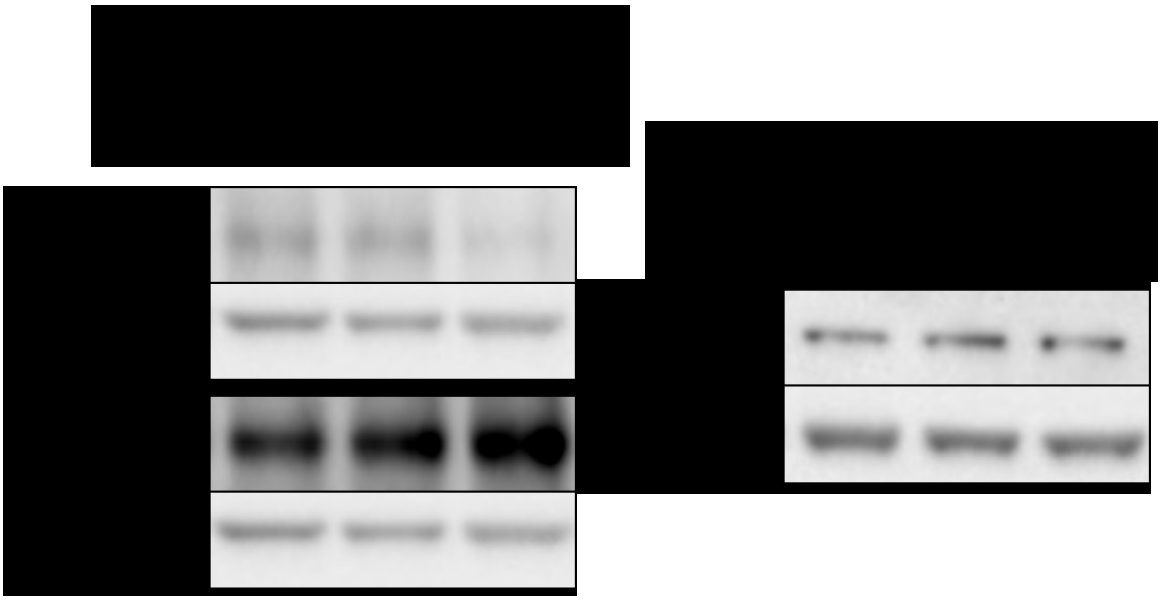

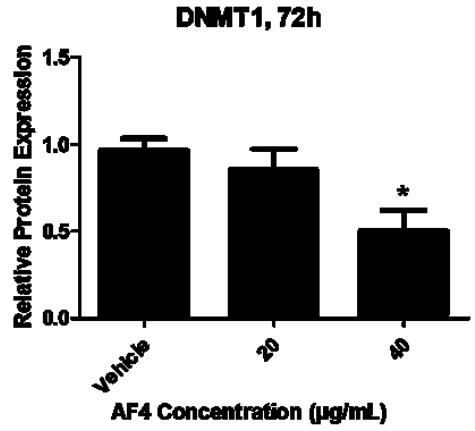

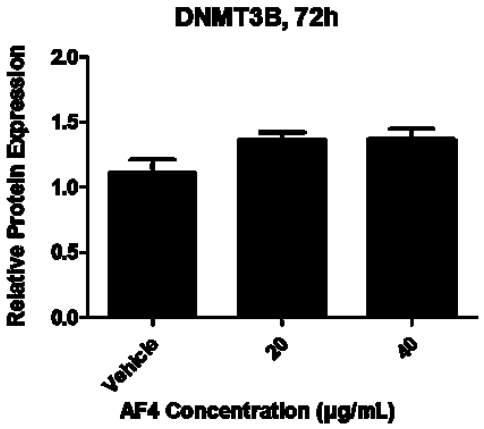

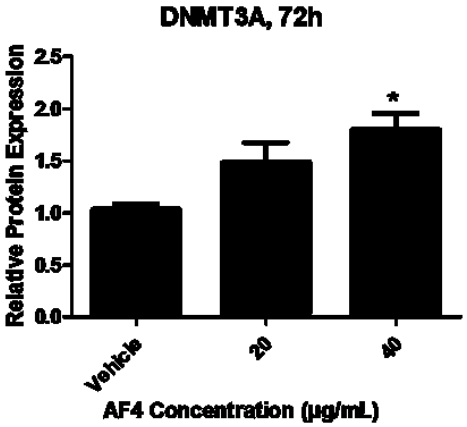

B. MDA-MB-468, 72 h

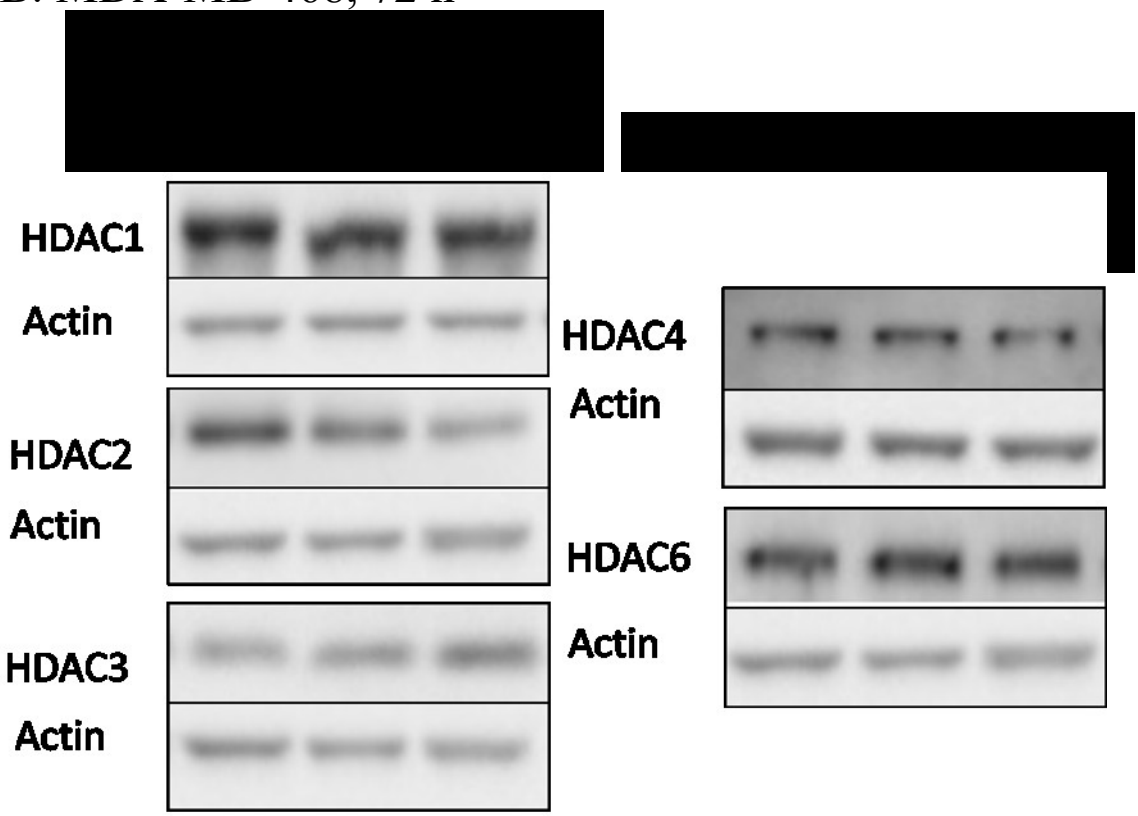

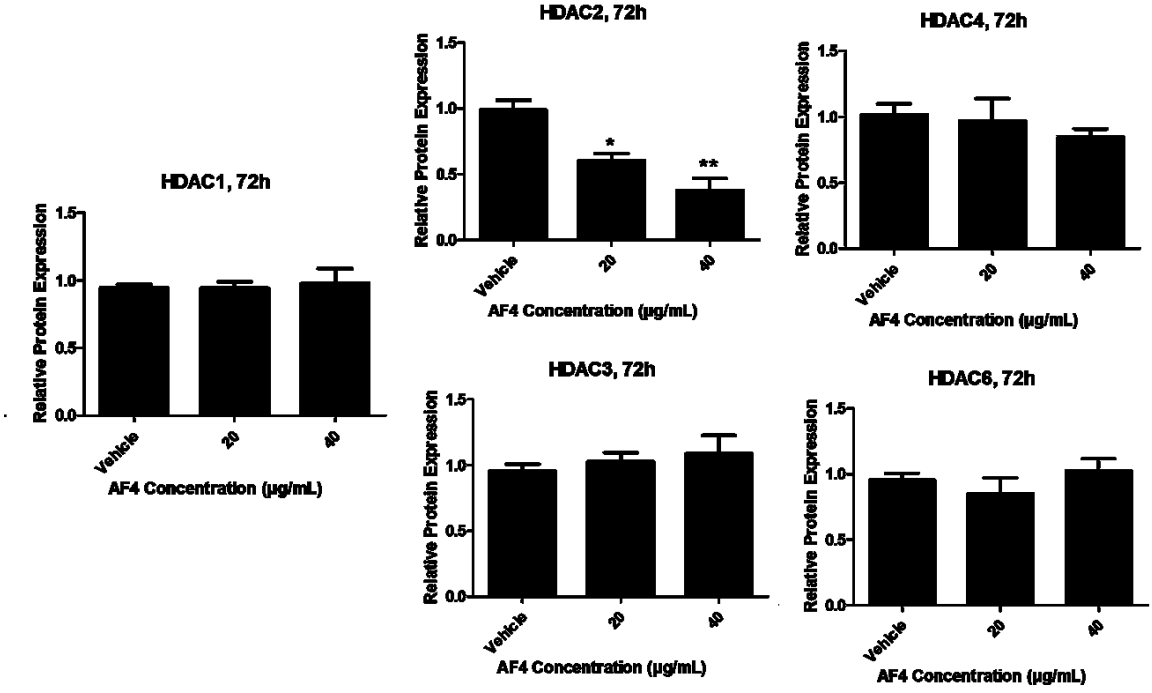

B. MDA-MB-468, 72 h

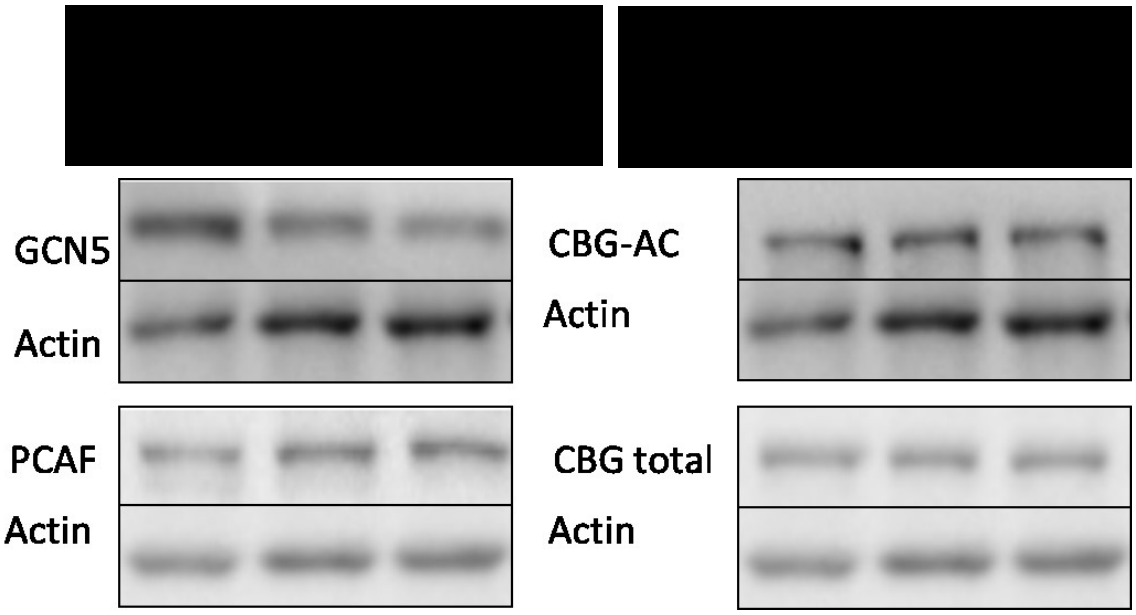

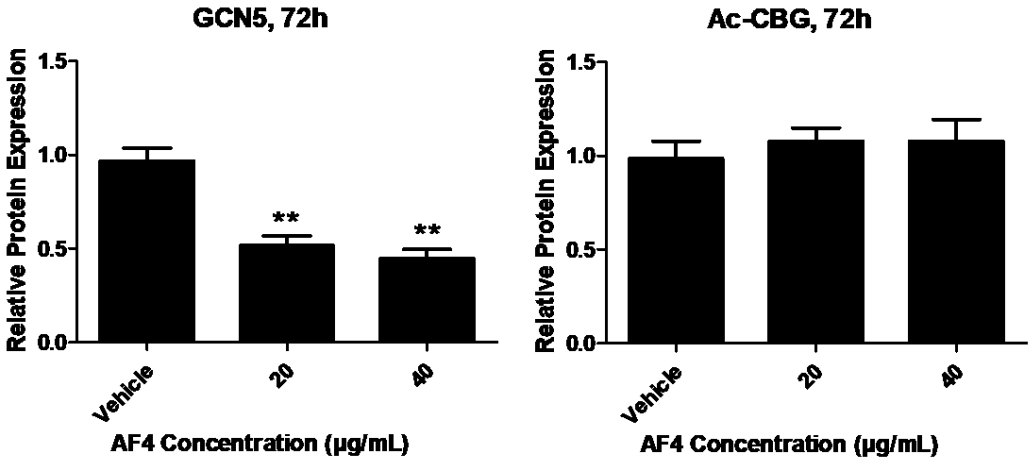

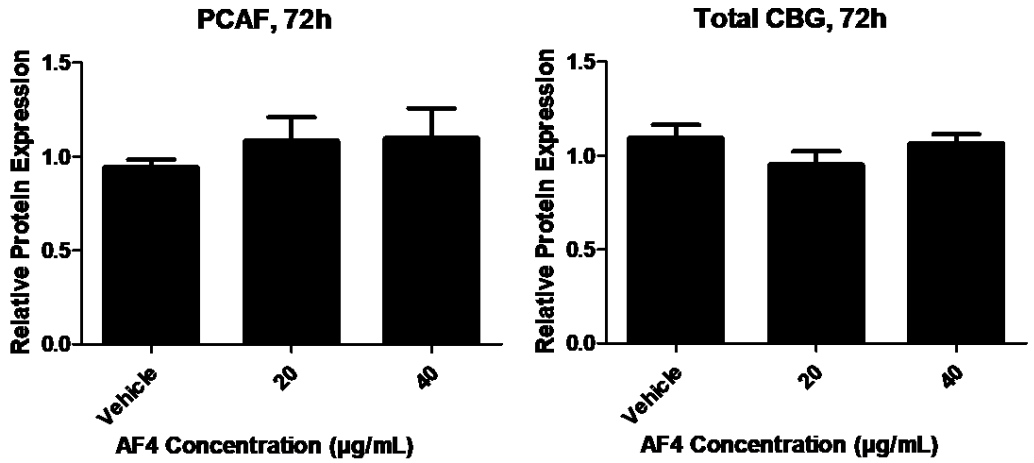

B. MDA-MB-468, 72 h

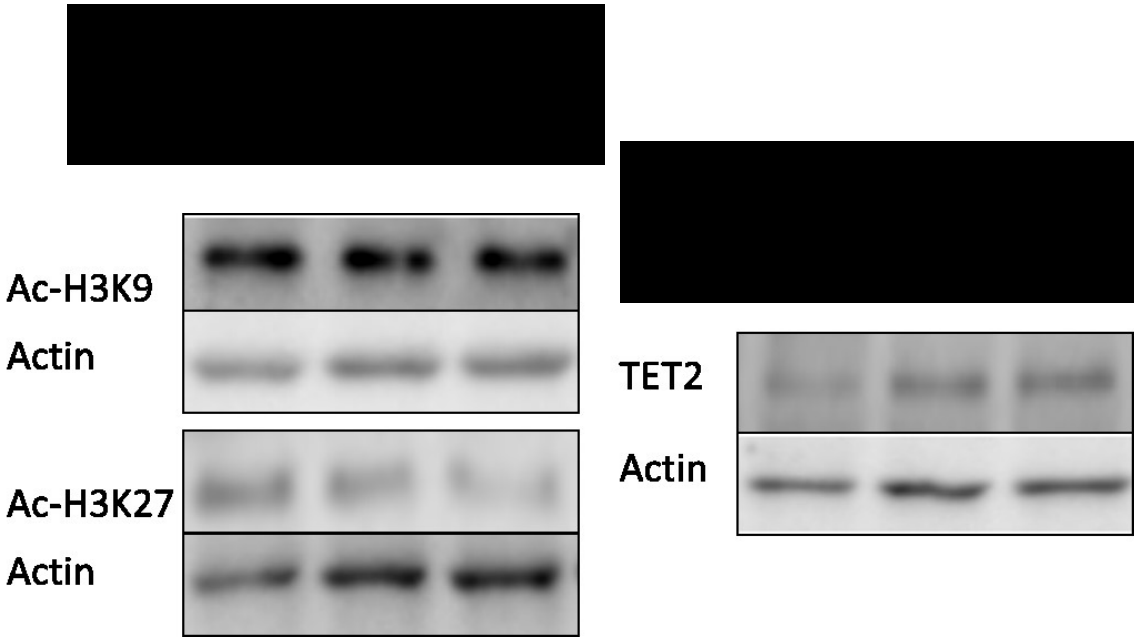

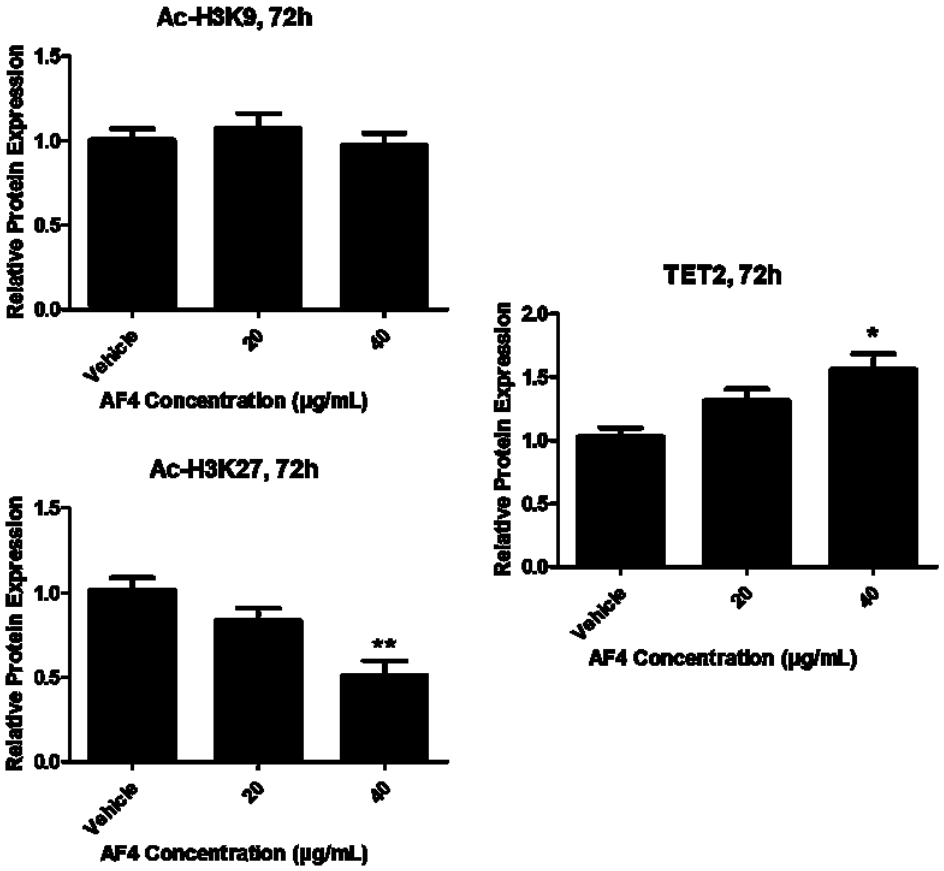

C. MCF10A, 48 h

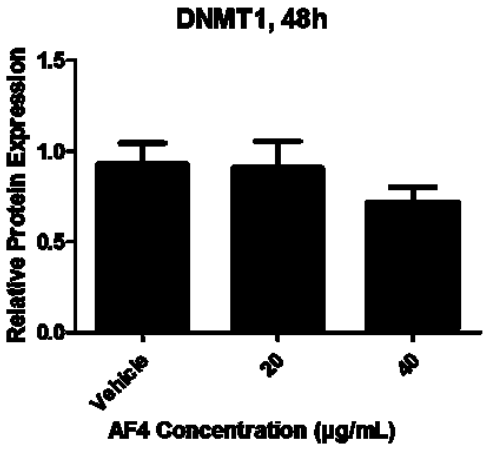
DNMT1, 48h
Relative Protein Expression
1.5
1.0
0.5
0.0
Vehicle
20
40
AF4 Concentration (µg/mL)

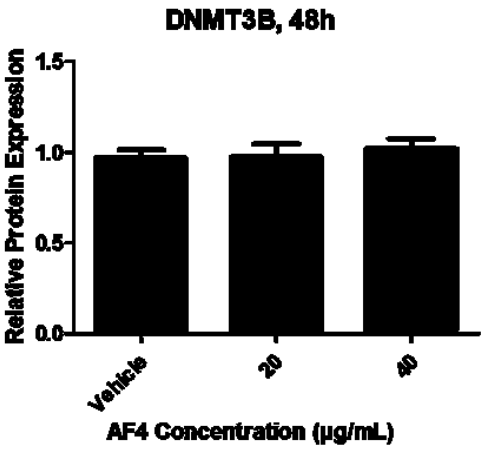
DNMT3B, 48h
Relative Protein Expression
1.5
1.0
0.5
0.0
Vehicle
20
40
AF4 Concentration (µg/mL)

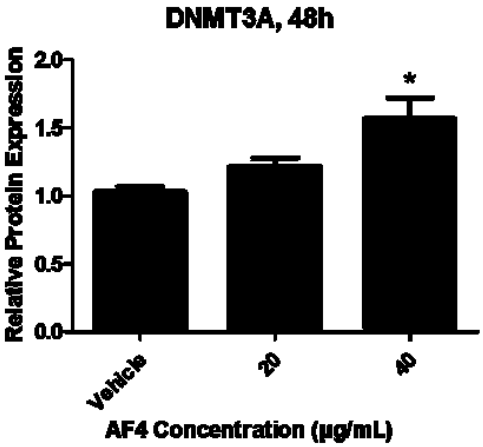
DNMT3A, 48h
Relative Protein Expression
2.0
1.5
1.0
0.5
0.0
*
Vehicle
20
40
AF4 Concentration (µg/mL)

C. MCF10A, 48 h

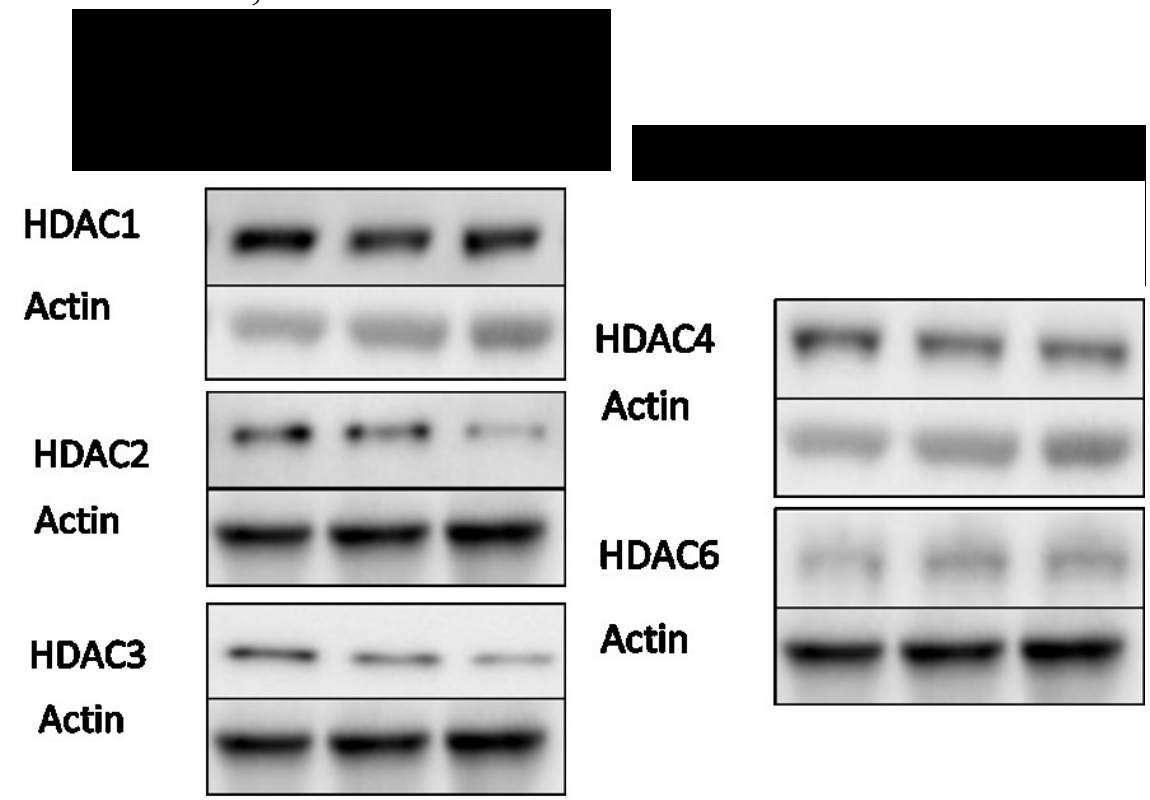
HDAC1
Actin
HDAC2
Actin
HDAC3
Actin
HDAC4
Actin
HDAC6
Actin

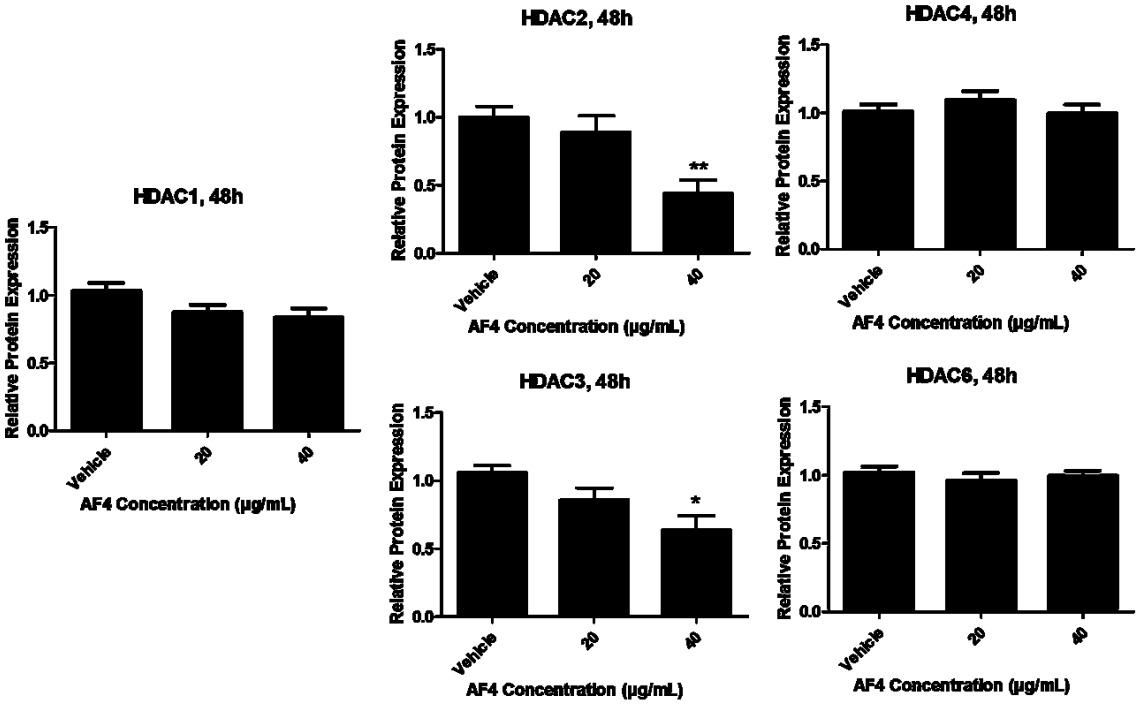
HDAC1, 48h
HDAC2, 48h
HDAC4, 48h
HDAC3, 48h
HDAC6, 48h
Relative Protein Expression
1.5
1.0
0.5
0.0
Vehicle
20
40
AF4 Concentration (µg/mL)
**
*

C. MCF10A, 48 h

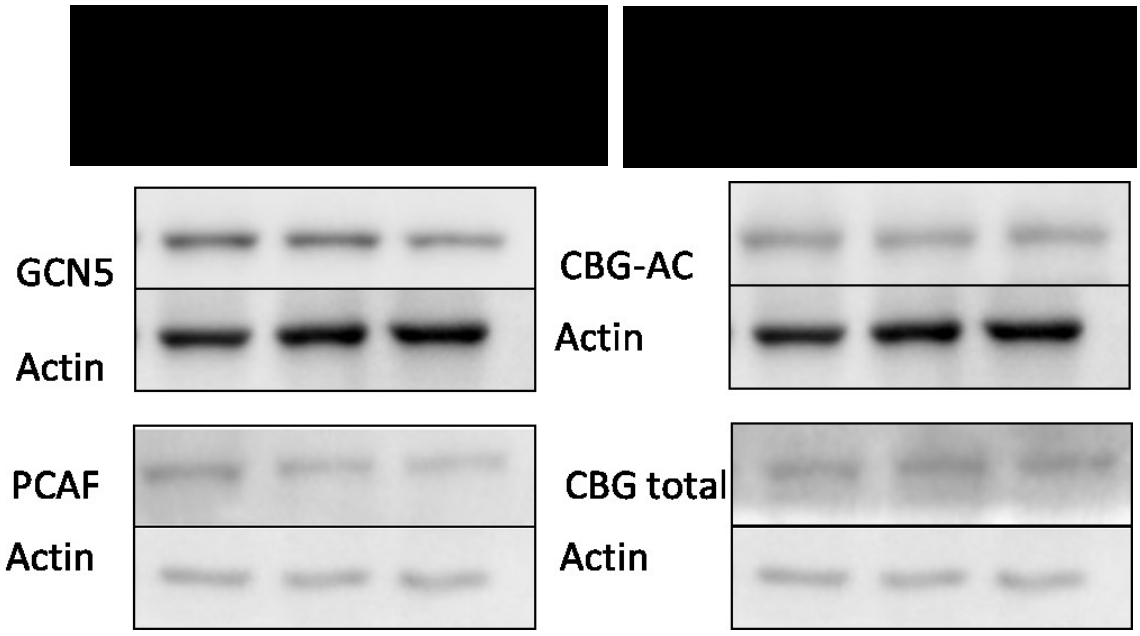
GCN5
Actin
CBG-AC
Actin
PCAF
Actin
CBG total
Actin

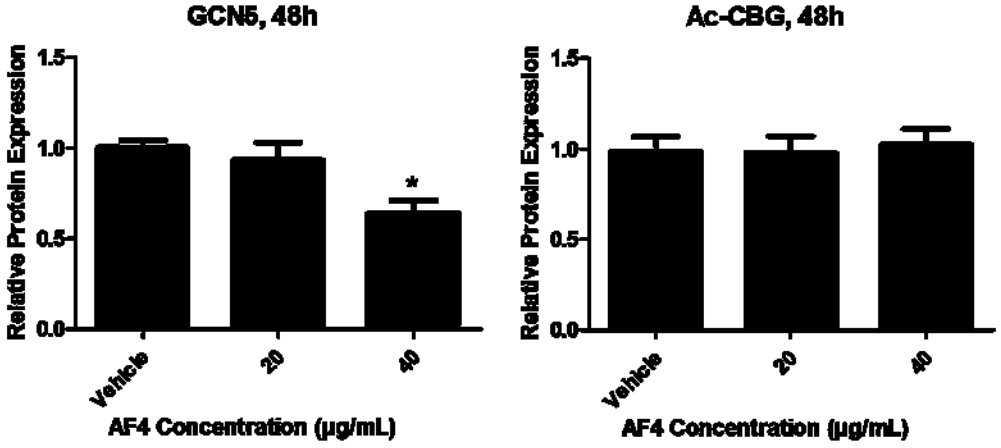
GCN5, 48h
Relative Protein Expression
1.5
1.0
0.5
0.0
*
Vehicle
20
40
AF4 Concentration (µg/mL)

Ac-CBG, 48h
Relative Protein Expression
1.5
1.0
0.5
0.0
Vehicle
20
40
AF4 Concentration (µg/mL)

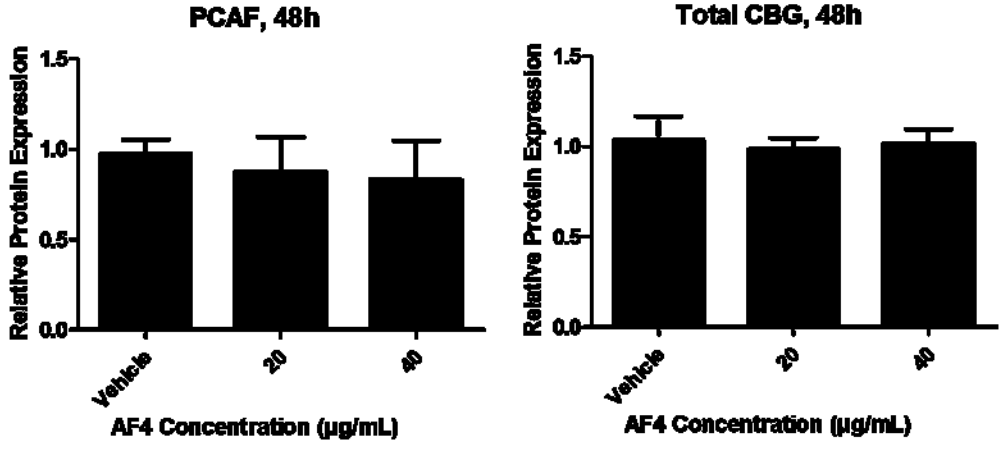
PCAF, 48h
Relative Protein Expression
1.5
1.0
0.5
0.0
Vehicle
20
40
AF4 Concentration (µg/mL)

Total CBG, 48h
Relative Protein Expression
1.5
1.0
0.5
0.0
Vehicle
20
40
AF4 Concentration (µg/mL)

C. MCF10A, 48 h

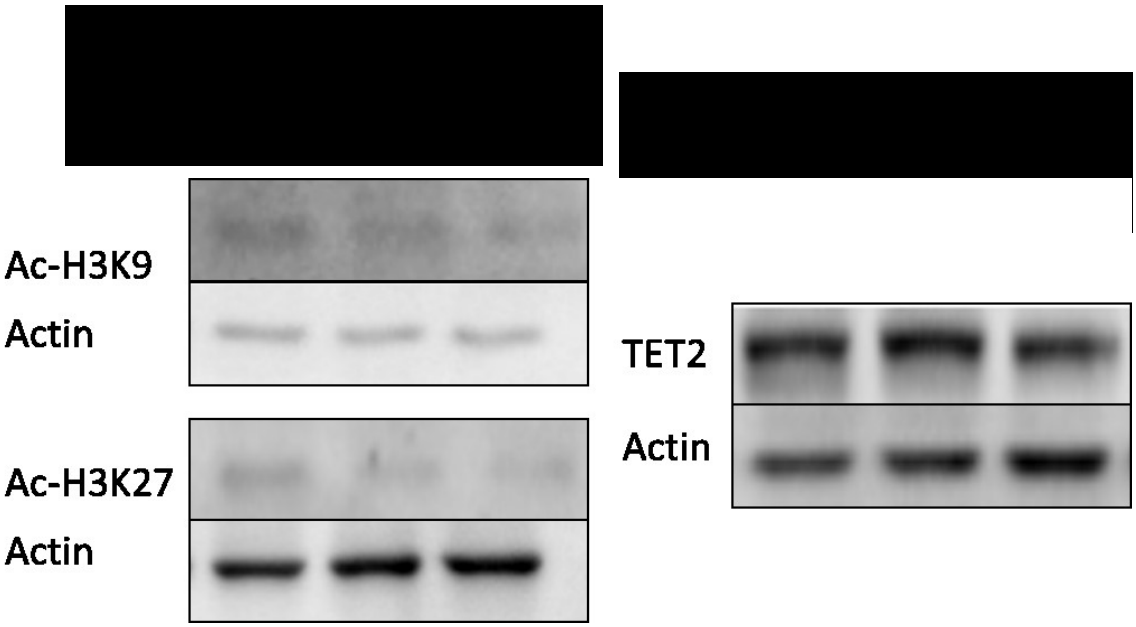
Ac-H3K9
Actin
Ac-H3K27
Actin
TET2
Actin

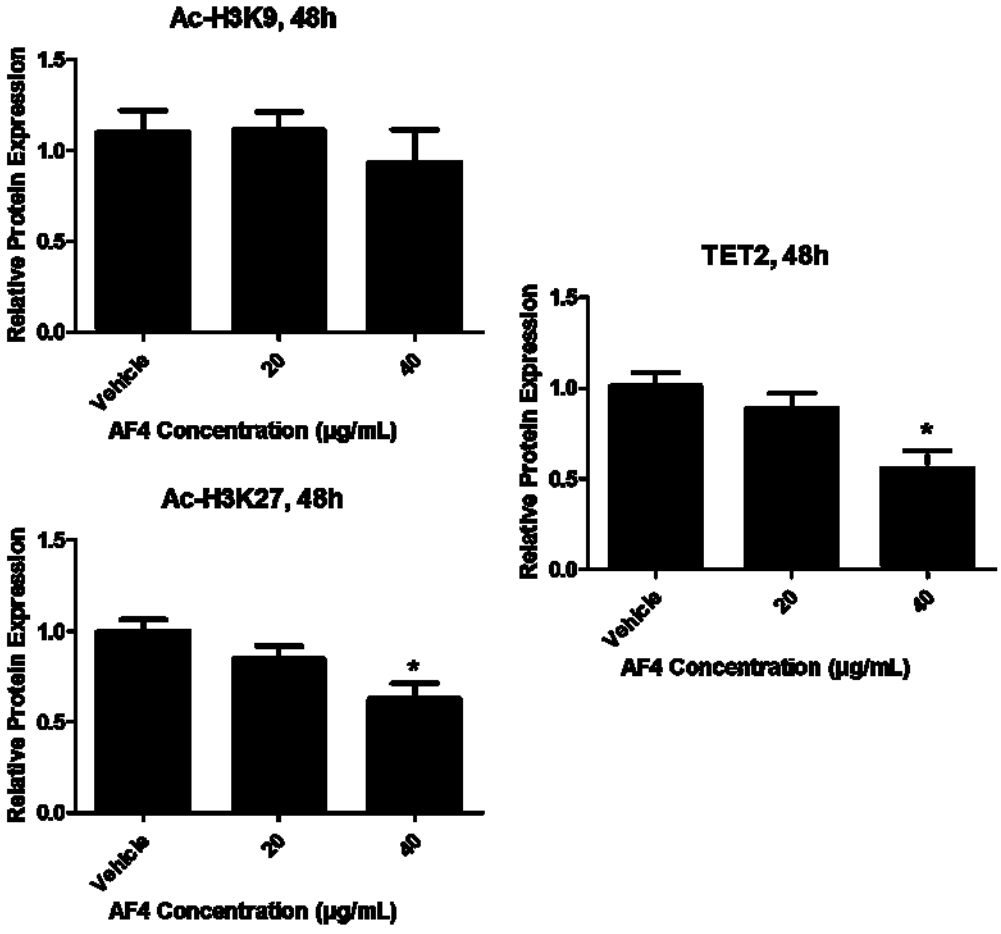
Ac-H3K9, 48h
Relative Protein Expression
1.5
1.0
0.5
0.0
Vehicle
20
40
AF4 Concentration (µg/mL)
Ac-H3K27, 48h
Relative Protein Expression
1.5
1.0
0.5
0.0
*
Vehicle
20
40
AF4 Concentration (µg/mL)
TET2, 48h
Relative Protein Expression
1.5
1.0
0.5
0.0
*
Vehicle
20
40
AF4 Concentration (µg/mL)

C. MCF10A, 72 h

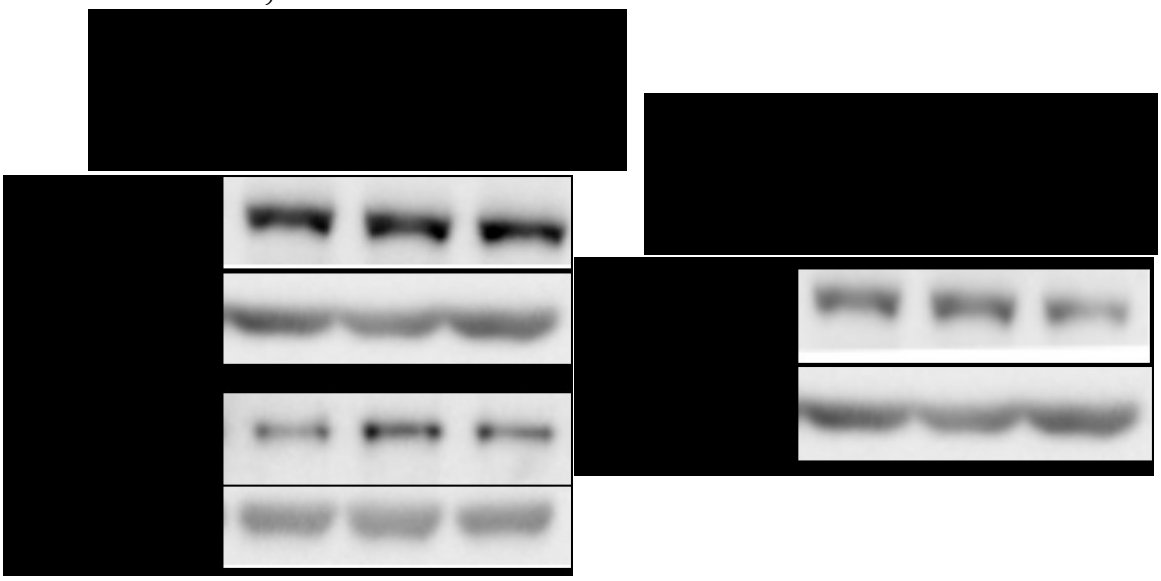

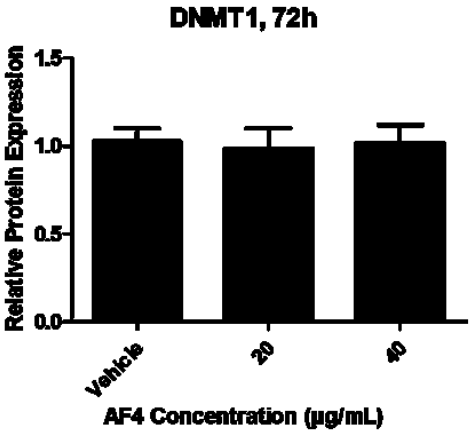
DNMT1, 72h
Relative Protein Expression
1.5
1.0
0.5
0.0
Vehicle
20
40
AF4 Concentration (µg/mL)

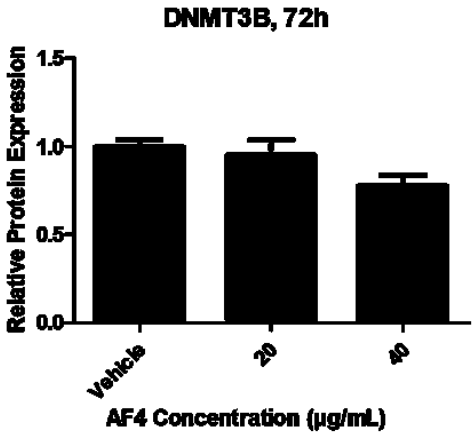
DNMT3B, 72h
Relative Protein Expression
1.5
1.0
0.5
0.0
Vehicle
20
40
AF4 Concentration (µg/mL)

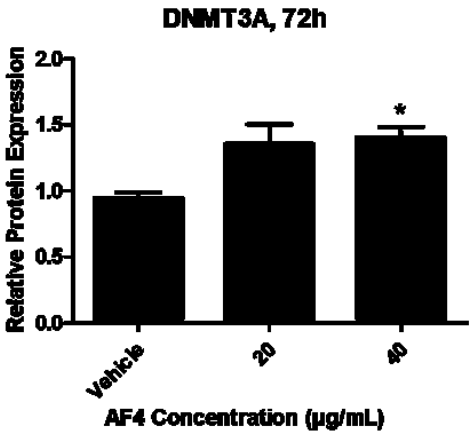
DNMT3A, 72h
Relative Protein Expression
2.0
1.5
1.0
0.5
0.0
*
Vehicle
20
40
AF4 Concentration (µg/mL)

C. MCF10A, 72 h

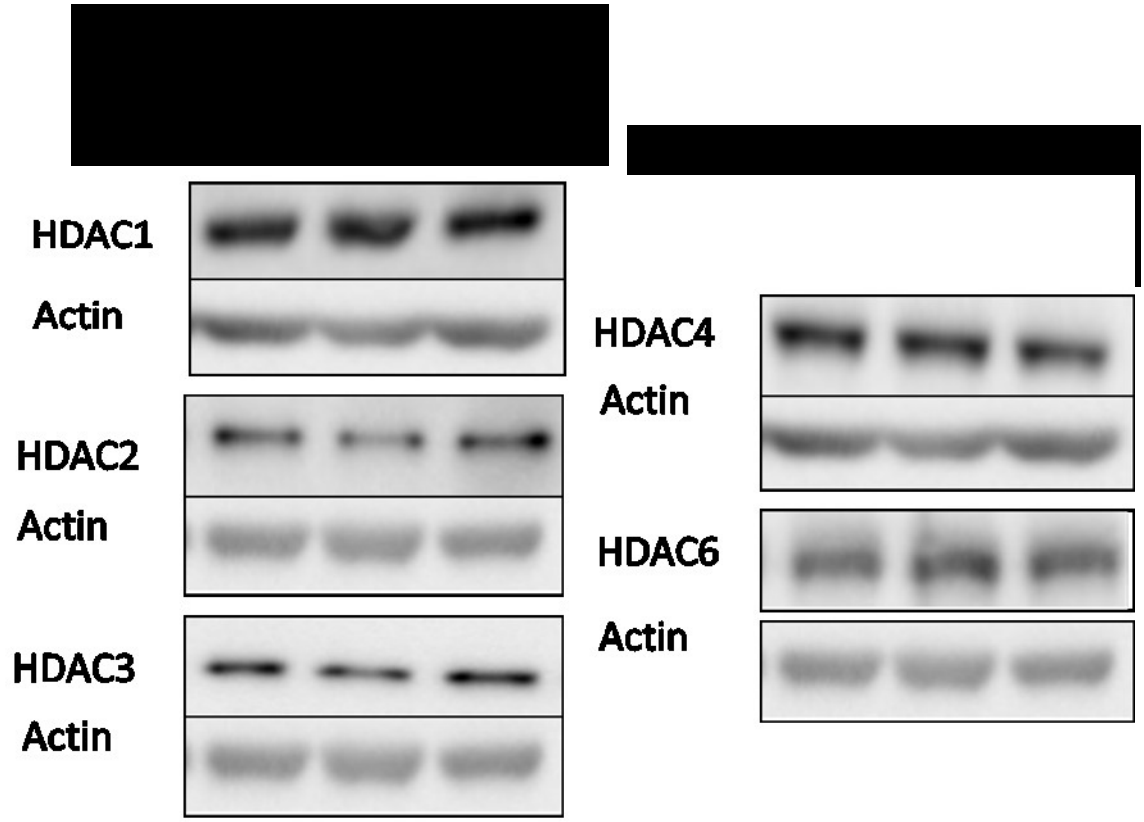
HDAC1
Actin
HDAC2
Actin
HDAC3
Actin
HDAC4
Actin
HDAC6
Actin

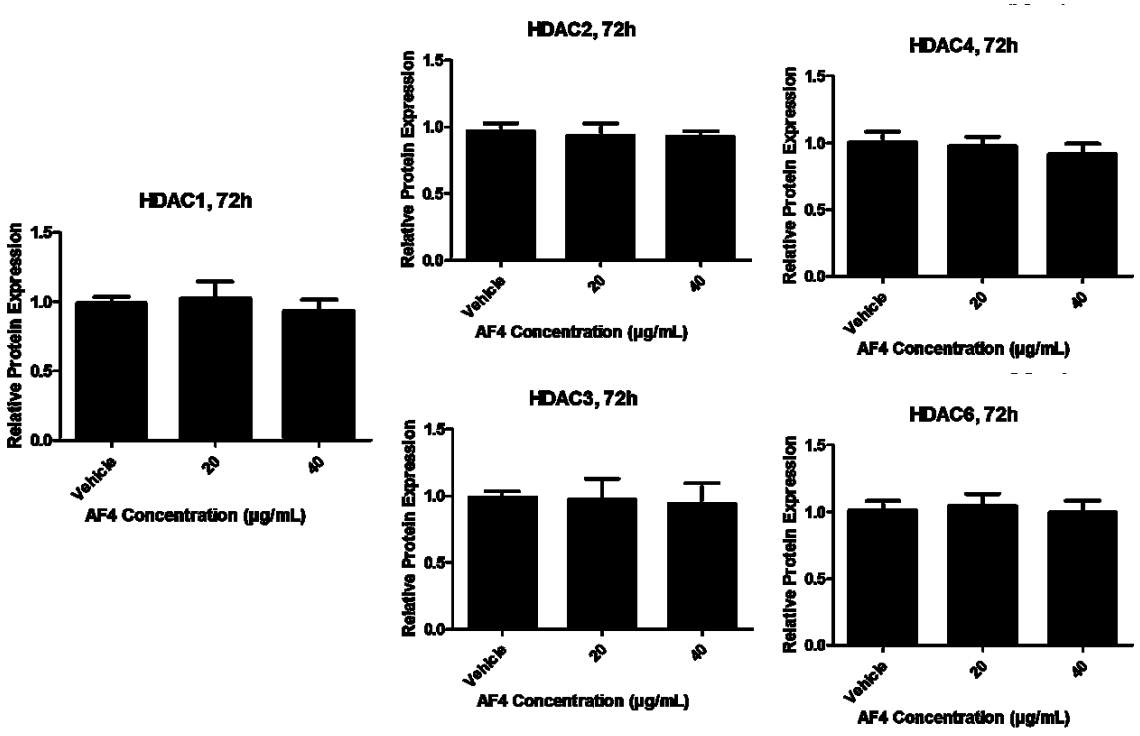
HDAC1, 72h
HDAC2, 72h
HDAC4, 72h
HDAC3, 72h
HDAC6, 72h
Relative Protein Expression
1.5
1.0
0.5
0.0
Vehicle
20
40
AF4 Concentration (µg/mL)

C. MCF10A, 72 h

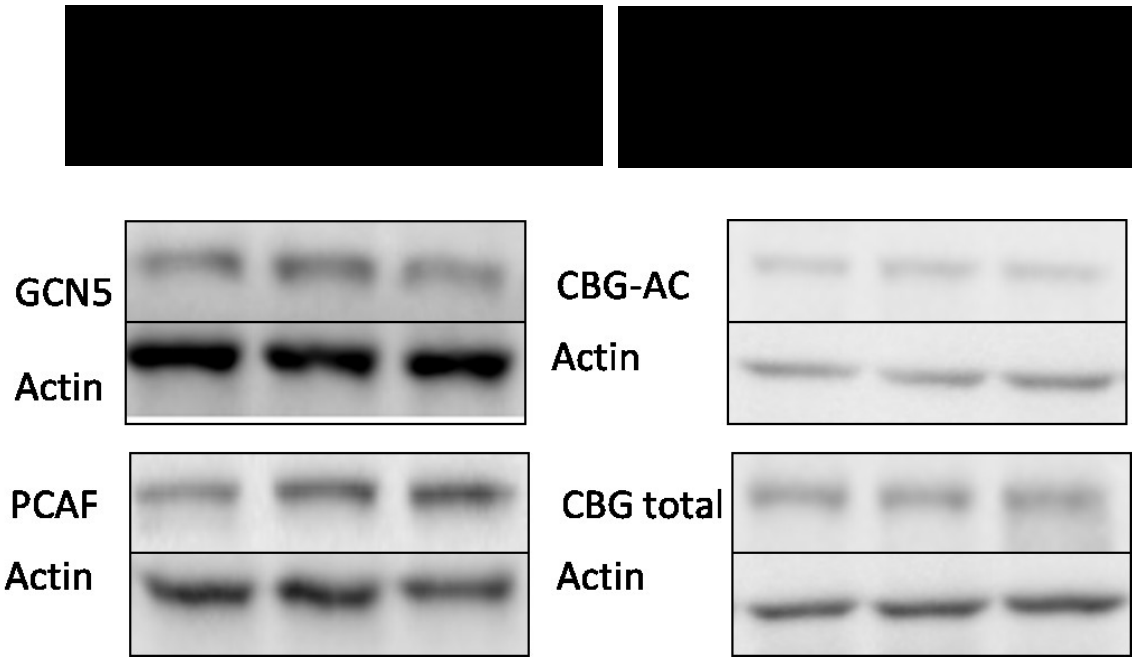
GCN5
Actin
CBG-AC
Actin
PCAF
Actin
CBG total
Actin

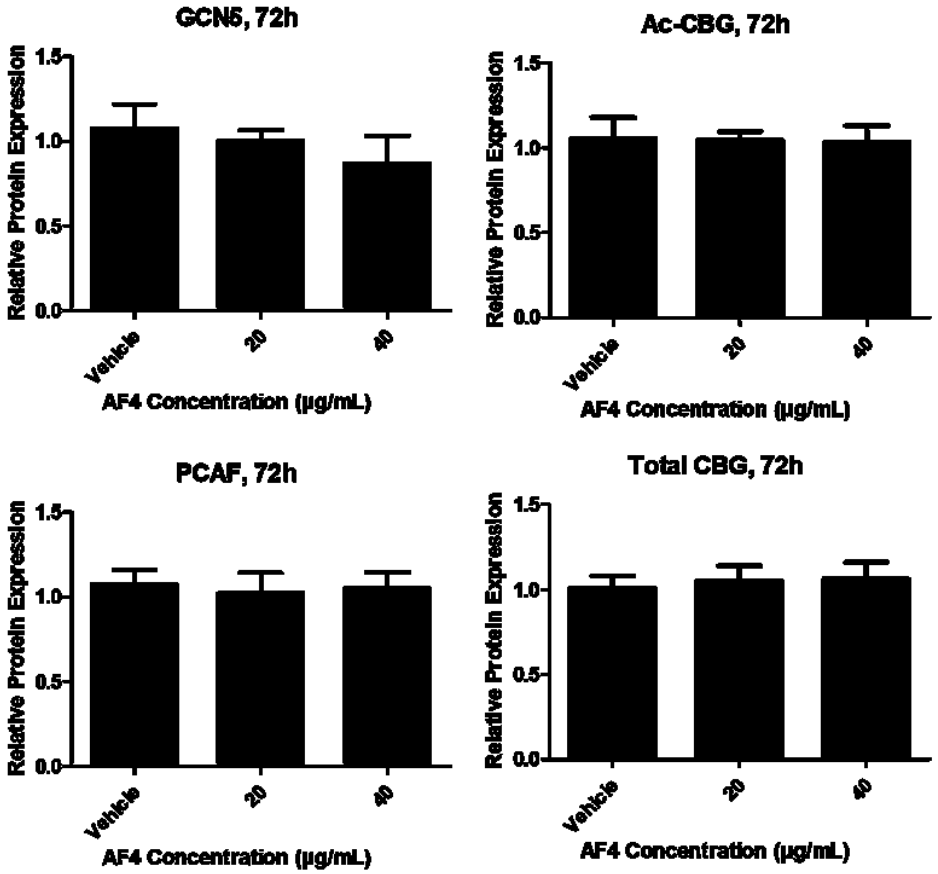
GCN5, 72h
Relative Protein Expression
1.5
1.0
0.5
0.0
Vehicle
20
40
AF4 Concentration (µg/mL)
Ac-CBG, 72h
Relative Protein Expression
1.5
1.0
0.5
0.0
Vehicle
20
40
AF4 Concentration (µg/mL)
PCAF, 72h
Relative Protein Expression
1.5
1.0
0.5
0.0
Vehicle
20
40
AF4 Concentration (µg/mL)
Total CBG, 72h
Relative Protein Expression
1.5
1.0
0.5
0.0
Vehicle
20
40
AF4 Concentration (µg/mL)

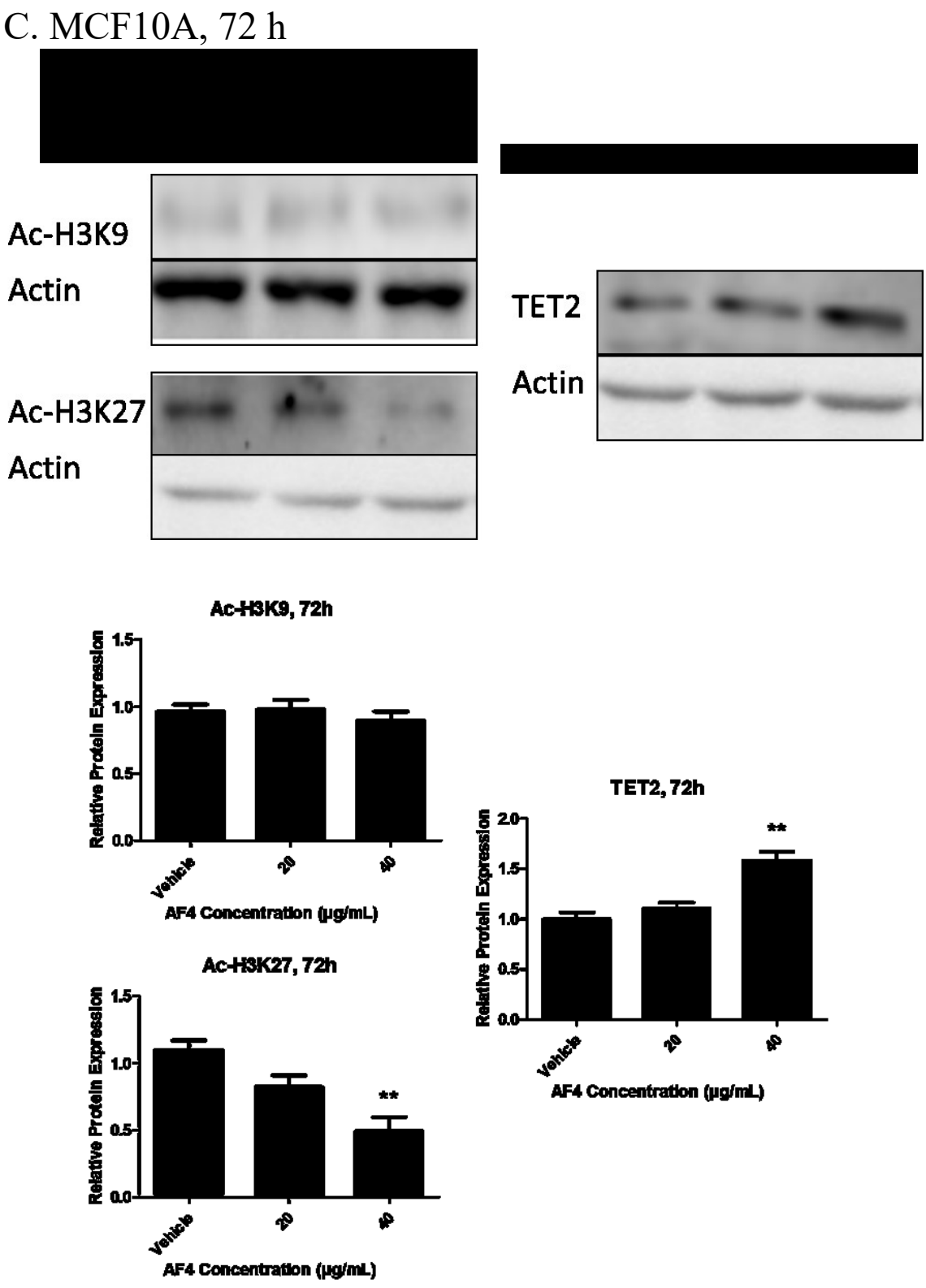

Figure 28. AF4 Affects the Protein Levels of Epigenetic Enzymes in MDA-MB-231 and MDA-MB-468 Breast Cancer Cells and MCF10A Epithelial Cells

Figure 29. Summary of AF4 Effects on Triple-negative Breast Cancer Cells. AF4 has a wide variety of effects, including inhibition of cell proliferation through a currently unknown pathway, induction of cytotoxicity via a ROS-dependent mechanism, and epigenetic effects.

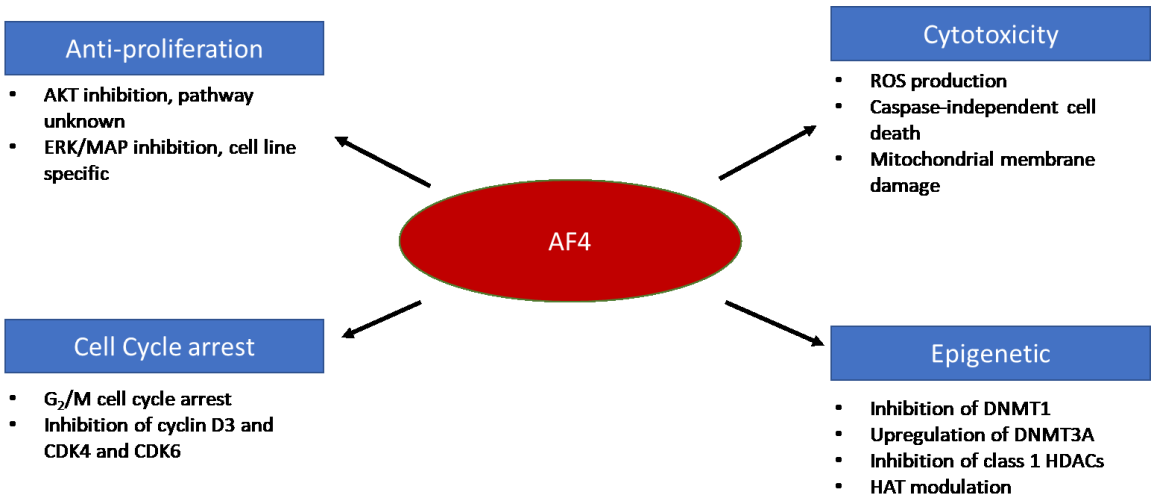

Figure 29. Summary of AF4 Effects

Supplementary Figure 1. AF4 is Cytotoxic to MCF10A Healthy Cells at High Doses in an Annexin-V 488/PI Flow Cytometry Assay. The cytotoxicity of AF4 in MCF10A cells at high doses only was confirmed by subtracting the percentage of dead cells from the medium control from experimental conditions. Data are shown as mean values ± SEM of three independent trials. Significance was determined by ANOVA with the Tukey-Kramer multiple comparisons post-test, and is denoted by * for $p < 0.05$, ** for $p < 0.01$, and *** for < 0.001.

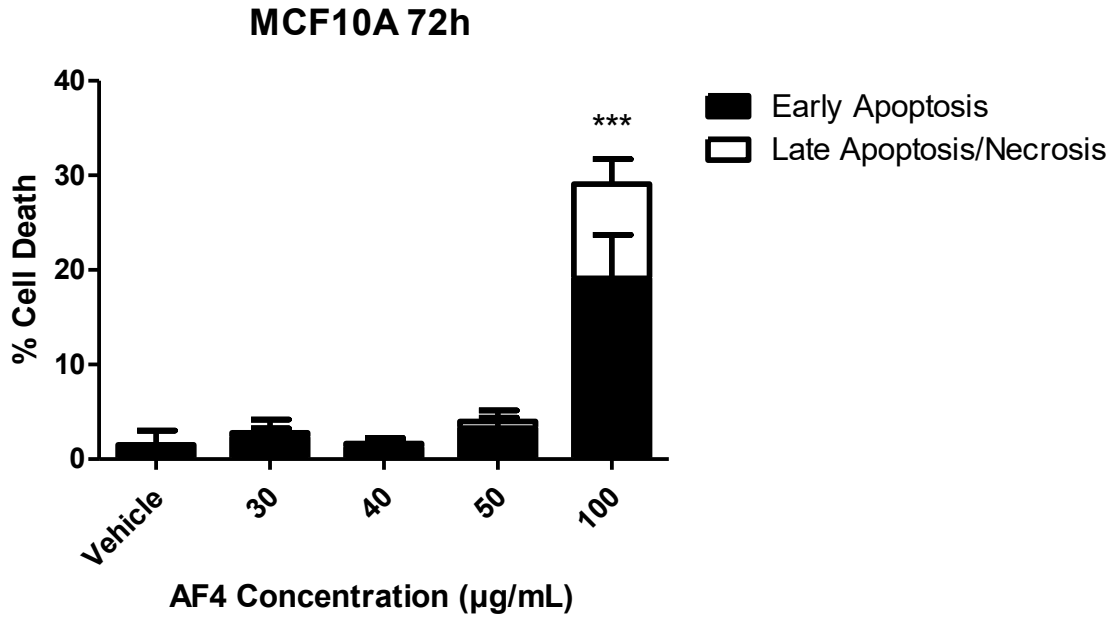

Supplementary Figure 1. AF4 is Cytotoxic to MCF10A Healthy Cells at High Doses in an Annexin-V 488/PI Flow Cytometry Assay.